

**CELLULAR INTERACTIONS WITH IRON CHELATORS**

**by**

**Katharine Pippin Hoyes**

**A thesis submitted for the Degree of Doctor of Philosophy of the  
University of London.**

**December 1991**

**Department of Haematology  
University College London**

ProQuest Number: 10609060

All rights reserved

INFORMATION TO ALL USERS

The quality of this reproduction is dependent upon the quality of the copy submitted.

In the unlikely event that the author did not send a complete manuscript and there are missing pages, these will be noted. Also, if material had to be removed, a note will indicate the deletion.



ProQuest 10609060

Published by ProQuest LLC (2017). Copyright of the Dissertation is held by the Author.

All rights reserved.

This work is protected against unauthorized copying under Title 17, United States Code  
Microform Edition © ProQuest LLC.

ProQuest LLC.  
789 East Eisenhower Parkway  
P.O. Box 1346  
Ann Arbor, MI 48106 – 1346

## ABSTRACT

The experiments contained within this thesis have characterized the ability of desferrioxamine (DFO) and 3-hydroxypyridin-4-one (3-HP-4-one) iron chelators to enter cells and mobilise iron from intracellular iron pools.

Radiolabelled 1,2-diethyl-3-hydroxypyridin-4-one (CP94) and DFO have been used to study their cellular uptake and subcellular distribution. CP94 had rapid passage into and out of K562 erythroleukaemia cells in both the iron-free and iron-complexed form by simple diffusion. In contrast, DFO was found to enter cells by a facilitated mechanism, possibly along an electrochemical gradient, and accumulated within cells at concentrations in excess of that in the extracellular medium. Iron chelated as FO passed out of the cell relatively slowly and it is proposed that the charged nature of FO may delay its egress from the cell. Whilst the major intracellular site of chelation by both compounds was the low molecular weight cytosolic iron pool, CP94 was more efficient at mobilising iron from intracellular organelles than DFO.

The effects of such iron depletion on cell function have been examined using *in vivo* and *in vitro* models of cellular proliferation. *In vitro* DFO and CP94 inhibited cell growth in a dose dependent manner. At chelator concentrations above 30 $\mu$ M this was concomitant with inhibition of DNA synthesis and ribonucleotide reductase activity. However, lower chelator concentrations exerted an inhibitory effect on cell growth that was independent of DNA synthesis suggesting that iron chelators may affect other intracellular iron dependent pathways necessary for proliferation. Unlike DFO, CP94 and other 3-HP-4-ones were found to act as potent cell cycle synchronisation agents. Inhibition of bone marrow progenitor growth *in vitro* was also dose dependent for DFO and the 3-HP-4-ones. Furthermore *in vivo* chronic administration of the chelators led to the suppression of haemopoiesis.

The 3-HP-4-ones possess a greater ability to mobilise iron from cells and intracellular organelles than DFO and these findings have important implications for the use of such compounds in both iron overloaded and non-overloaded conditions.

**For Guy**  
**in appreciation of his constant support and encouragement.**

*'A discovery is rarely.... a sudden achievement, nor is it the work of one man; a long series of observations, each in turn received in doubt and discussed in hostility are familiarised by time and lead at last to the gradual disclosure of truth.'*

Sir Berkeley Moynihan (1865-1936)

In: Surgery, Gynaecology and Obstetrics (1920) 31: 549

## ACKNOWLEDGEMENTS

I wish to express my gratitude to my supervisor, Dr John Porter, for all the advice, help and encouragement he has given me during the course of this study. I should also like to thank Professor Ernie Huehns for his help and in particular for his guidance in the preparation of this thesis.

I am particularly grateful to Professor Bob Hider and Paul Dobbin from the Department of Pharmacy, Kings College London for supplying the hydroxypyridinone iron chelators. I would also like to thank Dr Surinder Singh, of the same department, for carrying out the HPLC analysis. I am also indebted to Mark Jones, Department of Haematology, University College London for his help and advice with the bone marrow progenitor colony forming assays.

Finally I would like to thank all at 98 Chenies Mews, past and present, for their constant advice and encouragement over the last four years.

## INDEX

	PAGE
TITLE PAGE	1
ABSTRACT	2
DEDICATION	3
ACKNOWLEDGEMENTS	4
INDEX	5
LIST OF FIGURES	9
LIST OF TABLES	12
LIST OF ABBREVIATIONS	14
<b><u>CHAPTER 1: GENERAL INTRODUCTION</u></b>	<b>16</b>
1.1. INTRODUCTION	17
1.2. IRON PHYSIOLOGY	18
1.2.1. Iron Balance	18
1.2.2. Transferrin and the Transferrin Receptor	19
1.2.3. Cellular Iron Uptake	22
1.2.4. Cellular Iron Pools	25
1.2.5. Storage Iron	31
1.2.6. Cellular Iron Homeostasis	32
1.3. IRON OVERLOAD	33
1.4. IRON CHELATION	38
1.4.1. General Principles of Iron Chelation	38
1.4.2. Sites of Iron Chelation	41
1.4.3. Potential Oral Chelators	42
1.4.4. Use of Iron Chelators In Conditions Unrelated to Iron Overload	50

<b><u>CHAPTER 2: GENERAL MATERIALS AND METHODS</u></b>	<b>55</b>
2.1. INTRODUCTION	56
2.2 IRON CHELATORS	56
2.3. CELLS AND CELL CULTURE	58
2.3.1. Cell Culture Media	58
2.3.2. Culture of Cell Lines	59
2.3.3. Isolation and Culture of Human Peripheral Blood Lymphocytes	59
2.3.4. Isolation and Culture of Haemopoietic Progenitor Cells from Murine Bone Marrow	60
2.3.5. Cell Counting and Viability	61
2.3.6. Freezing and Thawing Cells	61
2.3.7. Cytospin Preparation	62
2.4. GENERAL METHODS	62
2.4.1. Transferrin Labelling	62
2.4.2. Cell Cycle Analysis	64
2.4.3. Assays Conducted on Fractionated Cells	64
2.4.4. Ribonucleotide Reductase Assay	66
2.4.5. Protein Assay	69
<b><u>CHAPTER 3: CELLULAR UPTAKE OF CP94 AND DFO</u></b>	<b>71</b>
3.1. INTRODUCTION	72
3.2. UPTAKE EXPERIMENTS WITH [ <sup>14</sup> C]DFO AND [ <sup>14</sup> C]CP94	73
3.2.1. Uptake of [ <sup>14</sup> C]DFO and [ <sup>14</sup> C]CP94 by K562 cells at 37°C	73
3.2.2. Initial Rate of Uptake of [ <sup>14</sup> C]CP94 and [ <sup>14</sup> C]DFO	74
3.2.3. Discussion	77
3.3. HPLC ANALYSIS OF INTRACELLULAR DFO	77
3.4. EFFECT OF TEMPERATURE AND SELECTIVE INHIBITORS ON CELLULAR UPTAKE OF [ <sup>14</sup> C]CP94 AND [ <sup>14</sup> C]DFO	82

3.5. IRON MOBILISATION FROM K562 CELLS BY CP94 AND DFO	85
3.6. GENERAL DISCUSSION	88
<b><u>CHAPTER 4: SUBCELLULAR DISTRIBUTION OF</u></b>	<b>90</b>
<b>CP94 AND DFO</b>	
4.1. INTRODUCTION	91
4.2. ANALYTICAL SUBCELLULAR FRACTIONATION OF K562 CELLS	92
4.3. SUBCELLULAR DISTRIBUTION OF [ <sup>14</sup> C]CP94 AND [ <sup>14</sup> C]DFO	96
4.4. SUBCELLULAR DISTRIBUTION STUDIES USING <sup>59</sup> Fe	101
4.4.1. Effect of 100µM IBE CP94 and DFO on the Subcellular Distribution of <sup>59</sup> Fe delivered by Receptor Mediated Endocytosis.	101
4.4.2. Mobilisation of Low Molecular Weight Iron by CP94 and DFO	107
4.4.3. Discussion	109
4.5. EFFECT OF PREINCUBATION WITH CP94 AND DFO PRIOR TO LOADING CELLS WITH <sup>59</sup> Fe TRANSFERRIN	111
4.6. GENERAL DISCUSSION	114
<b><u>CHAPTER 5: EFFECT OF DFO AND THE HYDROXPYRIDINONE</u></b>	<b>116</b>
<b>ON CELL CYCLE AND PROLIFERATION</b>	
5.1. INTRODUCTION	117
5.2. EFFECT OF CP94 AND DFO ON CELL CYCLE KINETICS	118
5.2.1. Dose Response Effect of DFO and CP94 on K562 and Daudi Cell Cycle.	118
5.2.2. Effect of DFO and CP94 on the Cell Cycle of Mitogen Stimulated Peripheral Blood Lymphocytes	125
5.2.3. Discussion	125
5.3. PHYSICOCHEMICAL PROPERTIES REQUIRED FOR EFFECTIVE CELL CYCLE ARREST	127



5.4.CELL CYCLE SYNCHRONISATION BY 3-HYDROXYPYRIDIN-4-ONES	128
5.5. INHIBITION OF RIBONUCLEOTIDE REDUCTASE BY CP94 AND DFO	137
5.6. EFFECT OF CP94 AND DFO ON CELL PROLIFERATION	138
5.6.1. Effect of CP94 and DFO on Cell Growth and Viability	140
5.6.2. Effect of CP94 and DFO on DNA,RNA and Protein Synthesis	144
5.6.3. Discussion	146
5.7. GENERAL DISCUSSION	149
<b><u>CHAPTER 6: IN VIVO AND IN VITRO EFFECTS OF DFO AND 3-HP-4-ONES ON MURINE HAEMOPOIESIS</u></b>	<b>152</b>
6.1. INTRODUCTION	153
6.2. <i>IN VIVO</i> STUDY	153
6.3. <i>IN VITRO</i> STUDY	159
6.3.1. Effects of DFO, CP94 and CP20 on Haemopoietic Colony formation	159
6.3.2. Effects of Iron-Complexed Chelators on Haemopoietic Colony Formation	162
6.3.3. Effect of Transferrin Saturation on Inhibition by Chelator Complexes	165
6.3.4. Relationship Between Complex Lipophilicity and Colony Inhibition	168
6.3.5. Discussion	170
6.4. GENERAL DISCUSSION	171
<b><u>CHAPTER 7: CONCLUSIONS</u></b>	<b>174</b>
7.1. INTRODUCTION	175

7.2. CELLULAR IRON MOBILISATION	176
7.2.1. Transit Across Cell Membranes	176
7.2.2. Access to Intracellular Iron Pools	178
7.2.3. Removal Of Iron From Cells	179
7.3. EFFECT OF IRON CHELATION ON CELL FUNCTION	181
7.3.1. The Antiproliferative Effects of Iron Chelators	181
7.3.2. The Use of Iron Chelators as Anti-neoplastic Agents	183
7.4. IRON CHELATOR TOXICITY	185
7.5. CONCLUSIONS AND FUTURE PERSPECTIVES.	188

<b><u>REFERENCES</u></b>	190
--------------------------	-----

<b><u>APPENDICES</u></b>	209
--------------------------	-----

APPENDIX 1. MANUFACTURERS OF REAGENTS	210
---------------------------------------	-----

APPENDIX 2. BUFFERS	215
---------------------	-----

APPENDIX 3. MEASUREMENT OF SERUM IRON LEVELS	216
--	-----

**LIST OF FIGURES**

FIGURE 1. Schematic Representation of the Human Transferrin Receptor.	20
---	----

FIGURE 2. The Receptor Mediated Transferrin to Cell Cycle.	23
--	----

FIGURE 3. Intracellular Iron Pools.	26
-------------------------------------	----

FIGURE 4. Schematic Description of the Interconversion of the 4Fe and 3Fe Cluster of Aconitase.	29
--	----

FIGURE 5. Schematic Representation of Ribonucleotide Reductase.	30
---	----

FIGURE 6. Co-ordinate Regulation of the Expression of the Transferrin Receptor and Ferritin.	34
---	----

FIGURE 7. The Chain Reaction of Lipid Peroxidation.	37
---	----

FIGURE 8. The Structure of Desferrioxamine B.	46
---	----

FIGURE 9. Bidentate Hydroxypyridinone Structures.	48
---	----

FIGURE 9. Bidentate Hydroxypyridinone Structures.	48
FIGURE 10. Labelling Transferrin with <sup>59</sup> Fe.	63
FIGURE 11. Measurement of Ferritin by ELISA.	67
FIGURE 12. Typical Standard Curve for the Ferritin ELISA.	68
FIGURE 13. Typical Standard Curve for the Protein Assay.	70
FIGURE 14. Uptake of [ <sup>14</sup> C]CP94 and [ <sup>14</sup> C]DFO by K562 cells.	75
FIGURE 15. Initial Uptake of [ <sup>14</sup> C]CP94 and [ <sup>14</sup> C]DFO by K562 cells.	76
FIGURE 16. Typical HPLC Chromatograms for DFO and FO.	79
FIGURE 17. Calibration Curves for the Measurement of DFO and FO by HPLC.	80
FIGURE 18. Effect of Temperature, Colchicine and Azide on uptake of [ <sup>14</sup> C]sucrose, [ <sup>14</sup> C]CP94 and [ <sup>14</sup> C]DFO by K562 cells.	84
FIGURE 19. Mobilisation of <sup>59</sup> Fe from K562 Cells by CP94 and DFO.	87
FIGURE 20. Fractionation Procedure.	95
FIGURE 21. Subcellular Distribution of [ <sup>14</sup> C]CP94 and [ <sup>14</sup> C]DFO in K562 cells at 20 minutes.	99
FIGURE 22. Subcellular Distribution of [ <sup>14</sup> C]CP94 and [ <sup>14</sup> C]DFO in K562 cells at 4 hours.	100
FIGURE 23. Pulse-chase Labelling of K562 cells with <sup>59</sup> Fe.	102
FIGURE 24. Distribution of <sup>59</sup> Fe in Control K562 Cells after 20 Minutes at 37°C.	104
FIGURE 25. Effect of 100µM IBE CP94 and DFO on Distribution of <sup>59</sup> Fe after 20 minutes.	105
FIGURE 26. Effect of 100µM IBE CP94 and DFO on Distribution of <sup>59</sup> Fe after 4 hours.	106
FIGURE 27. Incorporation of <sup>59</sup> Fe into Ferritin in Control and	108

Chelator Treated K562 cells.	
FIGURE 28. LMW <sup>59</sup> Fe in K562 Cells Treated with 100μM IBE CP94 or DFO.	110
FIGURE 29. Distribution of <sup>59</sup> Fe at 20 minutes following 4 hours Preincubation with CP94 and DFO.	113
FIGURE 30. Flow Cytometric DNA Histograms for Control K562 Cells.	119
FIGURE 31. DNA Histograms for K562 Cells Treated with 100μM IBE CP94 and DFO.	121
FIGURE 32. Relationship Between Partition Coefficient and Cell Cycle Arrest.	129
FIGURE 33. K562 Cell Cycle Arrest by DFO, CP130, CP94 and CP02.	130
FIGURE 34. Recovery of K562 Cells From Cell Cycle Arrest by CP94 and DFO.	132
FIGURE 35. Recovery of Daudi Cells From Cell Cycle Arrest by CP94 and DFO.	133
FIGURE 36. Recovery of K562 cells from Cell Cycle Arrest After Addition of 100μM IBE Ferric Ammonium Citrate.	134
FIGURE 37. Cell Cycle Synchronisation by 3-HP-4-ones.	135
FIGURE 38. Inhibition of Ribonucleotide Reductase by CP94 and DFO.	139
FIGURE 39. K562 Cell Growth in the Presence of CP94 and DFO.	141
FIGURE 40. Daudi Cell Growth in the Presence of CP94 and DFO.	142
FIGURE 41. Concentration Dependent Inhibition of Cell Growth by CP94 and DFO.	143
FIGURE 42. Concentration Dependent Inhibition of [ <sup>3</sup> H]Thymidine Incorporation in K562 and Daudi Cells.	147
FIGURE 43. Concentration Dependent Inhibition of CFU-G+CFU-Mac Growth by Iron Chelators.	160

FIGURE 44. Concentration Dependent Inhibition of BFU-E Growth by Iron Chelators.	161
FIGURE 45. Effect of Addition of Iron on Inhibition of CFU-G+CFU-Mac by Iron Chelators.	163
FIGURE 46. Dose Response Effect of FO, CP94-Fe and CP20-Fe on CFU-G+CFU-Mac Colony Growth.	164
FIGURE 47. Relationship Between Complex Partition Coefficient and Colony Inhibition.	169

### **LIST OF TABLES.**

TABLE 1. Desirable Properties for an Iron Chelator.	39
TABLE 2. Potential Oral Iron Chelators.	43
TABLE 3. Possible Applications for Iron Chelators in Conditions Unrelated to Iron Overload.	54
TABLE 4. Chelator Structure, Partition Coefficient and Stability Constant.	57
TABLE 5. HPLC Analysis of Intracellular DFO and FO.	81
TABLE 6. Distribution of Marker Enzymes Between Subcellular Fractions.	97
TABLE 7. Effects of CP94 and DFO on K562 Cell Cycle Kinetics.	122
TABLE 8. Effects of CP94 and DFO on Daudi Cell Cycle Kinetics.	123
TABLE 9. Effect of Low Concentrations of DFO and CP4 on the Percentage of Polynuclear and Mitotic Forms.	124
TABLE 10. Effects of CP94 and DFO on Peripheral Blood Lymphocyte Cell Cycle Kinetics.	126
TABLE 11. Effect of DFO and CP94 on the Viability of Daudi and K562 Cells.	145
TABLE 12. Cellular Incorporation of [ <sup>3</sup> H]Thymidine, [ <sup>3</sup> H]Uridine and [ <sup>3</sup> H]Leucine After 72 hours Exposure to CP94	148

and DFO.

TABLE 13. Haematology for Mice Treated with 60 Doses of 200mg/kg Chelator.	156
TABLE 14. Bone Marrow Cellularity and Haemopoietic Colony Formation for Mice Treated with 60 Doses of 200mg/kg Chelator.	157
TABLE 15. Haematology for Mice treated with 10 or 30 Doses of 200mg/kg Chelator.	158
TABLE 16. Transferrin Saturation and Inhibition of CFU-G+CFU-M Colony Growth by Iron Free and Iron Complexed CP94 and CP20.	167

## LIST OF ABBREVIATIONS

ADP	Adenosine diphosphate
AMP	Adenosine monophosphate
ATP	Adenosine triphosphate
BFU-E	Burst forming unit - erythroid
BSA	Bovine serum albumin
CDP	Cytidine diphosphate
CFU-G	Colony forming unit - granulocyte
CFU-Mac	Colony forming unit - macrophage
CPM	Counts per minute
DFO	Desferrioxamine
DNA	Deoxyribonucleic acid
EDTA	Ethylenediaminetetra-acetic acid
ELISA	Enzyme linked immunoassay
FCS	Foetal calf serum
FO	Ferrioxamine
GI	Gastrointestinal
GVHD	Graft versus host disease
HMW	High molecular weight
HPLC	High performance liquid chromatography
HPO	Hydroxypyridinone
3-HP-4-one	3-hydroxypyridin-4-one
3-HP-2-one	3-hydroxypyridin-2-one
IBE	Iron binding equivalents
IC <sub>50</sub>	Inhibitory concentration 50%
IRE	Iron regulatory element
IRE-BP	Iron regulatory element binding protein
LMW	Low molecular weight

MCV	Mean cell volume
NTBI	Non-transferrin bound iron
PBS	Phosphate buffered saline
PHA	Phytohaemagglutinin
RA	Rheumatoid arthritis
RNA	Ribonucleic acid
SEM	Standard error of the mean
UTR	Untranslated region



## **CHAPTER 1: INTRODUCTION**

## **1.1 INTRODUCTION**

This thesis will investigate the actions of iron chelators at a cellular level in order to further the understanding of their mode of action, help in their future development and identify their toxic effects.

The ideal iron chelator has a demonstrable ability to prevent or modify iron mediated pathological processes without undue toxicity. The clinical development of novel chelating agents necessitates an evaluation of their efficacy and potential toxicities in a variety of cellular and animal models. The use of such models can also provide valuable information regarding the biological source of mobilised iron and any resultant alteration of cell function.

Whilst the primary use of iron chelators has been alleviation of pathological iron overload, some attention has also been focused upon the ability of such compounds to modify disease unrelated to iron loading. However, even the only clinically proven chelator desferrioxamine (DFO), which has been used therapeutically for nearly three decades, has significant toxicity (Porter and Huehns, 1989). This is particularly prevalent in patients with minimal iron loading, suggesting that such toxicity may result from the depletion of iron vital to cellular function rather than any effect of DFO itself. This compound will be used in comparative studies with the hydroxypyridinones, a series of iron chelators with potential for clinical use. Initial studies will focus upon the ability of these chelators to enter cells and subcellular organelles and mobilise iron. Subsequent experiments seek to evaluate the effects of such chelation on cell physiology, taking the key area of cell proliferation as a model.

The introduction that follows will provide an overview of general iron physiology coupled with a discussion of the design and application of iron chelators in both iron overloaded and non-overloaded situations.

## **1.2 IRON PHYSIOLOGY**

### **1.2.1 Iron balance**

Eukaryotic cells have an obligate requirement for iron. This can be related to the critical role this metal plays in the function of a wide variety of biological redox systems, including the electron transport chains and ribonucleotide reductase. Consequently, the body's ability to maintain effective iron homeostasis is essential to health. Disturbances in iron balance are common but almost invariably result in a reduction in total body iron content, and iron deficiency affects 500-600 million people worldwide. In contrast, accumulation of excessive iron within the body is a relatively rare condition.

In man the average iron content is normally 40-50mg Fe/kg body weight. Levels are generally higher in men than women. The major proportion of body iron (approximately 30mg/kg) is bound in haemoglobin in circulating red cells. A further 4mg/kg is found in muscle as myoglobin and approximately 2mg/kg is in tissues as components of iron containing enzymes. Most of the remaining iron is stored within the liver, spleen, bone marrow and muscle as ferritin and haemosiderin (Bothwell et al, 1979)

In man iron metabolism is essentially a conservative process. Iron losses are compensated for by intestinal absorption but there is no specific mechanism for iron excretion. There is an inverse relationship between body iron stores and iron absorption in that as stores decrease absorption increases. Similarly, enhanced erythropoietic activity results in increased iron absorption. Iron absorption occurs primarily in the upper region of the gastrointestinal (GI) tract and is regulated by the intestinal mucosa which, under normal circumstances, absorb just enough iron to compensate for daily losses from the body. In men the average daily iron losses are approximately 1mg, two thirds of this from the GI tract by exfoliation of mucosal cells and loss of red blood cells and one third from the exfoliation of skin and urinary tract.

In women additional losses result from menstruation (0.6mg) and pregnancy (2.7mg) (Bothwell et al, 1979).

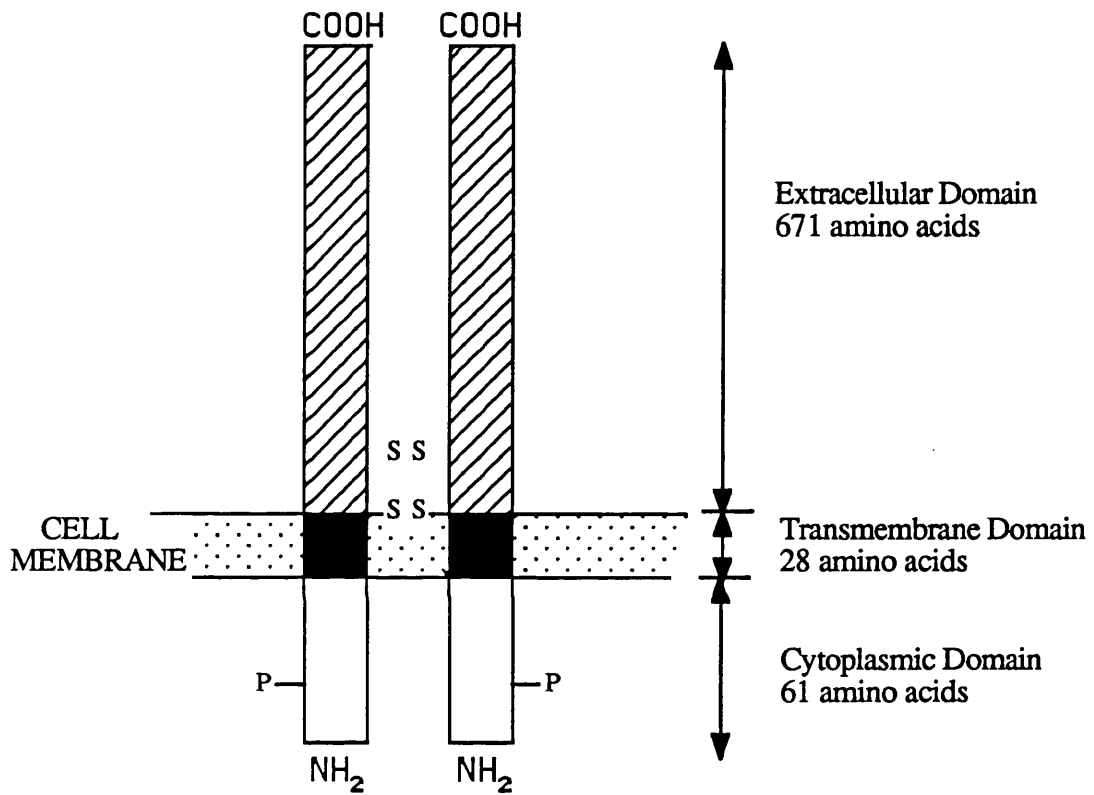
### 1.2.2 Transferrin and the Transferrin Receptor

In vertebrates serum transferrin provides the major physiological route for the extracellular transport of iron and its delivery to cells. The liver is the principal site of transferrin synthesis but other cell types including testicular Sertoli cells (Skinner and Griswold, 1982), cells in the central nervous system (Bloch et al, 1985) and lymphocytes (Soltys and Brody, 1970) also synthesize this protein.

Transferrin is a glycoprotein with a molecular weight of approximately 80,000. The molecule consists of a single polypeptide chain folded to form two globular domains termed N and C, relating to the N-terminal and C-terminal domains of the protein. Binding of iron (III) to each of the N and C lobes requires concomitant binding of a bicarbonate anion (Schlabach and Bates, 1975). The amino acid residues involved in the specific binding of iron by transferrin have been identified by X-ray crystallography. At both the N and C-terminals iron is directly co-ordinated to two tyrosines, one histidine and one aspartic acid and indirectly co-ordinated to an arginine via the bicarbonate anion which acts as a bridging ligand (Bailey et al, 1988). Under physiological conditions the apparent stability constants for the N and C binding sites are approximately  $10^{22}\text{M}^{-1}$  but this decreases rapidly with pH.

At the cell membrane the transferrin iron complex binds to specific receptors. The transferrin receptor is an integral membrane glycoprotein composed of two identical 95,000 dalton subunits linked by disulphide bonds (Enns and Sussman, 1981a). Studies on transferrin receptors isolated from both normal and malignant tissues (Enns and Sussman, 1981b; Stein and Sussman, 1983) have demonstrated similar proteolytic digest maps indicating that the receptor is identical in all tissues. Each subunit is a transmembrane polypeptide of 760 amino acids (McClelland et al, 1984; Schneider et al, 1984) consisting of three domains (Figure 1). The

**FIGURE 1: SCHEMATIC REPRESENTATION OF  
THE HUMAN TRANSFERRIN RECEPTOR**



(Adapted from McClelland et al, 1984)

intracellular N-terminal domain comprises the first 61 residues. This is followed by a hydrophilic transmembrane domain of 28 amino acids. This sequence appears to act as a signal for insertion of the receptor into the plasma membrane and its deletion confines the whole receptor to the cytoplasm (Zerial et al, 1986). The remaining 671 amino acids comprise the extracellular C terminal domain.

The cytoplasmic sequence contains a total of 4 serines, all potential phosphorylation sites. However only serine 24 appears to be a target for protein kinase C mediated phosphorylation (Davis et al, 1986). There has been some controversy over whether phosphorylation is required for receptor internalisation (Zerial et al, 1987; May and Tyler, 1987) but studies using site directed mutagenesis to substitute Ser 24 by alanine show that the mutation has no effect on the rate of transferrin receptor endocytosis (Davis and Meisner, 1987).

The transferrin receptor has very high affinity for diferric transferrin, with an estimated affinity constant of  $2.7 \times 10^9 \text{M}^{-1}$  at pH 7.4. Binding is pH dependent. At neutral pH the transferrin receptor has a higher affinity for diferric transferrin than for apotransferrin (Young, Bomford and Williams, 1984; Klausner et al, 1983; Dautry-Varsat et al, 1983). However at pH less than 7.0 the receptors affinity for apotransferrin increases to that of diferric transferrin (Dautry-Varsat et al, 1982; Klausner et al, 1983).

Transferrin receptor expression appears to be linked to cellular iron requirements. Proliferating cells express transferrin receptors at a high density (Sutherland et al, 1981) and receptors are expressed at high levels in reticulocytes but not in mature red cells (Seligman, 1983). Furthermore, in placenta there is a direct correlation between levels of placental transferrin receptor and foetal iron requirements (McCardle and Morgan, 1982).

### 1.2.3 Cellular Iron Uptake

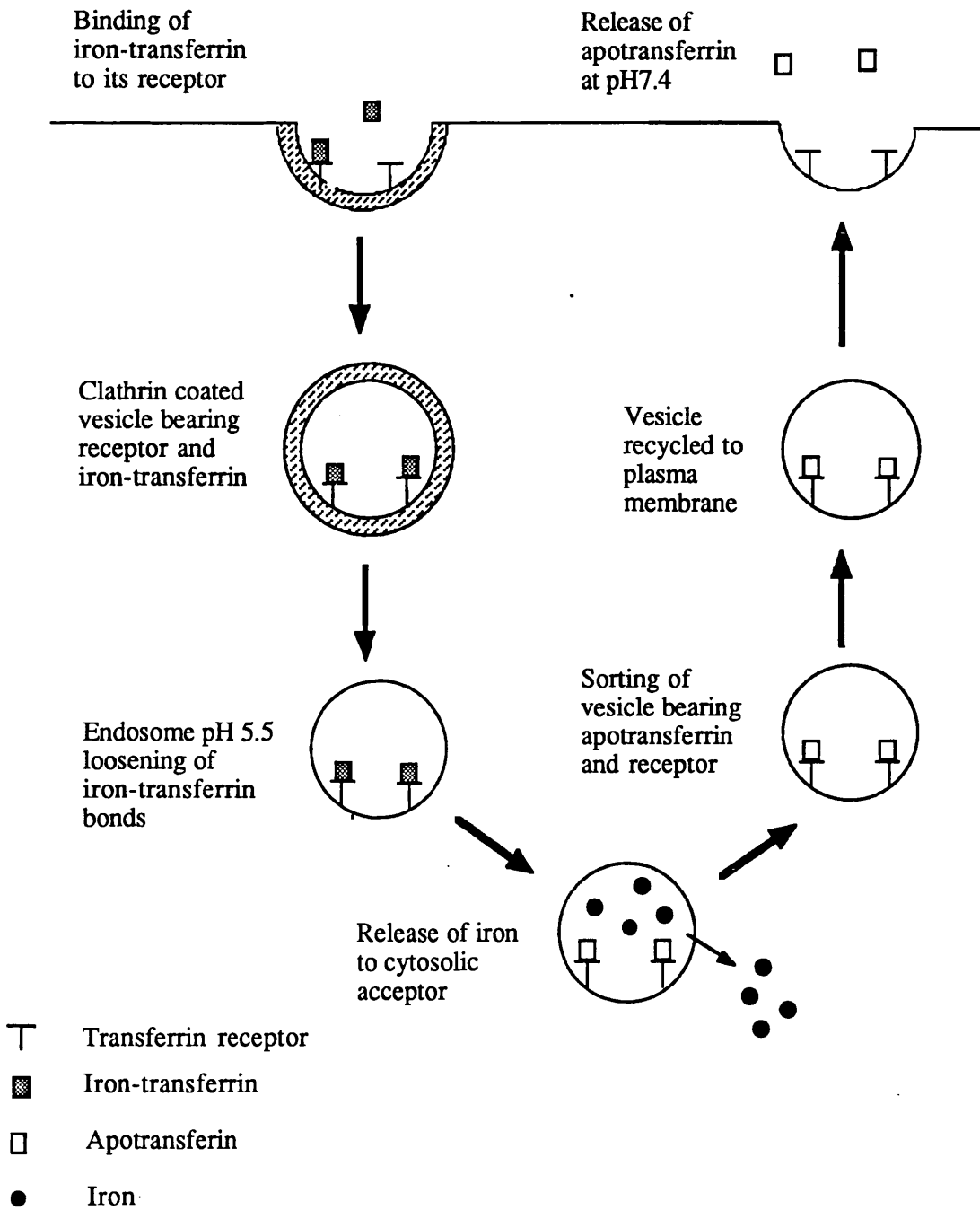
Many cells acquire iron by the receptor mediated endocytosis of transferrin (Figure 2). This process is initiated by the binding of transferrin to the transferrin receptor at the cell surface. The receptor-transferrin complexes localise in clathrin coated pits which bud off from the cell surface to form clathrin coated vesicles. The vesicles lose their coats, probably in an ATP dependent process, and fuse to form an endosome. Through the action of a proton pumping ATPase of the endosomal membrane, the vesicles interior is rapidly acidified (pH 5.5). The low pH facilitates the release of iron from transferrin and the iron is transported across the endosomal membrane into the cytosol leaving apotransferrin tightly bound by its receptor at the acidic pH. The apotransferrin-receptor complex is recycled back to the plasma membrane, possibly through the Golgi complex (Stoorvogel et al, 1988), where exposure to neutral pH effects release of the apotransferrin from the receptor (Dautry-Varsat et al, 1983; Klausner et al, 1983).

From studies in preparations of endocytotic vesicles from rabbit reticulocytes (Nunez et al, 1990) a four step model has been proposed for the dissociation of iron from transferrin and its subsequent transfer across the endosomal membrane:-

- (i) An acidification system which promotes iron (III) dissociation from transferrin and requires vesicle acidification promoted by a variety of membrane ATPases.
- (ii) A reduction system in which the dissociated iron (III) bound to an iron binding moiety on the *cis* side of the membrane is reduced to iron (II).
- (iii) A translocation system which moves iron (II) to the trans side of the vesicular membrane along a specific transmembrane pathway.
- (iv) A mobilization system in which iron (II) on the trans side of the membrane is mobilised by cytosolic low molecular weight carriers.

However *in vitro* release of iron from transferrin at the pH of the endosome may take hours (Foley and Bates, 1989), suggesting that more must be involved in this

**FIGURE 2: THE RECEPTOR MEDIATED TRANSFERRIN-TO-CELL CYCLE**





process than mere acidification. Furthermore, a recent study has indicated that the transferrin receptor itself may facilitate release of iron from transferrin within the endosome (Bali et al, 1991).

The receptor mediated endocytosis model has been derived mainly from studies utilising immature erythroid cells and established cell lines in culture. This model probably accounts for iron uptake in many cell types since transferrin receptors have been identified in many tissues (Reviewed by Huebers and Finch, 1987). However the mechanism by which hepatocytes accumulate iron is a subject of debate. Hepatocyte iron uptake does not reach saturation with increasing transferrin concentration, is increased by low oxygen concentration and is not significantly inhibited by weak bases and ionophores (Reviewed by Morley and Bezkorvainy, 1985; Thorstensen and Romslo, 1990). Consequently, a variety of mechanisms have been proposed to explain hepatocyte iron uptake. These include fluid phase endocytosis (Sibille et al, 1982; Page et al, 1984), the action of endogenous iron chelators (Page et al, 1984) and the mobilisation of iron from transferrin by a plasma membrane mediated redox process (Cole and Glass, 1983; Thorstensen and Romslo, 1988,1990; Morley and Bezkorvainy, 1985). These latter studies have led to the proposal of the redox model for hepatocyte iron uptake (Thorstensen and Romslo, 1990). This model starts, as the receptor mediated endocytosis model, with the binding of transferrin to the cell surface transferrin receptor. From this step the two models diverge and in the redox model the concerted actions of protons and reducing equivalents furnished by a NADH:ferricyanide oxireductase (Sun et al, 1987) in close proximity to the transferrin receptor evokes the destabilization of the transferrin iron complex and the reduction of iron. The ferrous iron is bound by a membrane binder/carrier specific for iron (II) and is translocated across the membrane where it is picked up by cytosolic iron acceptors.

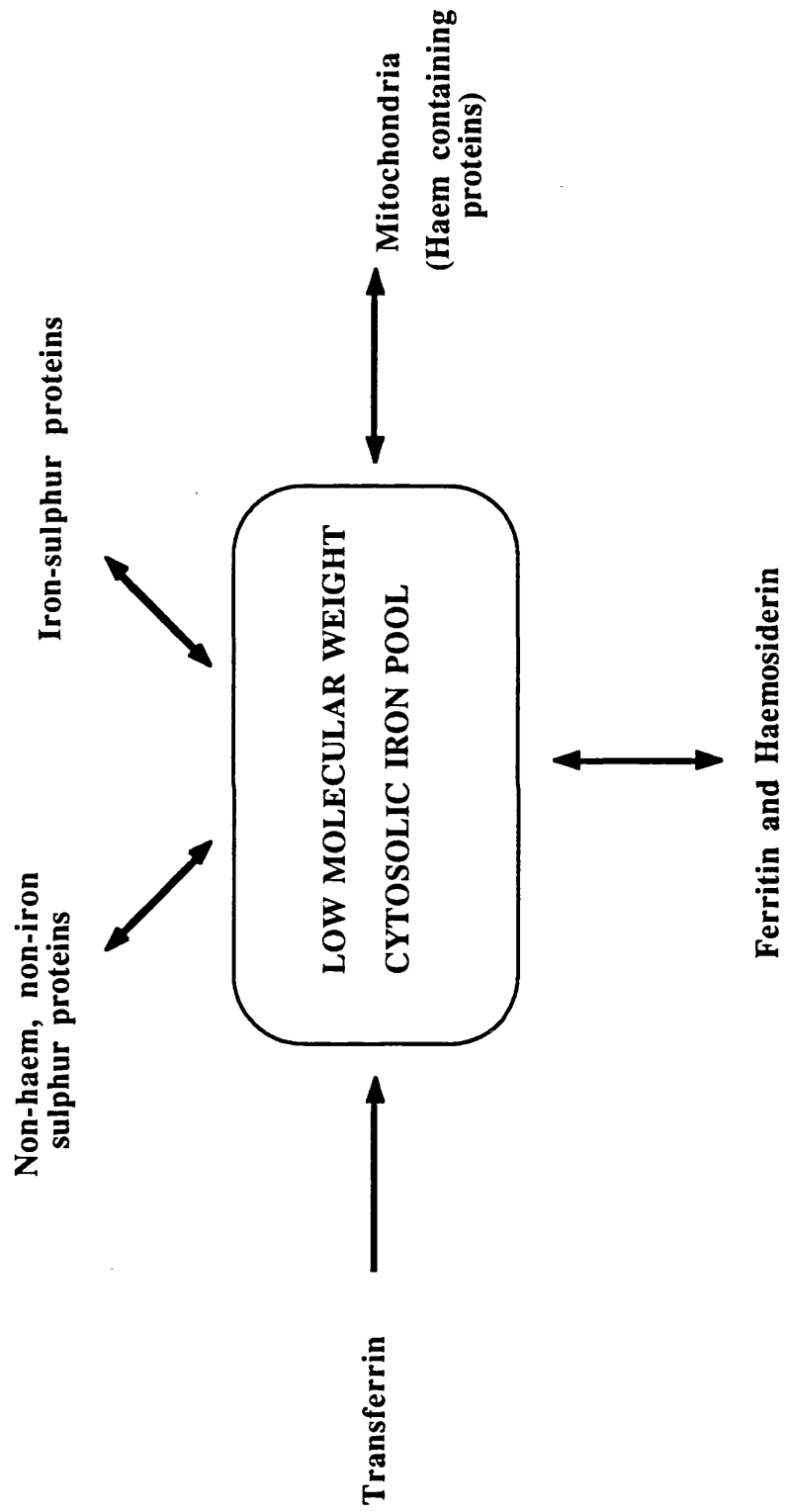
#### 1.2.4 Intracellular Iron Pools

When iron initially enters cells it transiently enters a low molecular weight (LMW) cytosolic pool before incorporation into iron-containing enzymes and ferritin (Jacobs et al, 1977) (Figure 3). The existence of this pool was originally inferred from indirect studies with the iron chelator DFO. Administration of repeated doses of DFO to normal rats provoked excretion of ferrioxamine (FO) in proportion to body iron stores. However, when the animals were hypertransfused, the resulting inhibition of erythropoiesis led to reduced FO excretion. As there was no reduction in the animals' iron stores, this suggests that ferritin and haemosiderin were not the direct donors of iron to DFO and compounds on the pathway between ferritin and transferrin were probably the immediate iron source (Libschitz et al, 1971). Furthermore, release of haemoglobin iron by the reticuloendothelial system in phenylhydrazine induced haemolysis increased FO excretion (Cummings et al, 1967), and similarly FO excretion increased 4-8 hours after transfusion of nonviable erythrocytes but returned to normal after 20 hours despite the increase in storage iron (Samson et al 1977).

Subsequent studies with  $^{59}\text{Fe}$  have supported the presence of a LMW iron pool in a number of cell types (White, 1976a,1976b; Pippard et al, 1982; Bakkeren et al, 1985; Mulligan et al, 1986). The transient nature of this pool makes characterisation of the iron complex difficult, but it has been shown that iron in this pool is bound primarily to ATP (Weaver and Pollack, 1989).

In addition to the LMW cytosolic pool there is evidence of a non-haem non-iron-sulphur mitochondrial iron pool which serves as a short term reserve for haem synthesis (Tangeras et al, 1980). Whilst maturing erythroid cells have the greatest capacity for haem synthesis, this takes place in virtually all cells due to the ubiquitous nature of haemoproteins. The mitochondrial iron pool represents approximately 1 nmol/mg mitochondrial protein, roughly one third of total mitochondrial iron (Tangeras et al, 1980). Its major function appears to be donation of iron to ferrochelatase for

**FIGURE 3: INTRACELLULAR IRON POOLS**



insertion into protoporphyrin IX, the final step in the haem biosynthetic pathway (Tangeras, 1985). *In vivo* this pool must be constantly resupplied with iron from a cytosolic source (Funk et al, 1986). Recent studies suggest that the major pathway by which iron is delivered to mitochondria may be through hydrolysis of cytosolic iron-ATP to iron-AMP which binds to specific mitochondrial receptors (Weaver and Pollack, 1990).

In addition to these endogenous pools, iron is an essential component of many cellular proteins. These may be classified into the haemoproteins, iron-sulphur proteins and non-haem non-iron-sulphur proteins.

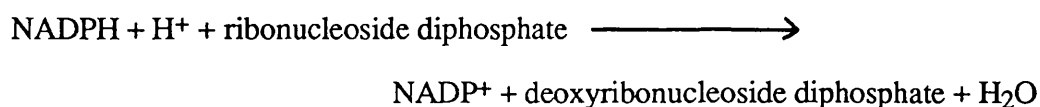
The haemoproteins include the oxygen transporters haemoglobin and myoglobin. The role of iron in the biology and chemistry of haemoglobin and myoglobin has been extensively studied and reviewed (Dickerson and Geis, 1983; Crichton, 1991) and since these proteins are somewhat peripheral to the theme of this thesis, they will not be discussed in detail here. Other haem containing proteins include the peroxidases, which constitute part of the microbicidal system in phagocytic cells (Klebanoff, 1975), catalase, which catalyses the dismutation of hydrogen peroxide to oxygen and water, cytochrome oxidase and various electron transport enzymes and cytochromes of the electron transport chain.

The iron-sulphur proteins are molecules which contain iron atoms bound to sulphide forming a cluster linked to a polypeptide chain by the thiol groups of cysteine residues. Several types of iron-sulphur cluster are known. In the simplest form a single iron atom is tetrahedrally co-ordinated to the sulphhydryl groups of four cysteine residues of the protein. A second kind denoted by [2Fe-2S] contains two iron atoms and two inorganic sulphides in addition to four cysteine residues. A third type is designated [3Fe-4S] and contains three iron molecules and four inorganic sulphides with the cysteine residues and the fourth type [4Fe-4S] contains four iron atoms four sulphides and four cysteine residues. The roles of iron-sulphur proteins are numerous and range from electron transport (such as components of the mitochondrial electron

transport chain) to enzymes with both redox and non-redox functions such as succinate dehydrogenase, and aconitase respectively.

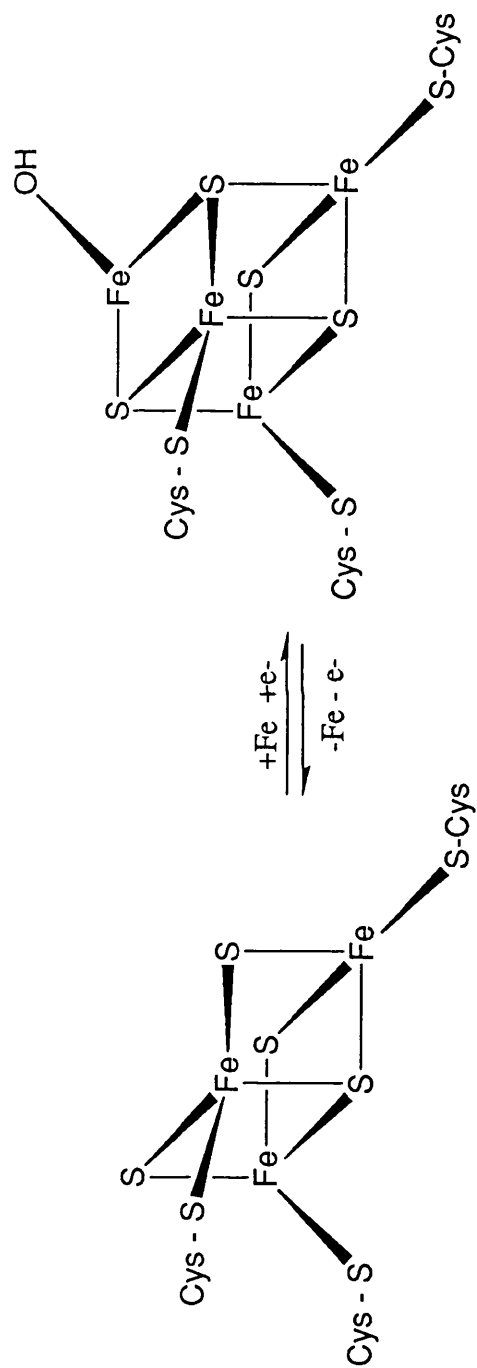
Aconitase is a mitochondrial enzyme of the citric acid cycle that catalyses the stereospecific dehydration and rehydration reactions that convert citrate to isocitrate via the intermediate cis-aconitate. Purified aconitase exists in an inactive  $[3\text{Fe-4S}]^+$  state which can be activated *in vitro* to the  $[4\text{Fe-4S}]^{2+}$  form by introduction of a fourth  $\text{Fe}^{2+}$  under reducing conditions (Beinert and Kennedy, 1989) (Figure 4). This is distinct from other iron-sulphur proteins in which the Fe-S centre is relatively stable. Thus aconitase provides an example of the possible way in which the activity of a protein is responsive to changes in iron availability.

The third class of iron containing proteins consists of a heterogeneous group of enzymes and proteins which contain non-haem, non-iron-sulphur iron. One notable member of this group is ribonucleotide reductase. The reduction of ribonucleotides to deoxyribonucleotides occurs through a series of redox reactions catalysed by thioredoxin reductase and ribonucleotide reductase (Thelander and Reichard, 1979) with the overall stoichiometry of:-



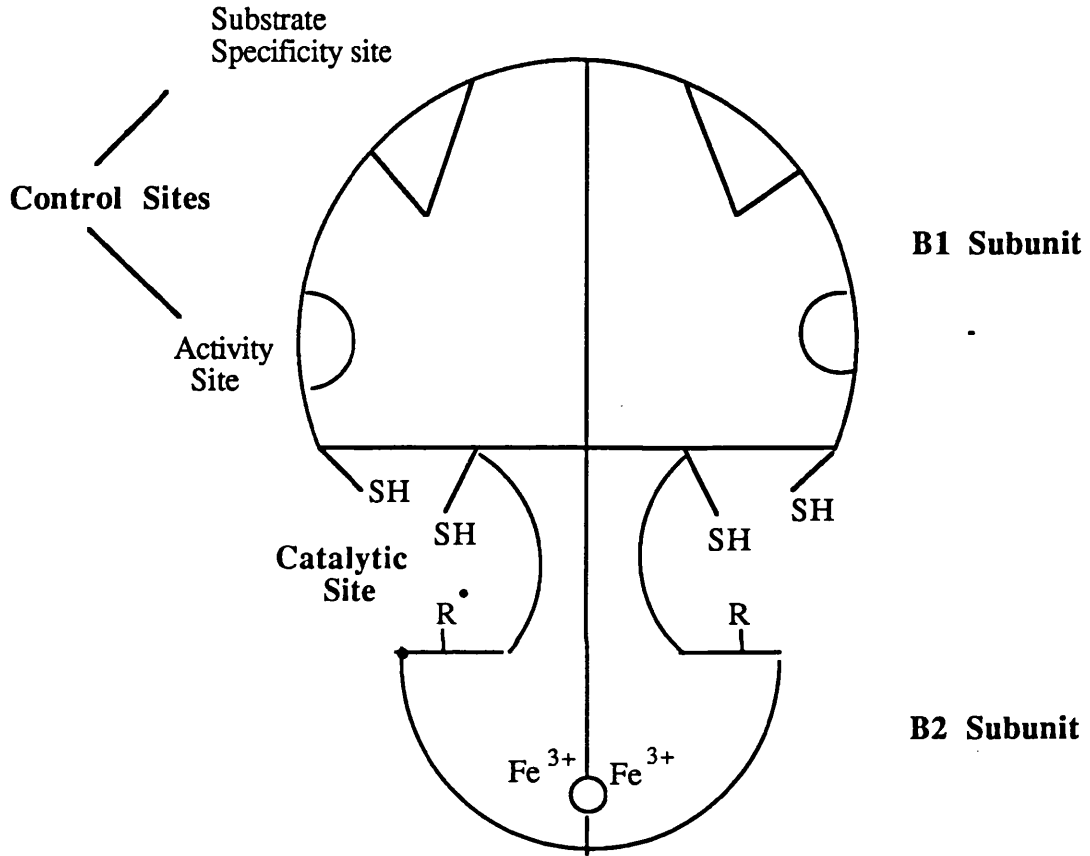
The best characterised form of this enzyme is from *E.coli* (Thelander and Reichard, 1979). This enzyme consists of two proteins B1 (a 160 kd dimer) and B2 (a 78 kd dimer) (Figure 5). B1 contains the binding sites for ribonucleotide substrates and allosteric effectors. B1 also contains sulphydryl groups that donate electrons for reduction of the ribose unit. B2 contains a tyrosyl radical cation stabilised by a di-iron centre. Mammalian ribonucleotide reductase has subsequently been demonstrated to have a similar structure with the two subunits designated M1 and M2 correlating with B1 and B2 in the *E.coli* enzyme (Thelander and Reichard, 1979)

FIGURE 4: SCHEMATIC DESCRIPTION OF THE INTERCONVERSION OF THE 4Fe AND 3Fe CLUSTER OF ACONITASE



(Adapted from Beinert and Kennedy, 1990)

**FIGURE 5: SCHEMATIC REPRESENTATION OF  
RIBONUCLEOTIDE REDUCTASE**



(Adapted from Thelander and Reichard, 1979)

### 1.2.5. Storage Iron

Any iron which is surplus to immediate functional needs is stored in cells as ferritin or haemosiderin. Ferritin is the major iron storage protein and is found in all living organisms with a consistent structure of an almost spherical protein shell surrounding an iron core of variable size (Harrison et al, 1980). The iron core is in the form of a polymeric iron hydroxide to which some phosphate groups may be attached. The amount of iron in the core is variable and ranges from zero (apoferritin) to a maximum of 4500 atoms. For iron to enter the ferritin molecule it must initially be in the ferrous form, as the protein subunits are arranged to leave a number of channels through which ferrous iron may pass. However once inside the molecule the iron is oxidised to the ferric form and polymerises. Release of iron *in vitro* requires the presence of reducing agents and is increased at low pH (Reviewed by Harrison, 1986; Crichton, 1991).

The protein shell is composed of 24 subunits of which three types have been identified: H (heavy or heart subunit) consisting of 182 amino acids with a molecular weight of approximately 21,000; L (light or liver) consisting of 174 residues with a molecular weight of approximately 19,000 and the G (glycosylated) subunit with a molecular weight of approximately 23,000. In human tissues H-rich isoferritins are more acidic and are found in cells which have high iron requirements such as heart muscle and nucleated red cells, and also in cells which are not involved in iron storage such as lymphocytes and monocytes. The more basic L-rich isoferritins appear to be required for iron storage and are found in liver, spleen and placenta (Wagstaff et al, 1978). The G subunit is found predominantly in serum. Serum ferritin is composed almost exclusively of L and G subunits (Cragg et al, 1981) containing little iron. The biological significance of this ferritin is obscure. However serum ferritin levels can be used as a clinical indicator of iron stores (Worwood, 1986).

In pathological iron overload the bulk of the excess iron is stored as haemosiderin (Selden et al, 1980). Haemosiderin is a heterogeneous compound



consisting of insoluble ferric hydroxide with variable amounts of phosphate and protein. It is localized in membranous structures termed siderosomes, which represent enlarged lysosomes and contain lysosomal enzymes (Richter, 1978). Similarities in the composition of the iron core of ferritin and haemosiderin led to the suggestion that haemosiderin is derived from lysosomal proteolysis of ferritin followed by aggregation of the naked cores (Fisbach et al, 1971). Subsequent electron microscopic studies of liver samples from iron overloaded patients and carbonyl-iron fed rats show that cytosolic ferritin appears to attain a maximum concentration, after which it aggregates and fuses with the lysosomal compartment, so forming a siderosome (Iancu and Neustein, 1977; Iancu, 1989).

Further evidence for the derivation of haemosiderin from ferritin comes from the observation that haemosiderin consistently contains peptides that may be ferritin degradation products (Weir et al, 1984a). However recent studies suggest that in certain pathological conditions haemosiderin may also be formed independently of ferritin (Mann et al, 1988; Dickson et al, 1988).

#### 1.2.5 Cellular Iron Homeostasis

Cellular expression of both the transferrin receptor and ferritin is highly regulated by the amount of available iron. Low cellular iron concentration results in an increase in the number of transferrin receptors expressed, whereas when iron is plentiful the number of transferrin receptors is decreased. Ferritin levels are regulated in the opposite direction increasing in the presence of iron and decreasing in its absence. The 3' untranslated region (UTR) of transferrin receptor mRNA contains potential stem loop sequences (Casey et al, 1988) similar to a cis-acting element of the 5' UTR of rat and human ferritin mRNA (Hentze et al, 1987; Aziz and Munro, 1987). These sequences have been termed iron responsive elements (IRE). These IREs interact with a common IRE-binding protein (IRE-BP) which exists in a high and low affinity state (Haile et al, 1989). As cellular iron levels become limiting a greater proportion of the

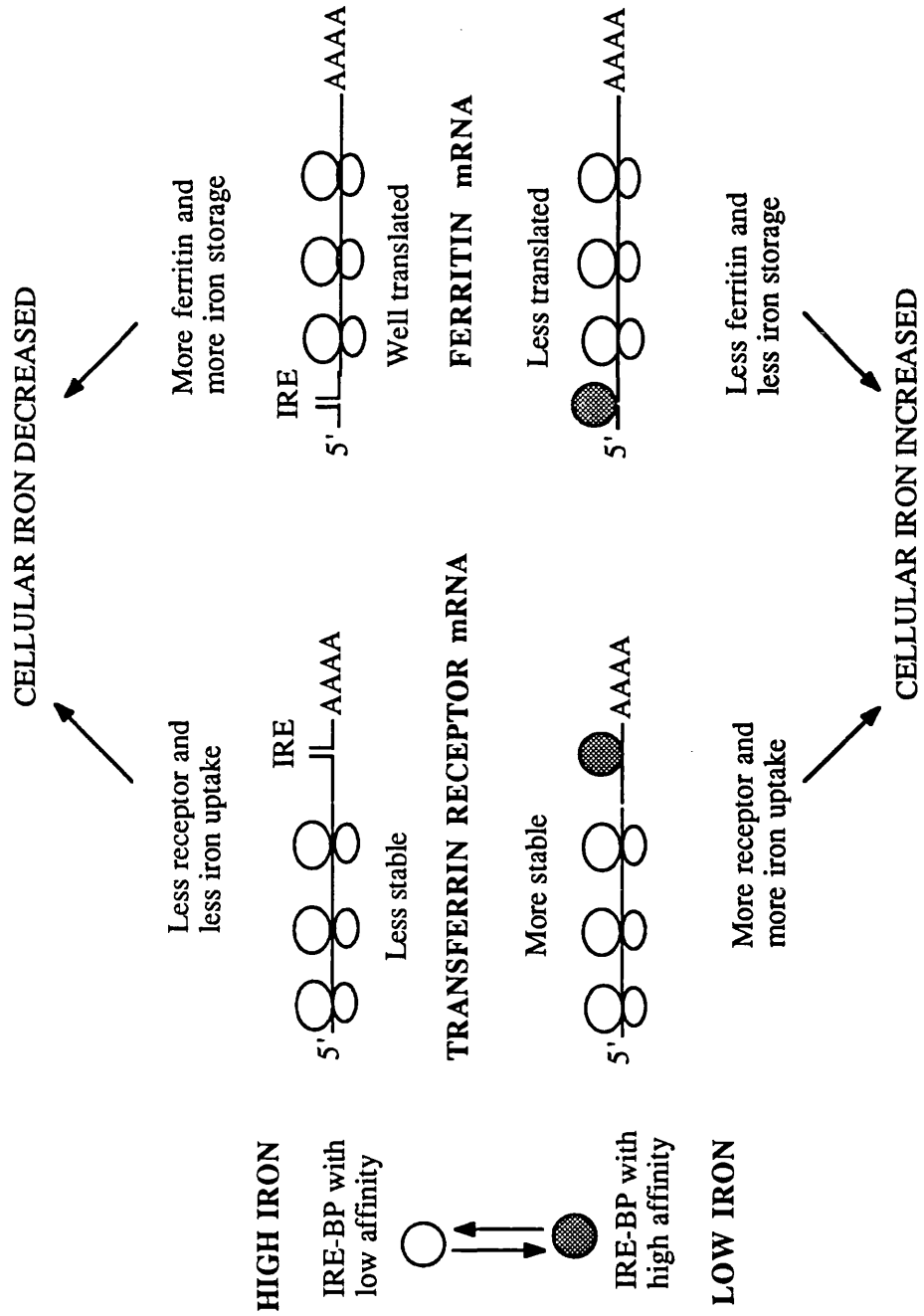
IRE-BP is recruited to the high affinity state. High affinity binding of this protein to a 3' IRE results in lower mRNA degradation and increased translation and protein synthesis. By contrast, binding to a 5' IRE results in repression of translation and inhibition of protein synthesis. Therefore iron deprivation leads to increased translation of transferrin receptor mRNA and reduced translation of ferritin mRNA (Figure 6). The iron status of the cell determines the affinity state of the IRE-BP through an iron mediated redox mechanism termed the sulphhydryl switch (Klausner and Harford, 1989). Recently the cDNA for human IRE-BP has been cloned (Rouault et al, 1990). There is extensive amino acid sequence homology between IRE-BP and mitochondrial aconitase (Rouault et al, 1991; Hentze and Argos, 1991). This suggests that IRE-BP itself may be an iron-sulphur protein which may respond to changes in cellular iron levels by a redox sensitive conversion between the [3Fe-4S] and the [4Fe-4S] forms in a similar manner to aconitase (Section 1.2.3).

Transferrin receptor expression is also linked to cell proliferation. Pelosi-Testa et al (1986) proposed that intracellular iron regulation and cell proliferation regulate expression by different mechanisms. Rao et al (1986) showed that desferrioxamine treatment of K562 cells causes an early increase in transferrin receptor mRNA, whilst haemin had the opposite effect. Transcriptional assays with isolated nuclei indicated that this regulation was at a transcriptional level. Furthermore, deletion of the 3' non-coding region of the cDNA abolishes the iron-dependent but not the proliferation dependent regulation of transferrin receptor expression (Owen and Kuhn, 1987).

### **1.3 IRON OVERLOAD**

Normal body iron stores are regulated between 0 and 2000mg depending on the balance between available dietary iron and the iron requirements of the individual (Bothwell et al, 1979). Iron overload can result when additional iron gains access to the body by increased oral absorption or parenteral iron administration.

**FIGURE 6: COORDINATE REGULATION OF THE EXPRESSION OF THE TRANSFERRIN RECEPTOR AND FERRITIN**



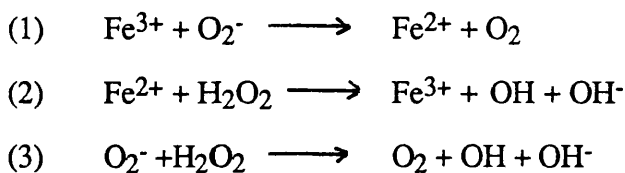
(Adapted from Kuhn, 1991)

Increased iron absorption may occur as a result of inappropriately large amounts of iron absorbed from a diet containing normal amounts of iron, as occurs in idiopathic haemochromatosis and the iron-loading anaemias (Cox, 1990). Alternatively oral iron overload may result from the consumption of large amounts of dietary or medicinal iron as in the South African Bantu population who drink large amounts of acidic beer brewed in iron pots (Bothwell et al, 1964).

Parenteral iron overload is produced by repeated blood transfusions in individuals suffering from dyserythropoietic anaemias such as  $\beta$  thalassaemia major. Haemoglobin has an iron content of 0.33% by weight so each 500ml of transfused whole blood represents 215mg of iron that cannot be excreted. Such patients require up to 50 units of blood annually depending on their age and size, therefore the burden of transfused iron is between 2.5 and 11g per year (Cox, 1990). Consequently patients who receive more than 100 units of blood usually develop iron overload. Furthermore, conditions such as  $\beta$  thalassaemia are characterised by a large degree of ineffective erythropoiesis resulting in enhanced absorption of dietary iron so contributing to the net positive balance of iron (Pippard et al, 1977).

This progressive accumulation of iron leads to cardiac, liver and endocrine damage, often with diabetes and failure to enter puberty. If this iron overload is untreated death often results from cardiac abnormalities before the end of the second decade of life (Moddell, 1979).

Biopsy samples from iron overloaded spleens from thalassaemic patients (Heys and Dormandy, 1981) and from livers of iron overloaded animals (Hanstein et al, 1975) have suggested that one of the primary mechanisms of cell and tissue damage in iron overload is iron induced lipid peroxidation via the following mechanism:-

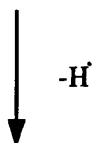
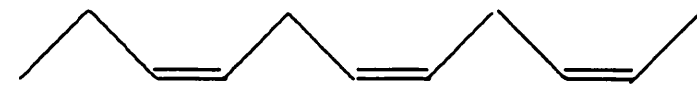


In this reaction  $\text{Fe}^{3+}$  is reduced to  $\text{Fe}^{2+}$  and molecular oxygen by superoxide (1). Catalytic  $\text{Fe}^{2+}$  is then available for the Fenton reaction (2) generating hydroxyl radicals and restoring  $\text{Fe}^{3+}$  for another catalytic cycle. The sum of these reactions (3), generally known as the Haber Weiss reaction, produces molecular oxygen, the hydroxyl radical (OH) and the hydroxyl anion.

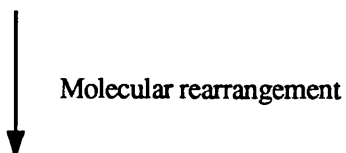
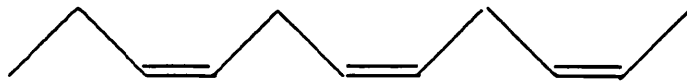
The hydroxyl radical is highly toxic and can initiate lipid peroxidation by abstraction of a hydrogen atom from polyunsaturated fatty acids in membrane lipids (Figure 7). This leaves an unpaired electron on the carbon atom from which it was abstracted and this carbon radical undergoes molecular rearrangement to form a conjugated diene which then reacts with  $\text{O}_2$  to give a peroxy radical. This radical converts itself to a lipid hydroperoxide by abstracting a proton from an adjacent fatty acid so propagating the chain reaction of lipid peroxidation (Gutteridge and Halliwell, 1989). Additionally, two peroxy radicals can react together to cause singlet oxygen formation with subsequent tissue damage. Lipid hydroperoxides can also decompose on exposure to transition metals and some iron proteins such as haemoglobin and cytochromes. The products of these reactions include hydrocarbon gases, radicals which can further stimulate the chain reaction of lipid peroxidation, and various cytotoxic carbonyl compounds. Extensive lipid peroxidation in biological membranes causes loss of fluidity, increased permeability and eventual rupture leading to release of cell and organelle contents. Increased lysosomal fragility has been demonstrated in liver biopsy material from patients with primary and secondary haemochromatosis (Seymour and Peters, 1978) and it is possible that iron from intralysosomal haemosiderin induces free radical formation resulting in lysosomal membrane disruption and release of hydrolytic enzymes into the cell causing cell death (Weir et al, 1984b).

**FIGURE 7: THE CHAIN REACTION OF LIPID PEROXIDATION**

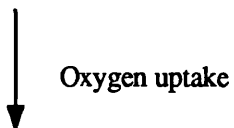
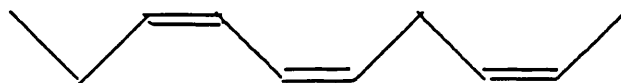
Polyunsaturated fatty acid



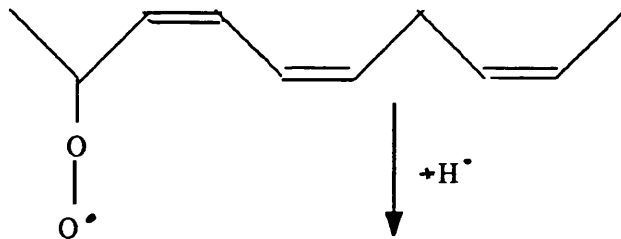
Hydrogen abstraction



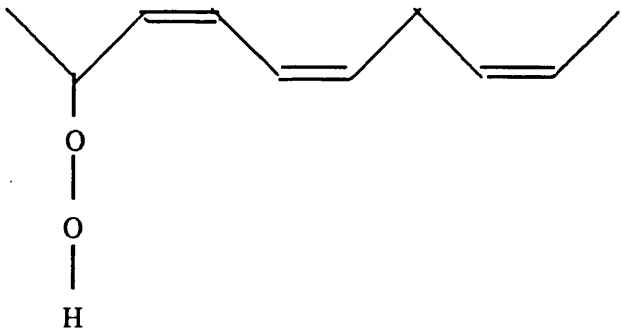
Conjugated diene



Peroxyl radical: propagates peroxidation by abstraction of H from another fatty acid.



Lipid hydroperoxide



(From Gutteridge and Halliwell, 1990)

## 1.4 IRON CHELATION

The only effective treatment for transfusional iron overload is chelation therapy. Currently DFO is the only iron chelator of proven clinical benefit. This drug is not effective when administered orally, and whilst the use of overnight subcutaneous infusions of DFO have markedly improved the life expectancy of transfusion dependent patients, poor patient compliance is a major problem. This combined with the high cost of DFO highlights the need for an inexpensive orally active iron chelator.

### 1.4.1 General Principles of Iron Chelation

An iron chelator is an organic molecule which contains two or more functional groups which are capable of forming co-ordinate bonds with iron to form a heterocyclic iron containing ring (Pippard, 1989). In order to be useful clinically an iron chelator should achieve iron balance in non-overloaded patients and negative iron balance in iron overloaded patients. In patients receiving regular blood transfusions a considerable amount of iron must be chelated, as the input from transfusions can be up to 0.02mg/kg daily (Modell, 1977) combined with an additional 2-8mg absorbed from the gastrointestinal tract dependent on the degree of ineffective erythropoiesis and transfusion regime (Pippard and Weatherall, 1984). It is necessary to have some degree of cellular penetration to obtain effective negative iron balance. However intracellular chelation may result in depletion of iron from essential sources such as iron containing enzymes. Hence a balance needs to be struck between effective iron chelation and toxicity when compounds are being designed for clinical use. The desirable properties of an oral iron chelator for the treatment of iron overload have been described by several authors (Porter et al, 1989; Porter, 1990; Pippard, 1989; Hershko et al, 1990) and are summarised in Table 1.

**TABLE 1: DESIRABLE PROPERTIES FOR AN IRON CHELATOR**

---

**a) Properties to maximize activity**

High rate of intestinal absorption

High affinity for  $\text{Fe}^{3+}$

Penetration of tissues, cells and subcellular sites  
of abnormal iron accumulation

Long half life of free chelate

**b) Properties to minimize toxicity**

High selectivity for  $\text{Fe}^{3+}$

Limited lipophilicity

Rapid excretion of iron-chelator complex

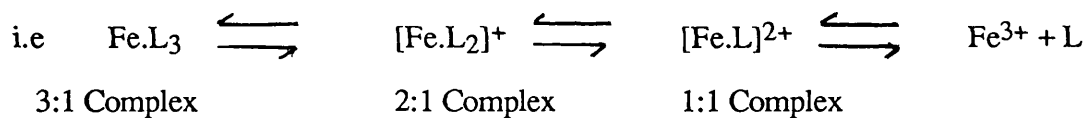
No redistribution or reabsorption of iron

No facilitation of micro-organism growth.

---



Such compounds should ideally display high affinity and selectivity for iron (III) and a low affinity for other transition metals such as copper and zinc. The structure of an iron chelator strongly influences its ability to bind iron. Iron (III) has a high charge density and tends to bind tightly to compounds with a similar charge density, in particular oxygen species such as hydroxamates, hydroxypyridinones and catecholates (Porter et al, 1989). The stability of the chelator-iron complex is also dependent on the number of covalently linked arms on the chelator. Iron (III) is most stable when linked with 6 oxygen atoms, these may be supplied by three bidentate chelators, donating two oxygen atoms each or one hexadentate chelator donating all six. Consequently complexes formed from hexadentate ligands are more thermodynamically stable than their bidentate counterparts (Martell, 1989) and so are less likely to dissociate at low concentrations. Bidentate complexes, however, can partially dissociate at low concentrations to form 2:1 and 1:1 complexes.



These complexes may generate hydroxyl radicals that can participate in free radical reactions. Therefore from a chemical viewpoint hexadentate chelators are more effective than bidentates.

However a key property of an oral iron chelator is the ability to cross biological membranes enabling absorption from the GI tract and penetration into intracellular iron pools. Absorption from the GI tract and passage across cell membranes will be impaired if the molecular weight exceeds 600, therefore low molecular weight bidentate chelators may have more access across the intestinal mucosa and into cells than relatively high molecular weight hexadentate compounds.

The membrane permeability of low molecular weight solutes is determined by their ability to partition from an aqueous phase into the lipid bilayer of the membrane (Oldendorf, 1974). The partition coefficient ( $K_{\text{part}}$ ) of a drug between octanol and

water at pH7.4 has been demonstrated to approximate to this partitioning (Leo et al, 1971).  $K_{part}$  values close to 1 signify approximately equal solubility in each phase. It has been established that the optimal balance between toxicity and efficacy of an iron chelator is attained when the  $K_{part}$  is between 0.2 and 1.0 (Gyparaki et al, 1987; Porter et al, 1988).

#### 1.4.2 Sites of Iron Chelation

Studies using a hypertransfused rat model have demonstrated the existence of two alternative pathways for *in vivo* iron chelation (Hershko and Weatherall, 1988). Iron may be chelated extracellularly in the plasma or from the breakdown of reticuloendothelial cells, or intracellular iron may be chelated by direct penetration of the chelators into cells. In the normal situation plasma iron is bound to transferrin and is unavailable for chelation (Hallberg and Hedenberg, 1965; Hershko et al, 1973). However, as iron overload develops the transferrin iron binding capacity becomes saturated and non-transferrin bound iron (NTBI) appears (Hershko et al, 1978). The NTBI pool is quantitatively small but plays an important role in the generation of free radical mediated lipid peroxidation of cell membranes (Gutteridge et al, 1985; Halliwell and Gutteridge, 1986). As NTBI is not bound to high affinity ligands, chelators in plasma may act on this pool and produce beneficial effects by decreasing lipid peroxidation without actually decreasing the body's iron stores. Another source of extracellular iron is from the reticuloendothelial system. The release of iron from macrophages in the liver, bone marrow and spleen following catabolism of senescent red cells is approximately 30mg/24h in normal subjects (Finch et al, 1970). This forms a considerable pool of chelatable iron and water soluble chelators act mainly at this site. Iron chelators may also compete with transferrin at the site of delivery of iron to cells such as hepatocytes which may accumulate iron by a redox process at the cell surface (Section 1.2.3) (Thorstensen and Romslo, 1988). Iron chelated from these extracellular pools is then excreted in the urine.

In contrast, lipid soluble compounds may enter cells such as hepatocytes and chelate iron *in situ* which is then excreted in the bile. A high proportion of intracellular iron is in haemoglobin, myoglobin or haem-containing proteins and, therefore, is not available for chelation. Ferritin is the major form of intracellular iron storage and in a normal adult represents approximately 1g of body iron and in iron overloaded subjects ferritin levels can reach 40-80g. However, direct chelation from ferritin occurs very slowly (Crichton et al, 1980). Evidence suggests that the major source of rapidly chelatable intracellular iron is the transient low molecular weight iron pool (White et al, 1976b) through which all intracellular iron traffic passes (Section 1.2.4). However other intracellular sites such as intralysosomal chelation may also be quantitatively important (Laub et al, 1985).

#### 1.4.3 Potential Oral Chelators

Over the last decade many potential oral iron chelators have been screened using *in vivo* and *in vitro* models. The most prominent of these compounds are summarised in Table 2. The experiments in this thesis will investigate the actions of 2 major chelator classes - the hydroxamates, in particular DFO, and the hydroxypyridinones.

#### **Desferrioxamine (DFO)**

This compound was first introduced for the treatment of transfusional iron-overload by Sephton-Smith in 1962 (Sephton-Smith, 1962). Early experiences with this DFO proved disappointing because urinary iron excretion was minimal until a substantial degree of iron overload occurred (Modell and Beck, 1974). However a study by Barry and co-workers (Barry et al, 1974) in thalassaemic children showed that regular intramuscular DFO stabilized liver iron concentrations and prevented the progression of liver fibrosis. Subsequent studies demonstrated that prolonged subcutaneous infusion of DFO mobilised considerably more iron than intramuscular injections (Modell and Beck, 1974; Propper et al, 1976). The advent of the small battery operated syringe

TABLE 2: POTENTIAL ORAL IRON CHELATORS

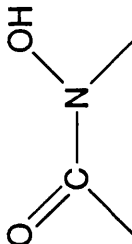
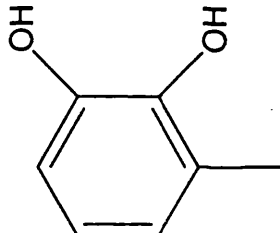
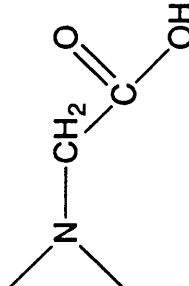
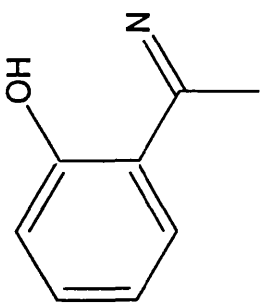
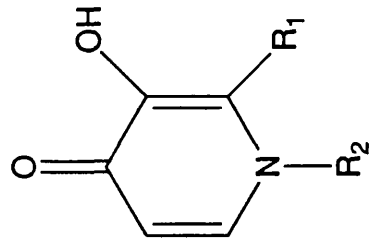
FUNCTIONAL GROUP	EXAMPLE	NET CHARGE		ORAL ACTIVITY
		Free	Complex	
Hydroxamate	Desferrioxamine (DFO)	+1	+1	Orally inactive (Keberle, 1964)
				
Catecholate	2,3-Dihydroxybenzoic Acid (DHB)	-1	-6	Inactive in clinical trials (Peterson et al, 1979)
				
Aminocarboxylate	Diethylenetriamine penta acetic acid (DTPA)	-5,+2	-2	Orally inactive. Poor selectivity for iron (Pippard, 1986)
				

TABLE 2 (CONT'D)

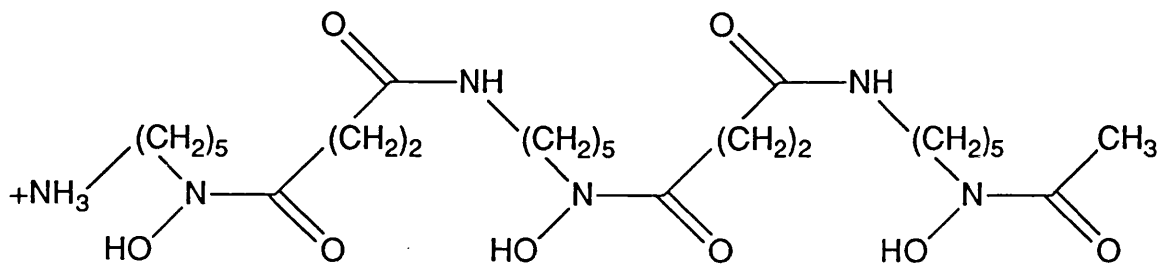
FUNCTIONAL GROUP	EXAMPLE	NET CHARGE		ORAL ACTIVITY	
		Free	Complex		
Orthosubstituted Phenolate		Pyridoxal Isonicotyl Hydrazone (PIH)	0	-1	Orally active in animals and man (Brittenham, 1990)
3-hydroxypyridin-4-ones		CP94 CP20(L1)	0	0	Orally active in animals and man (Porter et al, 1990, Kontoghiorghes et al, 1987)
Mixed Phenolate and aminocarboxylate	<p>(Adapted from Porter et al, 1989 and Pippard, 1990)</p>	N,N'-bis(2-hydroxy-1-benzoyl)-ethylenediamine N,N'-diacetic acid (HBED)	-2,+2	-1	Orally active in animals (Hershko and Grady, 1990)

pump has subsequently allowed overnight subcutaneous infusions of this drug to become a standard therapy for transfusional iron overload. The major disadvantage of DFO is that it possesses a net charge of +1 at neutral pH which limits intestinal absorption and is also susceptible to acid cleavage in the gastrointestinal tract and so orally inactive (Keberle, 1964). Furthermore the plasma half life of DFO is only 5-10 minutes (Summers et al, 1979) because it is rapidly metabolized and also excreted in the free form by the kidneys. In order to achieve negative iron balance DFO has to be administered by slow subcutaneous infusion over 8-12 hours, five days a week. As a result non-compliance has become a major problem with many patients.

DFO is a hydroxamate siderophore produced by *Streptomyces pilosus* (Keberle, 1964) (Figure 8) with high affinity and selectivity for iron (III) (binding constant =  $10^{31}$ ). DFO forms a neutral complex with iron to form ferrioxamine (FO). FO has low lipid solubility and so will not easily penetrate cells, resulting in minimal redistribution of chelated iron to other sites in the body. Whilst DFO has proved relatively non-toxic, prolonged use has revealed a number of adverse effects. The major concern surrounds ocular and auditory toxicities. These include retinal and visual field disturbances and high frequency hearing loss (Reviewed by Porter and Huehns, 1989). A further side effect of DFO treatment is the facilitation of the growth of the pathogen *Yersinia enterocolitica* thus increasing the possibility of enterocolitis in DFO treated patients (Robins-Browne, 1983).

Whilst DFO has several disadvantages, it remains the only clinically proven iron chelator and the standard against which any novel iron chelator should be compared. In view of this, DFO was selected for the studies that form the body of this thesis.

**FIGURE 8: THE STRUCTURE OF DESFERRIOXAMINE B**



## The Hydroxypyridinones

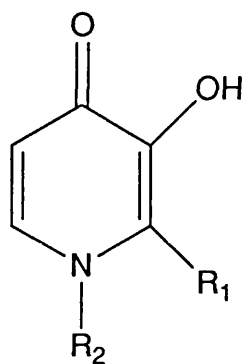
The hydroxypyridinones were designed by Hider and colleagues (Hider, Kontoghiorghes and Silver, 1982; Hider, Kontoghiorghes, Silver and Stockham, 1984a; and 1984b). These compounds are orally active due to their neutral charge in both the iron bound and iron free form and high chemical stability which protects against attack by digestive enzymes in the GI tract.

The hydroxypyridinones are hybrid compounds resembling both natural catechol and hydroxamate chelators. Both bidentate and hexadentate compounds have been investigated. There are three classes of bidentate hydroxypyridinones (Figure 9):- the 3-hydroxypyridin-2-ones (Hider, Kontoghiorghes and Silver, 1982), the 1-hydroxypyridin-2-ones (Hider, Kontoghiorghes, Silver and Stockham, 1984a) and the 3-hydroxypyridin-4-ones (Hider, Kontoghiorghes, Silver and Stockham, 1984b). Of these the 3-hydroxypyridin-4-ones (3-HP-4-ones) have the highest affinity for iron (III), with a binding constant ( $\text{Log } \beta_3$ ) of  $10^{36}$  (Taylor, Morrison and Hider, 1988) and so would be predicted to be the most active. This has been confirmed by studies on isolated ferritin (Brady et al, 1988) and in hepatocyte culture systems (Porter et al, 1988). The 1-hydroxypyridin-2-ones have the lowest affinity for iron (III),  $\text{log } \beta_3 = 10^{27}$  and have the additional disadvantage of bearing a net charge of -1 at pH 7.4 resulting in minimal oral activity. The presence of this charge also reduces the selectivity of these compounds. The 3-hydroxypyridin-2-ones (3-HP-2-ones) have a stability constant of  $10^{32}$  and in iron mobilisation studies these compounds were marked less active than the 3-hydroxypyridin-4-ones (Porter et al, 1988). Hence the bidentate 1-hydroxypyridin-2-ones and 3-hydroxypyridin-2-ones are unlikely to be clinically useful in the treatment of iron overload.

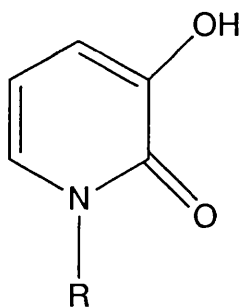
The 3-hydroxypyridin-4-one compounds form neutral complexes with iron (III) over the pH range 5.0-9.0. Modification of the  $R_1$  and  $R_2$  side chains allows the formation of a number of compounds with a wide range of partition coefficients. Studies with primary hepatocyte monolayer cultures have shown a strong correlation between iron mobilisation and the  $K_{\text{part}}$  value of the free ligand ( $r=0.94$ ) (Porter et al,



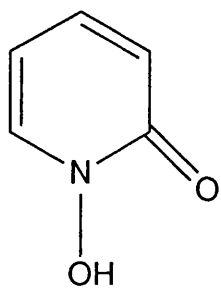
# FIGURE 9: BIDENTATE HYDROXYPYRIDINONE STRUCTURES



3-HYDROXYPYRIDIN-4-ONE



3-HYDROXYPYRIDIN-2-ONE



1-HYDROXYPYRIDIN-2-ONE

1988). Compounds with intermediate lipid solubility ( $K_{part}$  between 0.2 and 1.0) appear to have the optimal properties for iron mobilisation over a wide range of concentrations. Lipophilic chelators with  $K_{part}$  of greater than 1.0 were found to induce cell toxicity, whilst very hydrophilic compounds were ineffective at iron mobilisation.

The oral activity of 3-hydroxypyridin-4-ones has been demonstrated in an iron-overloaded  $^{59}\text{Fe}$  mouse model (Gyparaki et al, 1987; Porter et al, 1990), in rats pulsed with  $^{59}\text{Fe}$  ferritin (Kontoghiorghes et al, 1987a) and in overloaded rabbits (Kontoghiorghes and Hoffbrand, 1986). As in the *in vitro* isolated hepatocyte model, compounds with partition coefficients close to 1.0 displayed optimal oral activity whilst compounds with partition coefficients greater than 1.0 were toxic at relatively low doses (Porter et al, 1990).

1,2-dimethyl 3-hydroxypyridin-4-one, CP20 (L1), has been selected for clinical studies in man (Kontoghiorghes et al, 1987b; 1987c ). This compound has been shown to promote urinary iron excretion but no significant increase in faecal iron excretion has been observed (Kontoghiorghes et al, 1990; Olivieri et al, 1990). Furthermore, no reduction in serum ferritin has been reported, despite administration of this compound for up to 15 months. Transient agranulocytosis has been reported in one patient receiving long term L1 treatment (Hoffbrand et al, 1989) and other possible toxicities include transient arthralgia (Bartlett et al, 1990) and drug induced systemic lupus erythematosus (Mehta et al, 1991). Due to its low partition coefficient (Table 4), CP20 (L1) may not be as active as other 3-hydroxypyridin-4-one chelators since more lipophilic compounds may be better absorbed and have more access into cells such as hepatocytes, resulting in the increased faecal iron excretion necessary for significant negative iron balance.

Several 3-hydroxypyridin-4-ones have been shown to be more active than CP20 (L1) in primary hepatocyte cultures (Porter et al, 1988) and in short and long term animal studies (Porter et al, 1990; 1991; Hershko et al, 1990; 1991a). In particular the di-ethyl derivative CP94 has been identified as possessing the best therapeutic

safety margin (Porter et al, 1990). For this reason CP94 was selected as the lead compound for comparison to DFO in this thesis.

#### 1.4.4 Use of Iron Chelators In Conditions Unrelated To Iron Overload

Iron mediated free radical production has been implicated as a causative factor in the tissue damage associated with many disease states. DFO has been shown to interfere with free radical production both by iron chelation and by direct scavenging of the superoxide and hydroxyl radical (Hoe et al, 1982). Therefore iron chelators may have a role in the treatment of free radical mediated tissue injury.

Rheumatoid arthritis (RA) is often associated with abnormalities in body iron metabolism (Blake et al, 1981). The onset of inflammation is accompanied by a rapid fall in serum iron levels followed by a drop in haemoglobin concentration and deposition of ferritin in the synovial membrane (Muirden, 1966). Both low molecular weight iron complexes and ferritin are also found in synovial fluid (Blake and Bacon, 1981) and these may catalyse free radical production and lipid peroxidation. Iron may also act as a focus for the migration of lymphocytes and macrophages typically found in the synovium of affected joints (Blake et al, 1981).

Thus a viable rationale exists for the use of iron chelators to inhibit the inflammatory response in RA and prevent further tissue damage. In experimental models of RA daily administration of DFO markedly reduced chronic inflammation in guinea pigs (Blake et al, 1983) and reduced the joint inflammation associated with adjuvant disease in rats (Andrews et al, 1987). However the results of clinical studies with DFO in RA patients have been disappointing. No significant anti-inflammatory effect has been demonstrated for DFO and the advent of adverse effects in several patients has led to reduction of DFO dose to levels that are unlikely to have significant effects or the abandonment of chelation therapy (Blake et al, 1985; Polson et al, 1986).

Damage to aerobic tissues can be caused by the interruption of blood flow, resulting in lack of oxygenation followed by reoxygenation of the tissue

(ischaemia/reperfusion). It has been postulated that oxygen radicals generated during the reperfusion period have a major role in such tissue injury (McCord, 1985). Several studies have shown that DFO treatment may result in significant attenuation of reperfusion injury. In isolated perfused hearts administration of DFO at the time of postischaemic reflow resulted in greater recovery of myocardial function and energy metabolism (Ambrosio et al, 1987). Similarly studies in a cardiac arrest model in experimental dogs suggest that DFO plus a calcium antagonist can protect against reperfusion injury (Aust and White, 1985).

Free radical production on reperfusion may also impair successful organ transplantation. Rabbit kidneys subjected to warm ischaemia by clamping the renal artery followed by reperfusion show increased lipid peroxidation and subsequent functional derangement (Green et al, 1986a). However administration of intravenous DFO to the animal just before reperfusion effectively inhibited lipid peroxidation (Green et al, 1986b). Similarly single passage arterial flushing with saline containing 60mM DFO markedly reduced lipid peroxidation in kidneys stored at 0°C for 24 hours (Green et al, 1986c).

Tissue damage associated with the activation of complement and phagocytes is also closely related to hydroxyl radical production and may be inhibited by DFO. Infusion of cobra venom into rats causes systemic complement activation leading to aggregation and activation of neutrophils in pulmonary capillaries, ultimately resulting in injury to the endothelial cells of the lung microvasculature (Ward et al, 1983). Such lung injury can be prevented by pretreatment with DFO but not FO. Conversely infusion of iron greatly potentiates the lung damage. This model may approximate to the human adult respiratory distress syndrome (Ward et al, 1989) in which toxic oxygen metabolites from activated neutrophils may be responsible for the alveolar injury associated with this condition (Baldwin et al, 1986).

An entirely different therapeutic application for iron chelators is the reversible arrest of cell proliferation by inhibition of ribonucleotide reductase (Section 1.2.4), the rate limiting enzyme in DNA synthesis. In vitro studies with a variety of iron chelators

have shown reversible inhibition of proliferation in a range of cell types (Reviewed by Cazzola et al, 1990; see also Chapter 5). *In vitro* DFO inhibits the proliferation of mitogen and lectin stimulated T-cells and the induction of cytotoxic T cell activity (Lederman et al 1984, Bierer and Nathan 1990). These studies suggest that iron chelators may have a role as immunomodulating agents. In an *in vivo* model of murine pancreatic allografts DFO administration appeared to reduce chronic islet cell rejection (Bradley et al, 1986) and to reduce the severity and duration of experimental allergic encephalitis in rats (Bowerm et al, 1984). However it is unclear whether the beneficial effects of DFO in these *in vivo* studies were due to an immunosuppressive effect, or to the inhibition of free radical production from the respiratory burst of infiltrating phagocytes.

DFO has also been used to treat graft versus host disease (GVHD) in human bone marrow transplant allograft recipients (Weinberg et al, 1988). DFO at a dose of 50mg/kg/d resulted in prompt resolution of GVHD in association with inhibition of interleukin-2 receptor expression in lymphocytes. However when DFO was used for the prevention of GVHD after allogeneic transplantation in patients with thalassaemia major, it was found to delay significantly engraftment so its use was discontinued after a few cases (Luccarelli et al, 1989).

The inhibition of ribonucleotide reductase is probably responsible for the *in vivo* and *in vitro* antimalarial activity of iron chelators. *In vitro* micromolar concentrations of DFO and 3-HP-4-ones inhibit the growth of *Plasmodium falciparum* (Hershko et al, 1991b). DFO and the 3-HP-4-ones also inhibit *Plasmodium berghei* in rats (Hershko et al, 1991b) and DFO has been found to inhibit *P. vinckei* and *P. falciparum* in mice and monkeys respectively (Fritch et al, 1985; Pollack et al, 1987). Furthermore the phenolic aminocarboxylate chelator N,N'-bis(2-hydroxybenzoyl)-ethylenediamine-N,N'-diacetic acid (HBED) has also been demonstrated to have potent antimalarial activity (Yinnon et al, 1989).

The examples discussed above are by no means exhaustive and iron chelators potentially have many therapeutic applications as summarised in Table 3. However it

should be emphasised that all these observations are preliminary and much research is required before iron chelators can play a significant role in the clinical management of such conditions.

**TABLE 3: POSSIBLE APPLICATIONS FOR IRON CHELATORS  
IN CONDITIONS UNRELATED TO IRON OVERLOAD**

---

**Inhibition of Free Radical Production**

Post ischaemic reperfusion injury	Ambrosio et al, 1987
	Aust and White, 1985
Organ transplantation	Green et al, 1986b,c
Allograft rejection	Bradley et al, 1986
Drug Toxicity eg Bleomycin	Chandler and Fulwer, 1985
Paraquat	Osheroff et al, 1985

**Reduction of Inflammatory Reponse**

Rheumatoid arthritis	Blake et al, 1981
	Poulsen et al, 1986
Allergic encephalitis	Bowern et al, 1984
Neutrophil and complement-mediated tissue damage	Ward et al, 1989

**Effects on Haem Synthesis**

Pophyria cutanea tarda	Rocchi et al, 1986
Anaemia of renal failure	De La Serna et al, 1988

**Immunomodulating Actions**

Graft versus host disease	Weinberg et al, 1986
Allograft rejection	Bradley et al, 1986
Suppression of delayed type hypersensitivity	Saharrabudhe, 1991

**Inhibition of Infection**

Anti-malarial effects	Hershko et al, 1991
Inhibition of <i>Pneumocystis carinii</i>	Clarkson et al, 1990

**Antileukaemic effects**

Estrov et al, 1987
Dezza et al, 1987

---

## **CHAPTER 2: MATERIALS AND METHODS**



## **2.1 INTRODUCTION**

The methods used in the studies described in this thesis consist of a number of basic techniques brought together to serve the special investigations required for this research. The individual techniques used in later chapters are described here. The manufacturers from whom the various plastic and glassware as well as chemicals were obtained are given in Appendix 1. Recipes for the preparation of the buffers used in these methods are given in Appendix 2.

## **2.2 IRON CHELATORS**

Desferrioxamine mesylate (DFO) was obtained from Ciba Geigy Ltd (Basel, Switzerland). The hydroxypridinone (HPO) iron chelators were synthesized by the Department of Pharmaceutical Sciences, Kings College London, according to published procedures (Hider et al 1982) and supplied as the hydrochloride in the form of a white powder. The purity and stability of the HPO compounds was also assessed by Kings College. The purity of each HPO compound was tested by elemental analysis. The stability of the HPOs was monitored by high performance liquid chromatography (HPLC) using a PLRP-S column (150 x 4.6mm) with an isocratic mobile phase of 2mM pH7.0 EDTA, 20mM phosphate containing 15% methanol. Detection was at 280nm. All HPO compounds showed no detectable change when stored at 4°C for up to one month.

Table 4 lists the HPOs used in these studies with their partition coefficients and stability constants. Unless otherwise stated the chelators were dissolved in phosphate buffered saline (PBS) prepared with iron free water. The HPO compounds were prepared once a week and stored at 4°C. DFO is less stable and therefore was freshly prepared for each experiment

[<sup>14</sup>C]DFO and [<sup>14</sup>C]CP94 were the kind gift of Dr H.H. Peter of Ciba Geigy (Basel, Switzerland).

TABLE 4: CHELATOR STRUCTURE, PARTITION COEFFICIENT AND STABILITY CONSTANTS

CHELATOR	R <sub>1</sub>	R <sub>2</sub>	Partition Coefficient			Log β <sub>3</sub>
			Free Ligand	Iron Complex		
<b>3-Hydroxypyridin-4-ones</b>						
CP20	CH <sub>3</sub>	CH <sub>3</sub>	0.21	0.0009		36
CP21	CH <sub>3</sub>	CH <sub>2</sub> CH <sub>3</sub>	0.4	0.03		36
CP22	CH <sub>3</sub>	(CH <sub>2</sub> ) <sub>2</sub> CH <sub>3</sub>	1.35	0.65		36
CP24	CH <sub>3</sub>	(CH <sub>2</sub> ) <sub>3</sub> CH <sub>3</sub>	1.98	7.7		36
CP40	CH <sub>3</sub>	(CH <sub>2</sub> )OH	<0.002	<0.002		36
CP52	CH <sub>3</sub>	(CH <sub>2</sub> ) <sub>3</sub> OCH <sub>2</sub> CH <sub>2</sub>	0.3	0.005		36
CP94	CH <sub>3</sub>	CH <sub>2</sub> CH <sub>3</sub>	0.85	0.07		36
<b>3-hydroxypyridin-2-ones</b>						
CP02		CH <sub>2</sub> CH <sub>3</sub>	0.5	1.06		32
<b>Hexadentates</b>						
CP130			<0.001	<0.001		29 (K <sub>1</sub> )
DFO			0.01	0.03		33 (K <sub>1</sub> )

Hexadentate chelators such as DFO coordinate iron in a 1:1 ratio whereas the bidentate 3-HP-4-ones and 3-HP-2-ones coordinate in a 3:1 ratio. Hence three moles of HPO bind the equivalent amount of iron to one mole of DFO. Therefore in this thesis, all chelator concentrations are expressed in iron binding equivalents (IBE) rather than absolute concentration, unless otherwise stated.

The iron complexed forms of the chelators were prepared by the following procedure:-

- 1) 39.215mg ferrous ammonium sulphate was dissolved in 1ml 0.05M H<sub>2</sub>SO<sub>4</sub> to give a final concentration of 100µmoles/ml.
- 2) 110µl (11µmoles) of the iron solution was added dropwise to 10ml 1µmole/ml IBE chelator solution in PBS, and the pH was immediately raised to pH 7.4.
- 3) This results in a final iron : chelator molar ratio of 1.1:1 for the preparation of ferrioxamine (FO), the iron complexed form of DFO and 1.1:3 for the preparation of the bidentate 3-HP-4-one iron complexes, i.e iron : IBE = 1.1:1.

## **2.3 CELLS AND CELL CULTURE**

### **2.3.1 Cell Culture Media**

RPMI 1640 (Roswell Park Memorial Institute) media with L-glutamine and with or without 20mM HEPES was used for washing culturing and freezing cells.

FCS (foetal calf serum): screened batches that supported growth in culture were used as a growth supplement. FCS was heat inactivated at 56°C for 1 hour, aliquoted and stored at -20°C until required.

Penicillin and streptomycin at 100x concentration were added to tissue culture medium at 50 units/ml penicillin and 50µg/ml streptomycin where stated.

Iscoves modified Dulbeccos medium at single and double strength was used for bone marrow culture.

Double strength Iscoves modified Dulbeccos medium was prepared from powdered Iscoves modified Dulbeccos medium using the following procedure:

- 1) Two one litre packets of powdered Iscoves modified Dulbeccos medium were added to 800ml double distilled water and stirred gently at room temperature.
- 2) 2.6048g of NaHCO<sub>3</sub> was added per litre of final volume of medium
- 3) The volume was made up to one litre and filtered through 0.2µm millipore filters, aliquoted and stored at -20°C.

Agar was made up in double distilled deionised water at 0.9% and autoclaved. After cooling the agar was stored at 4°C and resolubilised for use by heating in a beaker of boiling water.

Methylcellulose was prepared in single strength IMDM at 2.7%, with antibiotics at tissue culture concentrations, and stored at -20°C until used.

### 2.3.2 Culture of Cell Lines

The human K562 erythroleukaemia cell line and the Daudi Burkitts Lymphoma cell line were grown in suspension culture in tissue culture flasks, in RPMI 1640 medium containing L-glutamine, supplemented with 5% (v/v) FCS at 37°C in a humidified atmosphere of 5% CO<sub>2</sub> in air. The cells were cultured at densities between 2-7x10<sup>5</sup> cells/ml to ensure exponential growth was maintained.

### 2.3.3 Isolation and Culture Of Human Peripheral Blood Lymphocytes

Peripheral blood from healthy volunteers was taken into preservative free heparin (2 IU/ml). Samples were diluted to approximately twice the original volume with RPMI 1640 medium and layered onto an equal volume of Ficoll-Hypaque. The mixture was centrifuged at 1000g for 20 minutes and low density mononuclear cells

were collected from the interface using a sterile pipette. The cells were washed twice with RPMI 1640 (400g, 5 minutes) and resuspended in RPMI with 10% FCS and antibiotics.

Mitogen stimulated lymphocytes were obtained by incubation of peripheral blood mononuclear cells for 72 h in RPMI 1640 medium containing 10% FCS and 2µg/ml purified PHA.

#### 2.3.4 Isolation and Culture of Haemopoietic Progenitor Cells From Murine Bone Marrow

Male Balb c mice were sacrificed by cervical dislocation. The femur was isolated and the progenitor cells were flushed from the bone cavity with 2mls of Iscoves modified Dulbeccos medium supplemented with 5% FCS and antibiotics, using a 25G sterile hypodermic needle. The isolated cells were washed twice with 2ml of the same medium and then resuspended to a volume of 1ml prior to culturing.

#### **Culture of CFU-G + CFU-Mac Colonies**

CFU-G + CFU-Mac (Colony forming unit - granulocyte, Colony forming unit-macrophage) were assayed using a modification of the method of Pelus et al (1982).

Murine bone marrow cells were plated at  $0.5 \times 10^5$ /ml in a culture medium consisting of 2.5 parts FCS, 3 parts Iscoves modified Dulbeccos medium (double strength) and 3 parts 0.9% agar. This was supplemented with 2000 units/ml recombinant human macrophage colony stimulating factor and 2ng/ml recombinant human granulocyte colony stimulating factor. One millilitre of the culture mixture was placed in 35mm plastic Petri dishes and incubated in a humidified incubator at 37°C and 5% CO<sub>2</sub>. After 6 days colony formation was assessed by counting using a stereo microscope. A colony was defined as a group of 40 or more cells .

## **Culture of BFU-E Colonies**

BFU-E (Burst forming unit-erythroid) colony growth was assessed by standard procedures (Lu et al,1984) with modifications.

Murine bone marrow cells were plated at  $0.5 \times 10^5$  cells/ml in Iscoves modified Dulbeccos medium containing 0.9% methylcellulose, 30% FCS,  $50 \mu\text{M}$   $\beta$ mercaptoethanol, 1U of human recombinant erythropoietin and 10% Wehi 3b conditioned medium as a source of burst promoting activity. Cultures were grown in 35mm dishes in conditions of high humidity at  $37^\circ\text{C}$  and 4%  $\text{CO}_2$ . BFU-E were scored after 14 days incubation using a stereo microscope.

### 2.3.5 Cell Counting and Viability

Cell number was determined manually, unless otherwise stated, by microscopic counting using an Improved Neubeaur counting chamber.

Cell viability was measured using an ethidium bromide/acridine orange viability stain. This was prepared by adding 4 ml of ethidium bromide (4mg/ml) to 10ml of acridine orange (0.1% solution) and this solution was made up to one litre with PBS. This was stored in the dark at  $4^\circ\text{C}$  until required.

Viability was assessed by mixing  $100 \mu\text{l}$  of cell suspension with  $100 \mu\text{l}$  of ethidium bromide/acridine orange viability stain. The percentage of viable cells was counted using a fluorescent microscope. A minimum of 500 cells were counted for each sample. Ethidium bromide selectively enters dead cells which then fluoresce an orange-red colour, whilst acridine orange is taken up by viable cells which appear a light green colour under UV light.

### 2.3.6 Freezing and Thawing Cells

For freezing cells were suspended at  $5-10 \times 10^6$  cells/ml in 10% dimethylsulphoxide and 20% FCS in RPMI 1640 medium. Aliquots of 1ml were frozen overnight in cryotubes at  $-70^\circ\text{C}$  and then transferred to liquid nitrogen for storage. Frozen cells were thawed rapidly in a  $37^\circ\text{C}$  waterbath and diluted by

dropwise addition of ice-cold RPMI to 20ml. Cells were washed once, resuspended in tissue culture medium and counted before use.

### 2.3.7 Cytospin Preparation

Cytospins are made by centrifugating cell suspensions so that cells are thrown onto slides under centrifugal force (Chanarin 1989). By adjusting the number of cells in the preparation suitable numbers can be adhered to slides without overcrowding.

Single cell suspensions were prepared at  $0.5 \times 10^6$  cells/ml and 100 $\mu$ l of cell suspension was added to each prepared funnel with labelled slide and filter attached. The cytocentrifuge (Cytospin 2, Shannon) was spun at 700rpm for 10 minutes. Slides were removed, air dried and fixed with methanol before staining with an appropriate stain.

## 2.4 GENERAL METHODS

### 2.4.1 Transferrin Labelling

Human apotransferrin (approximately 98% pure) was saturated to 90% with radiolabelled iron using a modification of the method of Huebers et al (1981), as described by Porter et al (1988). The method is summarised in Figure 10.

#### **Procedure**

- 1)  $^{59}\text{Fe}$  and  $^{56}\text{Fe}$  in the form of ferrous ammonium sulphate were randomized in a minimal volume of 0.05M  $\text{H}_2\text{SO}_4$ .
- 2) The iron was added dropwise to human transferrin dissolved in 1ml of 1M Tris HCl pH 8.5 containing 5mM bicarbonate and incubated at 37°C for one hour.
- 3) The labelled transferrin was dialysed against 0.05M Tris HCl pH8.0 overnight and then passed down a 20 x 70mm diethylaminoethyl sepharose CL-6B column and eluted with a linear 0.05M Tris HCl/0.05M Tris HCl + 0.5M NaCl ionic gradient.
- 4) The protein containing fractions were counted and pooled then dialysed against PBS prior to storage at 4°C.

**FIGURE 10: LABELLING TRANSFERRIN WITH  $^{59}\text{Fe}$**

**DISSOLVE TRANSFERRIN IN 1M TRIS-HCl  
BUFFER pH 8.5**



**RANDOMISE  $^{59}\text{Fe}$  AND  $^{54}\text{Fe}$  (AS FERROUS  
AMMONIUM SULPHATE IN 0.04M  $\text{H}_2\text{SO}_4$ )  
AND ADD TO TRANSFERRIN DROPWISE,  
WITH 5mM BICARBONATE.**



**DIALYSE OVERNIGHT AT 4°C AGAINST  
0.05M TRIS HCl pH8.0**



**PASS TRANSFERRIN THROUGH A DEAE  
SEPHAROSE CL6B COLUMN WASH THROUGH  
WITH 0.05M TRIS HCl pH8.0 FOR 2 HOURS**



**ELUTE TRANSFERRIN FROM COLUMN WITH  
0.05M TRIS HCl 0.05M TRIS HCl + 0.5M NaCl  
IONIC GRADIENT**



**COLLECT PROTEIN CONTAINING FRACTIONS,  
POOL AND DIALYSE AT 4°C OVERNIGHT  
AGAINST PBS.STORE AT 4°C**



### 2.4.2 Cell Cycle Analysis

Cells were stained with propidium iodide for cell cycle analysis by a modification of the method of Krishan (1975). Cell samples were washed with PBS and fixed in 1ml ice cold 70% ethanol for 1 hour. The cells were washed again and extraneous RNA was digested with 0.5mg/ml RNAase in PBS by incubation at 37°C for 30 minutes. After further washing with PBS the cells were stained with 50ug/ml propidium iodide for measurement of cellular DNA by flow cytometry.

### 2.3.3 Assays Conducted on Fractionated Cells

#### **Cytochrome *c* Oxidase**

Cytochrome *c* oxidase was measured by a modification of the method of Cooperstein and Lazarow (1951). A stock substrate solution of cytochrome *c* (1mg/ml in distilled water, horse heart Type V1) containing 50mM KH<sub>2</sub>PO<sub>4</sub>, 1mM Na<sub>2</sub>EDTA and 0.1% (v/v) Tween 80 at pH7.0 was reduced to 90% with sodium dithionite and stored at -20°C until used.

For the assay 1ml of substrate solution was placed in a warmed cuvette in a thermostatically controlled spectrophotometer chamber (SP-8-200, Pye Unicam UV/VIS) at 37°C. 100µl of sample suspension was added and mixed and the linear rate of decrease in absorbance was measured on a chart recorder against a buffer blank.

#### **5' Nucleotidase**

5' Nucleotidase was measured by the hydrolysis of <sup>3</sup>H-adenosine monophosphate ([2-<sup>3</sup>H]AMP) by an adaptation of the method of Avruch and Wallach (1971).

50µl of sample suspension was diluted with 50µl distilled water and added to tubes containing 100µl of each 500mM Tris-HCl (pH 8.0), 1.8mM MgCl<sub>2</sub> and 10mM [2-<sup>3</sup>H] AMP (0.5µCi/ml). The mixture was incubated for 60 minutes at 37°C. The

reaction was stopped by the addition of 300 $\mu$ l of each of 0.3M ZnSO<sub>4</sub> and 0.3M Ba(OH)<sub>2</sub>. The samples were left on ice for 30 minutes to precipitate protein and unhydrolysed AMP leaving adenosine in the supernatant. Samples were then centrifuged at 700xg for 20 minutes and 500 $\mu$ l of supernatant was added to vials containing 4ml Hisafe scintillant and counted for  $\beta$  emissions.

### **NADPH Cytochrome *c* Reductase**

NADPH cytochrome *c* reductase activity was measured by following the reduction of cytochrome *c* at 550nm by an adaptation of the method of Williams and Kamin (1962) as described by Graham and Ford (1983).

0.9ml of 50mM sodium phosphate buffer (pH 7.7) was placed in a warmed cuvette in a thermostatically controlled spectrophotometer chamber at 37°C with 50 $\mu$ l of 25mg/ml cytochrome *c* (horse heart type VI), 10 $\mu$ l 10mM EDTA (both dissolved in sodium phosphate buffer) and 20 $\mu$ l of sample suspension. The absorbance was recorded until steady then 0.1ml of 2mg/ml NADPH was added and mixed and the linear rate of increase in absorbance was measured on a chart recorder against a buffer blank.

### **$\beta$ -Galactosidase**

$\beta$  Galactosidase activity was assayed by the method of Graham et al (1990). The substrate solution contained 6mM *p*-nitrophenyl  $\beta$ -D-galactopyranoside in 0.05M citrate-phosphate buffer pH 4.3 containing 0.5% (v/v) Triton X-100. 200 $\mu$ l of the substrate solution was incubated with 50 $\mu$ l of sample suspension for 30 minutes at 37°C. The reaction was stopped by the addition of 0.25M glycine-NaOH pH10. Sedimentable material was removed by centrifugation at 1000 x g for 5 minutes and the absorbance of the supernatant was measured at 400nm.

## Measurement of Ferritin by Enzyme Linked Immunoassay.

Samples were assayed for intracellular ferritin using an enzyme linked immunoassay (ELISA) system incorporating the use of the labelled avidin biotin technique (Guesdon et al, 1979). The procedure is summarised in Figure 11.

96 well ELISA plates were coated with 50µl of polyclonal rabbit anti human-ferritin and incubated overnight at 4°C in a sealed container. Following 3 washes with PBS the wells were blocked with PBS containing 1% (w/v) bovine serum albumin for 1 hour at room temperature. After 2 washes with 0.1% (v/v) Tween 20/PBS 50µl aliquots of test samples or standards containing from 3-500ng/ml human ferritin were incubated at room temperature for 3 hours. Following 4 washes in 0.1% Tween/PBS 50µl of biotinylated polyclonal rabbit anti human-ferritin was added to each well for 1.5 hours at room temperature. After 4 further washes 50µl of 1/1000 avidin-peroxidase conjugate in borate saline buffer at pH8.4 was added to each well for 30 minutes. Unbound conjugate was removed by 4 washes with borate saline containing 0.1% (v/v) Tween and a substrate buffer containing 34mg of O-phenylenediamine in 100ml of citrate phosphate buffer, pH5.0, was added. The reaction was stopped with 100µl 12.5% H<sub>2</sub>SO<sub>4</sub> and the optical density read in an automated ELISA plate reader (Dynatech) at 492 nm. A standard curve, absorbance versus ferritin concentration was plotted and the concentrations of the samples read from the curve (Figure 12).

### 2.3.4 Ribonucleotide Reductase Assay

Ribonucleotide reductase activity was assessed in intact cells by the method of Hards et al, 1981. In brief cells were washed and resuspended at 10<sup>7</sup>/ml in permeabilization buffer containing 1% (v/v) Tween 80, 0.25M sucrose, 50mM 4-(2-hydroxyethyl)-1-piperazin-ethanesulfonic acid (Hepes) pH7.2 and 2mM dithiothreitol (DTT). Cells were incubated at 22°C for 30 minutes then centrifuged and resuspended in fresh permeabilization buffer at 2.5 x10<sup>7</sup>/ml. Aliquots corresponding to 5 x 10<sup>6</sup> cells were added to assay tubes containing reaction buffer to give a final volume of 300ul containing 0.167M sucrose, 50mM Hepes pH7.2, 2mM ATP, 8mM MgCl<sub>2</sub>,

**FIGURE 11: MEASUREMENT OF FERRITIN BY ELISA**

**COAT 96 WELL ELISA PLATE WITH  
POLYCLONAL RABBIT ANTI HUMAN FERRITIN**



**INCUBATE OVERNIGHT AT 4°C.  
WASH 3 TIMES WITH PBS**



**BLOCK FOR 1 HR WITH PBS/ BSA.  
WASH 3 TIMES WITH PBS/TWEEN**



**ADD STANDARDS OR SAMPLES  
INCUBATE FOR 3 HRS AND WASH 4  
TIMES WITH PBS/TWEEN**



**ADD BIOTINYLATED POLYCLONALRABBIT  
ANTI-HUMAN FERRITIN. INCUBATE FOR  
1.5 HRS, WASH 4 TIMES WITH PBS/TWEEN.**

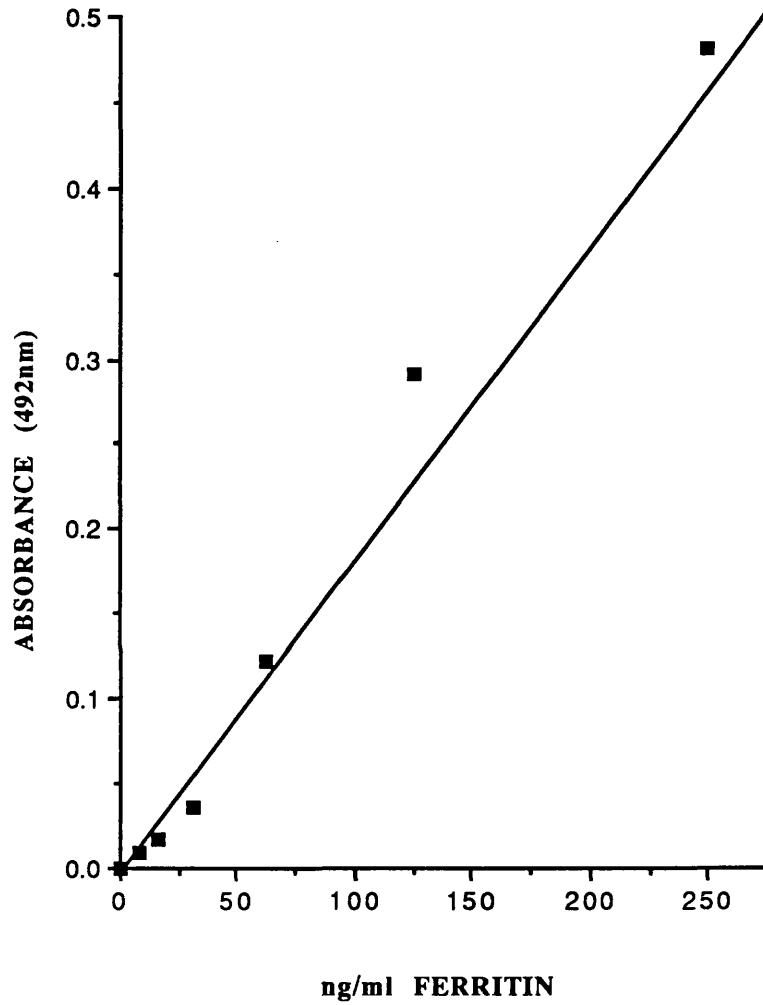


**ADD AVIDIN PEROXIDASE CONJUGATE  
IN BORATE SALINE. INCUBATE FOR 30  
MIN. WASH 4 TIMES WITH BORATE/TWEEN.**



**ADD O-PHENYLENEDIAMINE IN CITRATE  
PHOSPHATE BUFFER. AFTER COLOUR  
DEVELOPMENT STOP WITH H<sub>2</sub>S<sub>0</sub>4 AND READ  
ABSORBANCE AT 492nm.**

**FIGURE 12:**  
**TYPICAL STANDARD CURVE FOR FERRITIN ELISA**



6mM DTT, 0.67% (v/v) Tween 80 and 0.05 $\mu$ Ci [ $^{14}$ C]CDP (545 mCi/mMol). The assays were incubated at 37 $^{\circ}$ C in a shaking waterbath for 25 minutes and the reaction terminated by boiling. Nucleotides were converted to nucleosides by treatment with 2mg per tube *Crotalus atrox* venom, dissolved in 0.1M HEPES pH8.0 and 10mM MgCl<sub>2</sub>, for 2 hours at 37 $^{\circ}$ C. Again this reaction was terminated by boiling. Following the addition of 0.5ml distilled water to each tube, heat precipitated material was removed by centrifugation and the supernatant was passed down a 8 x 150mm Affigel 601 column to separate deoxycytidine from cytidine. The deoxycytidine was eluted from the column with 0.1M HEPES pH8.0 and 4ml of Aquasol liquid scintillation fluid added. Radioactivity was determined with an LKB liquid scintillation spectrophotometer.

### 2.3.5 Protein Assay

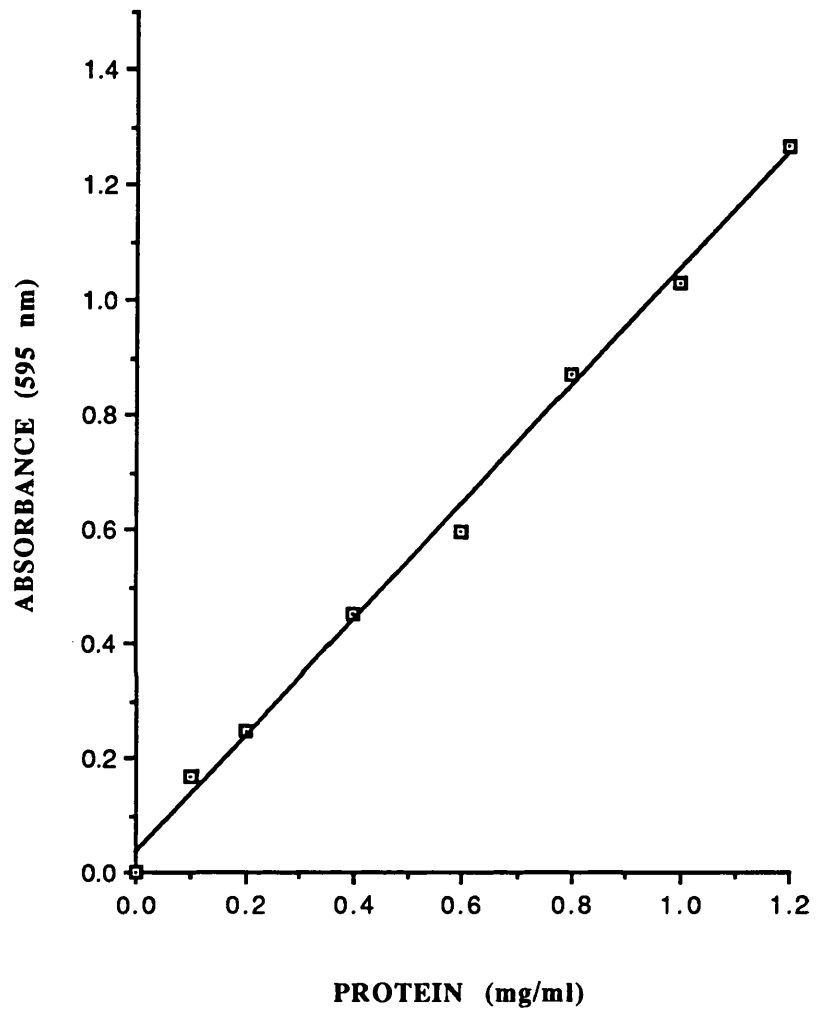
Cellular protein was measured using a Bio-Rad dye reagent based on the Bradford protein assay with Coomassie blue (Bradford, 1976).

Standards with a protein content ranging from 0.2 to 1.4mg/ml were prepared with bovine serum albumin dissolved in PBS. 20 $\mu$ l of standards or samples were added to test tubes containing 20 $\mu$ l 0.1M NaOH. The samples were incubated for one hour at room temperature then 1.0 ml of Bio-Rad dye reagent, diluted 1 in 5 with distilled water, was added to each tube. The samples were thoroughly mixed and incubated at room temperature for up to 30 minutes then the absorbance of standards and samples was measured at 595 nm.

A standard curve, absorbance versus protein concentration was plotted and the concentrations of the samples read from the curve. The curve is linear over the protein concentrations used and a typical example is shown in Figure 13.

**FIGURE 13:**

**TYPICAL STANDARD CURVE FOR THE PROTEIN ASSAY**



## **CHAPTER 3: CELLULAR UPTAKE OF CP94 AND DFO**



### 3.1 INTRODUCTION

Two of the major factors which may determine the effective mobilisation of intracellular iron by iron chelators are the entry of the iron-free ligand into the cell and the subsequent ability of the chelator-iron complex to exit the cell. The rate at which an iron chelator passes across the plasma membrane is dependent upon the size of the molecule, its charge and its partition coefficient ( $K_{part}$ ). Most drugs enter cells by simple diffusion through the hydrophobic region of the cell membrane, with uncharged compounds permeating cells more rapidly than charged compounds (Florence and Attwood, 1981). It would be expected that small, relatively lipophilic, neutral chelators such as the 3-HP-4-ones would cross membranes relatively rapidly. In contrast DFO is very hydrophilic ( $K_{part} = 0.01$ ) (Porter et al, 1988) with a net charge of +1, suggesting that this chelator should diffuse across cell membranes rather more slowly.

The exact mechanism of uptake of DFO has been a subject of much debate. Studies by Roberts and Bomford (1988) suggest that DFO enters K562 cells by a concentration dependent process of diffusion across the plasma membrane. However in these studies the intracellular concentration of DFO was measured indirectly by assessing the conversion of repeated pulses of [ $^{59}\text{Fe}$ ]transferrin to [ $^{59}\text{Fe}$ ]ferrioxamine, which was subsequently extracted in benzyl alcohol. Therefore the actual intracellular level of DFO was not determined. In contrast, Bottomley et al (1985) directly measured the uptake of [ $^{14}\text{C}$ ]DFO by K562 cells. These authors reported a progressive uptake of [ $^{14}\text{C}$ ]DFO over a 24 hour period with a resultant 14-fold intracellular accumulation of  $^{14}\text{C}$ -label. This suggests that a mechanism other than simple diffusion is responsible for the cellular uptake of DFO. More recent studies by Lloyd et al (1991) have suggested that the entry of [ $^{14}\text{C}$ ]DFO into rat visceral yolk sacs occurs by fluid phase pinocytosis, however it remains unclear to what extent these results can be extrapolated to other cell types which do not have such a high capacity for pinocytosis.

The human erythroleukaemia cell line K562 represents a suitable experimental model for the investigation of cellular interactions with iron chelators. These cells acquire iron by the receptor mediated endocytosis of transferrin and have been shown to possess a better developed iron handling capacity than many other human tumour cell lines (Forsbeck and Nilsson, 1985). These first experiments therefore examine the kinetics and mechanisms of cellular uptake of DFO and CP94 by K562 cells, and compare the relative abilities of these compounds to mobilise intracellular iron.

### **3.2 UPTAKE EXPERIMENTS WITH [<sup>14</sup>C]DFO AND [<sup>14</sup>C]CP94**

These first experiments examined the kinetics of uptake of <sup>14</sup>C-labelled DFO and CP94 into K562 cells. The studies initially examined chelator uptake over a prolonged incubation period to enable identification of the mechanisms involved in the cellular accumulation of these compounds. Subsequent experiments focussed upon the early uptake of [<sup>14</sup>C]CP94 and [<sup>14</sup>C]DFO into K562 cells so enabling a comparison of the relative rates at which these compounds enter cells.

#### **3.2.1 Uptake of [<sup>14</sup>C]DFO and [<sup>14</sup>C]CP94 by K562 Cells at 37°C**

##### **Experimental Procedures**

5x10<sup>7</sup> K562 per test sample, suspended in RPMI 1640 with 5% FCS were incubated with 100µM [<sup>14</sup>C]CP94 or [<sup>14</sup>C]DFO for up to 4 hours at 37°C. At the end of the incubation period the cells were washed twice with PBS and cell number and mean cell volume (MCV) were determined with a Coulter electronic particle counter. To remove any surface bound [<sup>14</sup>C] chelator the cells were incubated with 1ml pH 3.0 PBS at 4°C for 2 minutes then 20 mls of pH7.4 PBS containing 1% BSA was added to each sample tube and the cells were washed twice more with PBS. Cells were then solubilised with 500µl of 1% Triton X-100 and 4ml of Hisafe scintillation fluid was added to each sample. The amount of [<sup>14</sup>C] label incorporated by each test sample was

quantified with a beta counter. The intracellular volume of the samples was calculated from the MCV and the cell number. The intracellular concentration of each compound was determined from the radioactivity of the lysates and the specific activity of the labelled chelators.

## Results

At 37°C both [<sup>14</sup>C]DFO and [<sup>14</sup>C]CP94 were accumulated by K562 cells. As shown in Figure 14, the amount of cell associated [<sup>14</sup>C]CP94 increased rapidly to attain a maximum after one hour and then levelled off. By contrast [<sup>14</sup>C]DFO uptake appeared initially slower than that of CP94 but proceeded linearly over the entire period of incubation studied. After 4 hours the cells had accumulated  $590 \pm 12$  pmol [<sup>14</sup>C]CP94 and  $2001 \pm 420$  pmol [<sup>14</sup>C]DFO, as the MCV of K562 cells is 98 fl this corresponds to an intracellular concentration of  $118 \pm 25$  μM and  $402 \pm 104$  μM <sup>14</sup>C-labelled CP94 and DFO respectively.

### 3.2.2 Initial Rate of Uptake of [<sup>14</sup>C]CP94 and [<sup>14</sup>C]DFO

#### Experimental Procedures

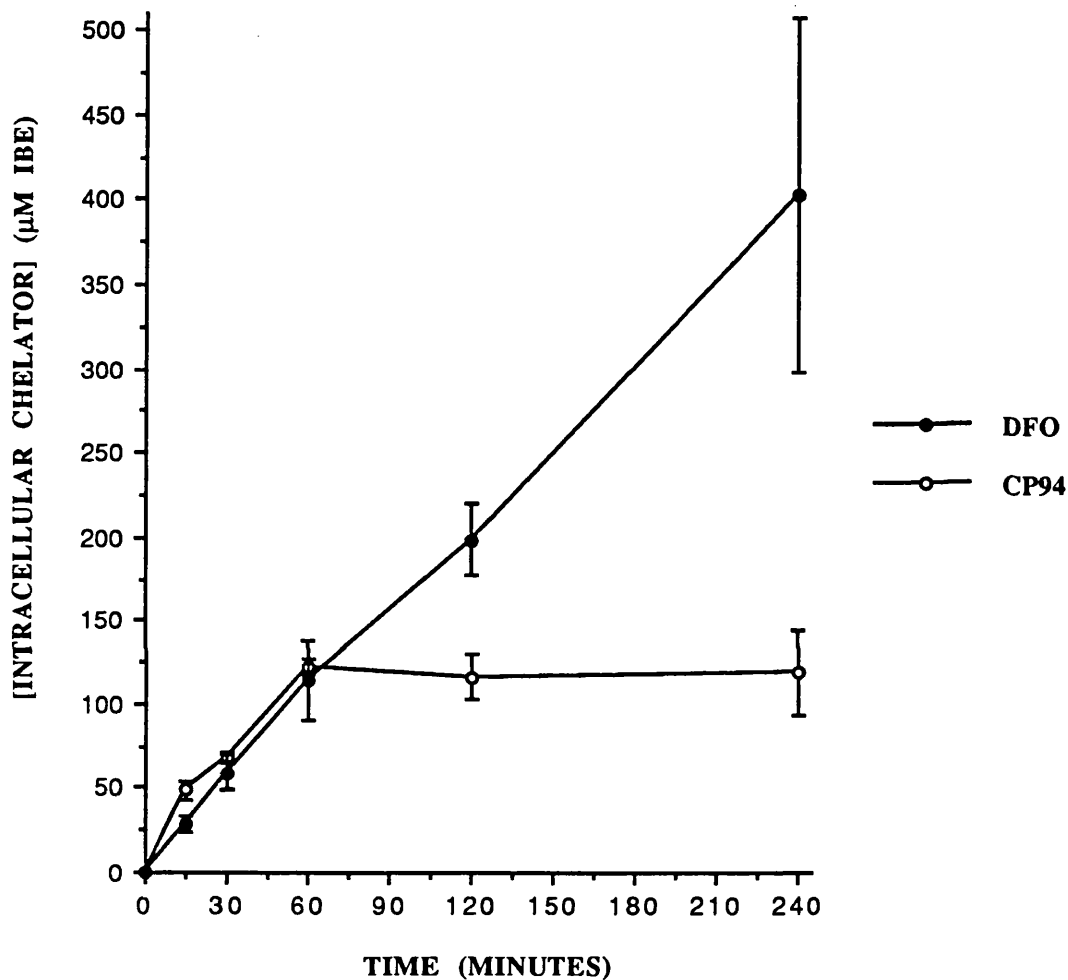
$5 \times 10^7$  K562 cells per sample were incubated with 100 μM [<sup>14</sup>C]CP94 and [<sup>14</sup>C]DFO for up to 30 minutes at 37°C. At the end of the incubation the cells were washed as described previously (Section 3.2.1). An aliquot of cells was set aside for protein analysis as described in Section 2.4.5. The remainder were solubilised with Triton X-100 and counted.

#### Results

Cellular uptake of both <sup>14</sup>C-labelled chelators was linear over the first 15 minutes (Figure 15) permitting the calculation of an initial rate of uptake for each compound. In 3 identical experiments the mean rate of uptake of [<sup>14</sup>C]CP94 was  $3.73 \pm 0.39$  pmol/mg cellular protein/minute, this is significantly higher than the initial

**FIGURE 14:**

**UPTAKE OF [<sup>14</sup>C] CP94 AND [<sup>14</sup>C]DFO BY K562 CELLS**

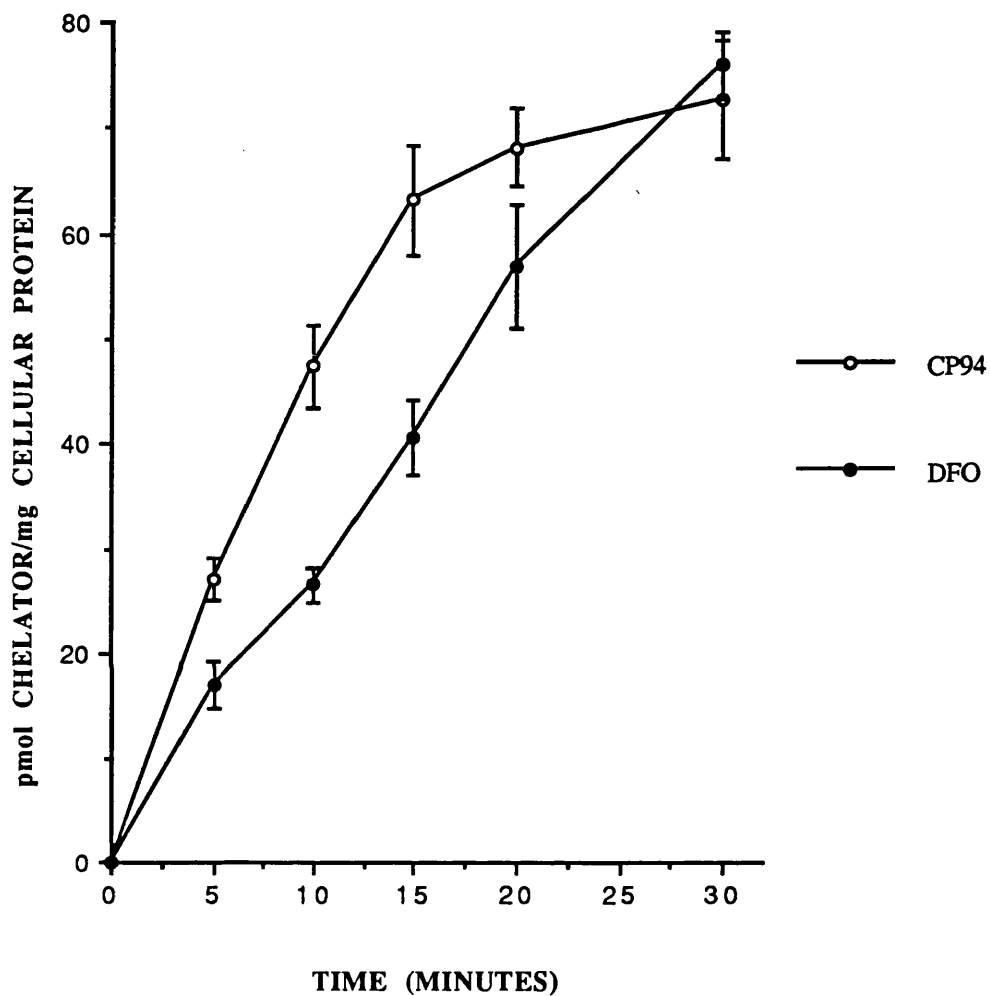


**LEGEND:**

K562 cells were incubated in the presence of 100µM IBE [<sup>14</sup>C]CP94 or DFO for up to 4 hours. At the end of incubation cells were washed as described in the text and analysed for cell number, MCV and radioactivity. The results represent the mean ± S.E.M of 3 separate experiments.

**FIGURE 15:**

**INITIAL UPTAKE OF [<sup>14</sup>C]CP4 AND [<sup>14</sup>C]DFO BY K562 CELLS**



**LEGEND:**

K562 cells were incubated in the presence of 100 $\mu$ M IBE [<sup>14</sup>C]CP94 or DFO for up to 30 minutes. At the end of incubation cells were washed as described in the text and analysed for protein and radioactivity. The results represent the mean  $\pm$  S.E.M of 3 separate experiments.

rate of uptake of [ $^{14}\text{C}$ ]DFO which was  $2.12 \pm 0.55$  pmol/mg cell protein/minute ( $p < 0.02$ ). After 15 minutes the rate of uptake of [ $^{14}\text{C}$ ]CP94 slowed but [ $^{14}\text{C}$ ]DFO continued to be accumulated in a linear manner.

### 3.2.3 Discussion

Cells incubated with [ $^{14}\text{C}$ ]DFO appeared to accumulate  $^{14}\text{C}$ -label at levels in excess of that in the extracellular medium (Figure 14). [ $^{14}\text{C}$ ]DFO was accumulated in a linear manner over the 4 hour incubation period, and achieved an intracellular concentration 4 fold higher than that present in the extracellular medium. In contrast [ $^{14}\text{C}$ ]CP94 was initially taken up significantly more rapidly than [ $^{14}\text{C}$ ]DFO (Figure 15) but uptake slowed as a concentration equilibrium was reached across the cell membrane.

The intracellular concentration of [ $^{14}\text{C}$ ]DFO could be a result of several factors; a) DFO itself maybe concentrated within the cell; b) the rate of transmembrane movement may be greater for DFO than FO. This could create a disequilibrium where DFO would enter the cell relatively rapidly, chelate iron and exit the cell more slowly in the form of FO. c) DFO or FO may be metabolised to a species unable to rapidly permeate cell membranes. An alternative explanation is that the  $^{14}\text{C}$  label does not accurately reflect intracellular chelator levels and the apparent cellular accumulation of DFO is a result of non-specific binding to the cell membrane despite the extensive washing procedure.

### 3.3 HPLC ANALYSIS OF INTRACELLULAR DFO

To demonstrate that DFO was present within the intracellular compartment and to determine its form K562 cells were incubated with DFO for various time intervals and analysed by high performance liquid chromatography (HPLC).

## **Experimental Procedures.**

$5 \times 10^7$  K562 cells per test sample were incubated with  $100 \mu\text{M}$  IBE DFO for up to 4 hours at  $37^\circ\text{C}$ . The cells were washed 3 times with PBS and resuspended to a final volume of 1.3ml. Cell number and MCV were determined with a Coulter automated cell counter. The cells were lysed by sonication and lysates were centrifuged for 2 minutes at  $13,000 \times g$  in a microcentrifuge to remove cellular membranes. The supernatant was then spun through an Amicon Centriflow CF-25 filtration cone to separate the high and low molecular weight portions of the lysates. DFO and its metabolites are unstable when stored frozen (S Singh, personal communication), therefore the low molecular weight supernatants were immediately passed to Dr Surinder Singh at Kings College London for HPLC analysis.

The samples were analysed by the method of Singh and colleagues (1990). A Hewlett-Packard Model 1090M HPLC system complete with an autoinjector, autosampler and diode-array detector was used together with a Waters (Milford, MA, USA) Novapack ODS radial compression column (10cm x 8mm) equipped with a precolumn cartridge (Waters, Bondapack ODS). The flow rate was 1ml/min and the eluent was monitored at 215nm and 430nm. The chromatographic conditions were as follows; Pump A (20mM phosphate, pH 7.0 containing 2mM nitriloacetic acid (NTA)); Pump B (20mM phosphate, pH7.0 containing 2mM NTA in 50% acetonitrile). The gradient programme was (min/%B): 0/0; 1/0; 20/18; 24/25; 28/35; 31/35; 32/0. A post run time of 10 minutes was allowed between injections for re-equilibration of the column.

## **Results and Discussion**

Typical HPLC profiles of the cell lysates are shown in Figure 16. FO absorbs both in the UV region at 215nm and in the visible region at 430nm. DFO only absorbs at 215nm. Therefore the HPLC chromatographs were monitored at both wavelengths. Standard curves of concentration versus peak area were plotted for DFO and FO (Figure 17) and the concentration of each compound in the cell lysates was read from

FIGURE 16: HPLC CHROMATOGRAMS FOR DFO AND FO

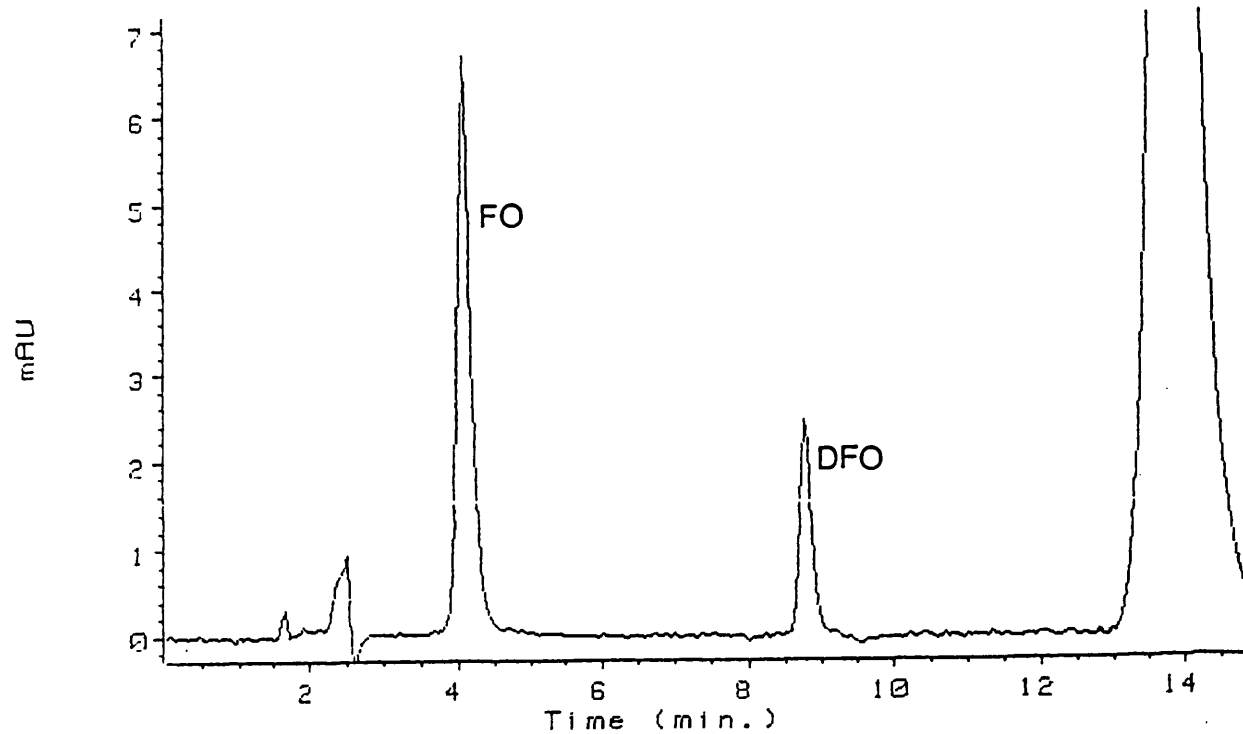
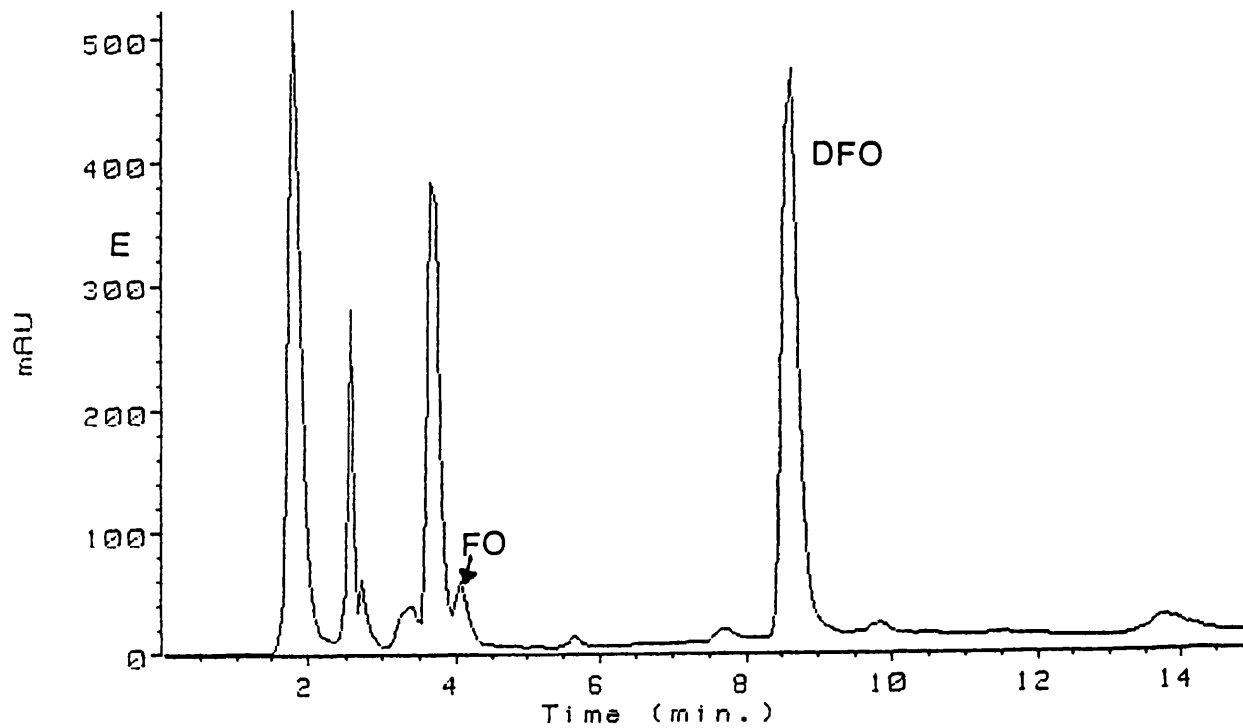




**FIGURE 17:**

**CALIBRATION CURVES FOR THE MEASUREMENT  
OF DFO AND FO BY HPLC**

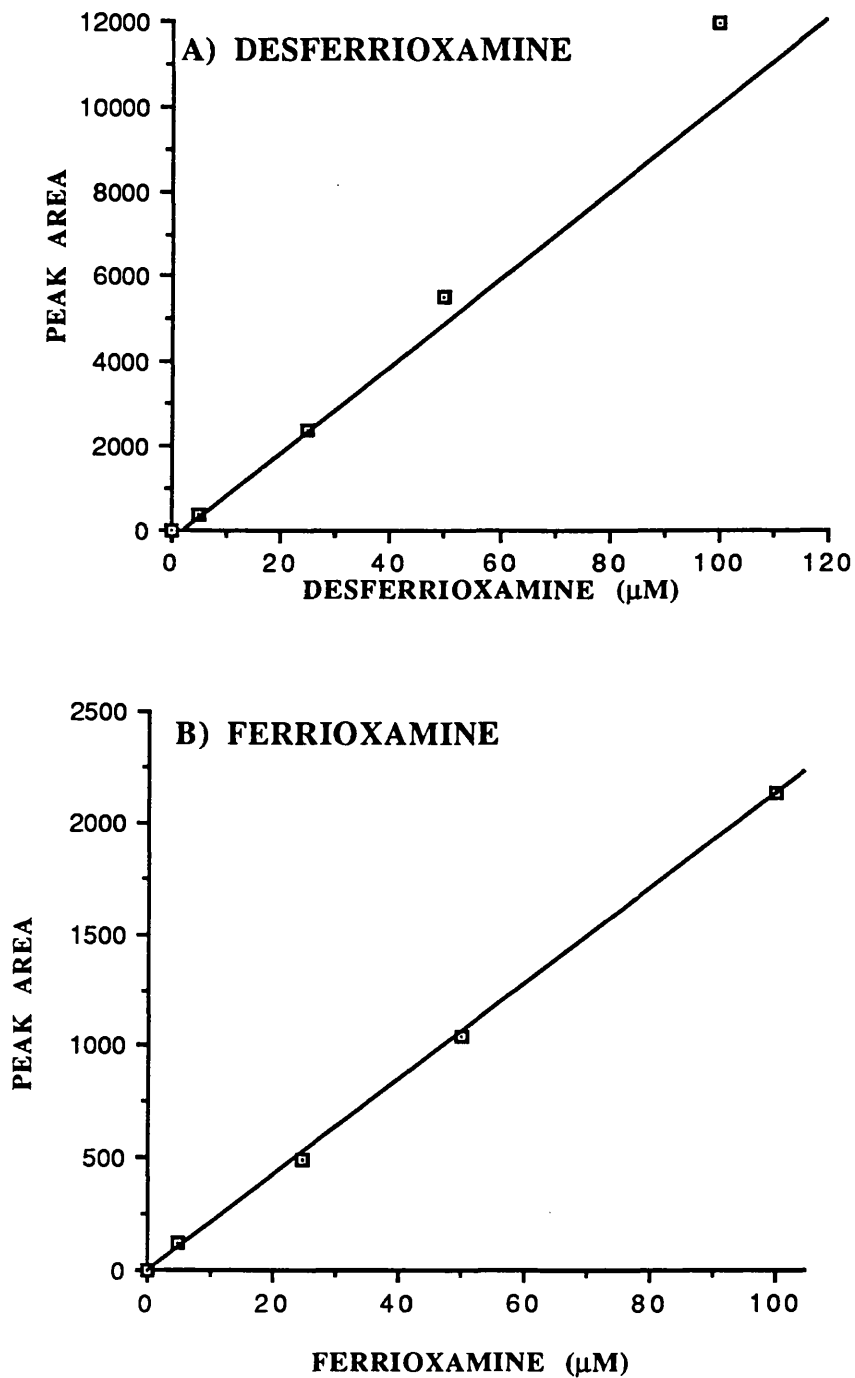


**TABLE 5: HPLC ANALYSIS OF INTRACELLULAR DFO AND FO**

TIME (minutes)	INTRACELLULAR CONCENTRATION( $\mu$ M)	
	DFO	FO
20	N.D	8.7
60	87.5	15.2
120	169	16.8
240	331	17.9

N.D = not detectable

K562 cells were incubated with 100 $\mu$ M DFO for up to 4 hours. At the end of incubation cells were washed, lysed and prepared for analysis as described. Intracellular levels of DFO and FO were determined by HPLC using the conditions described in the text.

the curves. The corresponding intracellular concentration was calculated from the cell number and the MCV (Table 5).

The levels of total intracellular chelator measured by HPLC were in agreement with those calculated from the cellular accumulation of  $^{14}\text{C}$ -labelled chelators (Section 3.2), thus confirming the accuracy of the  $^{14}\text{C}$ -labelled chelator methodology. However analysis by HPLC provides the additional advantage of separation of the iron free and iron bound ligand and allows the identification of any metabolites. Furthermore the HPLC assay is highly reproducible and sensitive with a limit of detection of 1.5 and  $1.0\mu\text{g/ml}$  for DFO and FO respectively (Singh et al, 1990).

The results in Table 5 show that DFO is progressively accumulated by K562 cells. After 20 minutes incubation only FO was detectable in the cell lysates, however by 60 minutes the majority of the intracellular chelator was in the iron free form. The intracellular concentration of DFO continued to rise in a linear manner throughout the duration of the experiment.

Intracellular levels of FO initially increased rapidly to give an intracellular concentration of  $15\mu\text{M}$  by 60 minutes. Since at this time DFO was in excess, the concentration of FO achieved may represent the amount of intracellular iron that was readily available for chelation from the low molecular weight cytosolic pool. After 60 minutes intracellular levels of FO continued to increase very slowly suggesting that a slight disequilibrium exists between the rate of formation of FO and its subsequent exit from the cell. In these experiments no metabolites of DFO or FO were observed at any time either within the cells or in the extracellular medium.

### **3.4 EFFECT OF TEMPERATURE AND SELECTIVE INHIBITORS ON CELLULAR UPTAKE OF $^{14}\text{C}$ CP4 AND $^{14}\text{C}$ DFO**

The experiments above indicate that DFO, unlike CP94, is concentrated within cells. This suggests that CP94 and DFO may enter cells by different mechanisms, with a possibility of active uptake of DFO. To investigate this further cellular uptake of  $^{14}\text{C}$

CP94 and [<sup>14</sup>C]DFO was examined in the presence of the microtubule inhibitor colchicine or the metabolic inhibitor sodium azide.

Colchicine blocks microtubule polymerization and therefore inhibits cell processes that depend on functioning microtubules. The metabolic inhibitor sodium azide acts by depletion of cellular ATP and therefore inhibits energy dependent active transport. As some cellular uptake processes may be temperature dependent uptake was also examined at 4°C.

Cellular accumulation of [<sup>14</sup>C] sucrose was also examined as a positive control, as the rate of intracellular accumulation of radiolabelled sucrose is an accepted method for the measurement of a cells capacity to accumulate molecules by processes such as fluid phase pinocytosis (Pratten et al, 1980).

## **Experimental Procedures**

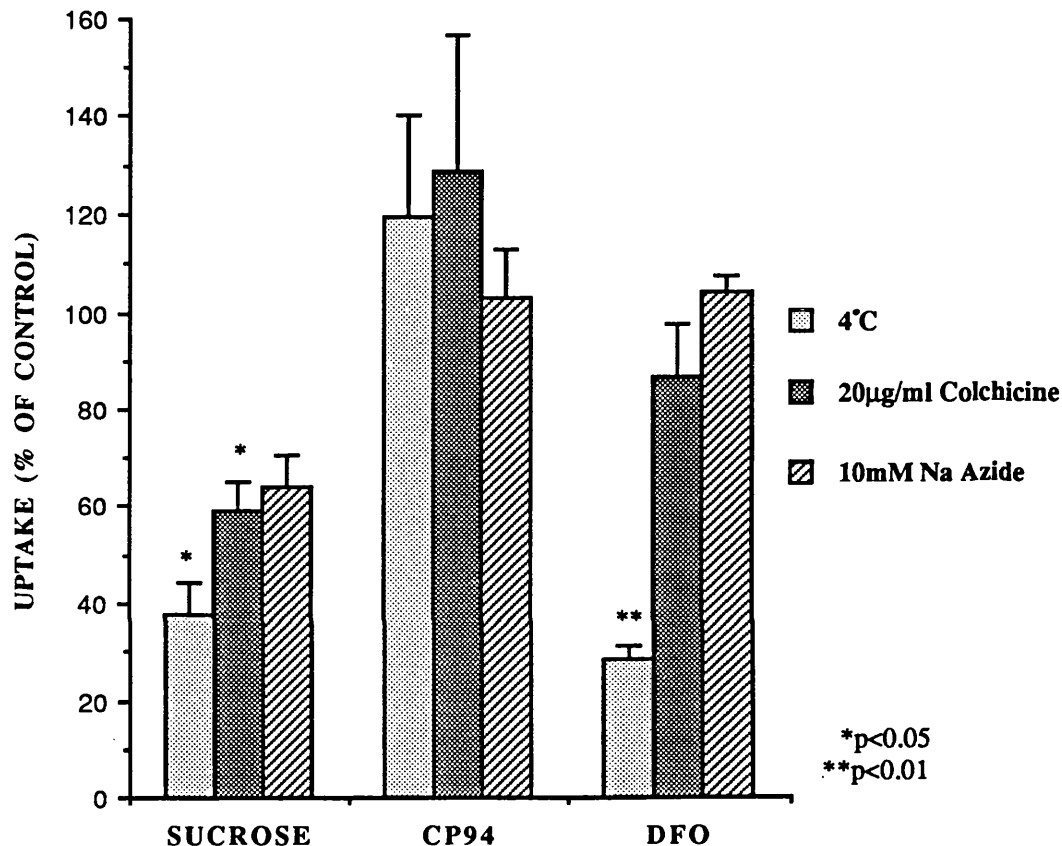
5x10<sup>7</sup> K562 cells per sample were incubated at 37°C, at 4°C and at 37°C with 20µg/ml colchicine or 20mM Na azide for 15 minutes. 100µM [<sup>14</sup>C]CP94 or [<sup>14</sup>C]DFO, or 0.4µCi/ml [<sup>14</sup>C]sucrose were added to the cultures and the cells were incubated for a further 4 hours. The cells were maintained at 37°C (controls), 4°C or at 37°C with colchicine or azide for the duration of the experiment. At the end of the incubation period samples were washed and counted as described in section 3.2.1.

## **Results and Discussion**

The results in Figure 18 show that uptake of [<sup>14</sup>C]DFO and [<sup>14</sup>C]CP94 by K562 cells was not significantly affected by the addition of colchicine or azide to the culture medium. However cellular accumulation of [<sup>14</sup>C]sucrose was reduced by more than 60% under these conditions, indicating that cellular capacity for uptake processes requiring microtubular function or metabolic energy was markedly decreased. Likewise cellular accumulation of [<sup>14</sup>C]sucrose was significantly reduced by incubation at 4°C, as was uptake of [<sup>14</sup>C]DFO. By contrast incubation at 4°C had no significant effect on the accumulation of [<sup>14</sup>C]CP94.

**FIGURE 18:**

**EFFECT OF TEMPERATURE, COLCHICINE AND AZIDE ON UPTAKE OF [<sup>14</sup>C] SUCROSE, CP94 AND DFO BY K562 CELLS**



**LEGEND:**

K562 cells were preincubated at 37°C (controls), 4°C or at 37°C with colchicine or azide for 15 minutes. 100µM IBE [<sup>14</sup>C]CP94 or [<sup>14</sup>C]DFO or 0.4µCi/ml [<sup>14</sup>C]sucrose were added to the culture medium and cells were incubated for a further 4 hours. At the end of incubation cells were washed as described in the text and analysed for protein and radioactivity. The results are expressed as the amount of <sup>14</sup>C label accumulated by cells for each compound as a percentage of that accumulated by controls over the 4 hour incubation period. The data represents the mean ± S.E.M of 3 separate experiments. Significant differences in the uptake of <sup>14</sup>C-label in test compared to control conditions were identified at the p<0.05 (\*) and p<0.01(\*\*) levels using unpaired Students t tests.

These results indicate that DFO enters cells by a process that is independent of microtubule function and cellular ATP levels. Thus it is unlikely that this chelator is taken into K562 cells by pinocytosis or an active transport mechanism. However the partition coefficient of DFO is too low to be compatible with passive diffusion across the cell membrane and it is therefore probable that DFO enters cells by a temperature dependent facilitated process.

The uptake of CP94 was also found to be independent of cellular energy levels and microtubule function. Furthermore cellular accumulation of this chelator was also unaffected by temperature. These data suggest that CP94 enters K562 cells by a process of simple diffusion across the plasma membrane.

### **3.5 IRON MOBILISATION FROM K562 CELLS BY CP94 AND DFO**

Mobilisation of intracellular iron may be influenced, not only by the rate at which the chelator enters the cell, but also by the efficiency with which the chelator-iron complex exits the cell. The next experiments were designed to compare the relative abilities of the CP94-iron complex and FO to egress from cells. HPLC analysis has already indicated that FO may accumulate within cells (Section 3.3), suggesting that this molecule only transits cellular membranes very slowly. However it was not possible to make a direct comparison between the relative rates at which the CP94-iron complex and FO exit from the cell. Therefore this was compared indirectly by monitoring the relative abilities of these chelators to mobilise intracellular  $^{59}\text{Fe}$  delivered to K562 cells by the receptor mediated endocytosis of transferrin.

#### **Experimental Procedure**

$2 \times 10^6$  K562 cells/ml, suspended in RPMI 1640 supplemented with 1% BSA, were incubated with  $100 \mu\text{g/ml}$   $^{59}\text{Fe}$  labelled diferric transferrin (see section 2.4.1) at  $37^\circ\text{C}$  for 3 hours and then washed 3 times with PBS.

The  $^{59}\text{Fe}$ -loaded cells were resuspended in culture medium containing  $100\mu\text{M}$  IBE of CP94 or DFO, or an equivalent volume of PBS for controls. This point is called TO. The cells were incubated at  $37^\circ\text{C}$  and 5ml aliquots were taken at the time points indicated. The samples were centrifuged and the supernatant removed and retained. The cells were washed 3 times with PBS and the amount of radioactivity in the cells, supernatant and each wash was measured using an LKB gamma counter.

## Results and Discussion

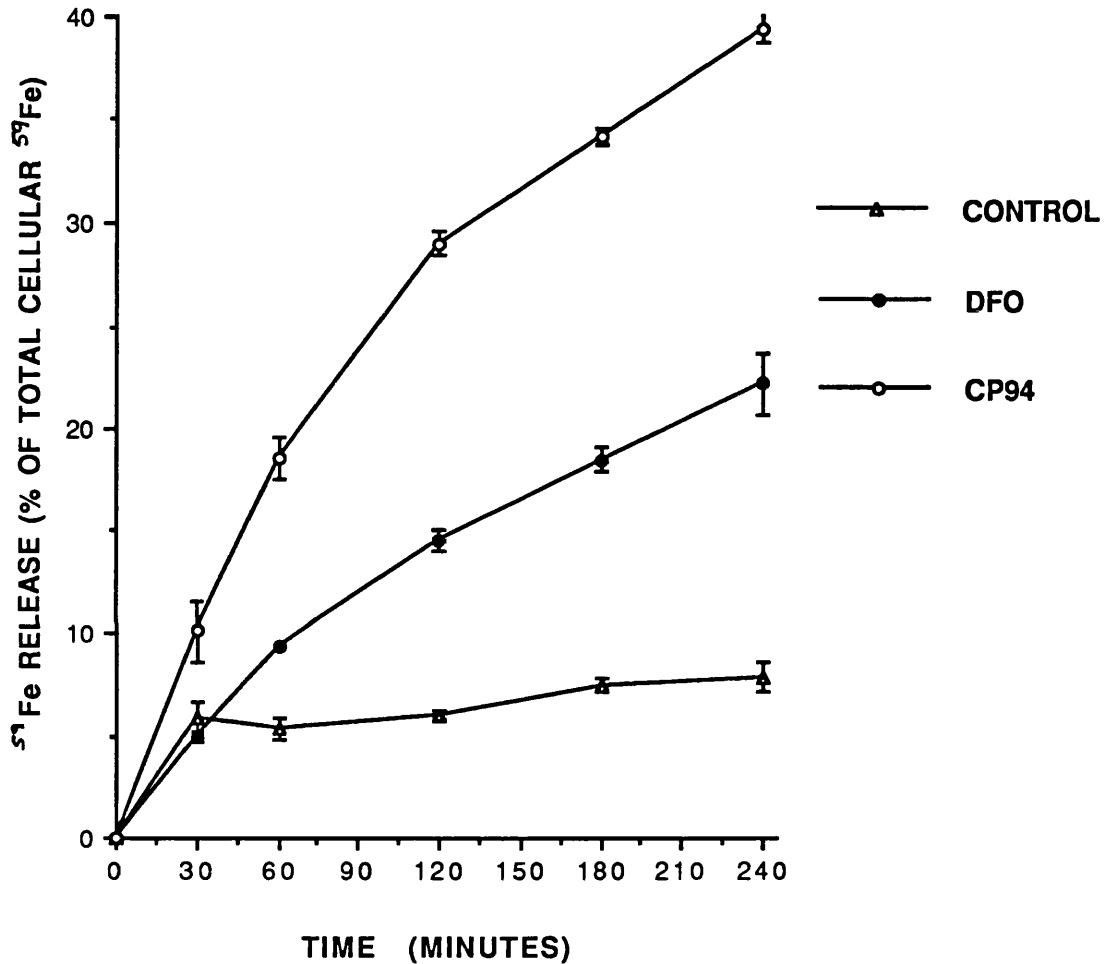
When  $^{59}\text{Fe}$  labelled cells were reincubated the amount of iron released from control cells was low (approximately 4%) and remained unchanged during the 4 hour incubation period (Figure 19). This iron release may represent a reflux of  $^{59}\text{Fe}$  labelled transferrin, accumulated during the preincubation, back into the culture medium.

In the presence of  $100\mu\text{M}$  IBE CP94 the intracellular  $^{59}\text{Fe}$  was rapidly mobilised (Figure 19). Twice as much  $^{59}\text{Fe}$  as controls was released into the culture medium over the first 30 minutes of culture and after 4 hours less than 60% of the  $^{59}\text{Fe}$  originally accumulated remained cell associated. By contrast release of  $^{59}\text{Fe}$  from DFO treated cells was markedly slower and more than 75% of the original  $^{59}\text{Fe}$  remained cell associated after 4 hours incubation.

These results show that DFO is markedly less active than CP94 in mobilising  $^{59}\text{Fe}$  from K562 cells. However it has been shown previously that intracellular concentrations ( $\mu\text{M}$  IBE) of DFO exceed those of CP94 after 1 hour (Figure 14). Thus the disparities in iron mobilisation by these chelators are unlikely to be as a result of DFO failing to enter cells. This suggests that the limiting factor in iron mobilisation by DFO is the slow rate at which FO exits from the cell in contrast to the CP94-Fe complex which appears to pass out of the cell relatively rapidly.

**FIGURE 19**

**MOBILISATION OF RADIOIRON FROM  
K562 CELLS BY CP94 AND DFO**



**LEGEND:**

K562 cells were preincubated with 100 $\mu\text{g}/\text{ml}$   $^{59}\text{Fe}$  transferrin for 3 hours. The cells were then washed and reincubated at TO in the presence or absence of 100 $\mu\text{M}$  IBE CP94 or DFO for up to 4 hours. At the end of incubation cells were washed and the amount of radioactivity in the cells, the extracellular medium and washings was analysed. The results show the amount of  $^{59}\text{Fe}$  released from cells at each time point expressed as a percentage of the total cell associated radioactivity at TO. The data represents the mean  $\pm$  S.E.M of 3 separate experiments.



### 3.6 DISCUSSION

Experiments investigating the uptake of  $^{14}\text{C}$ -labelled DFO and CP94 indicate that these compounds enter cells by distinct processes. The uptake of [ $^{14}\text{C}$ ]CP94 by K562 cells was initially more rapid than that of [ $^{14}\text{C}$ ]DFO (Figure 15) but formed a plateau after 1 hour when equilibrium between intracellular and extracellular concentration was reached (Figure 14). By contrast [ $^{14}\text{C}$ ]DFO uptake was continuous over the 4 hour period studied (Figure 14) resulting in a ratio of approximately 4:1 between the intracellular and extracellular DFO concentration.

Analysis of cell lysates by HPLC confirmed that K562 cells accumulate DFO at concentrations in excess of that present in the extracellular medium (Table 5). Furthermore these studies revealed that the majority of the intracellular oxamine was present as DFO rather than FO.

Experiments utilising the selective inhibitors colchicine and sodium azide demonstrated that the uptake of both DFO and CP94 was independent of microtubular function and cellular ATP levels (Figure 18) suggesting that neither pinocytosis or active transport plays a role in the accumulation of these chelators by K562 cells.

However the rate at which DFO enters cells is faster than can be accounted for by passive diffusion in view of the low lipid solubility of this compound. These studies therefore suggest that cellular accumulation of DFO is by a temperature dependent facilitated process.

A possible explanation for the apparent concentration of DFO by K562 cells is that this chelator enters cells by a facilitated transport process as a result of its charged nature. The transit of charged species across biological membranes is influenced both by the concentration gradient and also the electrical potential difference across the membrane. All plasma membranes have a voltage gradient across them with the inside being negative as compared to the outside. This potential difference favours the entry of positively charged molecules into cells but opposes the entry of negatively charged

molecules. If the resting membrane potential is known the ratio of internal and external concentrations of an ionic species may be calculated from the Nernst equation.

i.e The Nernst equation is  $V = \frac{RT}{zF} \ln \frac{C_o}{C_i}$

where V = the equilibrium potential in volts

(internal potential minus the external potential)

C<sub>o</sub> and C<sub>i</sub>=outside and inside concentration of the charged species respectively

R=the gas constant (8.3 J.K<sup>-1</sup>.mol<sup>-1</sup>)

T=the absolute temperature (K)

F= Faradays constant (96,500 Coulombs mol<sup>-1</sup>)

z= the valance (charge) of the ionic species

The average resting potential in vertebrate cells is approximately -70mV (Kumar-Jain, 1988), therefore using the formula shown above it may be calculated that an equilibrium distribution ratio of approximately 14:1 will result for a univalent species such as DFO at 37°C (Singh et al, 1990). Hence cells accumulate positively charged species and it is likely that DFO will accumulate within the cell in the absence of metabolism to a negatively charged species.

When DFO coordinates iron (III), three protons are displaced so conferring a net positive charge upon FO (Singh et al, 1990). Therefore FO, like DFO, will tend to be accumulated by cells and will only pass out of the cell slowly. These findings would explain why both DFO and FO tend to accumulate within K562 cells over the timecourse studied.

In contrast to DFO, CP94 is uncharged in both the iron free and iron-complexed form. Consequently, as demonstrated in these studies, CP94 and the CP94-Fe complex can pass in out of the cell relatively rapidly by simple diffusion down a concentration gradient.

## **CHAPTER 4: SUBCELLULAR DISTRIBUTION OF CP94 AND DFO**

## 4.1 INTRODUCTION

The experiments described in Chapter 3 demonstrate that CP94 rapidly transits the plasma membrane by simple diffusion due to its low molecular weight and neutral charge. Similarly CP94 should pass rapidly across intracellular membranes and into organelles. By contrast, DFO may have limited access into intracellular organelles due to its relatively low lipid solubility. An understanding of the intracellular site of action of iron chelators is important both in relation to their efficacy and potential toxicity. This has relevance for the therapeutic applications of iron chelators not only in the management of iron overload but also in situations unrelated to iron overload, where chelation of vital iron from intracellular organelles may compromise normal cell function.

Iron chelators may act intracellularly on several iron pools. Ferritin is the major intracellular iron storage molecule and represents potentially the largest pool of chelatable iron. However direct chelation from ferritin is unlikely to be a major source of chelator induced iron excretion since at physiological pH, in the absence of reducing agents, DFO is capable of removing iron from ferritin at a rate of less than 1% per hour (Crichton et al, 1980). It has been suggested, however, that smaller chelators such as the bidentate HPOs may be able to penetrate the protein shell of ferritin and mobilise iron more efficiently (Brady et al, 1988).

Studies by Pippard et al (1982) showed that  $^{59}\text{Fe}$  delivered to rat hepatocytes by transferrin is almost immediately available for chelation by DFO. In contrast, optimal chelation of iron delivered to the cell in the form of  $^{59}\text{Fe}$ -ferritin does not occur until 2-6 hours later, following lysosomal autolysis and before  $^{59}\text{Fe}$  incorporation into endogenous ferritin. These observations suggest that the direct source of chelatable intracellular iron is the transient low molecular weight (LMW) iron pool in equilibrium with storage iron (Section 1. 2.4). All intracellular iron traffic must pass through this LMW pool, therefore chelators acting at this site will have access to large amounts of chelatable iron.

Laub et al (1985) suggested that intralysosomal chelation is also quantitatively important. Studies utilising tritiated DFO analogues demonstrated a time dependent accumulation of these compounds within plasma-membrane related structures and lysosomes in cultured rat hepatocytes. These studies suggested that lysosomal catabolism of cytosolic ferritin may enhance the chelation of ferritin iron by the DFO analogues and that this may represent the chelatable intracellular iron pool.

The studies in this chapter therefore compare the subcellular distribution of [ $^{14}\text{C}$ ]DFO and [ $^{14}\text{C}$ ]CP94 in K562 cells and the effect of these compounds on the intracellular distribution of  $^{59}\text{Fe}$  delivered by the receptor mediated endocytosis of transferrin.

## **4.2 ANALYTICAL SUBCELLULAR FRACTIONATION OF K562 CELLS**

The first requirement for this series of experiments was the development of a reproducible cellular fractionation procedure which gave optimal separation of the subcellular organelles. Several different experimental approaches were tried and a brief description of each procedure follows:

a) Cells were homogenised and the nuclear fraction removed by centrifugation as described in experimental procedures. The post nuclear supernatant was layered onto a 13ml sucrose gradient (from 11-55% sucrose wt/wt, density 1.045-1.266 g/ml) over a cushion of 1ml 60% sucrose as described described by Roberts (1990). Gradients were centrifuged (25,000 rpm at 4°C) for 16 hours in a Beckman SW41 swinging bucket rotor with a Beckman L8M Ultracentrifuge.

With this system good separation of intracellular organelles was attained however the need to spin these gradients overnight made them unsuitable for analysis of the subcellular distribution of compounds such as CP94 which rapidly pass across cell membranes even at 4°C (Section 3.4).

b) The post nuclear supernatant was obtained as described and layered onto a discontinuous sucrose gradient consisting of 41, 26.5, 20, 15 and 10.5% (wt/wt) sucrose as described by Bakkeren et al (1987). The gradient was centrifuged for 60 minutes at 40,000 rpm in a Beckman SW41 rotor at 4°C. Fractionation by this protocol did not give adequate separation of the mitochondrial and lysosomal fractions.

c) The cells were fractionated by differential centrifugation as summarised in Figure 20 and described in experimental procedures below. This method gave relatively good separation of the nuclear, mitochondrial and lysosomal fractions but did not enable good separation of lysosomes and endosomes.

In order to attain better separation of these organelles the lysosomal and endosome containing particulate fractions were layered onto a discontinuous sucrose gradient of the type described in b). Whilst this protocol resulted in good resolution of the lysosomal and particulate fractions it proved to be impractical for the fractionation experiments involving <sup>14</sup>C-labelled chelators as the specific activity of these compounds was not sufficient to enable detection in the gradient fractions. Therefore it was decided to utilise the procedure described below for all subsequent fractionation experiments.

## **Experimental Procedure**

### **1) HOMOGENISATION**

50 x 10<sup>6</sup> K562 cells were suspended in 2.5mls of chilled homogenization buffer (HB: 0.25M sucrose, 5mM TrisHCl pH 7.2, 0.2mM EDTA supplemented with 1mM PMSF and 100U/ml aprotinin) and disrupted by sonication (5μ x 15 seconds, twice) (Roberts, 1990). Total cell lysis was established by light microscopy.

## 2)SUBCELLULAR FRACTIONATION

Subcellular fractionation was carried out according to isolation procedure 2 described by Bakkeren and coworkers (Bakkeren et al, 1987) with modifications. This procedure is summarised in Figure 20. All manipulations were carried out at 4°C.

The cell homogenates were centrifuged for 8 minutes at 2000 rpm to remove the nuclear fraction and unbroken cells. The pellet was resuspended in 2.5ml HB, the sonication process repeated and the homogenate centrifuged as before. The supernatants were pooled and the pellet was called the nuclear fraction. The pooled supernatants were centrifuged at 11,000 rpm in a Beckman SW55 rotor and a Beckman L8M ultracentrifuge for 8 minutes and the resulting pellet was resuspended, washed and called the mitochondrial fraction. The supernatant was centrifuged at 17,400 rpm for 20 minutes and the pellet called the lysosomal fraction. The supernatant was centrifuged at 40,000rpm for 60 minutes to give a final pellet called the particulate fraction and the final supernatant containing the cell cytosol. This fraction was further subdivided into high and low molecular weight (HMW and LMW) fractions by centrifugation through a CF-25 filtration cone for 30 minutes at 3000 rpm. The retention size of the cone was 25000 daltons so low molecular weight substances such as ferrioxamine or CP94-Fe complex would pass through the cone whilst high molecular weight molecules such as ferritin would be retained.

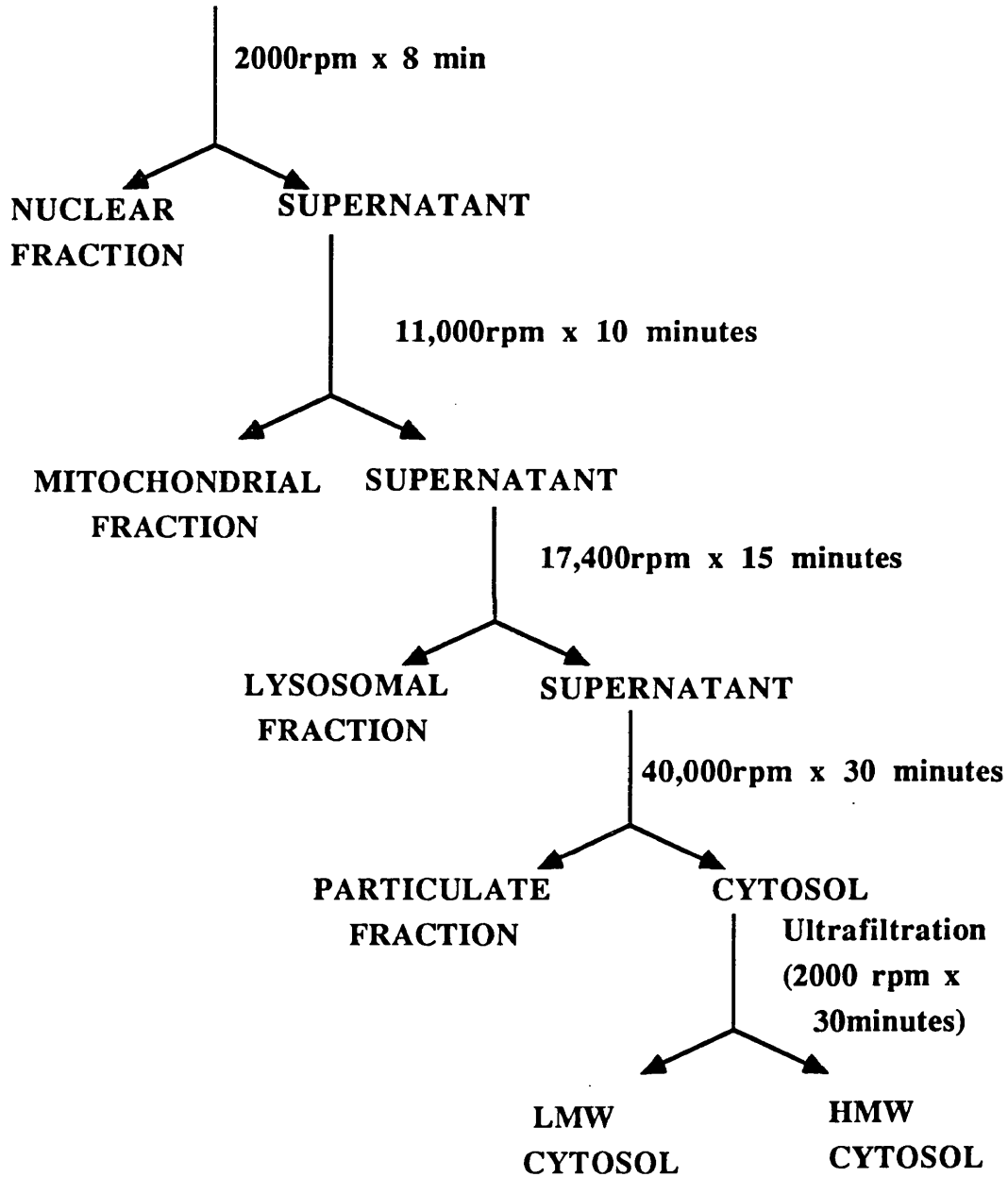
Each pellet was resuspended in HB to a final volume of 1ml and stored at -20°C until required for analysis.

## 3)ANALYTICAL PROCEDURES

The activity of the following enzymes was determined in each fraction using the protocols described in Section 2.4.4: cytochrome c oxidase (mitochondria), 5'-nucleotidase (plasma membrane), NADPH cytochrome c reductase (endoplasmic reticulum) and  $\beta$  galactosidase (lysosomes). The amount of ferritin in each fraction was determined by ELISA as described in Section 2.4.4.

**FIGURE 20: FRACTIONATION PROCEDURE**

**K562 HOMOGENIZED IN 0.25M SUCROSE BUFFER**





The enzyme composition of each fraction is summarised in Table 6. The data represents the activity (enzymes) or amount (ferritin and protein) of each marker expressed as a percentage of the total in the cell homogenate from a minimum 5 separate experiments. The preincubation of cells with iron chelators for up to 24 hours did not affect the subcellular distribution of the marker enzymes.

Since the lysosomal and particulate fractions displayed almost identical composition of marker enzymes these fractions were pooled in future experiments.

### **4.3 SUBCELLULAR DISTRIBUTION OF [<sup>14</sup>C]CP94 AND [<sup>14</sup>C]DFO**

Having established a reproducible subcellular fractionation protocol the intracellular distribution of [<sup>14</sup>C]CP94 and [<sup>14</sup>C]DFO was examined. In these experiments fractionation was carried out at 2 time points, a short time point (20 minutes) when differences in the subcellular distribution of these compounds may be most obvious due to differences in the rate at which these chelators move across cell membranes (Section 3.2.), and a longer time point (4 hours) when it would be expected that differences in rate of membrane movement would have been resolved as it has previously been shown that equilibrium is attained between intracellular and extracellular chelator concentrations after one hour (Section 3.2).

#### **Experimental Procedures**

1.5 x10<sup>8</sup> K562 cells per test sample were incubated in RPMI 1640 medium, supplemented with 5% FCS, with 100µM [<sup>14</sup>C]CP94 or [<sup>14</sup>C]DFO at 37°C for 20 minutes or 4 hours. At the end of the incubation period cells were washed twice with PBS at 4°C and resuspended in HB and fractionated as described in Section 4.2.1. Each pellet was resuspended in HB to a final volume of 1ml and 200µl was added to 4ml of Hisafe liquid scintillant for β counting.

TABLE 6: DISTRIBUTION OF MARKER ENZYMES BETWEEN SUBCELLULAR FRACTIONS

ENZYMES	% IN FRACTIONS					
	Nuclear	Mitochondrial	Lysosomal	Particulate	LMW cytosol	HMW cytosol
5'Nucleotidase	18±2	41±6	21±1	17±3	N.D	1±0.5
Cytochrome c oxidase	8±2	75±2	7±1	4±2	N.D	4±1
β Galactosidase	10±2	21±3	32±2	30±1	N.D	4±1
NADPH Cytochrome c Reductase	5±1	37±2	29±3	23±3	N.D	6±0.5
Ferritin	1±2	1±1	4±1	2±1	N.D	92±1
Protein	6±2	12±1	14±1	11±1	45±5	12±1

N.D. = not detectable

K562 cells were homogenized and separated into nuclear, mitochondrial, lysosomal, and particulate fractions. The final cytosolic fraction was further separated into a high molecular weight (HMW cytosol) fraction and a low molecular weight (LMW cytosol) fraction by ultrafiltration.

## Results and Discussion

After 20 minutes incubation the cells had accumulated  $1130 \pm 141$  pmol [ $^{14}\text{C}$ ]CP94 and  $784 \pm 102$  pmol [ $^{14}\text{C}$ ]DFO. This corresponds to an intracellular concentration of  $75 \pm 9$   $\mu\text{M}$  CP94 and  $52 \pm 8$   $\mu\text{M}$  DFO. By 4 hours the amount of intracellular chelator had risen to  $1825 \pm 131$  pmol [ $^{14}\text{C}$ ]CP94 and  $3668 \pm 632$  pmol [ $^{14}\text{C}$ ]DFO corresponding to  $106 \pm 8$   $\mu\text{M}$  CP94 and  $244 \pm 63$   $\mu\text{M}$  DFO. When the cells were fractionated  $92.15 \pm 15.6$  % of the [ $^{14}\text{C}$ ]CP94 and  $98 \pm 7.84$  % of the [ $^{14}\text{C}$ ]DFO present in the intact cells was recovered.

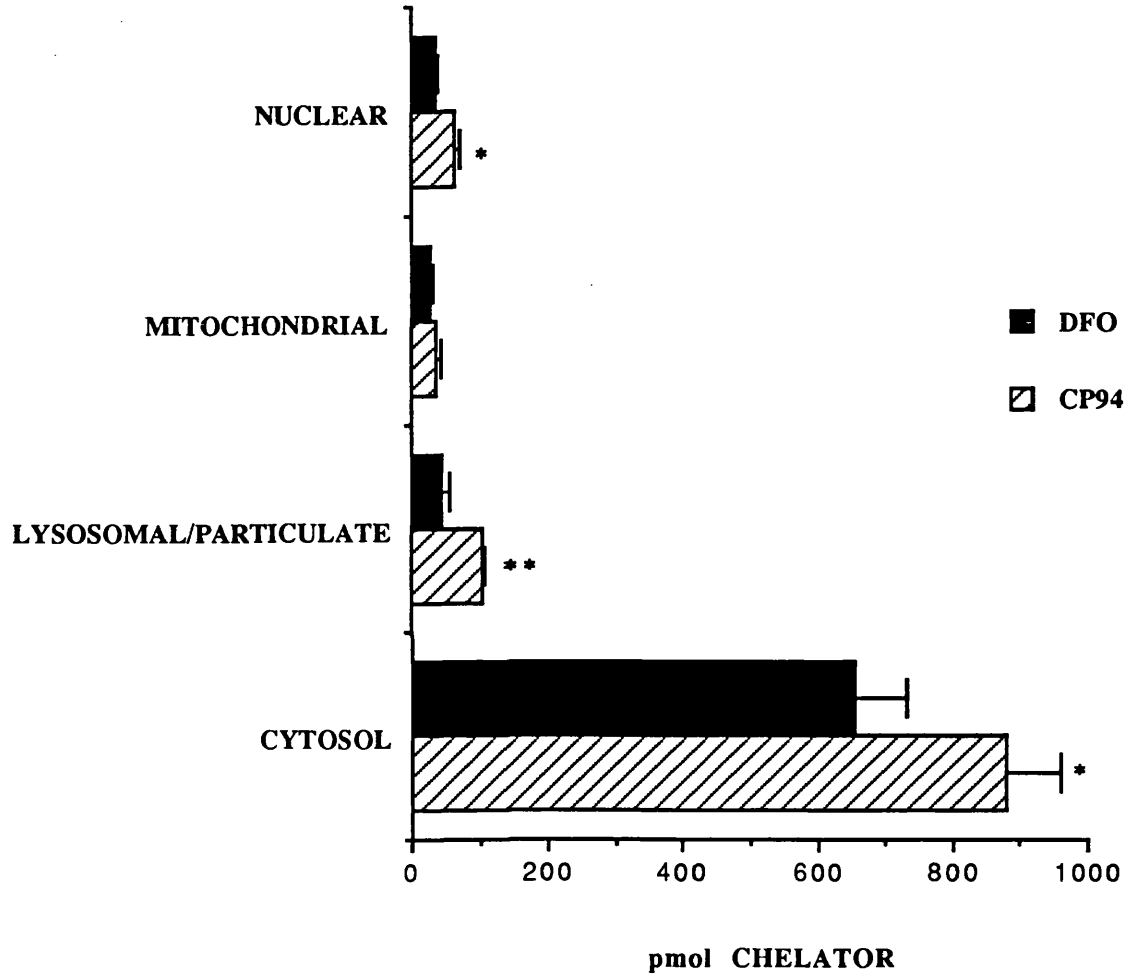
The intracellular distribution of the chelators at 20 minutes and 4 hours is shown in Figures 21 and 22. The majority of the  $^{14}\text{C}$ -label was associated with the cytosolic fraction in both CP94 and DFO treated cells at each timepoint. The amount of chelator associated with the nuclear, mitochondrial and lysosomal/particulate fractions increased, however, in a time dependent manner.

After 20 minutes incubation there was significantly more [ $^{14}\text{C}$ ]CP94 associated with the nuclear, lysosomal/particulate and cytosol fractions than [ $^{14}\text{C}$ ]DFO (Figure 21). The increased amount of CP94 in the nuclear and lysosomal/particulate fractions was not merely a consequence of the higher intracellular concentration of CP94 at this time (Section 3.2.2) since  $6 \pm 0.2$  % and  $12 \pm 1$  % of the intracellular  $^{14}\text{C}$ -label in CP94 cells is associated with the nuclear and lysosomal/particulate fractions respectively compared to  $4 \pm 0.5$  % and  $6 \pm 1$  % in DFO treated cells ( $p < 0.05$ ). This suggests that CP94 has more rapid access into these organelles than DFO.

When the subcellular distribution of [ $^{14}\text{C}$ ]CP94 and [ $^{14}\text{C}$ ]DFO was re-examined after 4 hours there were no significant differences between the amounts of each chelator associated with the nuclear, mitochondrial and lysosomal/particulate fractions, indicating that DFO has access into these organelles, but at a slower rate than CP94 (Figure 22). However there was significantly more [ $^{14}\text{C}$ ]DFO associated with the cytosolic fraction than [ $^{14}\text{C}$ ]CP94. This observation is consistent with the data discussed in Chapter 3 showing intracellular accumulation of [ $^{14}\text{C}$ ]DFO.

**FIGURE 21:**

**SUBCELLULAR DISTRIBUTION OF [<sup>14</sup>C]CP94  
AND [<sup>14</sup>C]DFO IN K562 CELLS AT 20 MINUTES**

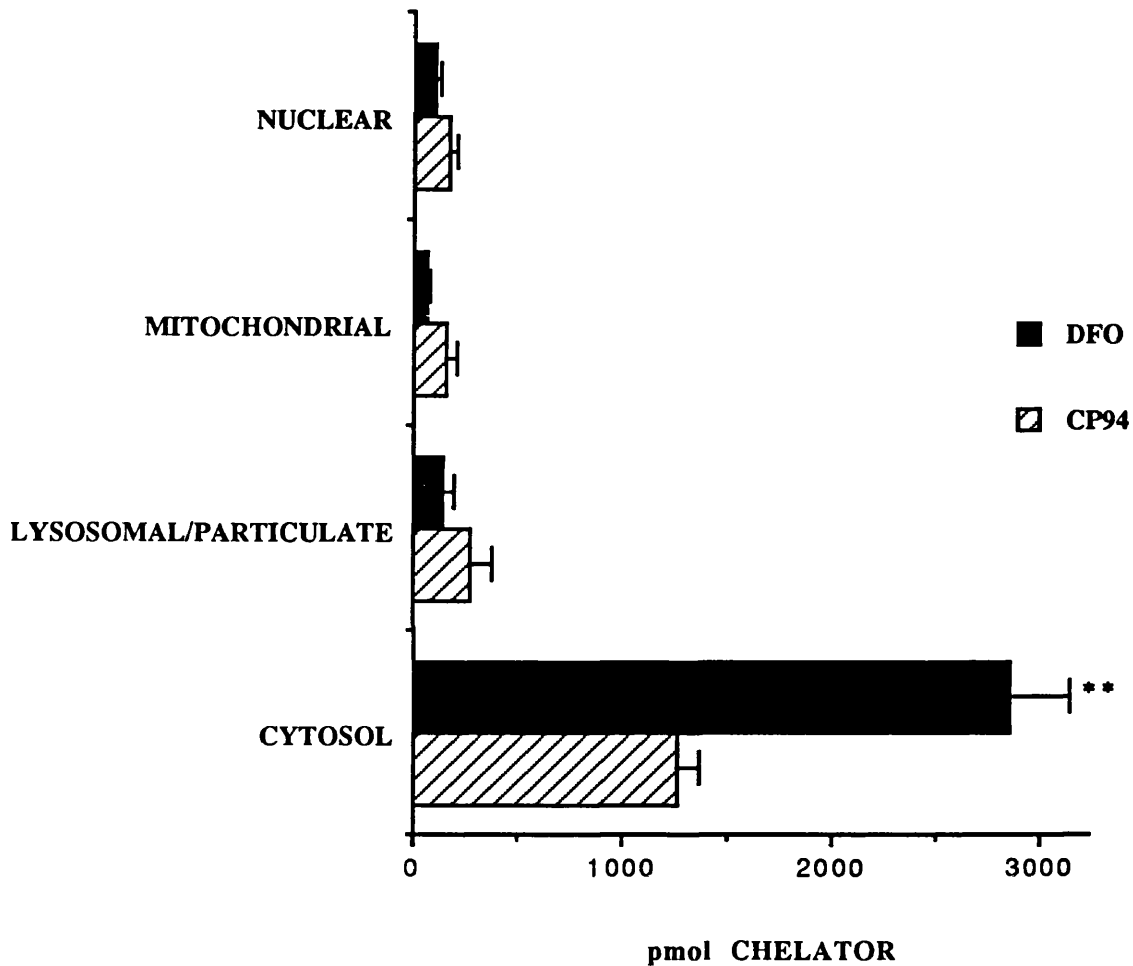


**LEGEND:**

K562 cells, incubated in the presence of 100 $\mu$ M [<sup>14</sup>C]CP94 or [<sup>14</sup>C]DFO for 20 minutes, were homogenised and separated into nuclear, mitochondrial, lysosomal, particulate and cytosolic fractions. The results represent the mean  $\pm$  S.E.M of 3 separate experiments. Significant differences in the subcellular distribution of [<sup>14</sup>C]CP94 and [<sup>14</sup>C]DFO at the p<0.05 (\*) and p<0.01 (\*\*) levels were determined using unpaired Students t tests.

FIGURE 22:

SUBCELLULAR DISTRIBUTION OF [<sup>14</sup>C]CP94 AND [<sup>14</sup>C]DFO IN K562 CELLS AT 4 HOURS



**LEGEND:**

K562 cells were incubated in the presence of 100 $\mu$ M [<sup>14</sup>C]CP94 or [<sup>14</sup>C]DFO for 4 hours and homogenised and fractionated as described for Figure 21. The results represent the mean  $\pm$  S.E.M of 3 separate experiments. Significant differences in the subcellular distribution of [<sup>14</sup>C]CP94 and [<sup>14</sup>C]DFO at the p<0.05 (\*) and p<0.01 (\*\*) levels were determined using unpaired Students t tests.

## **4.4 SUBCELLULAR DISTRIBUTION STUDIES USING <sup>59</sup>Fe**

### **4.4.1 Effect of 100µM IBE CP94 and DFO on the Subcellular Distribution of <sup>59</sup>Fe Delivered by Receptor Mediated Endocytosis.**

In order to determine whether the subcellular distribution of the chelators correlates with their relative abilities to mobilise iron from subcellular organelles the effect of the chelators on the subcellular distribution of <sup>59</sup>Fe, delivered by the receptor mediated endocytosis of transferrin, was investigated.

#### **Experimental Procedure**

The procedure used in these experiments is summarised in Figure 23.  $1 \times 10^8$  K562 cells per test sample were washed twice in PBS at 4°C and resuspended in prechilled 1% BSA, RPMI 1640 at 4°C. After 10 minutes 100µg/ml <sup>59</sup>Fe transferrin (Section 2.4.1) was added and cells were incubated for a further 30 minutes at 4°C to allow saturation of cell surface transferrin receptors. Excess transferrin was then removed by washing the cells three times with ice cold PBS.

At T=0 the cells were resuspended in 10ml 1% BSA, RPMI 1640 at 37°C containing 100µM IBE CP94 or DFO or an equivalent amount of PBS for controls. After 20 minutes and 4 hours the cells were harvested and the supernatant retained. Cells were washed 3 times with ice cold PBS and resuspended in 2.5ml HB prior to homogenisation and subcellular fractionation by differential centrifugation as described in Section 4.2.1

Each pellet was resuspended to a final volume of 1ml with HB and the amount of radioactivity determined using a gamma counter.

The amount of ferritin in each sample was assayed using an ELISA system as described in section 2.4.4. From the radioactivity of the HMW cytosolic fraction and

**FIGURE 23:  
PULSE-CHASE LABELLING OF K562 CELLS WITH  
<sup>59</sup>Fe-TRANSFERRIN**

**K562 SUSPENDED IN 1% BSA/RPMI 1640**



**INCUBATE 10 MINUTES 4°C**



**+ 100µg/ml <sup>59</sup>Fe-TRANSFERRIN**

**INCUBATE 30 MINUTES 4°C**



**WASH 3X WITH ICE COLD PBS**



**RESUSPEND IN 1% BSA/RPMI 1640  
WITH 100µM IBE CP94, DFO OR PBS AT 37°C**



**INCUBATE AT 37°C**



**WASH 3X WITH PBS AT 4°C AND  
RESUSPEND IN 2.5ml CHILLED HB**

the specific activity of the  $^{59}\text{Fe}$ -transferrin complex, the amount of  $^{59}\text{Fe}$  ( $\mu\text{g}$ ) per  $\mu\text{g}$  of ferritin was calculated for each test sample.

## Results

Over the first 20 minutes incubation at  $37^\circ\text{C}$  approximately 50% of the  $^{59}\text{Fe}$  associated with control cells was released to the culture medium (Figure 24). Of the intracellular  $^{59}\text{Fe}$  approximately one third was associated with the nuclear, mitochondrial and lysosomal/particulate fractions, one third was in the LMW cytosolic fraction and the remainder was found in the HMW cytosolic fraction where it was possibly associated with ferritin (Figure 24).

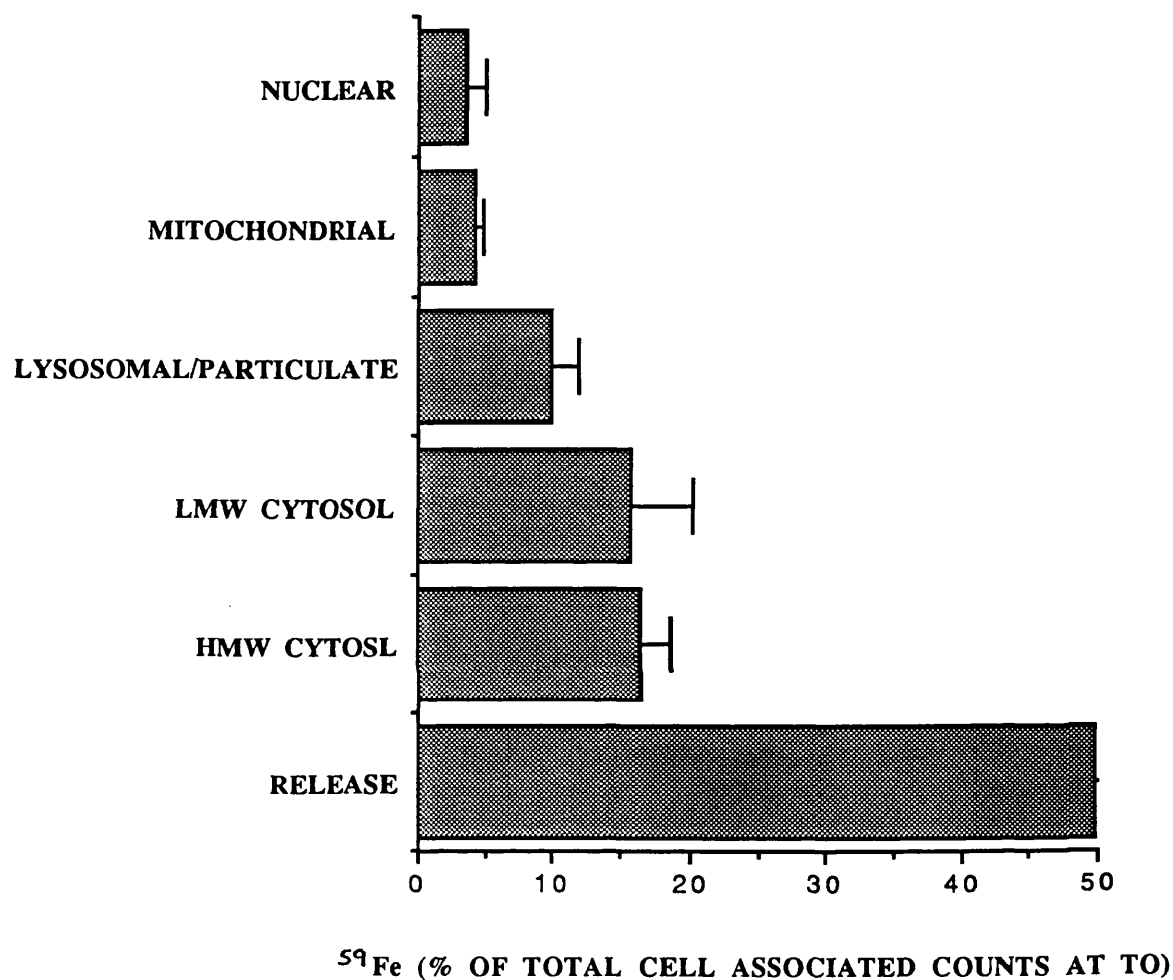
The presence of  $100\mu\text{M}$  IBE CP94 and DFO in the culture medium had marked effects on the subcellular distribution of  $^{59}\text{Fe}$ . After 20 minutes incubation there was significantly less  $^{59}\text{Fe}$  associated with the lysosomal/particulate and HMW cytosolic fractions in CP94 treated cells (Figure 25) when compared to controls. The radioiron content of the nuclear and mitochondrial fractions was also reduced but this did not reach statistical significance. In addition the  $^{59}\text{Fe}$  content of the LMW cytosol fraction was significantly increased.

There was also a trend of accumulation of  $^{59}\text{Fe}$  in LMW cytosolic fraction at the expense of the HMW fraction in DFO treated cells after 20 minutes incubation, however this was less marked and failed to reach statistical significance. When the subcellular distribution of the radioiron was re-examined after 4 hours (Figure 26) there was significant reduction in the  $^{59}\text{Fe}$  associated with the lysosomal/particulate and the HMW cytosolic fractions of both DFO treated cells and those which had been incubated with CP94. In addition the  $^{59}\text{Fe}$  content of nuclear, mitochondrial and LMW cytosol fraction was significantly reduced in CP94 treated cells and the amount of iron released from these cells was significantly enhanced above controls. By contrast the  $^{59}\text{Fe}$  in the LMW cytosolic fraction of DFO treated cells was significantly increased when compared with control cells and a less marked release of  $^{59}\text{Fe}$  was observed.



**FIGURE 24:**

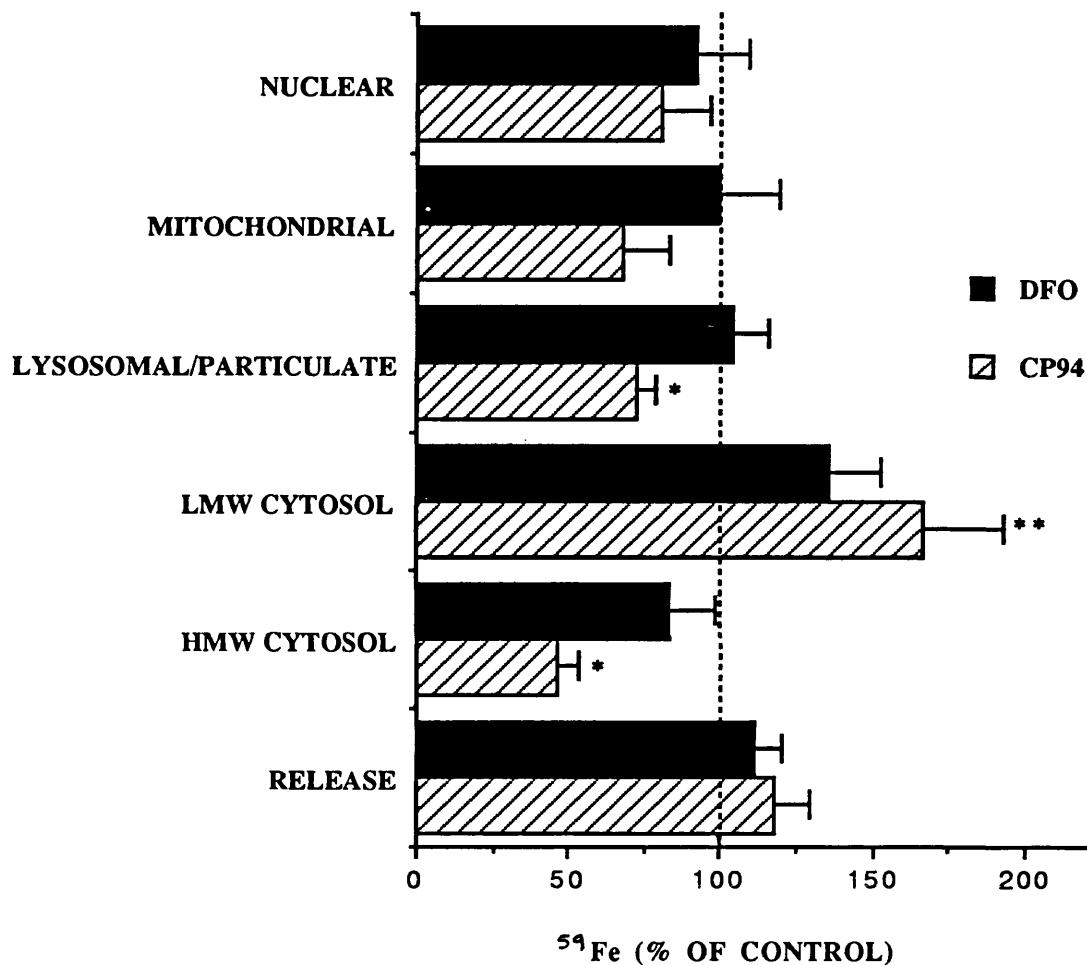
**DISTRIBUTION OF  $^{59}\text{Fe}$  IN CONTROL K562 CELLS AT 20 MINUTES.**



**LEGEND:**

K562 cells were labelled with  $^{59}\text{Fe}$ , washed and incubated at  $37^{\circ}\text{C}$  for 20 minutes as described in the text. The cells were homogenised and separated into nuclear, mitochondrial, lysosomal and particulate fractions. The final cytosolic fraction was further separated into a high molecular weight (HMW cytosol) fraction and a low molecular weight (LMW cytosol) fraction by ultrafiltration. The results are expressed as the percentage of total cell associated radioactivity at TO present in each fraction after 20 minutes incubation and represent the mean  $\pm$  S.E.M of 3 separate experiments.

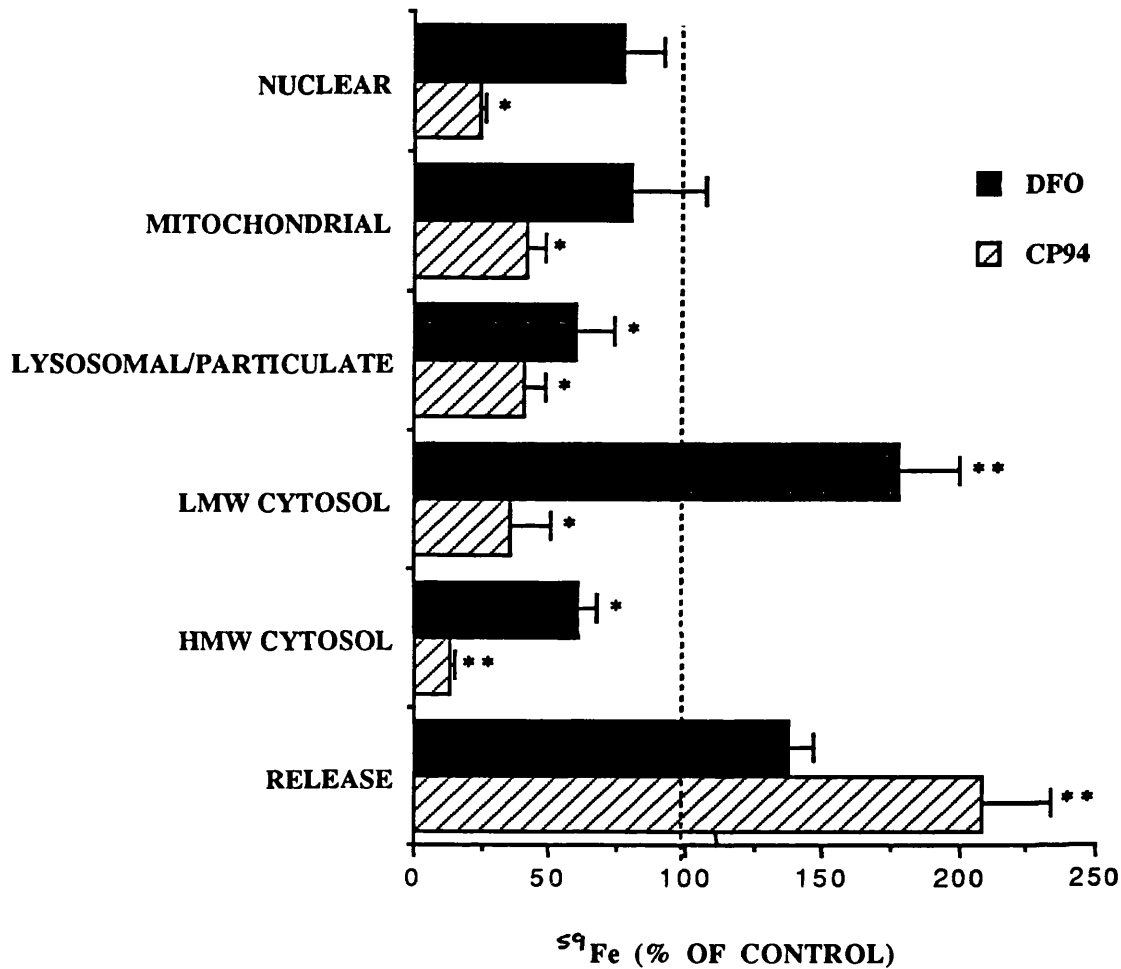
**FIGURE 25:**  
**EFFECT OF 100 $\mu$ M IBE ON DISTRIBUTION**  
**OF  $^{59}\text{Fe}$  AFTER 20 MINUTES**



**LEGEND:**

K562 cells were labelled with  $^{59}\text{Fe}$ , washed and incubated with 100 $\mu$ M IBE CP94 or DFO for 20 minutes as described in the text. The cells were homogenised and fractionated as indicated in Figure 24. The results are expressed as the percentage of radioactivity in each fraction as a percentage of control and represent the mean  $\pm$  S.E.M of 3 separate experiments. Significant differences between the percentage of radioactivity in fractions from control and chelator treated cells at the  $p < 0.05$  (\*) level were identified with the unpaired Students t test.

**FIGURE 26:**  
**EFFECT OF 100 $\mu$ M IBE ON DISTRIBUTION**  
**OF  $^{59}\text{Fe}$  AFTER 4 HOURS**



**LEGEND:**

K562 cells were labelled with  $^{59}\text{Fe}$ , washed and incubated with 100 $\mu$ M IBE CP94 or DFO for 4 hours as described in the text. The cells were homogenised and fractionated as indicated in Figure 24. The results are expressed as the percentage of radioactivity in each fraction as a percentage of control and represent the mean  $\pm$  S.E.M of 3 separate experiments. Significant differences between the percentage of radioactivity in fractions from control and chelator treated cells at the  $p < 0.05$  (\*) and  $p < 0.01$  (\*\*) levels were identified with unpaired Students t tests.

Treatment with CP94 produced a statistically significant reduction in the amount of  $^{59}\text{Fe}$  associated with ferritin compared with controls after 20 minutes incubation (Figure 27). A similar trend was observed in DFO treated cells but this failed to reach statistical significance. After 4 hours incubation the amount of  $^{59}\text{Fe}$  associated with ferritin was slightly reduced in all samples but no additional reduction in the chelator treated cells was observed (Figure 27).

#### 4.4.2 Mobilisation of Low Molecular Weight Iron by CP94 and DFO

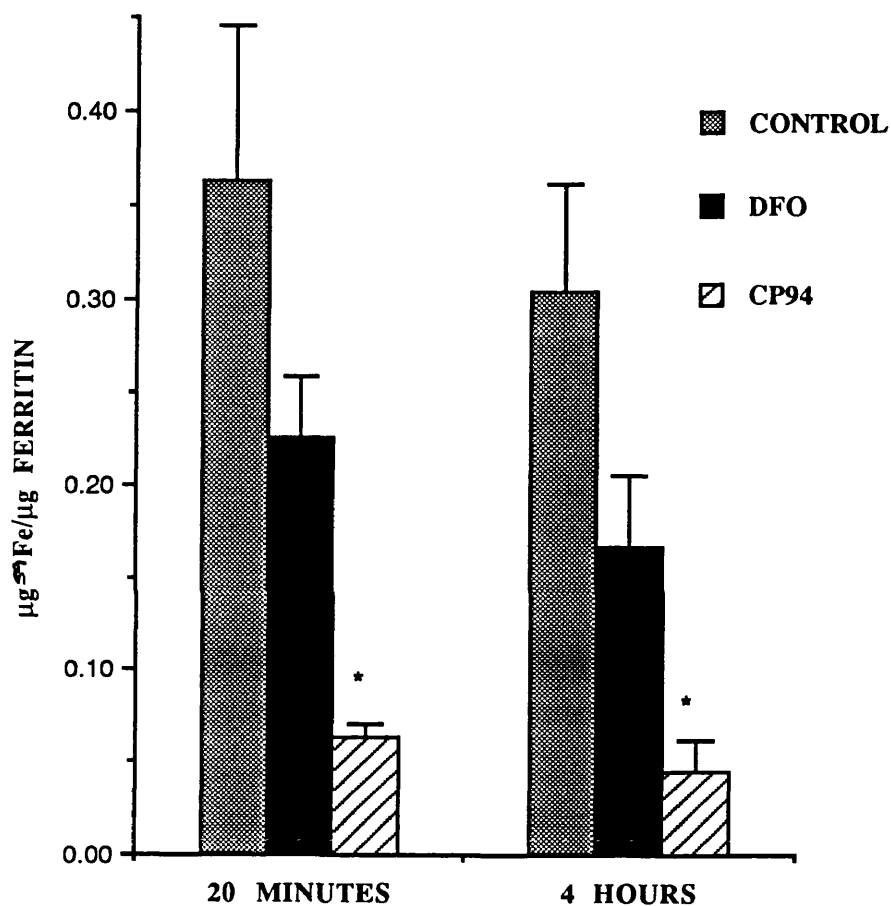
The previous experiment suggests that CP94 and DFO redistribute  $^{59}\text{Fe}$  to the LMW fraction at the expense of the other subcellular compartments. To investigate this further a detailed examination of the kinetics of formation and dissipation of this LMW  $^{59}\text{Fe}$  was performed. Due to the frequent and multiple time points required for this experiment it was not possible to carry out a full subcellular fractionation at each time point, therefore the intracellular organelles were rapidly separated from the cytosol which was then separated into LMW and HMW fractions as described below.

#### **Experimental Procedure**

K562 cells were pulsed with  $100\mu\text{g/ml}$   $^{59}\text{Fe}$ -transferrin and incubated with  $100\mu\text{M}$  IBE CP94 or DFO for up to 4 hours as described in Section 4.4.1 (Figure 23). At the time points shown aliquots were taken from each test sample and the cells were homogenised and lysed as previously described (Section 4.2). The cytosolic fraction was obtained by centrifuging the post nuclear supernatant onto a 60% sucrose cushion at 40,000rpm for 30 minutes to remove the organelles in a Beckman SW55 swinging bucket rotor using a Beckman L8M Ultracentrifuge. The LMW fraction of the cytosol was then isolated by spinning the samples through a CF-25 filtration cone (Section 4.2). The radioactivity of each fraction was obtained using a gamma counter.

**FIGURE 27:**

**INCORPORATION OF  $^{59}\text{Fe}$  INTO FERRITIN IN CONTROL AND CHELATOR TREATED K562 CELLS**



**LEGEND:**

K562 cells were labelled with  $^{59}\text{Fe}$ , washed and incubated in the presence or absence of 100µM IBE CP94 or DFO for up to 4 hours as described in the text. The cells were homogenised and fractionated as indicated in Figure 4.5. The amount of ferritin in the HMW cytosolic fraction was determined with an ELISA system. The results represent the mean  $\pm$  S.E.M of 3 separate experiments and significant differences between control and chelator treated cells at the  $p < 0.05$  level (\*) were determined with the unpaired Students t test.

## Results

In control cells 25% of the total radio-iron was found to be in a LMW form after 10 minutes incubation, by 20 minutes this had decreased to approximately 10% and remained constant over the rest of the experiment. Incubation of cells with CP94 or DFO resulted in an increase in the percentage of radioiron in the LMW cytosolic fraction (Figure 28).

In CP94 treated cells the amount of LMW iron rapidly rose to peak at almost 250% of control by 15 minutes and then decreased gradually over the remainder of the incubation period. The increase in LMW iron in DFO treated cells was slower and did not peak until 60 minutes, but then stayed almost constant for the remainder of the incubation period (Figure 28)

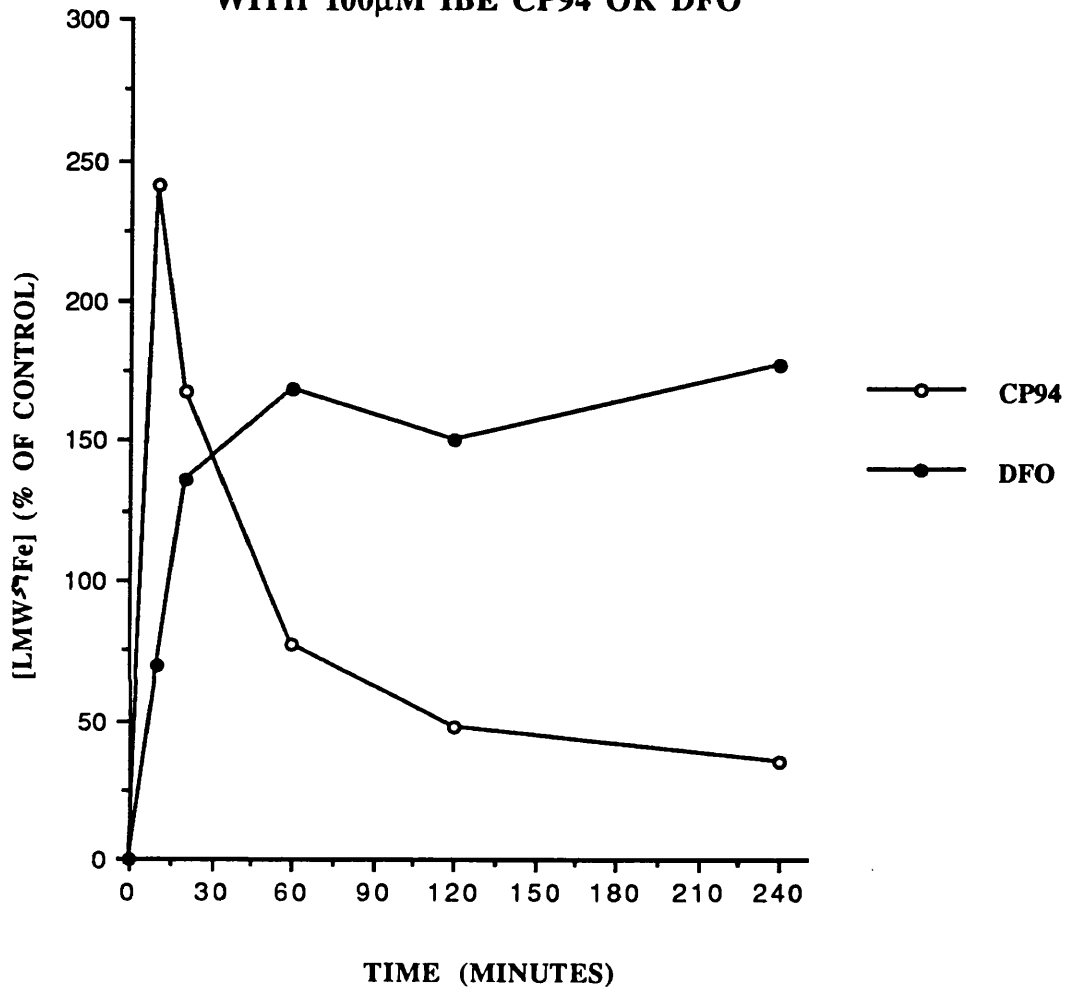
### 4.4.3 Discussion

These experiments suggest that CP94 is more effective at rapidly mobilising  $^{59}\text{Fe}$  from intracellular organelles than DFO. After 20 minutes incubation there was less  $^{59}\text{Fe}$  in the nuclear, mitochondrial and lysosomal/particulate fractions of CP94 treated cells than either control cells (Figure 24) or those treated with DFO (Figure 25). This was particularly marked in the lysosomal/particulate fraction and may be a result of CP94 entering endosomes and chelating iron as it is released from transferrin before it is passed into the cytosol.

When the subcellular distribution of the  $^{59}\text{Fe}$  was re-examined at 4 hours (Figure 26) there was significantly less  $^{59}\text{Fe}$  present in the lysosomal/particulate fraction of chelator treated cells than controls. However the  $^{59}\text{Fe}$  content of the nuclear and mitochondrial fractions of cells incubated with DFO did not significantly differ from controls, in contrast to CP94 treated cells. A possible explanation for this is that chelation of  $^{59}\text{Fe}$  from the cytosolic LMW pool reduces the amount of  $^{59}\text{Fe}$  available for incorporation into the nuclear and mitochondrial fractions. Therefore, under these conditions, CP94 will be more effective at inhibiting the incorporation of  $^{59}\text{Fe}$  into

**FIGURE 28:**

**LMW  $^{59}\text{Fe}$  IN K562 CELLS TREATED WITH  $100\mu\text{M}$  IBE CP94 OR DFO**



**LEGEND:**

K562 cells were labelled with  $^{59}\text{Fe}$ , washed and incubated in the presence or absence of  $100\mu\text{M}$  IBE CP94 or DFO for up to 4 hours as described in the text. The cells were homogenised and organelles removed by ultracentrifugation. The cytosol was further separated into a high and low molecular weight fraction by ultrafiltration. The results are expressed as the percentage of radioiron in the low molecular weight fraction as a percentage of control at each time point. The data are the mean  $\pm$  S.E.M of 2 separate experiments with duplicates at each point.

these fractions than DFO because cytosolic concentrations of CP94 are initially greater than those of DFO (Figure 25). By contrast after 4 hours intralysosomal  $^{59}\text{Fe}$  may result from the turnover of cytosolic ferritin. After 4 hours incubation the intralysosomal concentrations of DFO and CP94 are approximately equal (Figure 22). Therefore after this time period DFO would be as capable as CP94 of chelating intralysosomal iron.

CP94 appears to be more efficient at inhibiting the incorporation of iron into ferritin than DFO (Figure 28). This is possibly due to the higher cytosolic concentrations of CP94 present when iron is released from the endosome into the LMW pool for incorporation into ferritin (Section 4.2). However the amount of  $^{59}\text{Fe}$  in ferritin does not decrease over the 4 hour incubation period (Figure 27) in chelator treated cells suggesting that direct chelation from ferritin may not be a major route of iron mobilisation for the HPOs.

Both CP94 and DFO redistributed iron into the LMW cytosolic fraction at the expense of the HMW cytosolic fraction. The LMW cytosolic fraction includes intracellular  $^{59}\text{Fe}$  bound to CP94 or DFO. The amount of LMW iron in CP94 treated cells rose rapidly and then gradually decreased as the CP94-Fe complex diffused out of the cell (figure 28). LMW iron also increased in DFO treated cells and reached a peak at 1hr. However, the amount of LMW iron in DFO treated cells did not diminish over the remaining experimental period. This most likely represents  $^{59}\text{Fe}$  in the form of FO which will be retained within the cell and efflux very slowly as shown in the experiments in Chapter 3.

#### **4.5 EFFECT OF PREINCUBATION WITH CP94 AND DFO PRIOR TO LOADING CELLS WITH $^{59}\text{Fe}$ -TRANSFERRIN**

In the experiments described above  $^{59}\text{Fe}$  was introduced to the cell concurrently with the chelators. Therefore the ability of CP94 and DFO to modify the



intracellular distribution of the  $^{59}\text{Fe}$  were influenced by the relative rate at which the chelators entered the cell.

To investigate whether factors other than membrane permeability influenced the relative abilities of CP94 and DFO to redistribute intracellular iron the effects of the chelators on the subcellular distribution of  $^{59}\text{Fe}$  when intracellular concentrations of the chelators were already established have been investigated.

## Procedure

$1 \times 10^8$  K562 cells per sample were incubated for 4 hours in the presence of  $100\mu\text{M}$  IBE CP94 or DFO in RPMI 1640 medium containing 1% BSA. For the final 30 minutes of this incubation period the cells were incubated at  $4^\circ\text{C}$  with  $100\mu\text{g/ml}$   $^{59}\text{Fe}$  transferrin and the cells were then washed and resuspended in fresh medium containing CP94 and DFO at  $37^\circ\text{C}$  as described previously (Section 4.4.1). The samples were incubated at  $37^\circ\text{C}$  for 20 minutes and then washed 3 times with ice cold PBS and fractionated as described in section 4.2.

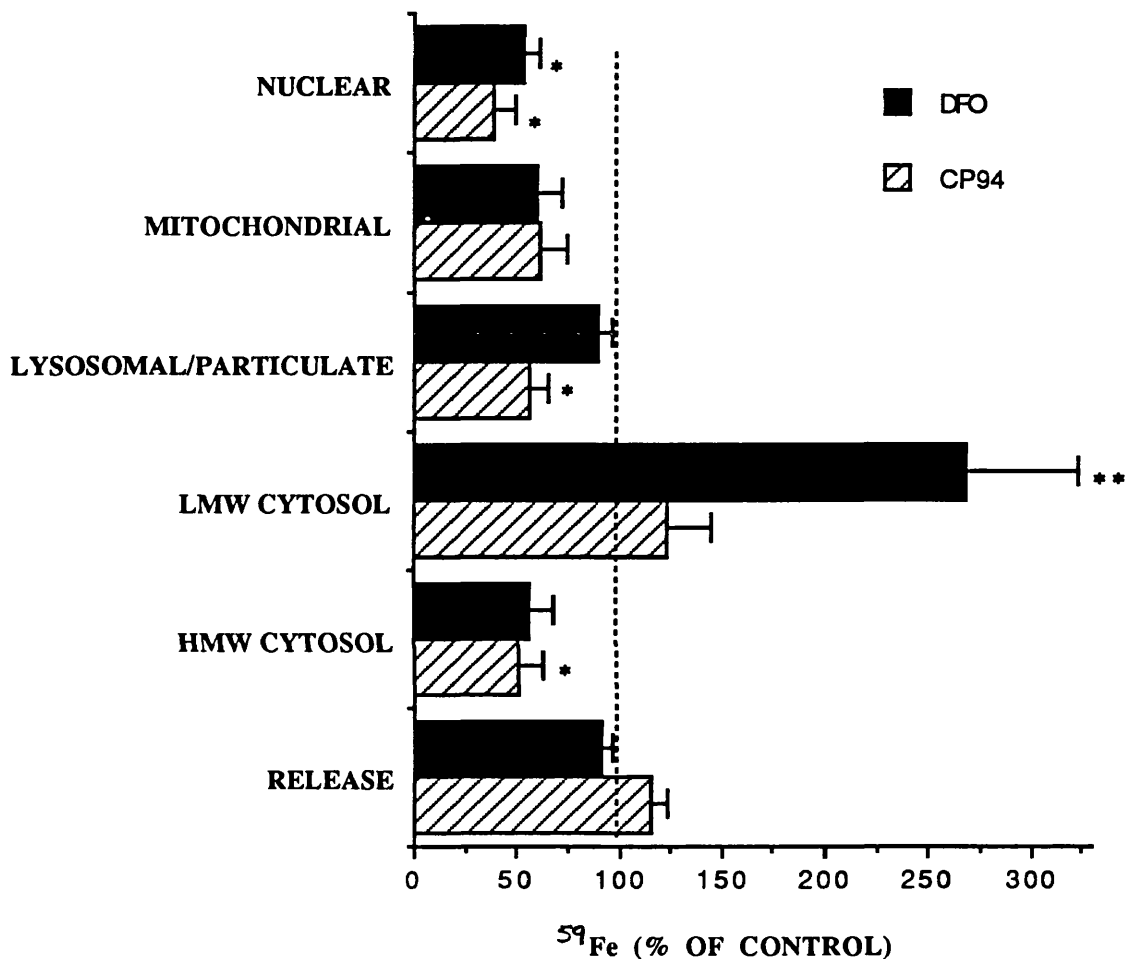
## Results and Discussion

When substantial intracellular chelator concentrations were already established there was little difference in the relative abilities of CP94 and DFO to redistribute intracellular  $^{59}\text{Fe}$  (Figure 29). As observed previously the radioiron was redistributed to the LMW cytosolic fraction, at the expense of the organelles and the HMW cytosolic fraction. The  $^{59}\text{Fe}$  content of the lysosomal/particulate fraction in CP94 treated cells was significantly less than control or DFO treated cells and may indicate that CP94, unlike DFO, can chelate intraendosomal iron.

There was a significant accumulation, in excess of control, of  $^{59}\text{Fe}$  in the LMW cytosolic fraction that was not apparent in CP94 treated cells. As observed previously this is probably due to intracellular accumulation of  $^{59}\text{Fe}$ -FO as a result of the slow rate at which this chelate exits the cell.

**FIGURE 29:**

**DISTRIBUTION OF  $^{59}\text{Fe}$  AT 20 MINUTES AFTER 4 HOURS PREINCUBATION WITH CP94 AND DFO**



**LEGEND:**

K562 cells were preincubated at 37°C with 100µM IBE CP94 or DFO for 4 hours. For the final 30 minutes of incubation cells were incubated at 4°C with  $^{59}\text{Fe}$  transferrin. Samples were washed and reincubated for a further 20 minutes at 37°C then homogenised and fractionated as indicated in Figure 24. The results are expressed as the percentage of radioactivity in each fraction as a percentage of control at each time point and represent the mean  $\pm$  S.E.M of 3 separate experiments. Significant differences between the percentage of radioactivity in fractions from control and chelator treated cells at the  $p < 0.05$  (\*) and the  $p < 0.01$  (\*\*) levels were identified with the Students t test.

## **4.6 GENERAL DISCUSSION**

Subcellular fractionation by differential centrifugation has indicated that a large proportion of the cell-associated  $^{14}\text{C}$ -label, accumulated during incubation of K562 cells with [ $^{14}\text{C}$ ]CP94 or [ $^{14}\text{C}$ ]DFO is recovered in the cytosol. Whilst there was a time dependent accumulation of both chelators within the organelle fractions, CP94 entered intracellular organelles significantly more rapidly than DFO (Figures 21 and 22).

To determine whether the subcellular distribution of the chelators was paralleled by their relative ability to mobilise iron from subcellular organelles cells were loaded with  $^{59}\text{Fe}$ . In these experiments  $^{59}\text{Fe}$  was introduced into the cell concurrently with the chelators. Therefore the relative abilities of CP94 and DFO to mobilise intracellular iron were influenced by the rate at which the chelator enters into the cell. Under these conditions CP94 was more efficient at redistributing intracellular  $^{59}\text{Fe}$  delivered by the receptor mediated endocytosis of transferrin than DFO (Figure 25).

Both CP94 and DFO redistributed  $^{59}\text{Fe}$  into the LMW cytosolic fraction at the expense of the HMW cytosolic fraction (Figures 27 and 28). In these studies it has been assumed that the  $^{59}\text{Fe}$  in this fraction was associated with ferritin. However whilst analysis by ELISA showed that over 90% of intracellular ferritin was present in the HMW cytosolic fraction (Table 6) these experiments have not conclusively demonstrated that the  $^{59}\text{Fe}$  was bound exclusively to this protein. Ideally immunoprecipitation experiments should be performed to confirm this.

It is clear from these experiments that CP94 has more rapid access into intracellular organelles than DFO resulting in enhanced mobilisation of intracellular iron. This is highlighted by the observation that the  $^{59}\text{Fe}$  content of the lysosomal/particulate fraction after 20 minutes at  $37^\circ\text{C}$  was consistently lower in CP94 treated cells than controls or those cells treated with DFO. This suggests that CP94 may enter endosomes and chelate intraendosomal iron, the resulting CP94-Fe complex

would then be released from the cell by exocytosis. However, since the transferrin containing endosome has a recycling time of only 5-10 minutes it is unlikely that effective concentrations of DFO could accumulate within the vesicle during this period.

When substantial intracellular chelator concentrations were already established by preincubation of the cells with chelators there was little difference between the relative abilities of CP94 and DFO to redistribute  $^{59}\text{Fe}$  into the LMW cytosolic fraction at the expense of the nuclear, mitochondrial and HMW cytosolic fractions (Figure 29). However, as previously observed, there was less  $^{59}\text{Fe}$  in the lysosomal/particulate fraction of CP94 treated cells than cells incubated with DFO. This reiterates the previous finding that CP94 may be able to chelate intraendosomal  $^{59}\text{Fe}$ .

These data suggest that whilst the primary site of iron chelator action appears to be the LMW cytosolic pool, chelator access to other intracellular iron pools is limited only by the rate at which the chelator crosses biological membranes. Such membrane transit is in turn dependent upon the physicochemical properties of the chelator.

**CHAPTER 5: EFFECT OF DFO AND THE HYDROXYPYRIDINONES  
ON CELL PROLIFERATION**

## **5.1 INTRODUCTION**

In Chapters 3 and 4 the ability of CP94 and DFO to access intracellular iron pools has been compared and contrasted. It has been shown that the entry of CP94 into K562 cells and subcellular organelles is more rapid than that of DFO. The potential of iron chelators to modify intracellular iron dependent metabolism would be expected to be influenced by their ability to enter cells and compete with cellular iron pools and iron transport mechanisms, therefore 3-HP-4-ones such as CP94 may affect cell function in an alternative way to DFO. In this chapter the effects of iron chelators on one aspect of cell function which is assumed to be iron dependent, namely cellular proliferation, has been investigated.

Iron deprivation has profound effects on cell growth and division (Titeux et al, 1984; Taetle et al, 1985). DFO has been demonstrated to inhibit the proliferation of normal human haemopoietic cells (Lederman et al, 1984), a variety of malignant cell lines (Foa et al, 1986; Blatt et al, 1987) and human bone marrow neuroblastoma cells (Becton et al, 1988). Additionally DFO has been shown to have anti-tumour activity in acute neonatal leukemia (Estrov et al, 1987).

There remains some debate over the exact mechanisms by which iron chelators exert their anti-proliferative effects. Incubation of cells with micromolar concentrations of DFO leads to cessation of DNA synthesis (Hoffbrand et al, 1976) and a blockade in cell cycle at the G<sub>1</sub>/S border (Lederman et al, 1984). Evidence suggests that competition with ribonucleotide reductase for iron is the causative mechanism (Ganeshaguru et al, 1980). This enzyme is responsible for the free radical mediated reduction of ribonucleotides to deoxyribonucleotides, the rate limiting step in DNA synthesis (Section 1.2.5). However, DFO has also been demonstrated to inhibit cellular proliferation independently of DNA synthesis in some cellular models (Reddel et al, 1985; Bomford et al, 1986) suggesting that other iron dependent cellular mechanisms may be involved (Sussman et al, 1989).

The experiments that follow have therefore compared the effects of CP94 and other HPOs with DFO on cell cycle arrest and subsequent cycle synchronisation. In addition the relationships between chelator concentration and relative effects on cell cycle, cell proliferation and ribonucleotide reductase activity were investigated.

## **5.2 EFFECT OF CP94 AND DFO ON CELL CYCLE KINETICS**

The initial studies in this section examined the relative abilities of CP94 and DFO to arrest cell cycle. Since K562 cells express a large number of transferrin receptors (Bomford et al 1986), these cells may be relatively insensitive to the antiproliferative effects of the chelators. Therefore K562 cells were compared with Daudi Burkitts lymphoma cells and mitogen stimulated human peripheral blood lymphocytes (PBL) to determine their relative sensitivities to cell cycle arrest by the chelators.

### **5.2.1 Dose Response Effect of DFO and CP94 on K562 and Daudi Cell Cycle**

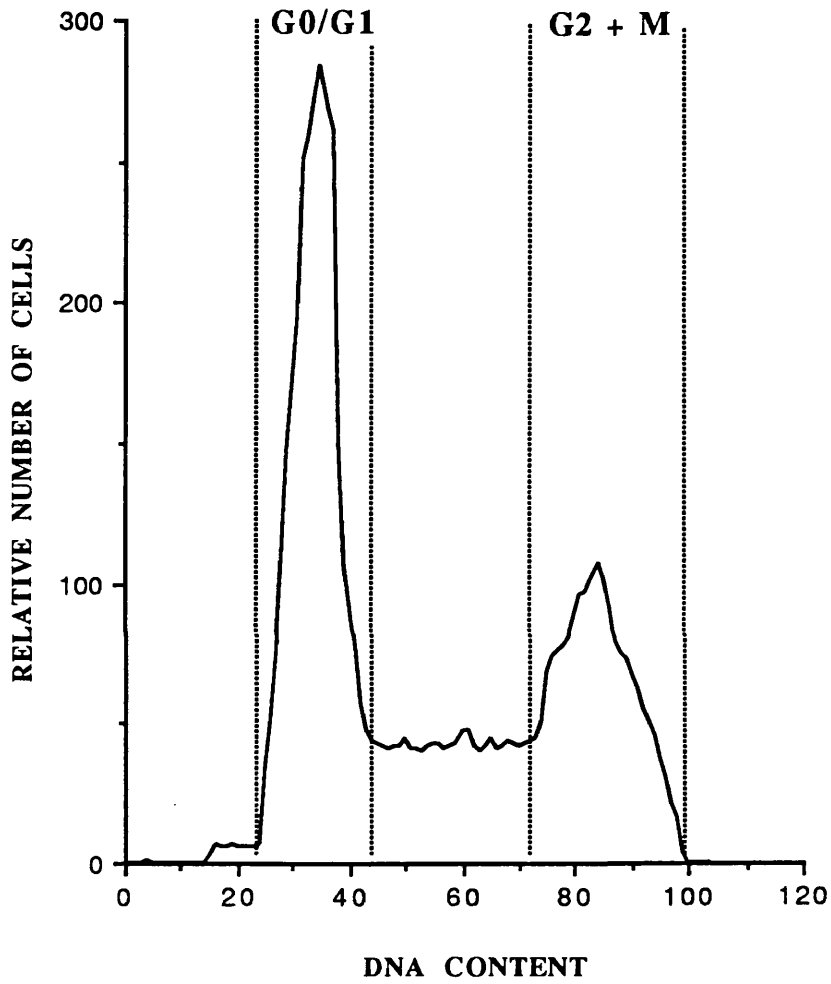
#### **Experimental Procedure**

K562 and Daudi cells in exponential growth were cultured with CP94 or DFO at concentrations of 3-100 $\mu$ M IBE for 24 hours. At the end of this time samples containing approximately  $5 \times 10^5$  cells were stained with propidium iodide for DNA cell cycle analysis as described in Section 2.4.2. using an EPICS CS flow cytometer (Coulter).

A typical DNA histogram for control cells is shown in Figure 30. The abscissa shows the DNA content in arbitrary units whilst the ordinate gives the frequency of cells with a given DNA content. In an asynchronous population of diploid cells two peaks can be distinguished: the first with a DNA complement of  $n$  representing the cells in  $G_0$  and  $G_1$  phase of the cell cycle, and the second, with a DNA content of  $2n$ ,

**FIGURE 30:**

**FLOW CYTOMETRIC DNA HISTOGRAM FOR CONTROL K562 CELLS**





containing cells in both G<sub>2</sub> and M phases. Cells with an intermediate DNA content (S phase) are registered between the two peaks.

Control cells were used as a diploid standard to establish a consistent location (channel number) of the G<sub>0</sub>/G<sub>1</sub> peak with the G<sub>2</sub>/M peak being twice this number. The proportion of cells in each cell cycle phase were obtained from planimetric analysis of the DNA histograms assuming a Gaussian distribution of the G<sub>1</sub> and G<sub>2</sub>+M peaks and attributing the remaining area to cells in S phase as described by Barlogie et al (1976).

## Results

Figure 31 shows typical DNA histograms obtained by flow cytometry of K562 cells cultured for 24h in the presence or absence of 100µM IBE CP94 or DFO. In control cultures approximately 45% of cells were in G<sub>1</sub> phase, 27% were in S phase and the remainder in G<sub>2</sub>+M phases, however the chelator treated cell populations exhibited a block in late G<sub>1</sub> phase with a concomitant decrease in the proportion of cells in G<sub>2</sub>+M phase.

The blockade of cell cycle was dose dependent and plateaued at 100µM IBE. Iron-saturation of the chelators prior to addition to the cell cultures abrogated the inhibitory effects of the chelators on cell cycle. Dose responses for CP94 and DFO are shown in Table 7 and Table 8 for K562 and Daudi cells respectively.

In K562 cells treated for 24 hours with chelator concentrations below 10µM IBE there was a significant accumulation of cells in G<sub>2</sub>/M phase. In separate experiments cytopins (Section 2.3.7) were prepared from cells which had been exposed to low concentrations of DFO or CP94 for 24h. Cytological examination after staining with haematoxylin revealed a higher proportion of both polyploid and mitotic cells in the chelator treated populations than in the control population (Table 9).

**FIGURE 31:**

**DNA HISTOGRAMS FOR K562 CELLS TREATED  
WITH 100 $\mu$ M IBE DFO AND CP94**

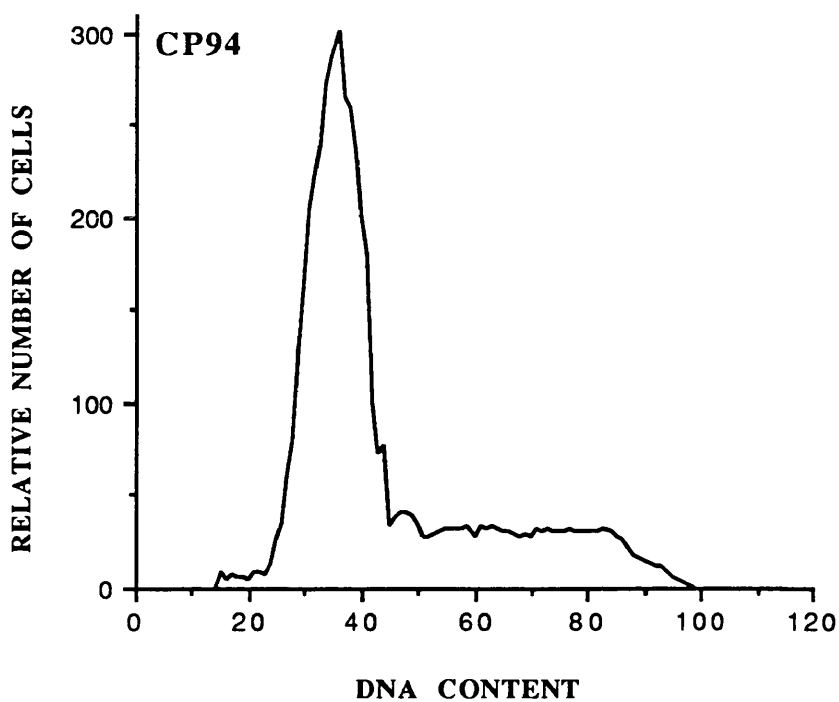
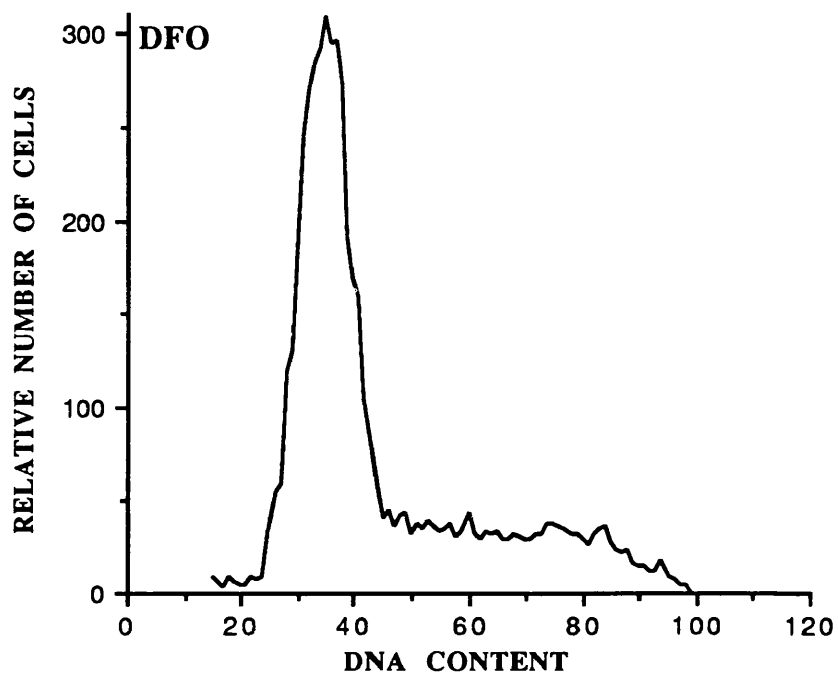


**TABLE 7: EFFECTS OF DFO AND CP94 ON  
K562 CELL CYCLE KINETICS**

Chelator Concentration		% of cells in phase		
$\mu$ M	IBE	G <sub>0</sub> /G <sub>1</sub>	S	G <sub>2</sub> /M
	Control	47±1	24±3	26±2
DFO	3	46±3	20±3	34±1*
	10	49±4	23±1	29±1
	33	55±2*	20±2	24±3
	100	61±2**	18±2	16±2*
CP94	3	45±1	21±2	34±1*
	10	46±5	23±3	31±3
	33	54±2*	22±3	20±4
	100	66±3**	16±1*	15±2*
FO	100	48±1	20±2	31±3
CP94-Fe	100	49±3	21±1	30±3

K562 cells were incubated with DFO or CP94 or their preformed iron saturated complexes at the concentrations shown for 24 hours. Cell cycle status was assessed by flow cytometry after staining with propidium iodide. Results are expressed as the percentage of cells in each phase of the cell cycle and represent the mean  $\pm$  S.E.M of 5 independent experiments in triplicate. Significant differences in the cell cycle kinetics between control and chelator treated cells were identified at the  $p < 0.05$  (\*) and  $p < 0.01$  (\*\*) levels using unpaired Students t tests.

**TABLE 8: EFFECTS OF DFO AND CP94 ON  
DAUDI CELL CYCLE KINETICS**

Chelator Concentration		% of cells in phase		
		G <sub>0</sub> /G <sub>1</sub>	S	G <sub>2</sub> /M
Control		48±3	25±2	22±2
DFO	3	57±4	22±2	22±2
	10	57±2	22±1	22±1
	33	64±1*	22±2	13±2**
	100	65±2**	22±2	12±2***
CP94	3	54±3	21±1	24±1
	10	55±3	26±2	20±2
	33	66±2***	23±1	12±1***
	100	65±2**	23±2	13±1***
FO	100	48±2	25±2	23±3
CP94-Fe	100	49±3	23±2	22±3

Daudi cells were incubated with CP94 or DFO or their preformed ion complexes for 24 hours. Cell cycle status was assessed by flow cytometry after staining with propidium iodide. The results are expressed as for Table 7 and represent the mean ± S.E.M of 3 separate experiments in triplicate. Significant differences in the cell cycle kinetics of control and chelator treated cells were identified with the unpaired Students t test at the p<0.05 (\*), p<0.01 (\*\*) and p<0.001 (\*\*\*) levels.

**TABLE 9:****EFFECT OF LOW CONCENTRATIONS OF DFO AND CP94 ON THE PERCENTAGE OF POLYNUCLEAR AND MITOTIC FORMS**

	% of mitotic cells	% of polynuclear cells	% of cells in G2/M phase
Control	3.92±0.3	0.25±0.1	26.10±2.1
DFO 3µM	5.79±0.2*	1.73±0.1***	29.04±0.7
10µM	7.58±0.4*	1.28±0.1*	30.07±1.2*
CP94 3µM	8.07±0.3***	1.57±0.1*	30.13±0.1*
10µM	8.83±0.67**	1.12±0.2*	27.64±0.6

K562 cells were incubated for 24 hours with CP94 or DFO. The proportion of mitotic and polynuclear cells was assessed by cytological examination after staining with haemotoxylin. The results are the mean ± S.E.M of 2 separate experiments in duplicate. Significant differences in the incidence of mitotic and polynuclear cells between control and chelator treated populations were identified at the  $p < 0.05$  (\*),  $p < 0.01$ (\*\*) and  $p < 0.001$ (\*\*\*) levels using unpaired Student t tests.

### 5.2.2 Effect of DFO and CP94 on the Cell Cycle of Mitogen Stimulated Peripheral Blood Lymphocytes

#### **Experimental Procedure**

Peripheral blood lymphocytes (PBL) from normal donors were isolated as described in Section 2.3.3 and cultured at  $0.5 \times 10^6$ /ml in RPMI 1640 supplemented with 10% FCS and 2 $\mu$ g/ml PHA. Concentrations of 3-30 $\mu$ M IBE CP94 or DFO were added at the initiation of the culture period. After 72 hours the lymphocytes were washed with PBS and fixed in 70% ethanol for flow cytometric analysis as previously described.

#### **Results**

When the cultures were initiated more than 99% of PBL were in G<sub>0</sub>/G<sub>1</sub> phase of the cell cycle. In the presence of PHA for 72 hours the cells were triggered into the cell cycle. Treatment with the chelators resulted in cell cycle arrest in late G<sub>1</sub> phase at relatively low chelator concentrations. The dose responses for CP94 and DFO are shown in Table 10.

### 5.2.3 Discussion

Incubation with CP94 or DFO arrested cell cycle in a dose dependent manner. In K562 cells G<sub>1</sub> arrest was observed at chelator concentrations of 33 $\mu$ M IBE and above (Table 7). At lower chelator concentrations there was significant accumulation of cells in G<sub>2</sub>+M phase. It is unlikely that iron is limiting for DNA synthesis at these low chelator concentrations since these cells had already traversed S phase and there was an increased incidence of polynuclear and mitotic forms (Table 9). Therefore this accumulation in G<sub>2</sub>+M phase may represent an alternative site of iron chelator action.

K562 cells appear to be less sensitive to iron deprivation than other cell types such as Daudi cells and PBL. Daudi cells were markedly more sensitive to chelator induced cell cycle arrest, than K562 cells, with accumulation of cells in G<sub>1</sub> phase at

**TABLE 10: EFFECTS OF DFO AND CP94 ON PERIPHERAL BLOOD LYMPHOCYTE CELL CYCLE KINETICS**

Chelator Concentration		% of cells in phase		
$\mu\text{M}$ IBE		G <sub>0</sub> /G <sub>1</sub>	S	G <sub>2</sub> /M
Control		53 $\pm$ 1	23 $\pm$ 2	24 $\pm$ 1
DFO	3	80 $\pm$ 2***	13 $\pm$ 3**	6 $\pm$ 1***
	10	89 $\pm$ 2***	6 $\pm$ 1***	5 $\pm$ 1***
	33	93 $\pm$ 1***	4 $\pm$ 1***	3 $\pm$ 1***
	100	94 $\pm$ 2***	3 $\pm$ 1***	3 $\pm$ 1***
CP94	3	82 $\pm$ 1***	10 $\pm$ 1**	8 $\pm$ 1***
	10	91 $\pm$ 1***	3 $\pm$ 1***	6 $\pm$ 1***
	33	91 $\pm$ 2***	3 $\pm$ 1***	5 $\pm$ 1***
	100	93 $\pm$ 2***	4 $\pm$ 1***	3 $\pm$ 1***

Human peripheral blood lymphocytes ( $5 \times 10^5/\text{ml}$ ) were isolated and cultured as described in the text and incubated for 72 hours with CP94 or DFO. Cell cycle status was analysed as described for Table 7. Results are expressed as in Table 7 and represent the mean  $\pm$  S.E.M of 3 separate experiments in triplicate. Significant differences in the cell cycle distribution of control and chelator treated lymphocytes were identified at the  $p < 0.01$  (\*\*) and  $p < 0.001$  (\*\*\*) level with unpaired Students t tests.

concentrations as low as 3 $\mu$ M IBE and maximal arrest at 33 $\mu$ M IBE (Table 8). PBL were also more sensitive to chelator action; less than 20% of the chelator treated cells were in S and G<sub>2</sub>+M phase after 72 hours at concentrations of 3 $\mu$ M IBE, compared to almost 50% of controls (Table 10).

Daudi cells and PBL displayed equal sensitivity to the chelators, therefore Daudi cells were selected for comparison with K562 for the remainder of these studies as they have a doubling time of approximately 20 hours, similar to K562 cells.

### **5.3 PHYSICOCHEMICAL PROPERTIES REQUIRED FOR EFFECTIVE CELL CYCLE ARREST**

The ability of HPO chelators to mobilise intracellular iron has been directly related to the partition coefficient of the iron free HPO and the iron (III) binding constant (Porter et al 1988). The experiments that follow were designed to determine whether these physicochemical properties exert a similar influence upon the ability of chelators to arrest cell cycle.

#### **Experimental Procedure**

The importance of partition coefficient was investigated by incubating K562 cells with a range of 3-HP-4-one chelators; CP20, CP21, CP22, CP24, CP40, and CP94 at 100 $\mu$ M IBE. After 24 hours the cells were washed with PBS and the cell cycle status of each sample was analysed as described in Section 5.2.1.

The antiproliferative effects of two additional HPOs CP130 and CP02 were compared with DFO and CP94. K562 cells were incubated for 24 hours with 3-100 $\mu$ M IBE CP130, CP94, CP02 or DFO then analysed by flow cytometry as described previously.



## Results and Discussion

The results in Figure 32 show the percentage of cells in G<sub>1</sub> phase of the cell cycle plotted against partition coefficient for each 3-HP-4-one compound. The correlation coefficient,  $R$ , was calculated to be 0.020 indicating poor correlation between chelator lipophilicity and cell cycle arrest for the bidentate 3-HP-4-ones. This suggests that the 24 hour period of incubation is sufficient for even relatively hydrophilic compounds to permeate the cell and arrest cell cycle.

By contrast, the 3-HP-2-one compound CP02 and the hexadentate HPO CP130 were significantly less active than DFO and CP94 (Figure 33). Significant arrest in G<sub>1</sub> was not observed with CP130 or CP02 at concentrations less than 300 $\mu$ M IBE. However at 33 $\mu$ M IBE both these chelators caused a significant accumulation of cells in G<sub>2</sub>+M phase (Control = 27%, CP130 = 31%, CP02 = 30%;  $p < 0.05$ ,  $n = 3$ ) as was observed previously with low concentrations of DFO and CP94.

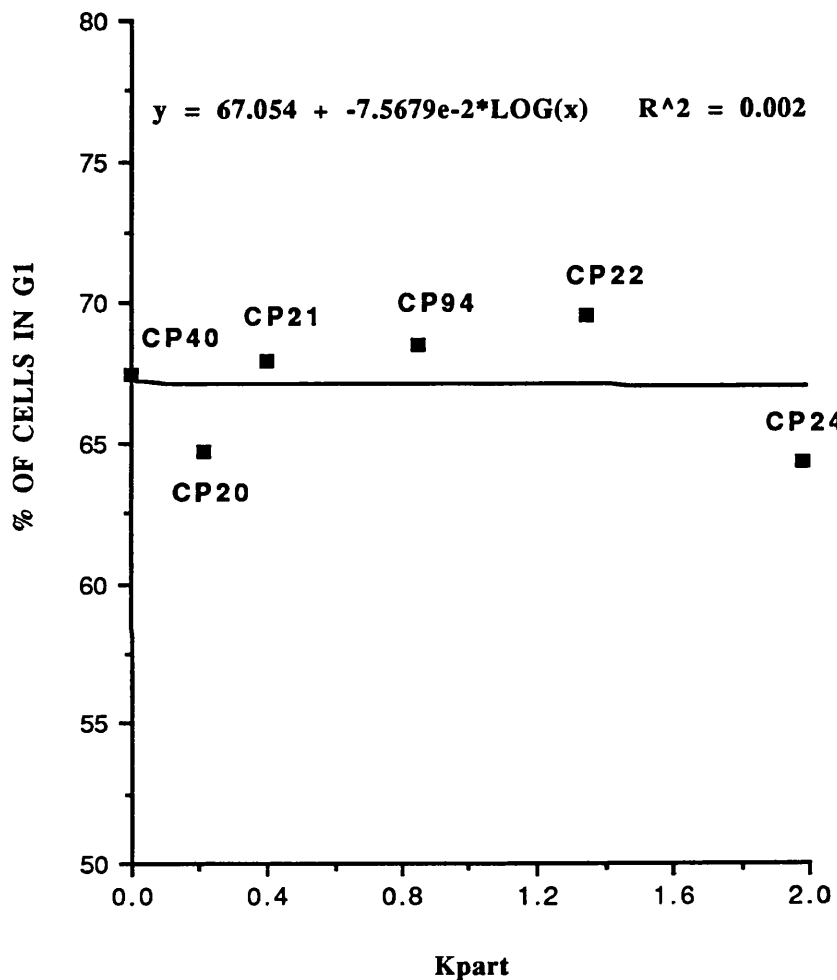
CP02 is a relatively lipophilic compound but has a low stability constant for iron ( $\log \beta_3 = 10^{32}$ ) when compared 3-HP-4-ones such as CP94 ( $\log \beta_3 = 10^{36}$ ). The hexadentate CP130 has a higher stability constant for iron but this compound is very hydrophilic (Table 4) and uncharged<sup>and</sup> consequently may enter cells relatively slowly compared to DFO. These results suggest that a degree of cellular penetration combined with a high stability constant is necessary for effective arrest of cell cycle.

### 5.4 CELL CYCLE SYNCHRONISATION BY 3-HYDROXYPYRIDIN-4-ONES

The microbial siderophore parabactin has been shown to be a potent cell cycle synchronisation agent and this has led to the suggestion that iron chelators may be used clinically to obtain a population of synchronised proliferating cells with enhanced sensitivity to cell cycle specific anti-tumour agents (Bergeron et al 1987). As CP94 distributes more freely within the intracellular compartment than DFO, the 3-HP-4-one chelator may have greater potential to act as a cell cycle synchronisation agent. This

**FIGURE 32:**

**RELATIONSHIP BETWEEN PARTITION  
COEFFICIENT AND CELL CYCLE ARREST**

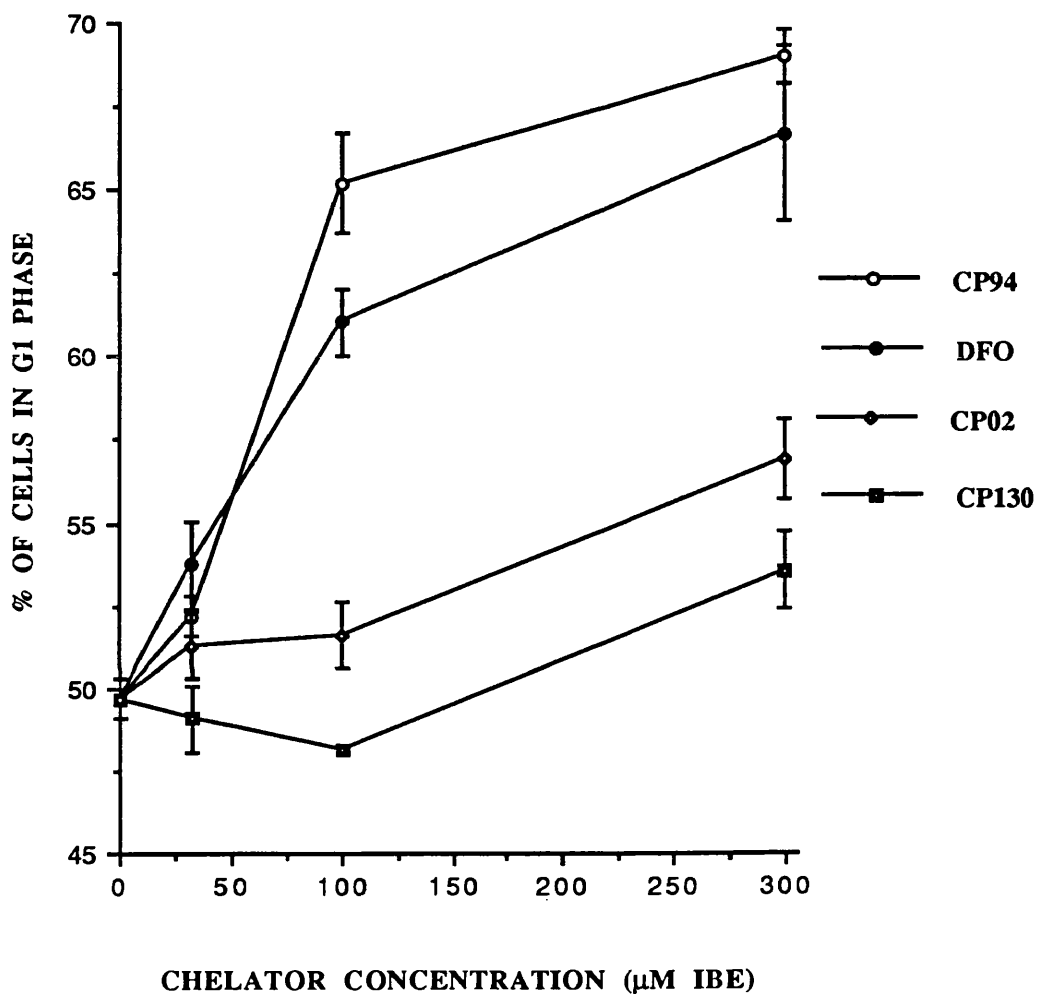


**LEGEND**

K562 cells were incubated with a range of 3-HP-4-ones at 100 $\mu$ M IBE for 24 hours. At the end of incubation cells were washed, fixed and stained with propidium iodide for cell cycle analysis as described in the text. The results show the percentage of cells in G<sub>1</sub> phase for each chelator and are the mean of duplicate experiments.

**FIGURE 33:**

**K562 CELL CYCLE ARREST BY DFO, CP130, CP94 AND CP02**



**LEGEND**

K562 cells were cultured in the presence of increasing concentrations of DFO, CP94, CP02 or CP130. After 24 hours cells were washed, fixed and stained with propidium iodide for cell cycle analysis as described in the text. The results show the percentage of cells in G<sub>1</sub> phase for each chelator and are the mean  $\pm$  S.E.M of 3 separate experiments in triplicate.

was investigated by monitoring the recovery of K562 cells from cell cycle arrest by DFO and CP94.

### **Experimental Procedure**

K562 and Daudi cells in exponential growth were cultured for 24 hours with 100 $\mu$ M or 33 $\mu$ M IBE respectively CP94 or DFO. At the end of the incubation period the cells were washed 3 times in sterile culture medium and re-cultured in fresh chelator free medium. Aliquots corresponding to 5x10<sup>5</sup> cells were taken at the start of reculture and then at 4 hour intervals for up to 24 hours. The cells were washed and prepared for cell cycle analysis by flow cytometry as described previously (Section 2.4.2).

### **Results and Discussion**

Figures 34 and 35 show the percentage of K562 and Daudi cells respectively in each phase of the cell cycle for the 24 hours following reculture as compared to controls. The blockade of cell cycle by both compounds was reversible and on reculture cells recommenced cycling after a lag phase of 4 hours. CP94 treated cells cascaded back into cycle in a synchronised manner and remained synchronised throughout the remainder of the cycle. In contrast cells which had been incubated with DFO re-entered cycle in a non-synchronous manner and cell cycle kinetics were similar to controls by 12 hours.

A less disruptive method of achieving cell cycle synchronisation may be to add iron directly to chelator treated cultures to overcome the chelator induced cellular iron deprivation. This hypothesis was tested by adding iron, in the form of ferric ammonium citrate, to a final concentration of 110 $\mu$ M to K562 cell cultures which had been preincubated for 24 hours with 100 $\mu$ M IBE CP94 or DFO. No washing step was included. Whilst the addition of iron had no effect on the cycling of control cells, chelator treated cells recommenced cycling after a lag period of 4-6 hours as above

FIGURE 34:

RECOVERY OF K562 CELLS FROM CELL  
CYCLE ARREST BY CP94 OR DFO

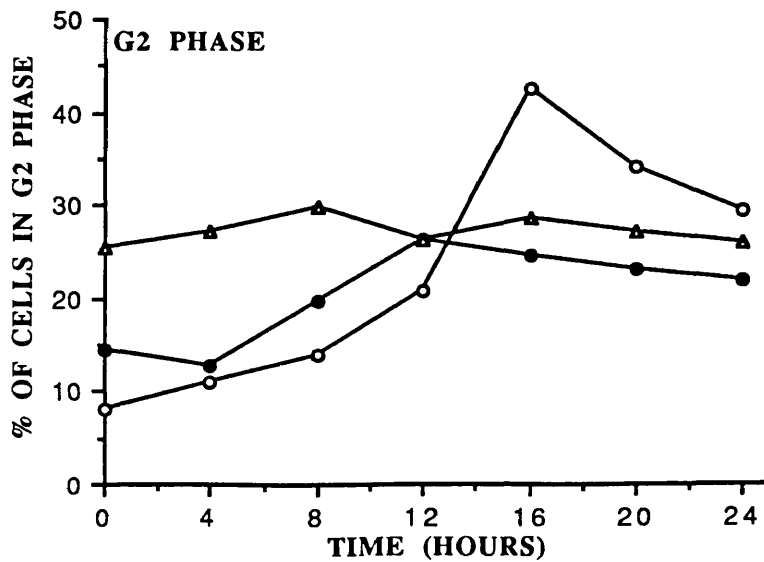
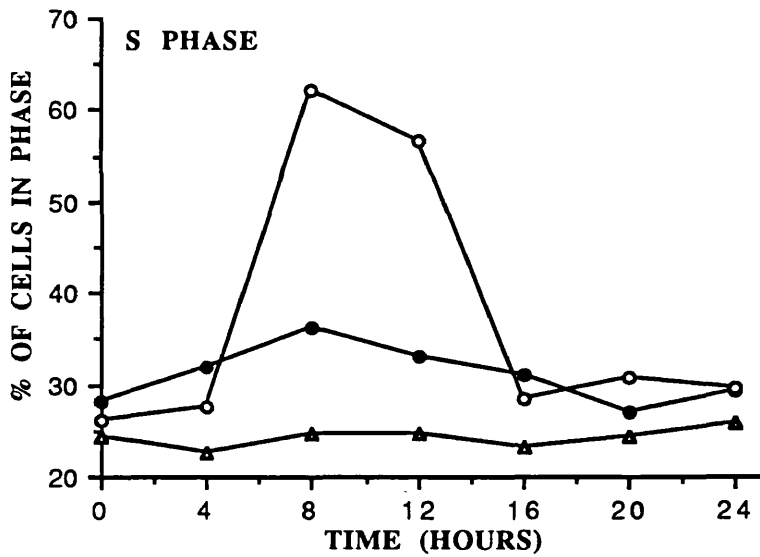
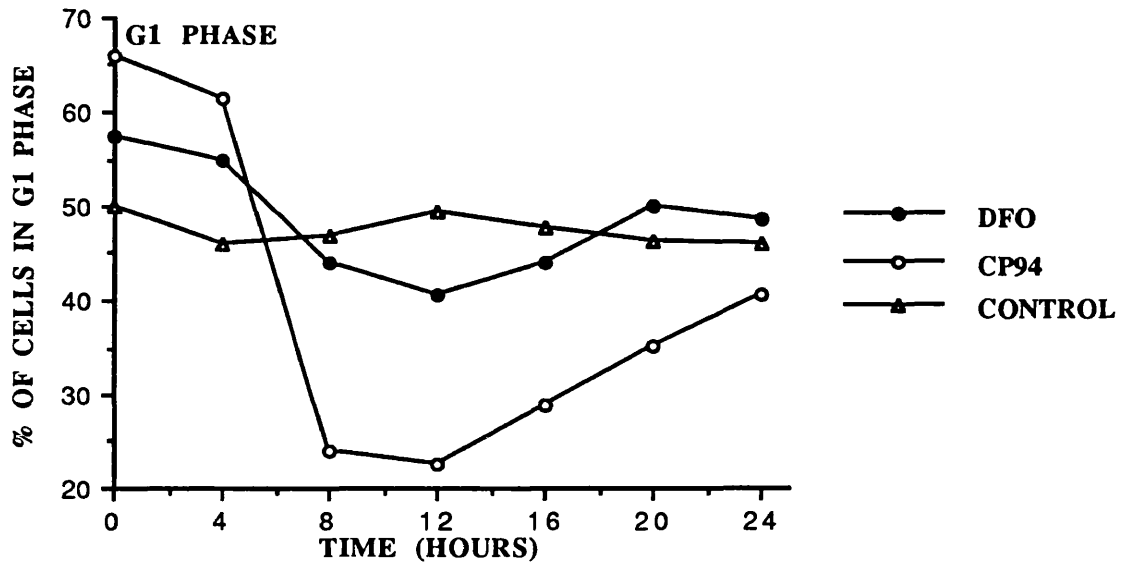


**FIGURE 35:**

**RECOVERY OF DAUDI CELLS FROM CELL  
CYCLE ARREST BY CP94 OR DFO**

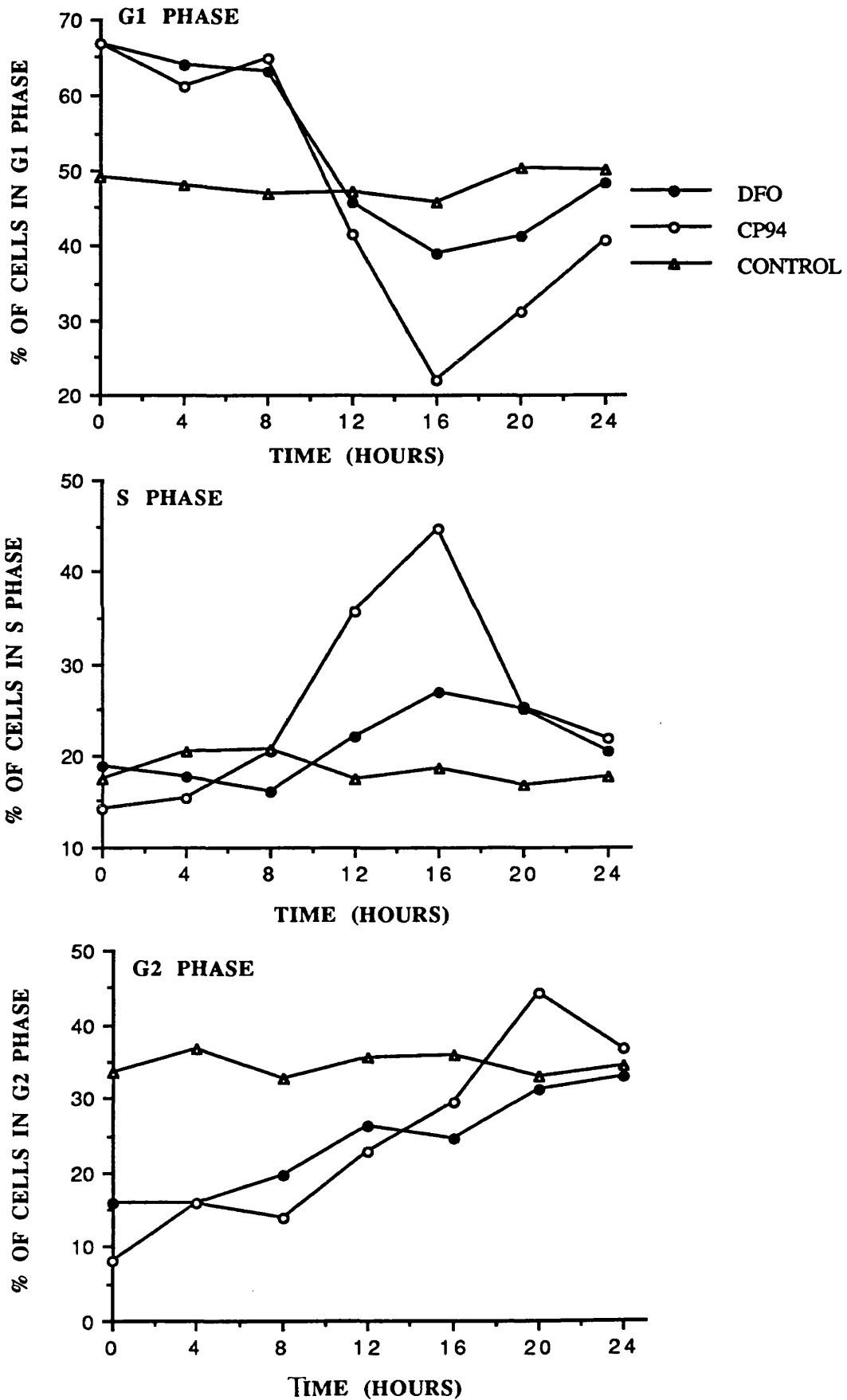


FIGURE 36:

RECOVERY OF K562 CELLS FROM CELL CYCLE ARREST AFTER ADDITION OF 100 $\mu$ M IBE FERRIC AMMONIUM CITRATE

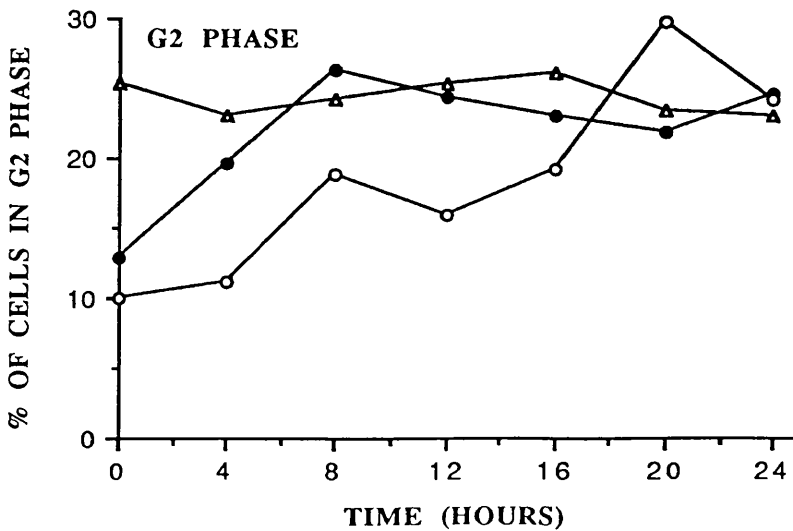
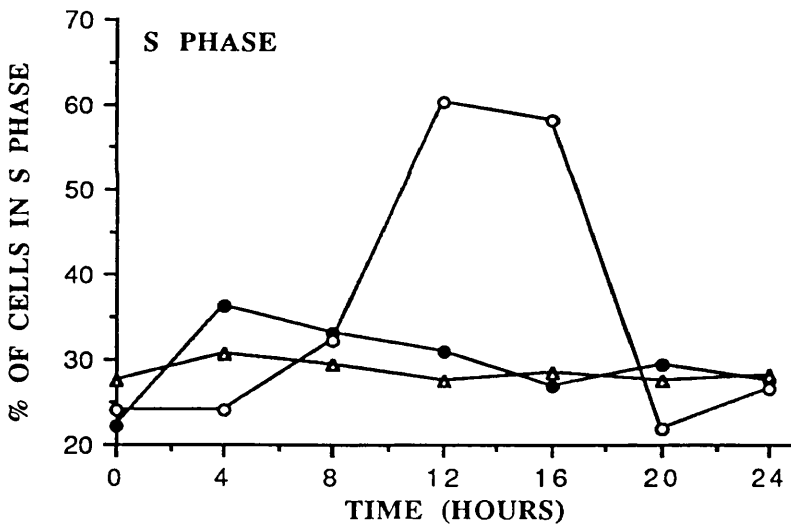
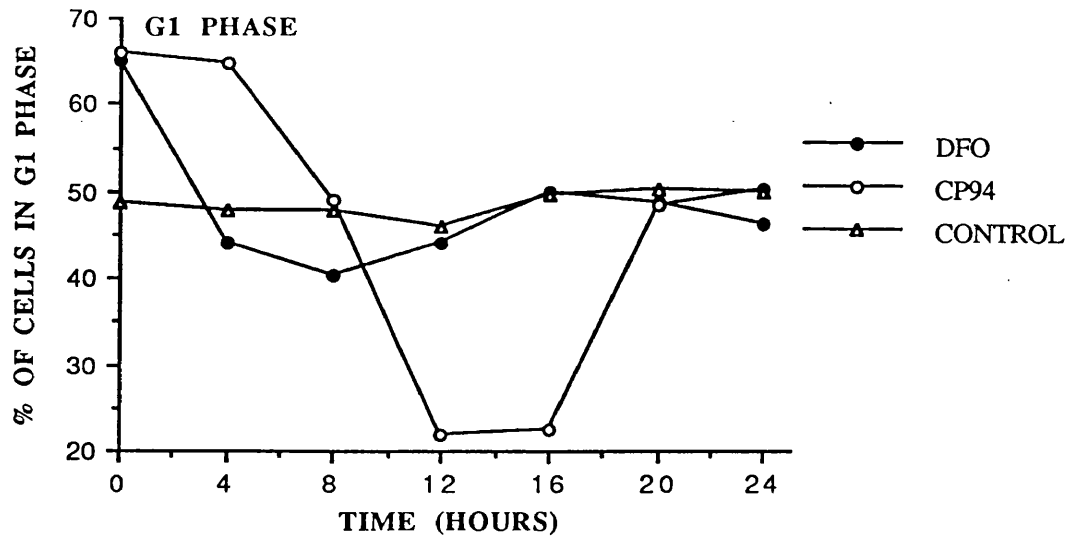
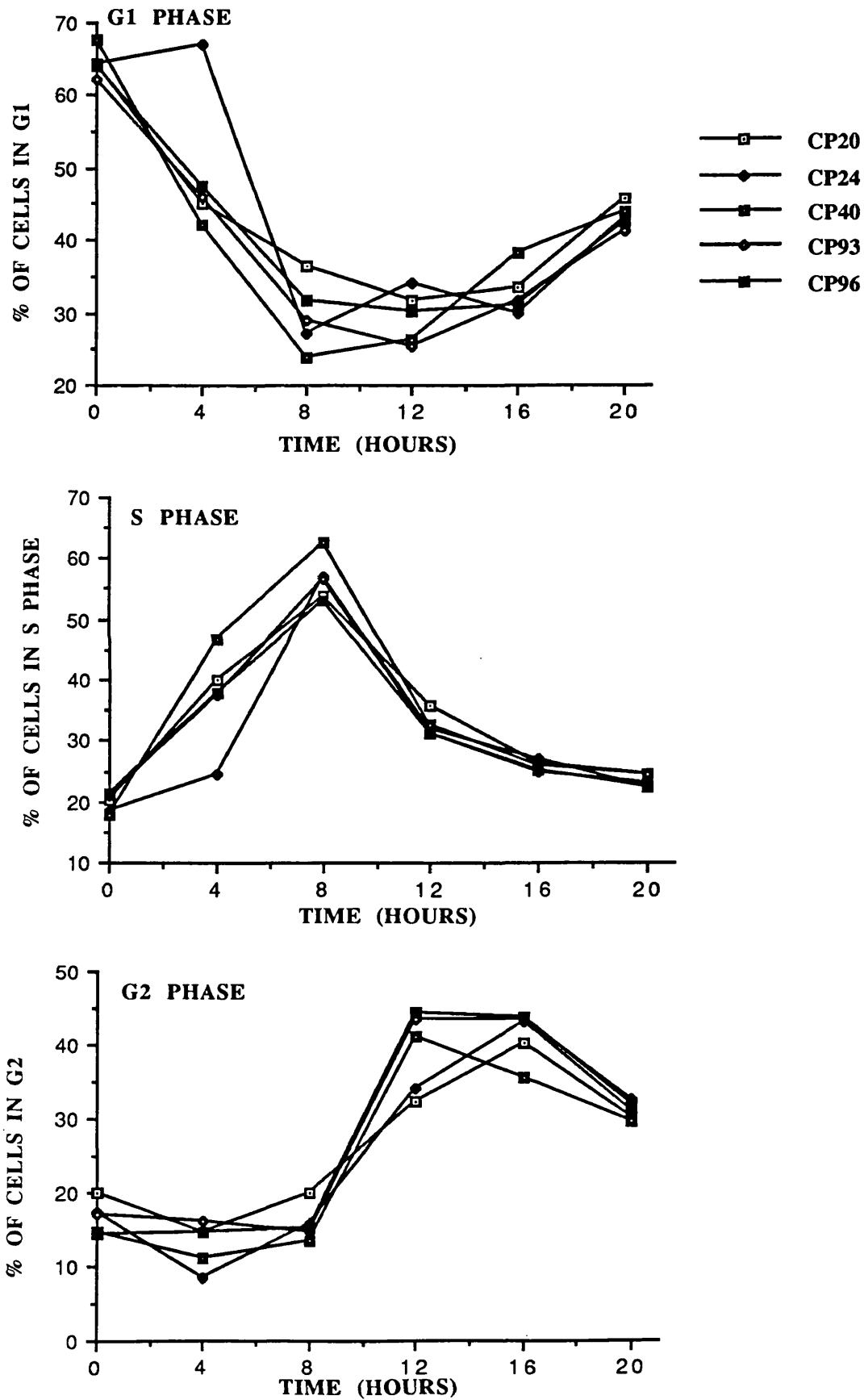


FIGURE 37:

K562 CELL CYCLE SYNCHRONISATION  
BY 3-HYDROXYPYRIDIN-4-ONES





**LEGEND: FIGURES 34, 35, 36 and 37**

K562 cells (Figure 34, 36 and 37) or Daudi cells (Figure 35) were cultured with 100 $\mu$ M (K562) or 33 $\mu$ M (Daudi) IBE iron chelator for 24 hours and then recultured as described in the text. At 4 hour intervals aliquots were taken for cell cycle analysis. The results show the percentage of cells in each phase of the cell cycle at each time point. The values shown are the means of duplicate observations from a representative experiment. 3 additional experiments gave similar results.

(Figure 36). Again synchronisation was observed in the CP94 treated cell population but not in the DFO treated population.

In order to assess whether synchronisation is a unique property of CP94 or common to all the 3-HP-4-one series the six HPO chelators used in section 5.3 were screened for their ability to synchronise cell cycle in K562 cells. Each of these compounds was found to be a potent cell cycle synchronisation agent (Figure 37), indicating little correlation between lipophilicity and ability to arrest or synchronise cell cycle.

## **5.5 INHIBITION OF RIBONUCLEOTIDE REDUCTASE BY CP94 AND DFO**

To confirm that inhibition of ribonucleotide reductase was associated with cell cycle arrest by CP94 and DFO, the activity of this enzyme was directly analysed in chelator treated K562 cells. Although previous studies have provided convincing demonstration of the effects of DFO on ribonucleotide reductase activity in cell free assays (Hoffbrand et al 1976) and intracellular levels of deoxyribonucleoside triphosphates (Barankiewicz 1987), direct *in vivo* effects on ribonucleotide reductase have not been demonstrated with DFO. Therefore in these experiments ribonucleotide reductase activity was assessed utilising an intact cell assay which directly measured ribonucleotide reduction in whole cells.

### **Experimental Procedure**

The activity of ribonucleotide reductase was determined in K562 cells, according to the intact cell method of Hards and Wright (1981), as described in Section 2.4.4, after 24 hours treatment with a range of concentrations of CP94 or DFO.

The number of cells used for these experiments was a crucial factor in obtaining consistent results. In initial experiments due to concern about the specific

activity of the [ $^{14}\text{C}$ ]CDP aliquots corresponding to  $1 \times 10^7$  cells, twice that used in the original method, were applied to the Affigel column. Under these circumstances the column rapidly became overloaded and incomplete separation of the deoxycytidine and the cytidine was attained. Reduction of the cell number to  $5 \times 10^6$  did not resolve this overloading and attempts to overcome this problem by using a larger column were unsuccessful due to the resulting large dilution of the eluted samples. Finally the number of cells was reduced to  $2.5 \times 10^6$ , half that utilised in the original method, and although the specific activity of the eluent was low reproducible data was obtained.

## **Results and Discussion**

As shown in Figure 38 there was a dose related reduction in enzyme activity with both chelators. Enzyme activity was decreased by 20% at concentrations of  $10 \mu\text{M}$  IBE with both CP94 and DFO and by more than 90% at concentrations of  $100 \mu\text{M}$  IBE. Quantification of DNA synthesis, as measured by cellular incorporation of [ $^3\text{H}$ ]thymidine, in the same experiments revealed no reduction in thymidine uptake at  $10 \mu\text{M}$  IBE but uptake was reduced by more than 90% at  $33 \mu\text{M}$  IBE.

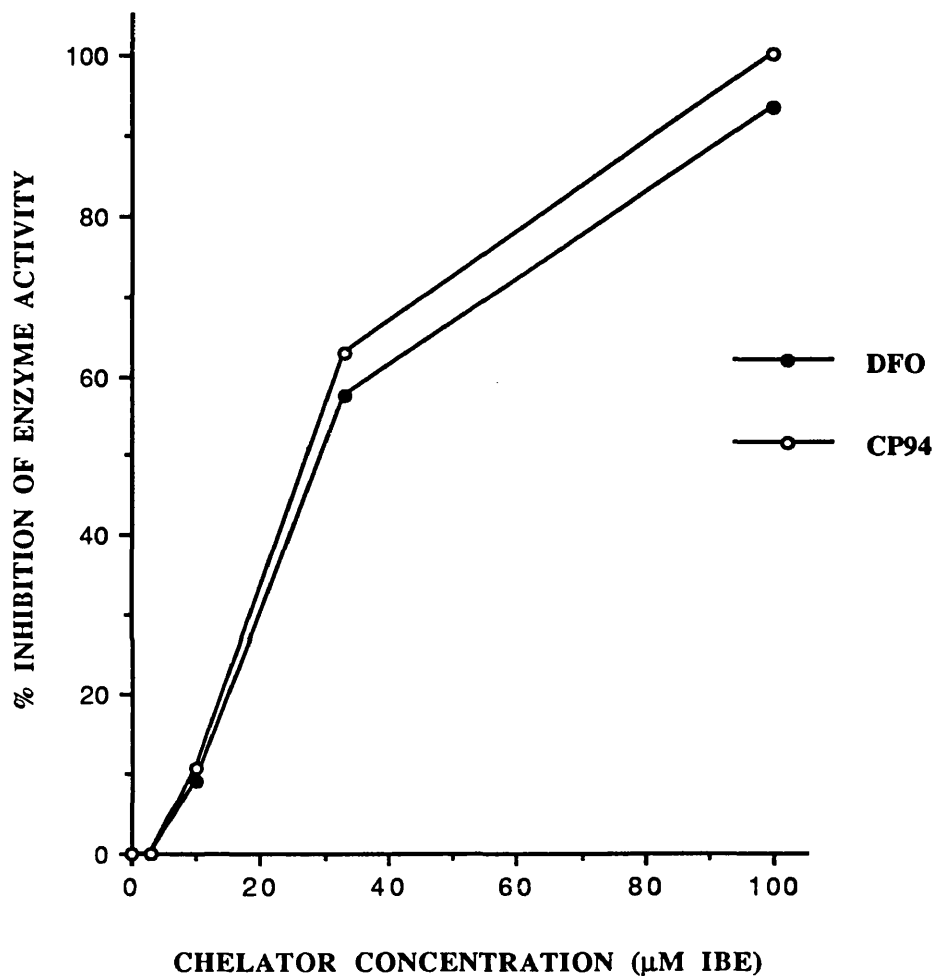
As indicated above considerable problems were encountered with this assay. An alternative method of measuring ribonucleotide reductase activity is by electron spin resonance (ESR) spectroscopy. This method monitors the characteristic ESR signal produced by the tyrosyl free radical in the M2 subunit which is directly correlated to enzyme activity (Eriksson et al 1984). Utilisation of this methodology may provide more consistent data and so allow closer examination of the kinetics and dose responses of chelator induced ribonucleotide reductase inhibition.

### **5.6 EFFECT OF CP94 AND DFO ON CELL PROLIFERATION**

The data above suggest that at chelator concentrations of  $10 \mu\text{M}$  IBE or less cell cycle arrest may occur in  $G_2/M$  phase independently of significant inhibition of ribonucleotide reductase. To investigate further the relationship between chelator

**FIGURE 38:**

**INHIBITION OF RIBONUCLEOTIDE  
REDUCTASE BY CP94 AND DFO**



**LEGEND:**

K562 cells were cultured for 24 hours with increasing concentrations of CP94 or DFO. Ribonucleotide reductase activity was assessed in cell pellets as described in the text. Results represent data from 2 independent experiments in duplicate.

concentration and inhibition of cell proliferation and DNA synthesis, K562 and Daudi cells were cultured with CP94 or DFO for up to 96 hours and cell growth and [<sup>3</sup>H]thymidine incorporation were monitored. To determine whether other cellular biosynthetic pathways are affected by chelator treatment the incorporation of the macromolecular precursors [<sup>3</sup>H]uridine and [<sup>3</sup>H]leucine were also monitored.

### 5.6.1 Effect of CP94 and DFO on Cell Growth and Viability

#### **Experimental Procedure**

K562 and Daudi cells were cultured at an initial density of  $0.1 \times 10^6$  cells/ml with a range of concentrations of CP94 and DFO for 96 hours. Growth curves were constructed by sampling the cells at 24 hour intervals to measure cell number and viability. Cell number was determined using an electronic particle counter (Coulter STK-R) and viability was assessed by fluorescence microscopy using ethidium bromide and acridine orange to mark live and dead cells respectively (Section 2.3.5)

#### **Results**

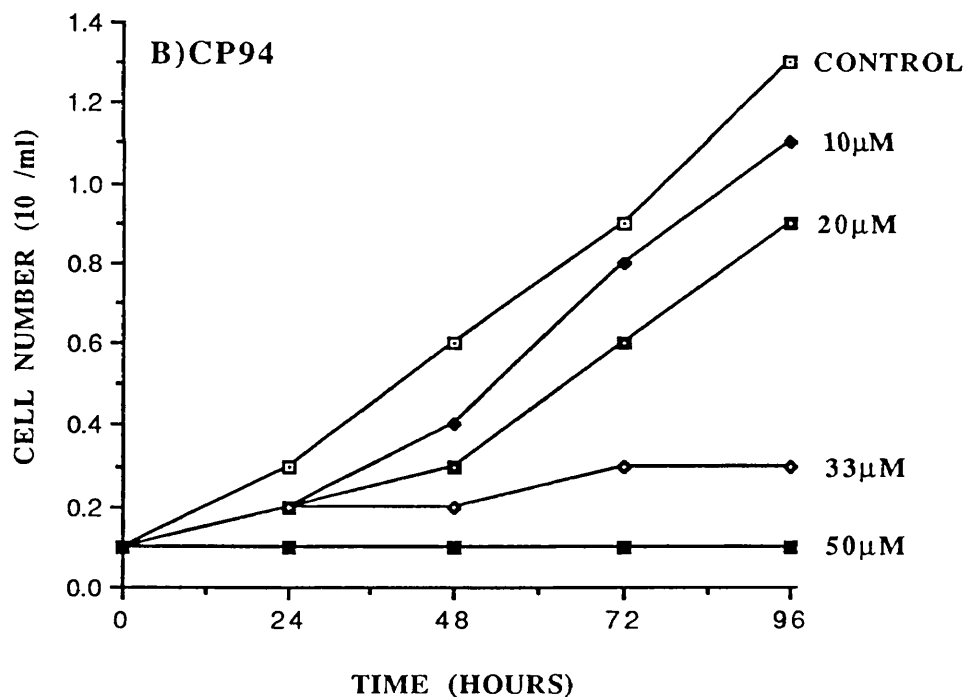
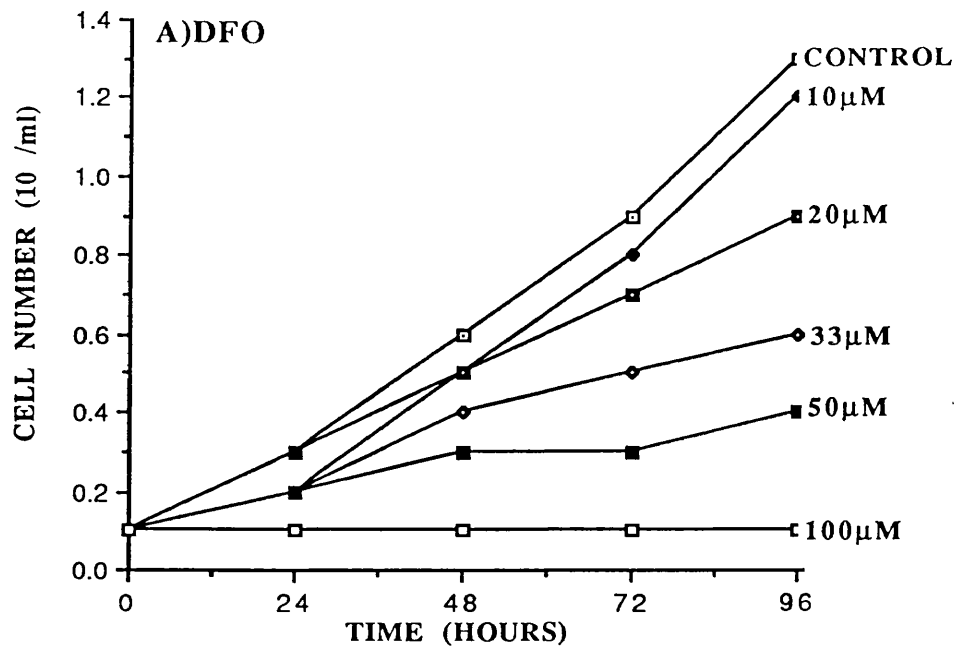
Whilst cell number in control cultures increased to  $1.4 \times 10^6$ /ml and  $1 \times 10^6$ /ml for K562 and Daudi cells respectively CP94 and DFO inhibited proliferation in a dose dependent manner (Figure 39 and 40).

At concentrations of  $10 \mu\text{M}$  IBE CP94 or DFO the number of K562 cells at 96 hours was reduced to 75-80% of control and at  $50 \mu\text{M}$  IBE there were only 5-15% of that in controls (Figure 39). Daudi cells were markedly more sensitive to growth inhibition by the chelators and maximal growth inhibition was observed at  $30 \mu\text{M}$  (Figure 40).

For easier observation of the results the percentage inhibition of cell growth at each chelator concentration is summarised in Figure 41. From these data the mean concentrations of each chelator required to inhibit proliferation by 50% ( $IC_{50}$ ) were

FIGURE 39:

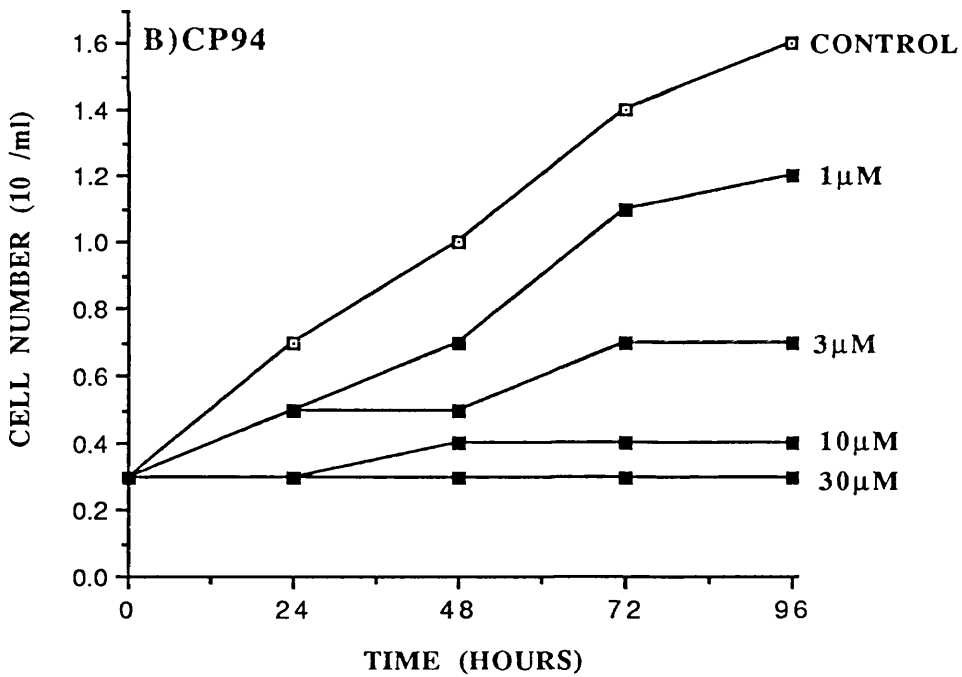
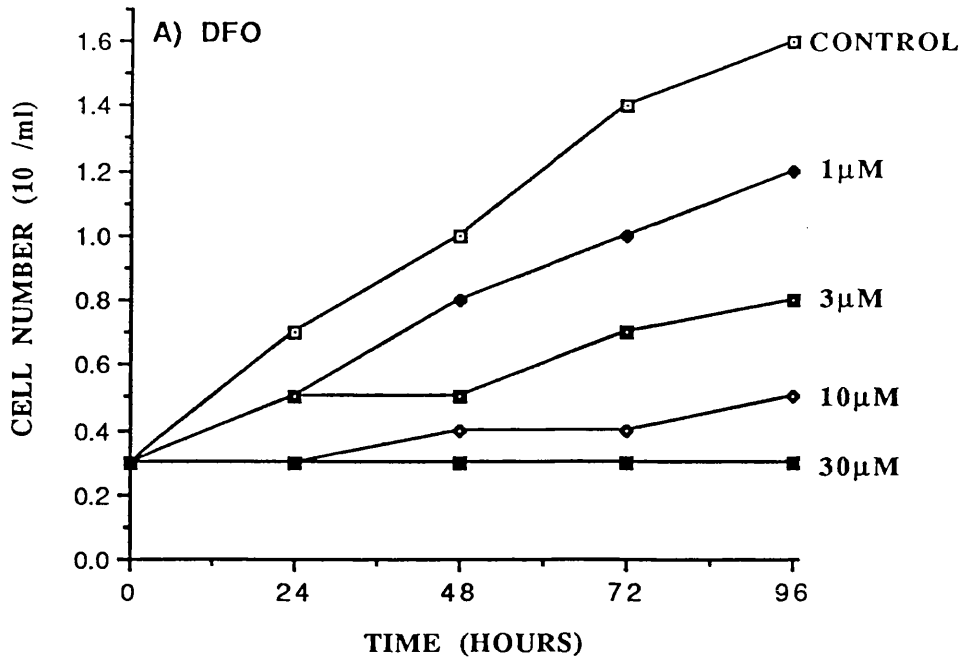
K562 CELL GROWTH IN THE PRESENCE OF DFO AND CP94



LEGEND

K562 cells were cultured in the presence of increasing concentrations of DFO or CP94. Controls received an equivalent volume of PBS. At 24 hour intervals cells were counted with an electronic particle counter. The results are the mean of 2 separate experiments with triplicates at each point.

DAUDI CELL GROWTH IN THE PRESENCE OF DFO AND CP94

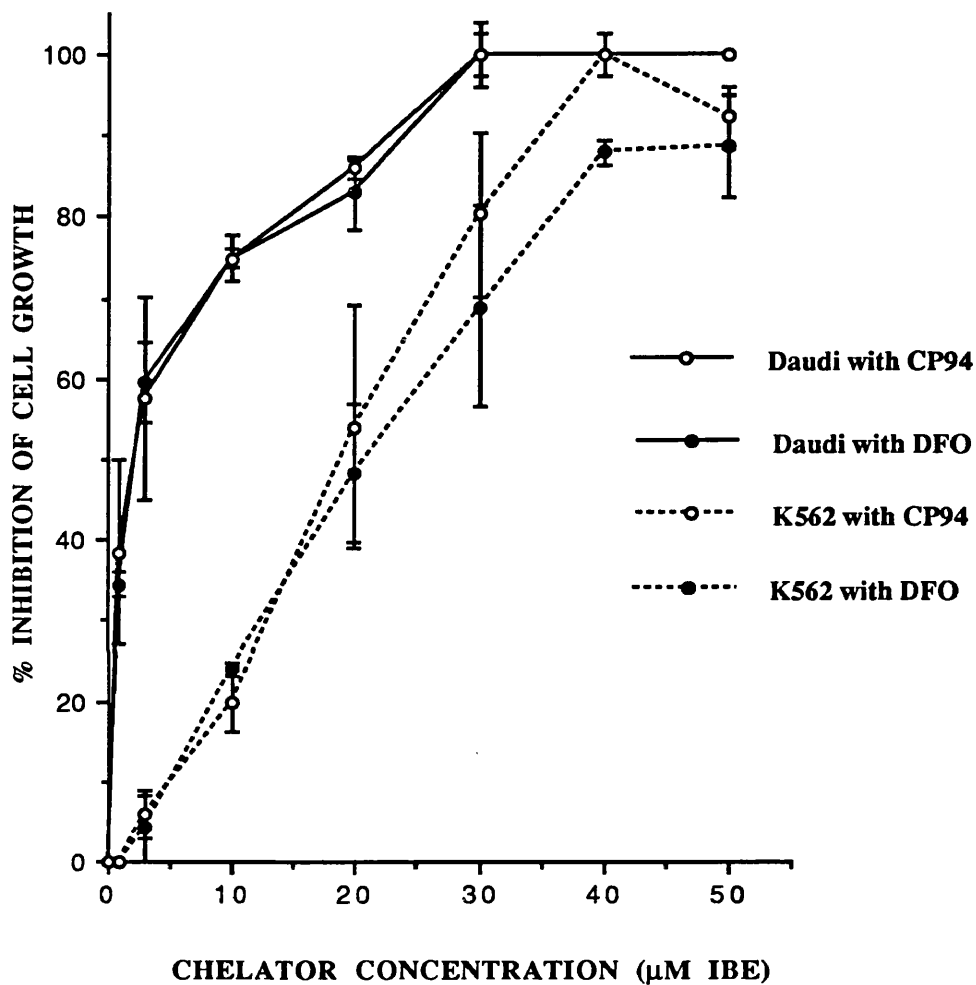


**LEGEND**

Daudi cells were cultured in the presence of increasing concentrations of DFO or CP94. Controls received an equivalent volume of PBS. At 24 hour intervals cells were counted with an electronic particle counter. The results are the mean of 2 separate experiments with triplicates at each point.

FIGURE 41:

CONCENTRATION-DEPENDENT INHIBITION  
OF CELL GROWTH BY DFO AND CP94



LEGEND

K562 and Daudi cells were cultured in the presence of increasing concentrations of DFO or CP94 as in Figures 39 and 40. Controls received an equivalent volume of PBS. The data shown are the percentage inhibition of cell growth compared to controls and represent the mean  $\pm$  S.E.M of 3 independent experiments in triplicate.



determined to be  $21.2 \pm 2.7 \mu\text{M}$  and  $24.9 \pm 4.3 \mu\text{M}$  IBE for CP94 and DFO respectively in K562 cells and  $3.1 \pm 0.2 \mu\text{M}$  and  $3.06 \pm 0.3 \mu\text{M}$  IBE respectively in Daudi cells.

Viability of the K562 cells at 72 hours was maintained at above 90% at concentrations up to  $10 \mu\text{M}$  IBE. Above this concentration cultures contained 15-20% non viable cells at 96 hours. The Daudi cells remained more than 90% viable at concentrations of  $3 \mu\text{M}$  IBE, at higher concentrations viability was significantly reduced (Table 11).

The addition of FO and CP94-Fe complex at concentrations of  $50 \mu\text{M}$  had no significant effect upon the growth or viability of K562 and Daudi cells over a 96 hour incubation period (Control cell number at 96 hours =  $1.2 \times 10^6/\text{ml}$ , FO =  $1.1 \times 10^6/\text{ml}$ , CP94-Fe =  $1.2 \times 10^6/\text{ml}$ ;  $n=3$ ,  $p>0.1$ )

### 5.6.2 Effect of CP94 and DFO on DNA, RNA and Protein Synthesis

#### **Experimental Procedure**

DNA, RNA and protein synthesis were indirectly quantified by measuring cellular incorporation of [ $^3\text{H}$ ]thymidine, [ $^3\text{H}$ ]uridine and [ $^3\text{H}$ ]leucine respectively.

K562 and Daudi cells cultured for 96 hours with varying concentrations of CP94 and DFO as described previously (Section 5.5.1). For the final 4 hours of incubation triplicate aliquots of  $2 \times 10^5$  cells from each test sample were plated in 96 well microtitration plates and  $0.5 \mu\text{Ci}$  [ $^3\text{H}$ ]thymidine, [ $^3\text{H}$ ]uridine or [ $^3\text{H}$ ]leucine in RPMI 1640 media was added to each well. The cells were harvested onto fibreglass filters using an Automash 2000 cell harvester. The filters were dried for 3 hours then put into scintillation vials and 4ml of Hisafe liquid scintillation fluid was added to each vial. Radioactivity was assessed using a LKB  $\beta$  counter.

#### **Results**

In the same experiment as described in Section 5.5.1 both CP94 and DFO caused a dose dependent reduction in [ $^3\text{H}$ ] thymidine uptake by K562 and Daudi cells.

**TABLE 11: EFFECT OF DFO AND CP94 ON THE VIABILITY OF DAUDI AND K562 CELLS**

Chelator Concentration		% of viable cells (mean± S.E.M)			
		Daudi		K562	
μM	IBE	24h	96h	24h	96h
Control		97±4	96±2	95±1	96±1
DFO	3μM	95±2	94±1	94±2	93±2
	10μM	91±2	88±4	93±1	92±2
	33μM	90±3	83±2 <sup>***</sup>	95±2	90±1 <sup>*</sup>
	100μM	92±1	68±1 <sup>***</sup>	94±3	79±1 <sup>***</sup>
CP94	3μM	94±1	94±1	95±4	93±3
	10μM	92±2	85±3 <sup>***</sup>	94±1	89±3
	33μM	91±2	80±4 <sup>***</sup>	92±1	84±1 <sup>***</sup>
	100μM	91±3	67±1 <sup>***</sup>	94±2	81±4 <sup>***</sup>

K562 and Daudi cells were cultured in the presence or absence of increasing concentrations of DFO or CP94. At the times indicated viability was assessed by fluorescence microscopy with ethidium bromide and acridine orange. The data is the mean ± S.E.M for 3 separate experiments. Significant differences in the viability of control and chelator treated cells were identified at the p<0.05 (\*) and p<0.001 (\*\*\*) levels with the unpaired Students t test.

(Figure 42). Whilst the mean incorporation of [<sup>3</sup>H]thymidine by control K562 cells was 6462cpm/10<sup>5</sup> cells, concentrations of 33μM IBE CP94 or DFO caused a reduction in [<sup>3</sup>H]thymidine uptake of more than 90%. Lower doses produced more moderate decreases in uptake and at concentrations of 10μM or less there was no apparent reduction in cellular [<sup>3</sup>H] thymidine incorporation despite the inhibition of cell growth observed at these concentrations.

Incorporation of [<sup>3</sup>H]thymidine by Daudi cells was reduced by more than 90% from 5442cpm/10<sup>5</sup> cells in control populations to less than 500cpm/10<sup>5</sup> cells in cells treated with CP94 or DFO at concentrations above 6μM IBE, at lower doses [<sup>3</sup>H]thymidine incorporation was reduced to a lesser extent.

In parallel experiments treatment of K562 and Daudi cells with concentrations of CP94 or DFO sufficient to inhibit [<sup>3</sup>H]thymidine incorporation by more than 90% had no significant effect on RNA or protein synthesis as measured by uptake of [<sup>3</sup>H]uridine and [<sup>3</sup>H]leucine (Table 12).

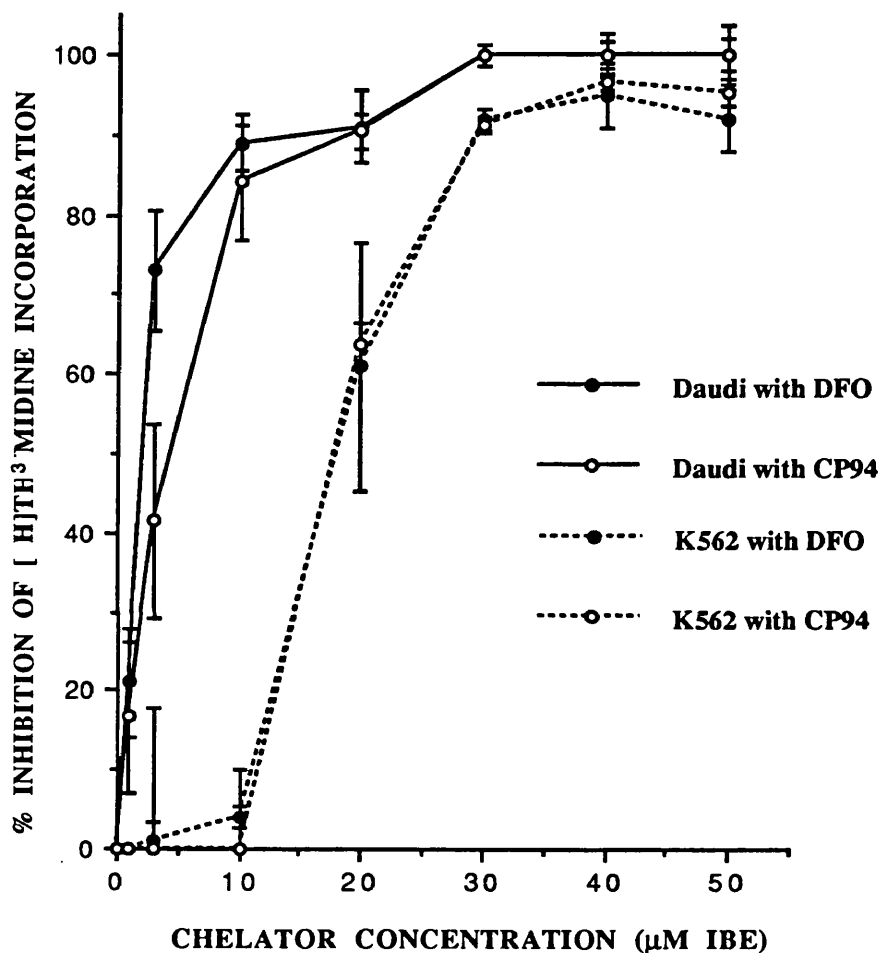
### 5.6.3 Discussion

Incubation with CP94 and DFO had pronounced effects on cell division and DNA synthesis. Exposure to relatively high chelator concentrations (above 33μM) caused concurrent cessation of growth and DNA synthesis in both K562 and Daudi cells (Figures 41 and 42). As observed previously Daudi cells were markedly more sensitive to iron chelation than K562 cells and this was reflected by the threefold difference in the IC<sub>50</sub> values for each cell type. Likewise prolonged exposure to the chelators had significantly greater effects on the viability of Daudi cells than K562 cells (Table 11). However global inhibition of RNA or protein synthesis was not observed in Daudi cells or K562 cells (Table 12) suggesting that such cytotoxicity results from specific chelation from iron dependent intracellular systems.

Whilst inhibition of Daudi cell DNA synthesis was observed at all chelator concentrations, exposure of K562 cells to concentrations of less than 10μM IBE

FIGURE 42:

CONCENTRATION-DEPENDENT INHIBITION OF [ H ] THYMIDINE INCORPORATION INTO K562 AND DAUDI CELLS



LEGEND

K562 and Daudi cells were cultured in the presence of increasing concentrations of DFO or CP94. Controls received an equivalent volume of PBS. After 96 hours cells were counted and thymidine incorporation was measured after a 4 hour pulse with  $[^3\text{H}]$ thymidine. The data shown are the mean  $\pm$  S.E.M of 3 independent experiments in triplicate and are expressed as a percentage of control values.

**TABLE 12:**  
**CELLULAR INCORPORATION OF [<sup>3</sup>H]THYMIDINE, [<sup>3</sup>H]URIDINE AND [<sup>3</sup>H]LEUCINE**  
**BY K562 AND DAUDI CELLS AFTER 72 HOURS EXPOSURE TO DFO OR CP94.**

Chelator concentration		cpm (mean ± S.E.M)		
μM IBE	[ <sup>3</sup> H]Thymidine	[ <sup>3</sup> H]Uridine	[ <sup>3</sup> H]Leucine	
<b>K562</b>				
Control	5853±860	4788±512	935±225	
50μM DFO	665±50***	3340±892	1228±197	
50μM CP94	578±28***	3928±200	1123±273	
<b>Daudi</b>				
Control	4417±467	393±18	290±52	
30μM DFO	455±91***	603±184	552±176	
30μM CP94	313±66***	647±237	377±120	

K562 or Daudi cells were cultured for 96 hours with CP94 or DFO. For the final 4 hours cells were pulsed with 0.5μCi/2x10<sup>5</sup> cells [<sup>3</sup>H]thymidine, [<sup>3</sup>H]uridine or [<sup>3</sup>H]leucine. Data shown are the mean cpm ± S.E.M from 3 separate experiments in triplicate. Significant differences in the incorporation of radioisotopes by control and chelator treated samples were identified at the p<0.001 (\*\*\*) levels by the unpaired Students t test.

caused selective inhibition on cell division without significant effect on DNA synthesis.

## **5.6 GENERAL DISCUSSION**

These experiments show that reversible cell cycle arrest occurs with bidentate 3-HP-4-ones and DFO at concentrations at which cell viability is preserved. Exposure of K562 cells to chelator concentrations in excess of 33 $\mu$ M IBE results in cell cycle arrest in late G<sub>1</sub> phase (Table 7). Lower chelator concentrations cause an accumulation of K562 cells in the G<sub>2</sub>+M phase of the cell cycle (Tables 7 and 9). The antiproliferative effects of DFO and CP94 appear to be a result of iron chelation with addition of preformed chelator-iron complexes to cultures having no effect on cell cycle or cell growth.

K562 cells have both a high ability to accumulate iron and large iron stores (Forsbeck and Nilsson 1983) and have been previously demonstrated to be relatively insensitive to the antiproliferative effects of iron chelators (Forsbeck et al 1986). Therefore the comparative effects of iron chelators on cell cycle in K562 cells, Daudi cells and PBL were examined. Daudi cells and PBL were considerably more sensitive to the effects of iron deprivation than K562 cells. This may be due to differences in iron requirement, iron utilisation and transferrin receptor expression on different cell types.

There were no differences observed between the relative abilities of the 3-HP-4-ones to synchronise cell cycle suggesting that this is a general property of this series of chelators (Figure 37). In contrast little cell cycle synchronisation is observed in DFO treated K562 or Daudi cells (Figure 34 and 35). One possible explanation for the differing behaviour of the chelators is that since 3-HP-4-ones such as CP94 have more rapid access into cells and organelles than DFO (Chapters 3 and 4) treatment with these compounds may result in more efficient chelation of intracellular iron necessary for proliferation resulting in cell cycle synchronisation.

The studies into ribonucleotide reductase activity show that this enzyme is inhibited in intact K562 cells by both DFO and CP94 (Figure 38). As the activity of ribonucleotide reductase is known to vary with cell cycle and in particular to be virtually undetectable in G<sub>1</sub> phase (Eriksson et al 1984), it is not possible to say with certainty that the low ribonucleotide reductase activity observed after 24h incubation with chelators is directly due to inhibition by iron chelation or secondary to cell cycle arrest by another mechanism. However as inhibition of ribonucleotide reductase activity occurs at a chelator concentration (33μM IBE in K562 cells) at which cell cycle kinetics (Table 7) and viability (Table 11) are similar to control cells, it is probable that ribonucleotide reductase inhibition precedes cell cycle arrest in G<sub>1</sub> phase.

At the low concentrations of chelators (3-10μM IBE of CP94 or DFO) where K562 cell growth is partially inhibited (Figure 39), a proportion of cells were arrested not in G<sub>1</sub>, as seen at higher chelator concentrations, but in G<sub>2</sub>+M phases (Table 7). This was associated with an increase in mitotic and polynuclear forms (Table 10) without a fall in cell viability (Table 11). Additionally there was no significant inhibition of ribonucleotide reductase activity (Figure 38) or [<sup>3</sup>H]thymidine (Figure 42) incorporation into K562 cells at these low concentrations. A similar observation has been made by Bomford et al (1986) who reported that the concentration of DFO required to inhibit K562 cell cycle and DNA synthesis was significantly above that required to slow cell growth. Similarly, Reddel and associates (1985) have reported that treatment of T47-D breast carcinoma cells with DFO concentrations of 10μM causes an accumulation of cells within the G<sub>2</sub>+M phase of the cell cycle with an increased incidence of polyploidy whilst higher concentrations result in arrest in late G<sub>1</sub> phase.

These results suggest that the cell cycle arrest in G<sub>2</sub>+M and inhibition of cell division observed at low chelator concentrations is caused by an alternative mechanism to ribonucleotide reductase inhibition. This could occur by iron deprivation from a variety of enzyme systems necessary for cell function and growth. Clearly however, protein synthesis is not affected globally at these low concentrations (Table 12)

indicating that the inhibition would have to act specifically on iron dependent molecules.

Inhibition of cell growth independently of DNA synthesis was not observed in Daudi cells or PBL. However as these cell types are more sensitive to iron deprivation than K562 these effects may occur at chelator concentrations lower than those used in these studies.



**CHAPTER 6: *IN VIVO* AND *IN VITRO* EFFECTS OF DFO AND THE  
HYDROXYPYRIDINONES ON MURINE HAEMOPOIESIS**

## **6.1 INTRODUCTION**

The previous experiments have utilised *in vitro* models to investigate the *modus operandi* of iron chelators and their consequent effects on cell proliferation. However, the mechanisms by which chelators inhibit proliferation may differ *in vivo* and *in vitro*. For example, *in vivo* factors such as metabolism of the chelators may decrease their antiproliferative effects, or conversely stable metabolites with their own inhibitory properties may be formed. This final series of experiments were therefore designed to compare the antiproliferative effects of iron chelators *in vivo* and *in vitro*.

It has been reported previously that prolonged administration of 1,2-dimethyl-3-HP-4-one (CP20) causes leucopaenia in mice (Porter et al, 1989) and rats (Kontoghiorghes et al, 1989). This provides a potentially useful model to determine the consequences of iron chelation both *in vivo* and *in vitro*. Therefore the effects of CP20, CP94 and DFO on haemopoiesis in mice given daily prolonged administration of chelators has been compared with their *in vitro* actions in colony forming assays.

## **6.2 IN VIVO STUDY**

To investigate the *in vivo* antiproliferative effects of the chelators mice were dosed at a level of 200mg/kg. Whilst this dose is above that which would be generally given to man it has been chosen because it was at this dosage that leucopaenia was initially observed (Porter et al, 1989) and it is not far removed from the levels of CP20 that have been administered to some patients (Kontoghiorghes et al, 1990). Previous data has demonstrated that 3-HP-4-ones have similar efficacy whether they are administered by the oral or intraperitoneal (i.p.) route (Porter et al, 1990), therefore the i.p. route was chosen for these studies to allow comparison with DFO which is inactive by the oral route. As there is evidence that iron overload can protect against

some of the toxic effects of iron chelation (Porter et al, 1991) non-overloaded animals were used in these studies.

## **Experimental Procedure**

6-8 week old male Balb c mice were obtained from Harlan OLAC. The weight of the animals at commencement of the study was 20-25g. Groups of 6 mice were kept in polypropylene cages with stainless steel lids. Tap water and diet were given *ad libidum* with Rat and Mouse S.Q.C Expanded Diet No.1.

The mice were dosed for 5 days per week by i.p injection of 0.2ml DFO, CP20, CP94 (200mg/kg) or PBS alone for up to 60 doses. Mice were observed immediately before dosing and for approximately 20 minutes afterwards. Animals that were obviously unwell were killed by cervical dislocation. During the dosing period five animals died, two from the control group and one from each of the chelator groups.

At the end of the study the mice were anaesthetised with Hypnorm (0.01ml/30g) and Diazepam (5mg/kg) by intraperitoneal injection and killed by exsanguination from the carotid artery. 130µl of blood was put into labelled siliconised polypropylene Eppendorf tubes containing 195µg dried dipotassium EDTA and samples were thoroughly mixed and analysed on a Coulter STK-R for haemoglobin (Hb), white cell count (WCC), mean corpuscular volume (MCV) and mean cell haemoglobin (MCH). For differential white cell counts blood films were made on glass microscope slides, stained with Geimsa stain and the percentage of each cell type was obtained by counting 200 cells.

For reticulocyte counts equivolumines of EDTA blood and a 1% solution of New Methylene Blue in citrate saline, were incubated at 37°C for 15-20 minutes. At the end of incubation cells were gently resuspended and blood films were made on glass microscope slides. The percentage of reticulocytes was determined by counting 1000 cells by light microscopy without further fixing or staining.

Bone marrow cells were flushed from the femoral bone cavity and counted prior to culture in agar or methylcellulose to assess the growth of CFU-G + CFU-Mac or BFU-E colonies as described in Section 2.3.4 .

## Results and Discussion

Table 13 shows the haematology for the chelator treated and control animals. The white cell count was reduced in all treated groups. This was most marked for CP20 ( $p < 0.01$ ) and DFO ( $p < 0.05$ ) but failed to reach significance for CP94. Differential counting showed that both lymphocyte and neutrophil counts were below control values although only the low lymphocyte count reached significance for CP20 ( $p < 0.01$ ) and DFO ( $p < 0.05$ ) whilst animals given CP94 showed the same trend but did not reach statistical significance. The animals dosed with CP20 had a significantly reduced Hb and RCC ( $p < 0.01$ ) and a raised MCV ( $p < 0.01$ ), furthermore these animals were reticulocytopenic ( $p < 0.05$ ). There was also a very small but significant increase in the MCV of mice dosed with CP94 or DFO ( $p < 0.05$ ) but other haematological parameters were unaffected.

Measurement of bone marrow cellularity showed that CP20 treated mice had a significant reduction in bone marrow cellularity ( $p < 0.05$ ) compared to control animals in contrast to CP94 and DFO treated mice. The number of CFU-G + CFU-Mac after 6 days and BFU-E at 14 days were significantly increased in marrow cultures from CP20 treated animals ( $p < 0.01$ ) when compared to control mice (Table 14). However in these experiments, marrow was plated at a constant cell density even though the absolute number of nucleated cells per femur was significantly lower in the CP20 treated mice. When the number of CFU-G + CFU-Mac and BFU-E formed are corrected for marrow cellularity there are no significant differences between CP20 treated animals and controls (Table 14). These data therefore, strongly suggest that CFU-G + CFU-Mac and BFU-E are unaffected by *in vivo* administration of CP20.

In contrast to the results obtained after 60 doses, no changes were observed in the haematology or bone marrow cellularity of chelator treated animals when compared

**TABLE 13: HAEMATOTOLOGY FOR MICE TREATED WITH 60 DOSES OF 200mg/kg CHELATOR**

COMPOUND	n	WCC x10 <sup>9</sup> /l	Lymphs x10 <sup>9</sup> /l	Neuts x10 <sup>9</sup> /l	Hb g/dl	RBC x10 <sup>12</sup> /l	MCV fl	Retics %
Control	11	6.8±0.4	5.2±0.5	1.5±0.7	17.3±0.5	10.8±0.3	45.5±0.2	3.8±0.2
CP20	12	3.9±0.5**	2.6±0.5**	1.2±0.2	14.9±0.5*	8.7±0.3**	50.2±0.5**	2.6±0.1*
CP94	12	5.4±0.5	3.7±0.4	1.4±0.1	16.8±0.3	10.5±0.2	46.2±0.2*	3.2±0.5
DFO	11	4.7±0.5*	3.2±0.3*	1.2±0.2	16.1±0.4	10.4±0.3	46.2±0.1*	3.2±0.3

Mice were given 60 daily doses of 200mg/kg CP20, CP94, DFO or an equivalent amount of PBS for controls. At the end of dosing animals were killed and blood was taken and analysed for white cell count (WCC), number of lymphocytes (Lymphs), number of neutrophils (Neuts), red cell count (RCC), haemoglobin Hb, mean corpuscular volume (MCV) and % reticulocytes (% retics). Data is expressed as the mean ± S.E.M for n animals in each group. Significant differences between control and chelator treated animals were identified at the p<0.05(\*) and the p<0.01(\*\*) levels by the Mann Whitney U test.

**TABLE 14: BONE MARROW CELLULARITY AND HAEMOPOIETIC COLONY FORMATION  
FOR MICE TREATED WITH 60 DOSES OF 200mg/kg CHELATOR**

COMPOUND	Cells/Femur X 109	CFU-G+CFU-Mac/50000	BFU-E/50000	CFU-G+CFU-Mac	BFU-E
		Cells Plated	Cells Plated	Per Femur	Per Femur
Control	12.7±2	30.2±3	6±2	43±7	20±6
CP20	6.7±1**	70±8**	12±2**	61±16	21±3
CP94	11.3±1	44±7	4±1	54±11	13±3
DFO	14.1±2	35±6	6±2	52±15	14±4

Mice were dosed with chelators or PBS as described for Table 6.1. At the end of dosing the animals were killed and the cellularity of one femur (Cells/femur) was measured. Isolated bone marrow cells were cultured in soft agar or methylcellulose with growth factors to assay the formation of Colony forming unit-granulocyte and Colony forming unit-macrophage (CFU-G + CFU-M) and Burst forming unit-erythroid (BFU-E) colony formation as described in the text. The results are expressed as the mean ± S.E.M for a minimum of 9 animals in each group. Significant differences between control and chelator treated animals were identified at the p<0.01 level (\*\*) by the Mann Whitney U test.

**TABLE 15: HAEMATOLOGY FOR MICE TREATED WITH 10 OR 30  
DOSES OF 200mg/kg CHELATOR**

COMPOUND	WCC x10 <sup>9</sup> /l	Hb g/dl	RBC x10 <sup>12</sup> /l	MCV fl	Cells/Femur x10 <sup>9</sup>
Control	6.4±0.9	16.3±0.3	10.7±0.5	45.3±0.3	12.3±1.4
CP20					
10 Doses	6.5±0.7	17.0±0.4	10.9±0.4	46.0±0.3	13.7±0.9
30 Doses	5.9±0.2	16.1±0.2	9.9±0.3	46.2±0.4	11.7±0.3
CP94					
10 Doses	6.7±0.3	16.2±0.4	10.1±0.3	45.6±0.2	12.6±0.4
30 Doses	7.1±0.5	16.7±0.2	10.4±0.3	46.0±0.3	12.4±0.4
DFO					
10 Doses	6.8±0.3	15.9±0.2	10.1±0.2	45.4±0.1	11.3±1.0
30 Doses	7.2±0.5	16.4±0.1	9.8±0.4	45.9±0.2	11.6±0.9

Mice were given 10 or 30 daily doses of 200mg/kg CP20, CP94, DFO or PBS for controls. At the end of dosing animals were killed and blood was taken and analysed for white cell count (WCC), red cell count (RCC), haemoglobin (Hb) and mean corpuscular volume (MCV). Data is expressed as the mean ± S.E.M for 4 animals in each group.

to controls after 10 or 30 doses of 200mg/kg chelator (Table 15). This suggests that the myelosuppressive effects result from chronic rather than acute exposure to CP20 at these doses.

### **6.3 IN VITRO STUDIES**

#### **6.3.1 Effects of DFO, CP94 and CP20 on Normal Haemopoietic Colony Formation**

##### **Experimental Procedure**

To determine the effects of iron chelators on CFU-G + CFU-Mac and BFU-E formation, bone marrow cells isolated from the femurs of normal untreated mice were cultured in agar or methylcellulose (Section 2.3.4) with a range of chelator concentrations. After 6 or 14 days the number of CFU-G + CFU-Mac or BFU-E colonies respectively, were counted with a stereo microscope, a colony was defined as a group of 40 or more cells.

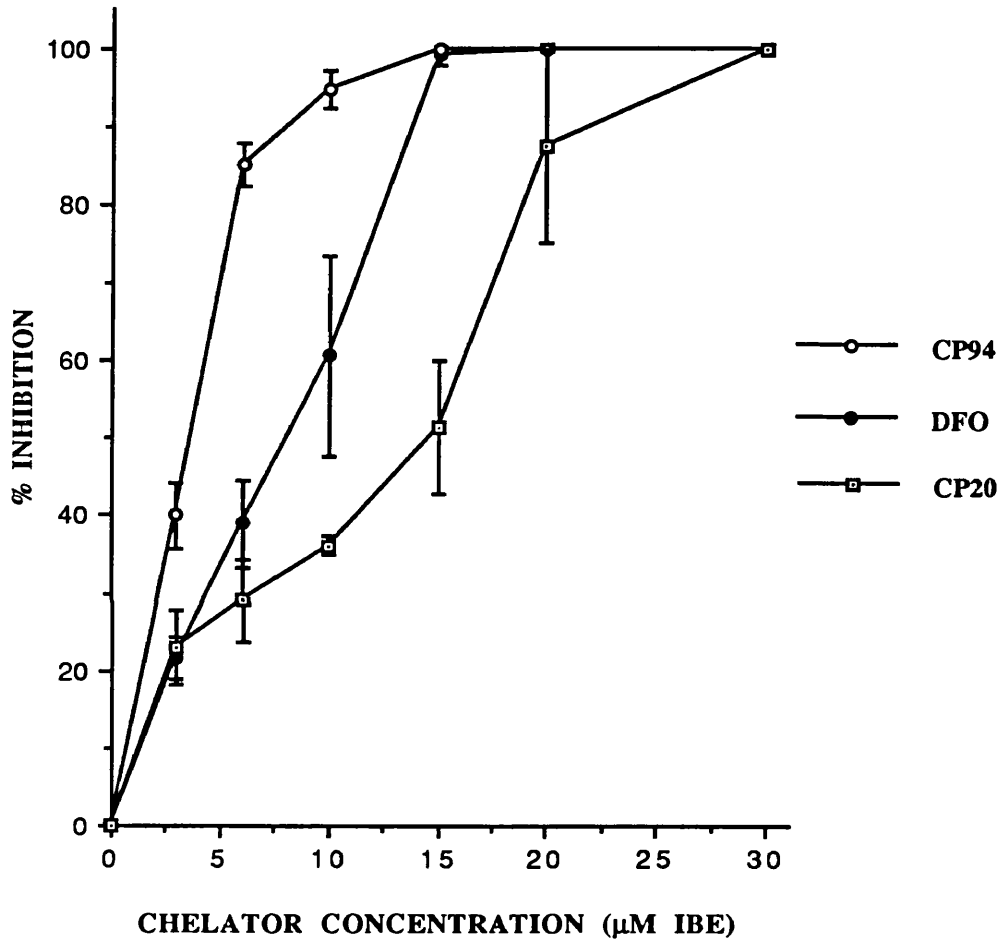
##### **Results**

Dose responses for CP94, CP20 or DFO on CFU-G + CFU-Mac and BFU-E colony formation are shown in Figures 43 and 44 respectively. Whereas the mean colony number in the control cultures was  $120 \pm 8.8$  and  $18 \pm 0.66$  for CFU-G + CFU-Mac and BFU-E respectively the chelators inhibited colony formation in a concentration dependent manner. From these data the mean concentrations required to inhibit colony formation by 50% (IC<sub>50</sub>) were calculated by linear regression to be  $3.5 \mu\text{M}$  IBE CP94,  $7.7 \mu\text{M}$  IBE DFO and  $12.9 \mu\text{M}$  IBE CP20 for CFU-G + CFU-Mac colonies and  $2.5 \mu\text{M}$  CP94,  $5.5 \mu\text{M}$  CP20 and  $8.7 \mu\text{M}$  DFO for BFU-E.



**FIGURE 43:**

**CONCENTRATION DEPENDENT INHIBITION OF CFU-G + CFU-Mac COLONY GROWTH BY IRON CHELATORS**

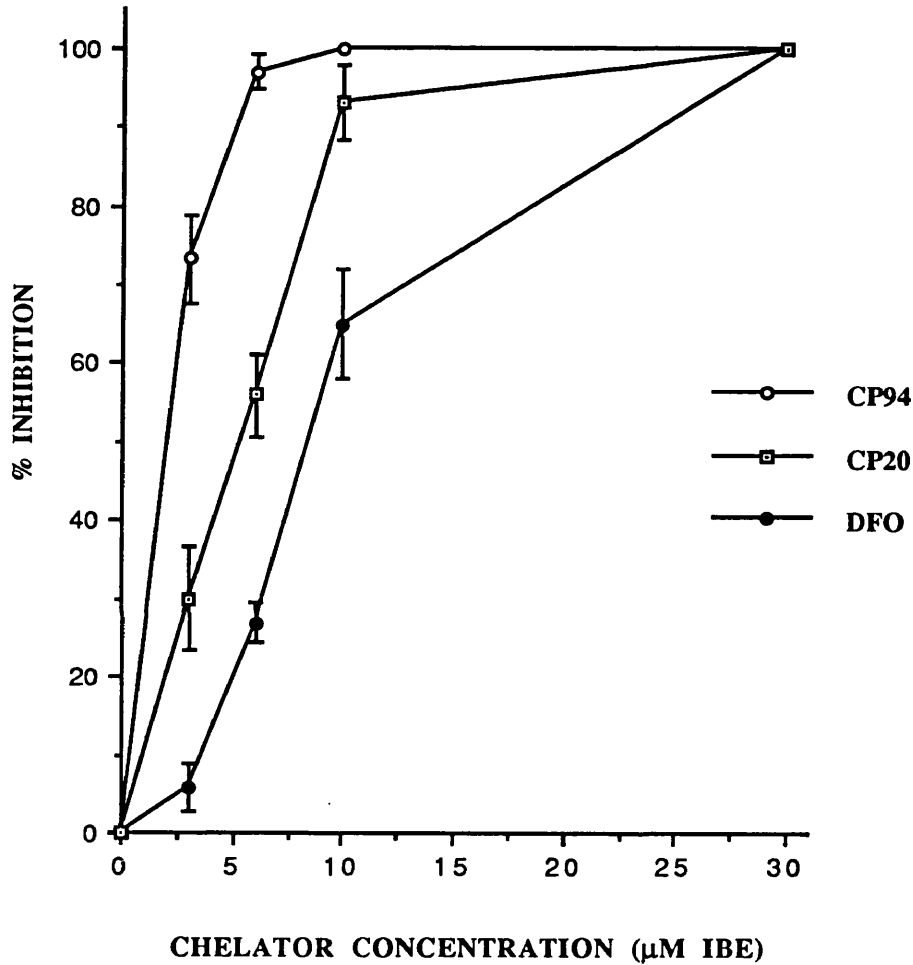


**LEGEND**

Unseparated bone marrow cells from normal Balb c mice were plated at  $1 \times 10^5$ /ml in soft agar and exposed to varying concentrations of DFO, CP20 and CP94. CFU-G + CFU-Mac colonies were counted after 6 days culture. The data is expressed as the percentage inhibition of colony formation of controls and represents the mean  $\pm$  S.E.M of 3 separate experiments with triplicates at each point.

**FIGURE 44:**

**CONCENTRATION DEPENDENT INHIBITION  
OF BFU-E GROWTH BY IRON CHELATORS**



**LEGEND**

Unseparated bone marrow cells from normal Balb c mice were plated at  $1 \times 10^5$ /ml in methylcellulose and exposed to varying concentrations of DFO, CP20 and CP94. BFU-E colonies were counted after 14 days culture. The data is expressed as the percentage inhibition of colony formation of controls and represents the mean  $\pm$  S.E.M of 3 separate experiments with triplicates at each point.

### 6.3.2 Effects of Iron Complexed Chelators on CFU-GM Colony Formation.

In order to investigate whether the inhibitory effects observed *in vitro* were due to iron chelation or to other mechanisms, sufficient iron to saturate the chelators was added to CFU-G + CFU-Mac cultures at the start of the experiment. This was done either by adding ferric ammonium citrate directly to the culture medium or by adding the chelator as preformed iron-chelator complexes.

#### **Experimental Procedure**

Isolated mouse bone marrow cells were cultured for 6 days in soft agar culture medium containing 30 $\mu$ M IBE DFO, CP20 or CP94 in the presence or absence of 33 $\mu$ M iron, added directly to the culture mixture as ferric ammonium citrate. In parallel experiments increasing concentrations (3-100 $\mu$ M IBE) of FO, CP20-Fe and CP94-Fe the iron complexed forms of DFO, CP20 and CP94 respectively (Section 2.2), were added directly to the culture medium. At the end of incubation colony formation was assessed by counting as in Section 6.3.1.

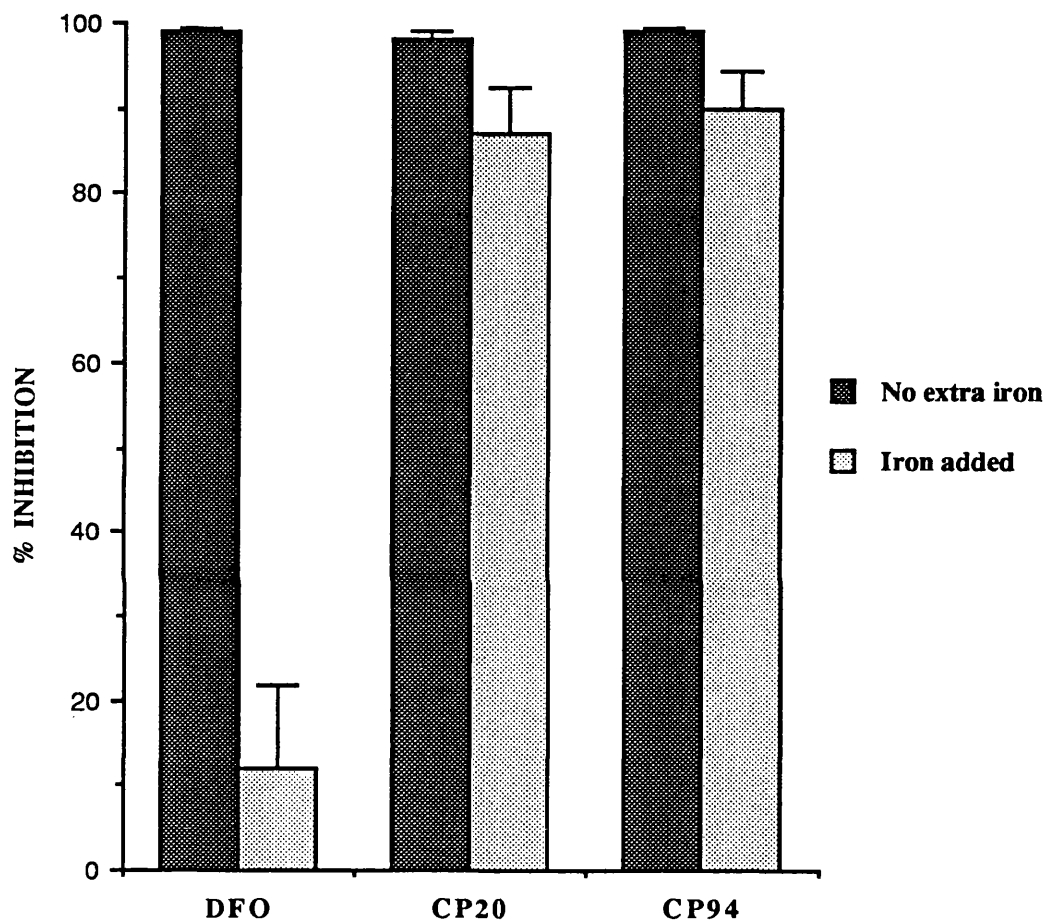
#### **Results**

Addition of saturating amounts of iron, in the form of ferric ammonium citrate, directly to the CFU-G + CFU-Mac cultures had no significant effect on the growth of controls but totally abrogated the inhibitory effects of 30 $\mu$ M IBE DFO on colony formation. In contrast CP94 and CP20 continued to inhibit colony formation by almost 90% (Figure 45).

When the iron complexes were added directly to the cultures, the number of CFU-G + CFU-Mac colonies formed in the presence of ferrioxamine did not differ significantly from the control value of  $103 \pm 7.8$  colonies. However CP94-Fe and CP20-Fe complexes suppressed CFU-G + CFU-Mac colony formation (Figure 46).

**FIGURE 45:**

**EFFECT OF THE ADDITION OF IRON ON INHIBITION  
OF CFU-G + CFU-Mac BY IRON CHELATORS**

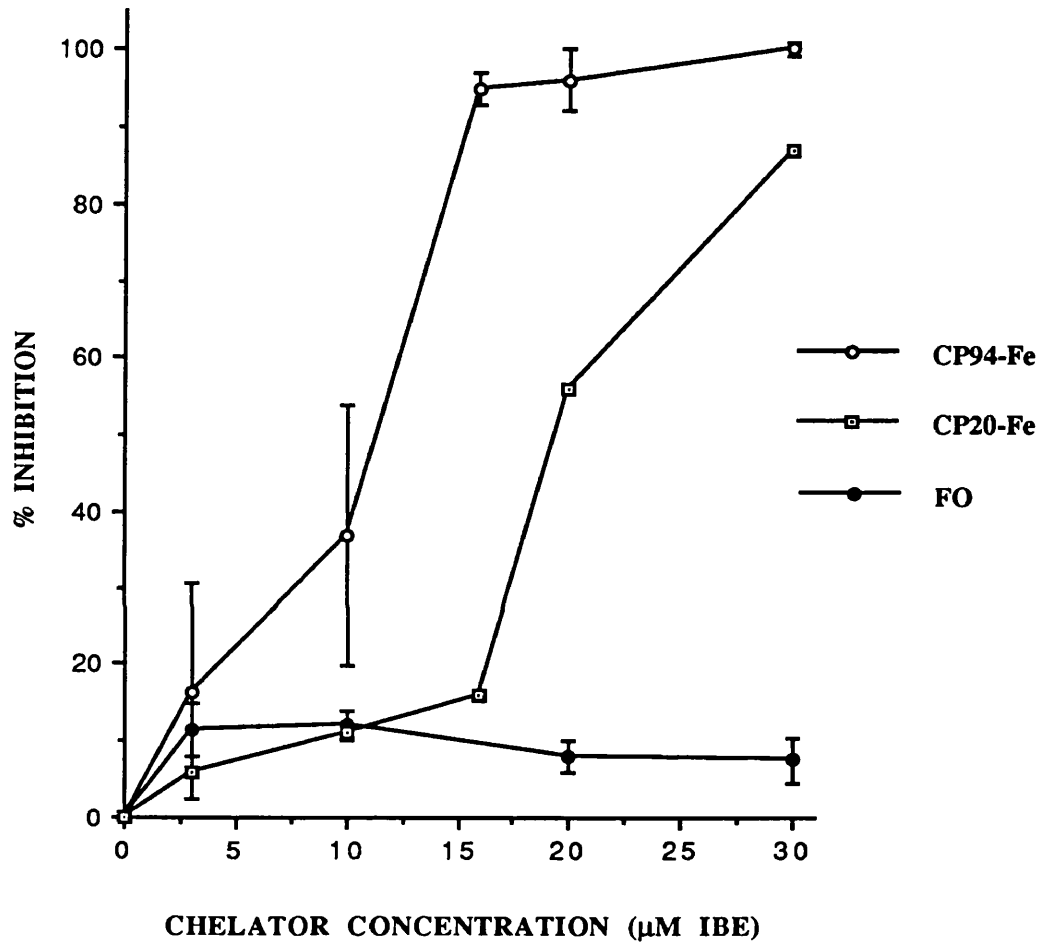


**LEGEND**

Unseparated bone marrow cells from normal Balb c mice were plated at  $1 \times 10^5$ /ml and cultured for 6 days in soft agar culture medium with  $30 \mu\text{M}$  IBE DFO, CP20 or CP94 in the presence or absence of  $33 \mu\text{M}$  iron, in the form of feric ammonium citrate. The data is expressed as the percentage inhibition of colony formation of controls and represents the mean  $\pm$  S.E.M of 2 separate experiments with triplicates at each point.

**FIGURE 46:**

**DOSE RESPONSE EFFECT OF FO, CP94-Fe AND CP20-Fe ON CFU-G + CFU-Mac COLONY GROWTH**



**LEGEND**

Unseparated bone marrow cells from normal Balb c mice were plated at  $1 \times 10^5$ /ml and cultured for 6 days in soft agar culture medium with varying concentrations of FO, CP20-Fe or CP94-Fe. The data is expressed as the percentage inhibition of colony formation of controls and represents the mean  $\pm$  S.E.M of 3 separate experiments with triplicates at each point.

The CP94-Fe iron complex was markedly more active with an approximate IC<sub>50</sub> of 12µM compared to 21µM for the CP20-Fe complex.

### 6.3.3 Effect of Transferrin Saturation on Inhibition by Chelator Complexes.

One mechanism by which the 3-HP-4-one iron complexes may inhibit colony formation is by donation of iron to unsaturated transferrin in the culture medium. This could promote the formation of iron free chelator with potential for the inhibition of cell proliferation. The influence of transferrin saturation on the inhibitory effects of free and iron-complexed chelators was therefore examined by iron-saturating the transferrin in the culture medium.

#### **Experimental Procedure**

The iron content and total iron binding capacity (TIBC) of three batches of FCS were measured by the method of Ruutu (1975) (Appendix 3). The TIBC was found to be  $135 \pm 3\mu\text{M}$  and the serum iron content was  $32 \pm 2\mu\text{M}$ . Therefore, 103 µmoles/l of iron, in the form of ferric ammonium citrate, were added to FCS in the presence of bicarbonate to increase the transferrin saturation to 100%. In some experiments iron equivalent to twice the TIBC was added as ferric ammonium citrate, this is shown as '2 x 100%' saturated transferrin. In other experiments additional iron was added in the form of iron saturated human transferrin to FCS containing 100% saturated transferrin. These experimental manipulations of transferrin saturation can be summarised as follows:

- A. 27% saturated - normal FCS.
- B. 100% saturated - sufficient iron added to saturate transferrin to the TIBC
- C. 2x100% saturated- total iron added equals twice the TIBC.
- D. 100% saturated + human transferrin - transferrin saturated to the TIBC then equivalent amount of iron added as 100% saturated human transferrin.

After the transferrin saturation of the FCS had been appropriately adjusted, soft agar culture medium was prepared as described previously (Section 2.3.4).

Bone marrow cells were isolated from normal Balb c mice and cultured in agar with increasing concentrations of CP94 and CP20 or their preformed iron complexes (Section 2.2) and the transferrin saturation of the culture medium was adjusted as described above. After 6 days culture the number of CFU-G + CFU-Mac colonies was counted using a stereo microscope as described previously (Section 6.3.1).

## Results

Table 16 shows the number of CFU-G + CFU-Mac colonies formed after 6 days culture. Whilst saturation of the transferrin in the culture medium had no significant effect on the proliferation of control cultures the inhibitory effects of the 3-HP-4-one complexes were significantly modified. When the transferrin was iron saturated there was no significant inhibition of CFU-G + CFU-Mac colony formation by CP20 or the preformed CP20-Fe complex. In contrast, although the suppression of colony formation by CP94 in both the iron free and iron complexed forms was reversed at 10 $\mu$ M IBE, a marked inhibition was apparent at higher concentrations. Furthermore increasing the iron concentration of the culture medium to 2x100% TIBC failed to reverse this trend (Table 16).

As inhibition was not abrogated by either of these methods additional iron was made available to the cultures in the form of fully iron saturated human transferrin. Under these conditions the inhibitory effects of CP94-Fe were overcome at all concentrations of the chelator-iron complex. The inhibitory effects of the free chelate, however, were only fully overcome at 10 $\mu$ M IBE (Table 16) and highly significant suppression of colony formation was observed at higher concentrations.

**TABLE 16: TRANSFERRIN SATURATION AND INHIBITION OF  
CFU-G+ CFU-MAC COLONY GROWTH BY IRON-FREE AND IRON-  
COMPLEXED CP94 AND CP20**

Chelator concentration		% Transferrin Saturation				
		$\mu$ M IBE	27%	100%	2 x100%	100%+hTf
<b>Control</b>			41±1	48±9	37±2	44±2
<b>CP94</b>	10	1±.3	44±2	30±3	45±4	
	20	0	3±2	18±2	20±2	
	30	0	0	4±2	2±1	
<b>CP94-Fe</b>	10	18±3	49±4	30±3	45±2	
	20	3±1	31±6	20±2	35±6	
	30	1±1	21±2	16±3	40±1	
<b>CP20</b>	10	19±6	43±2	N.D	N.D.	
	20	1±1	41±1	N.D.	N.D.	
	30	0	35±2	40±3	37±2	
<b>CP20-Fe</b>	10	40±3	48±2	N.D	N.D.	
	20	21±5	44±4	N.D.	N.D.	
	30	0	35±3	40±1	42±2	

N.D. = not determined.

Bone marrow cells from mouse femurs were cultured for 6 days in the presence or absence of chelators. The saturation of the transferrin present in the culture medium was unchanged (27%), saturated to 100% with ferrous ammonium sulphate (100%), saturated to a twofold excess with ferric ammonium citrate (2 x 100%) or saturated to 100% then an equimolar amount of human iron saturated transferrin added (100%+hTf). The data is expressed as the mean number of colonies  $\pm$  1 SE for triplicate samples.



### 6.3.4 Relationship Between Chelator Lipophilicity and Colony Inhibition.

To identify any relationship between the lipid solubility of chelators and their iron complexes and suppression of colony formation, a range of 3-hydroxypyridin-4-ones of varying lipophilicity were added to CFU-G + CFU-Mac cultures in both the iron free and iron complexed form.

#### **Experimental Procedure**

Bone marrow cells isolated from normal Balb c mice were incubated in soft agar culture medium (Section 2.3.4) in the presence or absence of 16 $\mu$ M IBE CP20, CP21, CP22, CP40, CP52 or CP94 in the iron free and iron saturated form. The iron complexes of the chelators were prepared as described previously (Section 2.2). After 6 days culture the number of CFU-G + CFU-Mac colonies was counted using a stereo microscope as described previously (Section 6.3.1)

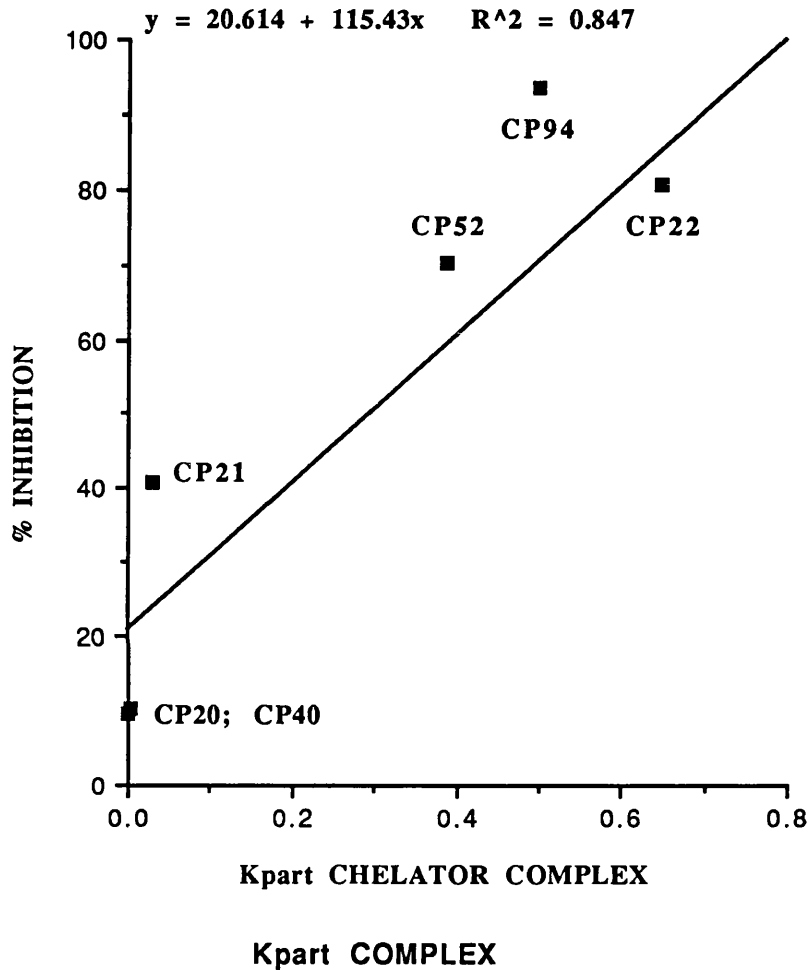
#### **Results**

The results in Figure 47 show the percentage inhibition of CFU-G + CFU-Mac growth plotted against partition coefficient for each 3-hydroxypyridin-4-one iron-complex. The correlation coefficient, R, was calculated to be 0.89 indicating good correlation between chelator lipophilicity and inhibition of CFU-G + CFU-Mac growth.

All the chelators screened totally inhibited colony formation in the free form with the exception of CP40 and CP20 which inhibited colony formation by 18% and 73% respectively.

**FIGURE 47:**

**RELATIONSHIP BETWEEN PARTITION COEFFICIENT AND INHIBITION OF CFU-G + CFU-Mac BY CHELATOR COMPLEXES**



**LEGEND**

Unseparated mouse bone marrow cells were cultured in soft agar culture medium with a range of preformed iron complexes of 3-HP-4-ones at 16 $\mu$ M IBE for 6 days. The transferrin saturation of the culture medium was 100%. The data is expressed as the percentage inhibition of colony formation of controls and represents the mean  $\pm$  S.E.M of 2 separate experiments with triplicates at each point.

### 6.3.5 Discussion

Micromolar concentrations of DFO and the 3-HP-4-ones caused dose dependent inhibition of haemopoietic progenitor growth from normal murine bone marrow (Figure 43 and 44). The IC<sub>50</sub> values obtained for DFO of 7.6 $\mu$ M and 8.7 $\mu$ M for CFU-G + CFU-Mac and BFU-E respectively agree closely with previously reported values for the inhibitory actions of this compound on the growth of human haemopoietic progenitors (Dezza et al, 1987). While the relative sensitivities of BFU-E and CFU-G + CFU-Mac to DFO and CP94 were approximately equal, their sensitivities to CP20 differ. The IC<sub>50</sub> for CP20 was 5.5 $\mu$ M for BFU-E and 12.9 $\mu$ M for CFU-G + CFU-Mac suggesting that different cell lineages may have differing sensitivities to this compound.

Whilst FO did not display any significant antiproliferative activity on CFU-G + CFU-Mac, the iron complexes of CP94 and CP20 continued to inhibit colony formation (Figures 45 and 46) although not to the same extent as the corresponding free chelator. When the transferrin in the medium was iron saturated, no significant inhibition of colony formation was observed with the hydrophilic CP20-Fe complex but the inhibitory effects of the more lipophilic CP94-Fe were only partially abrogated (Table 16), even when the transferrin saturation was doubled. However, when further iron-saturated human transferrin was added to the culture medium, inhibition of colony formation by CP94-Fe complex was completely reversed (Table 16).

These results suggest that 3-HP-4-one chelator-iron complexes may dissociate both in the extracellular medium with donation of iron to transferrin, and intracellularly with the released iron being sequestered into intracellular pools. The resulting free chelator would then be available to interfere with iron-dependent cellular function. When the concentration of iron-saturated transferrin in the culture medium is increased, however, sufficient iron is delivered to the cell to overcome the chelator induced intracellular iron depletion and proliferation may proceed normally. This

hypothesis is further supported by the observation that colony inhibition by 3-HP-4-one iron complexes correlates markedly with complex lipophilicity under conditions of 100% transferrin saturation (Figure 47).

#### **6.4 GENERAL DISCUSSION**

The results of these studies show that, like DFO, CP20 and CP94 are potent inhibitors of *in vitro* haemopoietic colony formation. *In vivo*, mice treated with CP20 displayed significant alterations to their haematology (Table 13). These results are consistent with previous findings in mice (Porter et al, 1989) and rats (Kontoghiorghes et al, 1989). In addition bone marrow cellularity in these animals was significantly reduced suggesting that chronic exposure to CP20 affects the production of cells in the bone marrow rather than increasing the consumption of circulating cells. Furthermore the antiproliferative effects do not appear to be selective for any single cell type as neutrophil, lymphocyte and red cell counts were decreased in the CP20 treated animals, suggesting a general antiproliferative effect.

When bone marrow cells isolated from the treated mice were cultured *in vitro*, the number of CFU-G + CFU-Mac and BFU-E colonies from mice receiving CP20 were significantly increased when compared to the other treatment groups (Table 14), however when colony number was normalised to account for the differences in bone marrow cellularity no alteration in colony formation could be detected in CP20 treated mice compared to controls. This suggests that CFU-G + CFU-Mac and BFU-E are not affected by *in vivo* administration of CP20. The exact cells which are being depleted is unclear but are unlikely to be earlier than the CFU-G + CFU-Mac and BFU-E stage.

Whilst DFO and CP94 had no significant effect on marrow cellularity a trend of lymphopaenia was observed with these chelators (Table 13). This observation is in accordance with the sensitivity of lymphocytes to cell cycle arrest by chelators observed in Section 5.2.2 and suggests that lymphocytes may be particularly

vulnerable to iron deprivation. It is unclear whether any one particular subclass of lymphocytes is particularly sensitive as phenotyping experiments were not performed in the current study. It would be interesting to conduct further experiments involving phenotyping to elucidate the mechanisms involved more clearly.

Whilst the *in vivo* effects of CP20 on marrow cellularity and haematology took several weeks to develop, it is clear from the *in vitro* studies that the iron chelators have antiproliferative effects on haemopoietic colony formation over the relatively short term of the culture. Micromolar concentrations of CP94, DFO and CP20 inhibited colony formation in a dose dependent manner. CP94 was the most active chelator, possibly because of its high lipid solubility.

Unlike FO, the iron complexes of the 3-HP-4-ones inhibited CFU-G + CFU-Mac colony formation (Figure 45). One major difference between the 3-HP-4-ones and DFO is that due to its bidentate nature the 3:1 HPO : iron complex has a tendency to dissociate into 2:1 and 1:1 iron complexes unlike the hexadentate FO (Porter et al, 1989). This occurs particularly at low ligand concentration and may result in donation of iron to unsaturated transferrin (Hider et al, 1991) leaving free chelator to inhibit colony formation. Hence there is a potential mechanism for the inhibition of cell proliferation for the bidentate 3-HP-4-ones which is not available to the hexadentate DFO.

Lipophilic chelators and their iron complexes would be predicted to have greater access into cells and organelles than the hydrophilic compounds and there is a clear correlation between complex lipophilicity and augmentation of suppression of colony formation (Figure 47). This observation is consistent with previous data demonstrating significant correlation between lipophilicity and antiproliferative activity for a range of bacterial siderophores by Bergeron and coworkers (Bergeron et al, 1984). However, these results contrast with the data shown in Sections 5.3 and 5.4 which indicate little relationship between lipophilicity and arrest of K562 cell cycle within the 3-HP-4-one series, when the chelators are in the iron free rather than the iron complexed state. The reasons for these differences are unclear but may be due to

the lower concentrations of iron-free chelator available to inhibit CFU-G + CFU-Mac colony formation, as only 16 $\mu$ M IBE was added to marrow cultures compared to 100 $\mu$ M IBE used in the cell cycle studies.

However, these results do not explain the relatively marked myelosuppressive effect of CP20 *in vivo*. It is unlikely that the suppression observed *in vivo* is a direct effect on BFU-E or CFU-G + CFU-Mac as the number of these colony types formed per femur was not significantly altered in CP20 treated animals compared to controls (Table 14). Furthermore, several other 3-HP-4-ones had a more marked effect on CFU-G + CFU-Mac than CP20 *in vitro* (Section 6.3.4). Clearly some additional property of CP20 is interacting with haemopoiesis *in vivo* which is not seen in simple *in vitro* cultures. For example CP20 or its metabolites may affect accessory cells necessary to maintain haemopoiesis *in vivo* relatively more than CP94 or DFO.

It is possible that the myelosuppressive effects of CP20 may not relate directly to iron chelation. Other bidentate 3-HP-4-ones which have been shown to be more effective than CP20 in removing iron from cells (Porter et al, 1988; Hershko et al, 1991) and animals (Porter et al, 1990; Hershko et al, 1990) had less effect on white cell count with *in vivo* administration to mice (Porter et al, 1989b). Furthermore previous studies have shown that that iron overload did not protect against leucopaenia induced by CP20 (Porter et al, 1989b). A potential difference between CP20 and other HPOs is its marked hydrophilicity in the iron complexed state (Table 4) resulting in a relative inability to transit cell membranes in the iron complexed form. This may mean that 3:1 iron complexes would remain within cells longer than more lipophilic 3-HP-4-one-iron complexes (e.g CP94-Fe), resulting in increased potential to cause toxicity.

## **CHAPTER 7: CONCLUSIONS**

## 7.1 INTRODUCTION

In order to optimise the clinical effectiveness of iron chelators whilst minimizing toxicity, in both iron-overloaded conditions and those unrelated to iron overload, it is important to understand how chelators interact with cells. In iron overload the aim of chelator therapy is to mobilise iron from cells or intracellular pools containing excess iron, whilst minimising iron removal from enzymes essential for normal cell function. In non iron-overloaded conditions the goals may be different, as the use of chelators in such circumstances depends upon the ability of these compounds to interfere with iron-dependent processes. However in both situations it is necessary to understand how the physicochemical properties of chelators influence their ability to mobilise iron from intracellular pools and so affect cell function.

The *in vitro* evaluation of iron chelators has been traditionally performed utilising cellular models with particular reference to the treatment of iron overload; namely hepatocytes (Porter et al, 1988) which represent the major site of iron accumulation, myocardial cells (Hershko et al, 1991) representing a major site of toxicity and reticuloendothelial cells (Ponka et al, 1979) representing a major site of iron turnover and release. While these systems have the advantage of allowing a thorough investigation of chelator function in iron-overloaded situations this in effect limits investigation into their potential toxicities and uses in alternative cell types in non-iron overloaded conditions.

In the current study the K562 cell line has been employed specifically because these cells are unrelated to iron storage cells but retain a high capacity to acquire and utilise iron via the receptor mediated endocytosis of transferrin. (Forsbeck and Nilsson, 1983). The studies presented in this thesis have sought to clarify the relationship between the physicochemical properties of DFO and the HPOs and their relative abilities to chelate iron from intracellular pools and so modify cell function. *In vivo* studies have also been performed utilising non-iron overloaded animals to



investigate how the *in vitro* effects of chelators on cell proliferation are paralleled by their *in vivo* effects with particular reference to haemopoiesis.

In these concluding sections the major findings of this thesis are discussed with particular reference to the relationship between iron chelator structure and subsequent ability to access intracellular iron pools and so modify cell function. The potential role of iron chelators as antineoplastic agents is also considered.

## **7.2 CELLULAR IRON MOBILISATION**

### **7.2.1 Transit Across Cell Membranes**

A key property for an iron chelator is the ability to cross biological membranes and so enter cells and mobilise iron from endogenous pools. The ability of chelators to mobilise intracellular iron has previously been related to their lipophilicity, measured by the  $K_{part}$  value, (Porter et al, 1988; Ponka et al, 1988; Hershko et al, 1991a) and their iron binding constant (Porter et al, 1988). Furthermore, the intracellular access of iron chelators will also be influenced by their charge (Florence and Attwood, 1981).

From the above criteria it is predicted that DFO would have limited access to intracellular iron pools. However, *in vitro* studies in a variety of cell types including hepatocytes (Octave et al, 1983), Chang cells (White et al, 1976b) and myocardial cells (Hershko et al, 1991a) have demonstrated the ability of DFO to mobilise intracellular iron. However the mechanisms involved in the entry of DFO into cells remain unclear.

The studies described in this thesis utilised the K562 cell line to assess the mechanisms of cellular accumulation of  $^{14}\text{C}$ -labelled DFO. The results in Chapter 3 suggest that DFO enters cells by a facilitated transport mechanism, most likely along an electrochemical gradient as a result of its charged nature. These results are in accordance with those of Bottomley and colleagues (1985) who reported a 14-fold accumulation of [ $^{14}\text{C}$ ]DFO in K562 cells over a 24 hour incubation period. Further

support for this concept is provided by the studies of Rice-Evans and associates (1989) who reported that DFO penetrates erythrocytes poorly. In contrast to most cell types the surface of the red cell membrane has a negative charge due to the presence of charged glycoprotein side chains (Gordon-Smith, 1981). Thus the ability of DFO to enter cells by an electrochemical gradient may be perturbed in red cells resulting in minimal DFO uptake.

In contrast to the above data, it has recently been proposed that pinocytosis may account for cellular accumulation of DFO by rat visceral yolk sacs (Lloyd et al, 1991). However, the observation in Section 3.4 that [ $^{14}\text{C}$ ]DFO uptake is not significantly impaired by the microtubule inhibitor colchicine suggests that pinocytosis is not a major route of uptake by K562 cells. Furthermore, DFO accumulated by this mechanism would be expected to be predominantly localised within the lysosomal compartment, but subcellular fractionation studies show that significant concentrations of intralysosomal [ $^{14}\text{C}$ ]DFO in K562 cells are not apparent until after 4 hours incubation (Section 4.3).

It is conceivable however, that pinocytotic uptake of DFO may play a more significant role in other cell types. Leukaemic cell lines such as K562 may have a limited capacity for pinocytosis when compared to hepatocytes (Pratten et al, 1980). Therefore hepatocytes may accumulate DFO relatively rapidly in comparison to other cell types by the dual processes of pinocytosis and a facilitated uptake mechanism. Further evidence for this hypothesis is provided by observations from preliminary experiments with isolated hepatocytes showing that these cells accumulate [ $^{14}\text{C}$ ]DFO more rapidly than K562 cells and this can be reduced by incubation with colchicine (Personal observation). In the treatment of iron overload it would be advantageous for chelators to interact rapidly with hepatocytes, as these cells are the major site of iron storage. Such preferential uptake would reduce the possibility of toxicity to other cell types. Therefore this observation may be one reason for the relatively low toxicity of DFO.

In contrast to DFO, the studies in Sections 3.2 and 3.4 of this thesis have clearly demonstrated that [ $^{14}\text{C}$ ]CP94 enters K562 cells by simple diffusion across the cell membrane. The close structural similarities in the 3-HP-4-one series, which differ only in the nature of the alkyl substituents on position  $\text{R}_1$  and  $\text{R}_2$  of the 3-HP-4-one ring (Figure 9), make it probable that this uptake mechanism applies to all 3-HP-4-one chelators. This concept is further supported by previous studies showing a direct relationship between the  $K_{\text{part}}$  value of 3-HP-4-one compounds and iron mobilisation from both primary hepatocyte monolayer cultures (Porter et al, 1988) and rat myocardial cell cultures (Hershko et al, 1991a). Similarly, studies in mice (Porter et al, 1990) have shown a linear relationship between  $K_{\text{part}}$  value and oral activity for 3-HP-4-one chelators.

### 7.2.2 Access to Intracellular Iron Pools

Many previous studies have suggested that the LMW cytosolic pool represents the most readily accessible intracellular source of chelatable iron for DFO (Jacobs et al, 1976; White et al, 1976b; Baker et al, 1985b; Mulligan et al, 1986). However, there has been considerable debate upon the contribution of alternative sites of iron sequestration, such as lysosomes or mitochondria, to net DFO iron mobilisation (Laub et al, 1985; Jin et al, 1989). Furthermore, there have previously been no detailed investigations of the intracellular source of iron mobilised by 3-HP-4-one chelators.

Therefore in this thesis the intracellular sites of action of DFO and CP94 were studied in K562 cells. The results of the experiments described in Chapter 4 show clearly that the LMW cytosolic pool is the major site of chelation for both DFO and CP94, so confirming the previous studies described above. Furthermore, the data in Section 4.4 indicates that chelation from the LMW cytosolic pool is at the expense of incorporation of iron into ferritin and organelles such as mitochondria and the nucleus. Access to this pool is only limited by the rate at which chelators cross the cell membrane. Therefore iron contained within the LMW pool is equally accessible to

CP94 and DFO when cytosolic concentrations of these chelators are equivalent (Section 4.6)

The access of iron chelators to other iron pools contained within organelles will be determined by the ability of the chelator to diffuse across intracellular membranes. Therefore, as shown in Section 4.3, relatively lipophilic LMW neutral chelators such as CP94 permeate into subcellular organelles more rapidly than hydrophilic higher molecular weight charged compounds such as DFO. The relative ease at which CP94 can transit intracellular membranes also raises the possibility that this compound can directly chelate intra-endosomal iron prior to its translocation across the endosomal membrane to the LMW pool. However further experiments utilising both subcellular fractionation and isolated endosome techniques are required to confirm this hypothesis

Rapid chelator transit across intracellular membranes may be advantageous in the treatment of iron overload where a significant amount of iron is present as intralysosomal haemosiderin (Selden et al, 1980). Several studies have identified the lysosome as a key organelle in iron mediated peroxidative damage (Seymour and Peters, 1978, Selden et al, 1980). It is unlikely that haemosiderin itself is responsible for such iron toxicity as the addition of haemosiderin to liposomes (O'Connell et al, 1985,1986) or to normal liver homogenates (Bacon et al, 1985) does not promote lipid peroxidation. It is more probable that the low intralysosomal pH dissolves the exposed haemosiderin core and the resultant released iron is able to participate in free radical reactions (Weir et al, 1984b). Such released iron would also be available for chelation and it is therefore important that chelators have rapid access to the lysosomal compartment. Thus the relatively slow rate at which DFO enters organelles may limit its effectiveness in iron over-loaded situations.

Whilst it is desirable that chelators have access to the lysosomal compartment, penetration of other organelles may result in toxicity from the removal of essential iron from iron containing enzymes. Iron contained in haemoproteins and iron-sulphur centres is difficult to remove with chelators at neutral pH, however non-haem,non-

iron-sulphur iron-containing enzymes such as ribonucleotide reductase (Ganeshaguru et al, 1980) or 5'lipoxygenase (Barradas et al, 1989) may be more susceptible to chelation and this, in turn, may lead to toxicity particularly in circumstances of minimal iron loading.

### 7.2.3 Removal of Iron From Cells

Once intracellular iron has been chelated the resulting iron-complex should be able to transit cell membranes and so remove iron from the cell. Therefore, like the free ligand, chelator complexes should be uncharged and relatively lipophilic for optimal passage across the plasma membrane.

The 3-HP-4-ones bind iron to form a neutral complex that generally has a markedly lower  $K_{part}$  than the corresponding free ligand (Table 4). In the current study CP94 has been shown to rapidly mobilise  $^{59}\text{Fe}$  from K562 cells (Sections 3.5 and 4.3). Previous studies in isolated hepatocyte culture models have revealed that the  $K_{part}$  of the 3-HP-4-one iron complex exerts little influence upon iron mobilisation (Porter et al, 1988). Hepatocyte isolates are capable of active excretion and bio-transformation of drugs (Bock et al, 1976; Waterkyn et al, 1987) and it is probable that such mechanisms account for the poor correlation between complex  $K_{part}$  and iron removal. However other cell types, such as the K562 model utilised in the present study, are unlikely to possess such properties and it would be expected that the  $K_{part}$  of the iron complex may exert a larger influence upon the removal of iron from the cell.

Unlike the 3-HP-4-one iron complexes, FO has a net positive charge and so would be expected to egress only slowly from cells by simple diffusion. This is confirmed by the experiments described in Chapter 3 of this thesis which show that DFO is less efficient at rapidly mobilising intracellular iron from K562 cells than CP94 (Section 3.5, Figure 19). This can be attributed to the intracellular retention of FO, as demonstrated by HPLC, rather than any inability of DFO to enter cells, as it has been

demonstrated previously that DFO has rapid access into K562 cells by a facilitated uptake mechanism (Section 7.2.1). Furthermore subcellular fractionation studies utilising both radiolabelled DFO and  $^{59}\text{Fe}$  show that FO rapidly accumulates within the LMW cytosolic fraction of the cell (Sections 4.2 and 4.3) and only egresses slowly from the cell (Section 4.3)

In contrast to these data, several studies have demonstrated that DFO rapidly mobilises iron from hepatocytes (Octave et al, 1983; Baker et al, 1985a; Porter et al, 1988) and it is possible that FO may egress from hepatocytes by an active excretion mechanism as discussed above. In the absence of such mechanisms FO would take many hours to pass out of the cell as observed in the current study.

### **7.3 EFFECT OF IRON CHELATION ON CELL FUNCTION**

Iron is required for a wide variety of cellular functions. Individual cellular pathways may have varying sensitivities to iron deprivation depending upon the availability of iron for chelation and the rate of turnover of iron dependent enzymes involved. Iron chelators may modify cell function by general iron depletion resulting mainly from chelation from the low molecular weight pool, or by direct removal of iron from iron containing enzymes. In this thesis the influence of iron chelation on cell function has been investigated using cell proliferation as a model.

#### **7.3.1 The Antiproliferative Effects of Iron Chelators.**

Experiments with K562 cells, Daudi cells and PBL have shown that cellular iron deprivation due to exposure to CP94 and DFO has a profound effect on DNA synthesis whilst having minimal effect on the synthesis of RNA and proteins (Sections 5.2 and 5.6). Furthermore a dose dependent reduction in ribonucleotide reductase activity was shown in K562 cells treated with CP94 and DFO (Section 5.4). These data are in agreement with the observations of others (Ganeshaguru et al, 1980;

Lederman et al,1984; Cavanaugh et al, 1985) which suggest that the primary mechanism by which iron chelators inhibit cell proliferation is the inhibition of ribonucleotide reductase, thereby preventing cells traversing S phase of the cell cycle (Section 5.2). However, it is unclear whether such inhibition of ribonucleotide reductase activity results from general cellular iron depletion or specific chelation of iron from the enzyme itself.

The activity of ribonucleotide reductase is cell cycle dependent, increasing markedly at the time of DNA synthesis. Extracts from resting cells contain very low or undetectable activity whilst there is a dramatic increase in activity as cells enter S-phase (Turner et al, 1968; Elford et al, 1970). Studies by Eriksson and colleagues (1984) have demonstrated that this S-phase associated increase in activity is regulated by *de novo* protein synthesis of the M2 subunit of ribonucleotide reductase, which has a half life of approximately 3 hours. Once formed, the M2 subunit gains its tyrosyl free radical which has a half life of approximately 10 minutes. Therefore constant regeneration of this radical is required with an obligate need for oxygen and iron (Thelander et al, 1983). Thus, it is conceivable that a general cellular iron depletion may result in the inhibition of tyrosyl radical formation in the M2 subunit so leading to cell cycle arrest without the need of specific iron chelation from this site. The ability of an iron chelator to inhibit ribonucleotide reductase activity and so arrest cell cycle would therefore be dependent upon the access of the chelator to the LMW cytosolic pool, which in turn is dependent upon transit of the cell membrane by the chelators.

Bergeron and colleagues (1984) have demonstrated a clear correlation between the antiherpetic and antineoplastic properties of a range of catecholamide iron chelators and their  $K_{part}$  values. However in the K562 model employed in current study, whilst the hydrophilic hexadentate HPO CP130 had minimal effect upon cell proliferation, no correlation between  $K_{part}$  value and antiproliferative effect was observed within the 3-HP-4-one series. The reasons for these contrasting results are unclear, but one possible explanation is that the chelator concentration of 100 $\mu$ M IBE used in the current study was so high as to mask any differences between the antiproliferative

activities of the 3-HP-4-one chelators. However, in the Bergeron study the chelators were used at considerably lower concentrations between 0.4 $\mu$ M and 50 $\mu$ M. This suggests that greater correlation between lipophilicity and antiproliferative effects may become apparent at low chelator concentrations. This concept is further supported by the clear correlation between chelator-iron complex lipophilicity and inhibition of CFU-G + CFU-Mac colony growth in Section 6.3.4 when the 3-HP-4-one complexes were present at a concentration of 16 $\mu$ M IBE.

Several studies have demonstrated that the effect of iron chelators on cellular proliferation is more complex than can be explained by ribonucleotide reductase inhibition alone (Barankiewicz and Cohen, 1987; Cavanaugh et al, 1985; Reddel et al, 1985). Similarly, the results shown in Sections 5.5 and 5.6 of this thesis suggest that low concentrations of CP94 and DFO selectively inhibit K562 cell proliferation with minimal inhibition of ribonucleotide reductase activity and DNA synthesis. Such effects may be a result of chelation of iron vital to the functioning of other iron dependent cellular systems.

One such system may be the mitochondrial respiratory enzymes (Hibbs et al, 1984). Included in this group are several enzymes containing non-haem bound iron in the form of iron-sulphur clusters (Section 1.2.3). In particular the citric acid cycle enzyme aconitase has been implicated as a target enzyme in the inhibition of tumour cell proliferation by cytotoxic activated macrophages by selective iron depletion (Drapier and Hibbs, 1986) and may be a target for chelator action. As previously described (Section 1.2.3) aconitase undergoes redox sensitive conversion between its active and inactive forms which is possibly influenced by intracellular iron levels.

Furthermore it is interesting to note that IREs, similar to that in transferrin receptor and ferritin mRNA (Section 1.2.6) have been observed in the 5'UTR of aconitase mRNA (Dandaker et al, 1991). It is conceivable that cellular iron depletion by iron chelators may promote an interaction between the IRE-BP and the 5'UTR of aconitase mRNA so inhibiting aconitase expression (Section 1.2.6). This may result in



functional incompetence of the citric acid cycle enzyme system which could result in inhibition of cytokinesis causing the observed arrest of cell cycle in G<sub>2</sub>+M phase.

It is possible that other, as yet undiscovered, IRE systems may be responsible for the regulation of the expression of other cellular proteins and so depletion of intracellular iron may result in the inhibition of alternative enzymes systems. For example, an IRE has also been observed in the 5' UTR of erythroid ALA synthase mRNA (May et al, 1990), the enzyme which catalyses the initial reaction in haem biosynthesis; the condensation of succinyl co-enzyme A with glycine to form  $\delta$ -aminolaevulinic acid (ALA). As with ferritin mRNA, IRE-BP binding to this IRE affects translation (Cox et al, 1991), thus cellular iron deprivation may impair ALA synthase expression and so ultimately inhibit haem biosynthesis.

### 7.3.2 The Use of Iron Chelators as Antineoplastic Agents

As a result of the essential role iron serves in cellular proliferation, iron depletion has been investigated as a potential anti-cancer therapy. Several different approaches have been employed including the blockade of transferrin uptake by anti-transferrin receptor antibodies (Mendelsohn et al, 1986), the substitution of iron transferrin by gallium transferrin (Chitamber and Seligman, 1986) or indium-transferrin (Moran and Seligman, 1989), and the use of iron chelators (Estrov et al, 1987; Dezza et al, 1989).

Iron chelators may act as antineoplastic agents either by exhibiting direct cytotoxicity themselves or by potentiating the effects of other chemotherapeutic agents. Whilst several *in vitro* studies have demonstrated the cytotoxicity of DFO and other iron chelators (Blatt et al, 1989; Bergeron et al, 1987), it is unlikely that such effects could be achieved *in vivo*, as it would be necessary to achieve high plasma chelator concentrations over a prolonged period of time to attain significant cytotoxicity. This is demonstrated in Section 5.6 of this thesis where exposure of K562 and Daudi cells to chelator concentrations of 100 $\mu$ M IBE (equivalent to a plasma concentration of 300 $\mu$ M

3-HP-4-one) caused minimal cytotoxicity after 24 hours exposure. Furthermore, even after 96 hours continuous incubation with 100µM IBE CP94 or DFO, only approximately 20% of K562 cells and 30% of Daudi cells were non-viable (Table 11).

However the observation in Section 5.4 that 3-HP-4-ones act as cell cycle synchronisation agents has implications for the use of iron chelators prior to chemotherapy of neoplasia. When used in this context iron chelators may enhance the actions of cell cycle specific chemotherapeutic regimes. Chelator-treated cells offer two opportunities for the potentiation of growth inhibition:-

a) Drugs such as bischloroethyl nitrosurea (BCNU) which act at the G1-S border of the cell cycle (Bjerkvig et al, 1983) would be more effective since chelators hold cells in this phase.

b) Agents which act during S phase such as cytosine arabinoside (Ara-C) (Nicoloini, 1976) should have improved activity since a larger percentage of the cell population will be synchronised in S-phase when the chelator induced block is released.

The catecholamate iron chelator parabactin has previously been demonstrated to be a potent cell cycle synchronisation agent (Bergeron et al, 1987). Preincubation with parabactin prior to the addition of Ara-C or BCNU to murine L1210 leukaemia cells potentiated the cytotoxic effects of these compounds. Furthermore, Estrov and associates (1987) have demonstrated an apparent synergism between DFO and Ara-C in the treatment of acute neonatal leukaemia. As the 3-HP-4-ones were substantially more effective than DFO in synchronising K562 and Daudi cell cycle (Section 5.3) it is possible that these compounds would be more effective in enhancing the effects of cell cycle specific anti-tumour agents.

For this to be useful clinically, an effect should be demonstrable at concentrations that are achievable *in vivo* without undue toxicity. The concentration of chelator necessary to achieve cell cycle synchronisation varies with different cell types. In the experiments described in Sections 5.2 and 5.6 of this thesis the Daudi cell line and PBL were observed to be considerably more sensitive to the antiproliferative

effects of iron deprivation than the K562 cell line. Such differences could be exploited with particular tumour cell types. The concentration at which cell cycle synchronisation of the Daudi cell line occurred (33 $\mu$ M IBE; equivalent to a plasma concentration of 99 $\mu$ M) was within the plasma levels of 132 $\mu$ M that have been achieved with CP20 (L1) in clinical studies following oral administration (Kontoghiorghes et al, 1990).

#### **7.4 IRON CHELATOR TOXICITY**

It is perhaps inevitable that removal of iron, which is an essential element for cellular metabolism, will result in some adverse effects, especially in individuals with a low iron burden. However it is important to distinguish between toxicities that are a result of effective iron chelation, and therefore are dependent on the degree of iron loading, and those which are independent of the chelation mechanism.

The development of new iron chelators has employed a wide variety of *in vivo* and *in vitro* models. Cellular systems are particularly suitable for the initial evaluation of candidate compounds when the efficacy of a number of chelators can be compared at the same time. Such systems can also provide information regarding cytotoxicity by examination of cell morphology and viability. Furthermore cellular models also permit assessment of the ability of chelators to interfere with iron dependent cell metabolism and so modify cell function. However studies utilising these *in vitro* systems do not allow for substantial toxicity evaluation and for the influence of metabolism. Therefore it is also necessary to evaluate iron chelators in animal models.

Unfortunately many of the physicochemical properties that ensure oral activity and cellular access also tend to lead to increased chelator toxicity either by penetration of the blood brain barrier giving access to the central nervous system (CNS), or by penetration of intracellular organelles leading to chelation of iron necessary for metabolic function. Compounds with a molecular weight below 400 can penetrate the CNS in a manner directly proportional to their lipid solubility (Levin, 1980). This may

be of particular concern with the 3-HP-4-ones as these chelators are of low molecular weight and cross membranes by simple diffusion (Section 3.2.1). Acute CNS toxicity has been observed in mice treated with high doses of 3-HP-4-ones and this occurs more rapidly with lipophilic compounds ( $K_{part}>1$ ) than with hydrophilic chelators (Porter et al, 1990). Iron-overload appears to have a protective effect against such toxicities and acute CNS toxicity was observed at markedly lower chelator doses in non-iron-loaded mice than in iron-loaded mice.

In contrast to the above examples, previous studies have demonstrated that iron overload does not protect against the leucopaenia observed in CP20 treated mice (Porter et al, 1989, 1991). The reasons for this leucopaenia are unclear but one possible explanation may be due to the marked hydrophilicity of CP20 in the iron complexed state ( $K_{part}<0.002$ ). This may result in a relative inability of the CP20-Fe complex to transit cell membranes and so lead to the retention of the CP20-Fe-complex within cells. Whilst studies by Singh and Hider (1988) have shown that the 3-HP-4-one iron complexes are chemically inert and do not generate hydroxyl radicals at physiological pH, it is possible that at sub-optimal concentrations a substantial proportion of the intracellular chelated iron may exist in the  $[Fe.L]^{2+}$  and the  $[Fe.L_2]^+$  forms. This may promote hydroxyl radical formation and cause cytotoxicity. An alternative explanation is that the *in vivo* myelo-suppressive effects of CP20 are due to a metabolite. Analysis of urine from rats has shown marked differences in the major metabolic routes for CP20 and CP94. Whereas glucuronidation is the dominant route for CP20, CP94 is metabolised to a more hydrophilic hydroxylated derivative which retains the ability to chelate iron (III) (Hider et al, 1990).

It has been reported in Chapter 5 and Chapter 6 of the present study that lymphocytes exhibit particular sensitivity to iron deprivation both *in vitro* (Section 5.2.2) and *in vivo* (Section 6.2). In common with other cell types, lymphocyte transferrin receptor expression is linked to proliferative activity. Resting lymphocytes have minimal transferrin receptor expression (Galbraith et al, 1980) however stimulation of resting T lymphocytes with the mitogenic lectin PHA induces T cells to

enter the G<sub>1</sub> phase of the cell cycle where they produce interleukin-2 (IL-2) and express the IL-2 receptor. Occupation of the IL-2 receptor by IL-2 leads to the induction of a second set of surface molecules including the transferrin receptor (Neckers and Cossman, 1983). Blockade of either the transferrin receptor or the IL-2 receptor with monoclonal antibodies inhibits lymphocyte proliferation (Neckers and Cossman, 1983; Mendelsohn et al, 1983) and cells treated with anti-IL-2 receptor do not go on to express transferrin receptors (Neckers and Cossman, 1983). It has been suggested that DFO may limit T cell proliferation not only through inhibition of DNA synthesis but also by interfering with interleukin-2 (IL-2) receptor expression (Carotenuto et al, 1986) however Brierer and Nathan (1990) found no such effect with the orthosubstituted phenolate chelator desferrithiocin. Thus the exact role of iron and transferrin in lymphocyte proliferation remain to be elucidated. However, it is clear from the data presented in Section 6.2 that, whilst granulocyte and red cell precursors are sensitive to iron deprivation, in mice lymphocytes are particularly vulnerable to chelator toxicity. Consequently lymphopaenia may be a potential toxicity in patients with minimal iron loading, although as described in Section 1.4.4 this also presents iron chelators with a potential therapeutic role as immuno-modulating agents.

In situations of iron overload, problems may arise from the redistribution of iron from relatively non-toxic sites such as the liver to more harmful ones such as the heart. Such redistribution could occur if the iron complex can freely cross membranes and so deliver iron directly to the cell or if the chelate donates iron to transferrin. Hexadentate chelates such as FO are less likely to penetrate cells due to their high molecular weight and hydrophilicity and, as a result of their high thermodynamic stability, are unlikely to donate iron to transferrin (Martell, 1989). By contrast, it has previously been shown that HP-4-one chelator iron complexes can donate iron to transferrin (Hider et al, 1991). Furthermore, the experiments in Section 6.3 of the current study demonstrate that 3-HP-4-one iron complexes inhibit CFU-G+CFU-Mac colony formation even when transferrin in the culture medium is fully iron saturated. These results suggest that bidentate complexes can both donate iron to transferrin and

enter cells and subsequently dissociate and thus are potentially toxic. However this may be of potentially therapeutic benefit in the treatment of disorders associated with abnormal iron sequestration such as the anaemia of chronic disorders (Pippard et al, 1991).

## **7.5 FUTURE PERSPECTIVES**

The studies presented in this thesis demonstrate that DFO and the 3-HP-4-one iron chelators have the potential to modify various aspects of cellular iron metabolism resulting in the inhibition of cellular proliferation. The ability of iron chelators to enter cells and organelles and subsequently affect cellular function can be directly related to the physicochemical properties of molecular weight, charge and partition coefficient. Whilst some of the consequences of iron chelation may result in toxicity, particularly in situations of minimal iron loading, other effects may have clinical application in the treatment of malignant disease and other conditions unrelated to iron overload.

It has become clear during the course of this study that the future development of orally active iron chelators requires detailed examination of the relationship between chelator structure, efficacy and toxicity. In particular, further experiments are required to elucidate the mechanism of the myelo-suppression observed with CP20. Furthermore it would be prudent to screen all potential iron chelators for this type of toxicity.

Iron chelators have considerable potential as antineoplastic agents. The observation that the 3-HP-4-ones act as cell cycle synchronization agents is of particular interest. Further work is required to investigate how cells differ in their relative sensitivities to iron deprivation by iron chelators. Additional studies in tumour cell lines on the use of these compounds with cell cycle specific chemotherapeutic agents, followed by *in vivo* experiments in mice infected with one of the transmissible leukaemias would elucidate whether the 3-HP-4-ones are significantly more effective in this respect than other iron chelating agents.

## REFERENCES

- Aisen, P, and I Litowsky.( 1980). Iron transport and storage proteins. *Ann. Rev. Biochem.* 49 : 357-393.
- Ambrosio, G, JL Zweier, WE Jacobus, ML Weisfeldt, and TJ Flaherty.( 1987). Improvement of postischemic myocardial function and metabolism induced by administration of deferoxamine at the time of reflow: the role of iron in the pathogenesis of reperfusion injury. *Circulation* 76 : 906-915.
- Andrews, FJ, CJ Morris, C Kondratowicz, and DR Blake.( 1987). Effect of iron chelation on inflammatory joint disease. *Ann. Rheum. Dis.* 46 : 859-865.
- Aust, SD, and BC White.( 1985). Iron chelation prevents tissue injury following ischaemia. *Adv. Free.Radical. Biol. Med.* 1 : 1-17.
- Avruch, J, and DFH Wallach.( 1971). Preparation and properties of plasma membrane and endoplasmic reticulum fragments from isolated rat fat cells. *Biochim. Biophys. Acta* 233 : 334-347.
- Aziz, N, and HN Munro.( 1987). Iron regulates ferritin mRNA translation through a segment of its 5' untranslated region. *Proc. Natl. Acad. Sci. USA* 84 : 8478-8482.
- Bailey, S, RW Evans, RC Garratt, B Gorinsky, S Hasnain, C Horsburgh, H Jhoti, PF Lindley, A Mydin, R Sarra, and JL Watson.( 1988). Molecular structure of transferrin at 3.33Å resolution. *Biochemistry* 27 : 5804-12.
- Baker, E, M Page, and EH Morgan.( 1985). Transferrin and iron release from rat hepatocytes in culture. *Am. J. Physiol.* 248 : G93-G97.
- Baker, E, M Page, J Torrance, and R Grady.( 1985b). Effect of desferrioxamine, rhotorulic acid and cholyhydroxamic acid on transferrin and iron exchange with hepatocytes in culture. *Clin. Physiol. Biochem.* 3 : 277-288.
- Bakkeren, DL, CMH de Jeu-Jaspers, C van der Heul, and HG van Eijk.( 1985). Analysis of iron binding components in low molecular weight fraction of rat reticulocyte cytosol. *Int. J. Biochem.* 17 : 925-930.
- Bakkeren, DL, CMH de Jeu-Jaspers, MJ Kroos, and HG van Eijk.( 1987). Release of iron from endosomes is an early step in the transferrin cycle. *Int. J. Biochem.* 19 : 179-186.
- Baldwin, SR, CM Grum, and LA Boxer.( 1986). Oxidant activity in expired breath of patients with adult respiratory distress syndrome. *Lancet* 1 : 11-14.
- Bali, P, O Zak, and P Aisen.(1991). A new function for the transferrin receptor in modulating the release of iron from transferrin (Abstr.). 10th International Conference on Iron and Iron Proteins, Oxford, UK.
- Barankiewicz, J, and A Cohen.( 1987). Impairment of nucleotide metabolism by iron-chelating deferoxamine. *Biochem. Pharmacol.* : 2343-2347.



- Barlogie, B, B Drewinko, DA Johnston, T Buchner, WH Hauss, and EJ Freireich.( 1976). Pulse cytophotometric analysis of synchronised cells in vitro. *Cancer Res.* 36 : 1176-1181.
- Barradas, MA, JY Jeremy, GJ Kontoghiorghes, DP Mikhailidis, AV Hoffbrand, and P Dandona.( 1989). Iron chelators inhibit human platelet aggregation, thromboxane A<sub>2</sub> synthesis and lipoxygenase activity. *FEBS Lett.* 245 : 105-109.
- Barry, M, DM Flynn, EA Letsky, and RA Risdon.( 1974). Long term chelation therapy in thalassaemia: effect on liver iron concentration, liver histology and clinical progress. *Br. Med. J.* 2 : 16-20.
- Bartlett, AN, AV Hoffbrand, and GJ Kontoghiorghes.( 1990). Long-term trial with the oral iron chelator 1,2-dimethyl-3-hydroxypyridin-4-one. *Brit. J. Haematol* 76 : 301-304.
- Becton, DL, and P Bryles.( 1988). Deferoxamine inhibition of human neuroblastoma viability and proliferation. *Cancer Res.* 48 : 7189-7192.
- Beinert, H, and MC Kennedy.( 1989). Engineering of protein bound iron-sulfur clusters. *Eur. J. Biochem.* 186 : 5-15.
- Bergeron, R J, P F Cavanaugh, S J Kline, R G Hughes, G T Elliott, and C W Porter.( 1984). Antineoplastic and antiherpetic activity of spermidine catecholamide iron chelators. *Biochem. Biophys. Res. Commun.* 121 : 848-854.
- Bergeron, RJ, and MJ Ingeno.( 1987). Microbial iron chelator induced cell cycle synchronisation in L1210 cells: potential in combination chemotherapy. *Cancer Res.* 47 : 6010-6016.
- Bierer, BE, and DG Nathan.( 1990). The effect of desferrithiocin, an oral iron chelator, on T-cell function. *Blood* 76 : 2052-2059.
- Blake, DR, ND Hall, and PA Bacon.( 1981). The importance of iron in rheumatoid disease. *Lancet* 2 : 1142-1144.
- Blake, DR, and PA Bacon.( 1981). Synovial fluid ferritin in rheumatoid arthritis: an index or cause of inflammation. *Br. Med. J.* 282 : 189.
- Blake, DR, HD Hall, PA Bacon, PA Dieppe, B Halliwell, and JMC Gutteridge.( 1983). Effect of a specific iron chelating agent on animal models of inflammation. *Ann. Rheum. Dis.* 42 : 89-93.
- Blake, DR, P Winyard, J Lunec, A Williams, PA Good, SJ Crewes, JMC Gutteridge, D Rowley, B Halliwell, A Cornish, and RC Hider.( 1985). Cerebral and ocular toxicity induced by desferrioxamine. *Q. J. Med* 56 : 345-355.
- Blatt, J, and S Stitley.( 1987). Antineuroblastoma activity of desferrioxamine in human cell

lines. *Cancer Res.* 47 : 1749-1750.

Blatt, J, SR Taylor, and GJ Kontoghiorghes.( 1989). Comparison of activity of deferoxamine with that of oral iron chelators against human neuroblastoma cell lines. *Cancer Res.* 49 : 2925-2927.

Bloch, BT, MJ Popovici, D Levin, D Tuil, and A Kahn.( 1985). Transferrin gene expression visualised in the oligodendrocytes of the rat brain by using in situ hybridisation and immunohistochemistry. *Proc. Nat. Acad. Sci. USA* 82 : 6706-6710.

Bomford, A, J Isaac, S Roberts, A Edwards, S Young, and R Williams.( 1986). The effect of desferrioxamine on transferrin receptors, the cell cycle and growth rates of human leukaemic cell lines. *Biochem. J.* 236 : 243-249.

Bothwell, TH, H Seftel, P Jacobs, JD Torrance, and N Baumslag.( 1964). Iron overload in Bantu subjects. Studies of the availability of iron in Bantu beer. *Amer. J. Clin. Nutr.* 14 : 47-51.

Bothwell, TH, RW Charlton, JD Cook, and CA Finch.(1979).*Iron Metabolism In Man.* Oxford: Blackwell.

Bottomley, SS, LC Wolfe, and KR Bridges.( 1985). Iron metabolism in K562 erythroleukemic cells. *J. Biol. Chem.* 260 : 6811-6815.

Bowern, N, IA Ramshaw, IA Clark, and PC Doherty.( 1984). Inhibition of autoimmune neuropathological process by treatment with an iron-chelating agent. *J. Exp. Med.* 160 : 1532-1543.

Bradford, MM.( 1976). A rapid and sensitive method for the quantitation of microgram quantities of protein utilizing the principle of protein-dye binding. *Anal. Biochem.* 72 : 248-254.

Bradley, B, SJ Prowse, P Bauling, and KJ Lafferty.( 1986). Desferrioxamine prevents chronic islet allograft damage. *Diabetes* 35 : 550-555.

Brady, MC, KS Lilley, A Treffry, PM Harrison, PD Taylor, and RC Hider.( 1988). Release of iron from ferritin molecules and the iron cores by 3-hydroxypyridinone chelators *in vitro*. *J. Inorg. Biochem* 32 : 1-14.

Brittenham, GM.( 1990). Pyridoxal Isonicotonyl Hydrazone: An effective iron-chelator after oral administration. *Semin. Haematol.* 27 : 112-116.

Carotenuto, P, O Pontesilli, JC Cambier, and AR Hayward.( 1986). Desferrioxamine blocks IL2 receptor expression on human T lymphocytes. *J. Immunol.* 136 : 2342-2347.

Casey, JL, MW Hentze, DM Koeller, S Caughman, TA Rouault, RD Klausner, and JB Harford.( 1988). Iron responsive elements: regulatory RNA sequences that control mRNA levels and translation. *Science* 240 : 924-928.

- Cavanaugh, PF, CW Porter, D Tukalo, OS Frankfurt, ZP Pavuchi, and RJ Bergeron.( 1985). Characterization of L1210 cell growth inhibition by the bacterial iron chelators parabactin and compound II. *Cancer Res.* 45 : 4754-4759.
- Cazzola, M, G Bergamaschi, L Dezza, and P Arosio.( 1990). Manipulations of cellular iron metabolism for modulating normal and malignant cell proliferation: Achievements and prospects. *Blood* 75 : 1903-1919.
- Chanarin, ID.(1989). Leucocyte preparation and separation. In *Laboratory Haematology*. Edited by I. Chanarin. Churchill Livingstone.
- Chandler, DB, and JD Fulwer.( 1985). The effect of deferoxamine on bleomycin-induced lung fibrosis in the hamster. *Am. Rev. Respir. Dis* 131 : 596-598.
- Chitamber, CR, and PA Seligman.( 1986). Effects of different transferrin forms on transferrin receptor expression, iron uptake and cellular proliferation of human leukemic HL60 cells. *J. Clin. Invest.* 78 : 1538-15456.
- Clarkson, AB, M Saric, and RW Grady.( 1991). Deferoxamine and Eflornithine (DL-Diflouromethylornithine) in a rat model of *Pneumocystis carinii* pneumonia. *Antimicrob. Agents. Chemother.* 34 : 1833-1835.
- Cole, ES, and J Glass.( 1983). Transferrin binding and iron uptake in mouse hepatocytes. *Biochim. Biophys. Acta* 762 : 102-110.
- Conrad, MD, and JC Bonton.( 1981). Factors affecting iron balance. *Am. J. Haematol.* 10 : 199-231.
- Cooperstein, SJ, and A Lazarow.( 1950). A microspectrophotometric method for the determination of cytochrome oxidase. *J. Biol. Chem.* 189 : 665-670.
- Cox, TM.( 1990). Haemochromatosis. *Blood Rev.* 4 : 75-87.
- Cox, TC, MJ Bawden, A Martin, and BK May.( 1991). Human erythroid 5-aminolevulinate synthase: promotor analysis and identification of an iron responsive element in the mRNA. *EMBO J.* 10 : 1891-1902.
- Cragg, SJ, M Wagstaff, and M Worwood.( 1981). Detection of a glycosylated subunit in human ferritin. *Biochem. J.* 199 : 565-571.
- Crichton, RR, F Roman, and F Roland.( 1980). Iron mobilisation from ferritin by chelating agents. *J. Inorg. Biochem* 13 : 305-316.
- Crichton, RR.(1991). *Inorganic Biochemistry of Iron Metabolism*. Edited by J. Burgess. London: Ellis Horwood.
- Cummings, RLC, A Goldberg, J Morrow, and JA Smith.( 1967). Effect of

phenylhydrazine-induced haemolysis on the urinary excretion of iron after desferrioxamine. *Lancet* *1* : 71-74.

Dandekar, T, R Stripecke, NK Gray, B Goossen, A Constable, HE Johanssen, and MW Hentze.( 1991). Identification of a novel iron-responsive element in murine and human erythroid delta aminolevulinic acid synthase mRNA. *EMBO J.* *10* : 1903-1909.

Dautry-Varsat, A, A Ciechanover, and HF Lodish.( 1982). pH and the recycling of transferrin during receptor mediated endocytosis. *Proc. Nat. Acad. Sci. USA* *80* : 2258-2262.

Davis, RJ, GL Johnson, DJ Kelleher, JK Anderson, JE Mole, and MP Czech.( 1986). Identification of serine 24 as the unique site on the transferrin receptor phosphorylated by protein kinase C. *J. Biol. Chem.* *261* : 9034-9041.

Davis, RJ, and H Meisner.( 1987). Regulation of transferrin receptor recycling by protein kinase C is independent of receptor phosphorylation at serine 24 in Swiss 3T3 fibroblasts. *J. Biol. Chem.* *262* : 10641-10647.

Dezza, L, M Cazzola, M Danova, G Bergamaschi, S Brugnattelli, R Invernizzi, G Mazzini, A Riccardi, and E Ascari.( 1987). Effects of desferrioxamine on normal and leukemic human haematopoietic cell growth: in vivo and in vitro studies. *Leukemia* *3* : 104-109.

Dickerson, RE, and I Geis.(1983) *Haemoglobin Structure, Function, Evolution and Pathology*. Menlo Park, California: Benjamin.

Dickson, DPE, NMK Reid, S Mann, VJ Wade, RJ Ward, and TJ Peters.( 1988). Mossbauer spectroscopy, electron microscopy and electron diffraction studies of the iron cores in various human and animal haemosiderins. *Biochim. Biophys. Acta* *957* : 81-90.

Drapier, JC, and JB Hibbs.( 1986). Murine cytotoxic macrophages inhibit aconitase in tumour cells. *J. Clin. Invest* *78* : 790-797.

Elford, HL, M Freese, E Passamani, and HP Morris.( 1970). Ribonucleotide reductase and cell proliferation. 1. Variation in ribonucleotide reductase activity with tumor growth rates in a series of rat hepatomas. *J. Biol. Chem.* *245* : 5228-5233.

Enns, CA, and HH Sussman.( 1981a). Physical characterization of the transferrin receptor in human placenta. *J. Biol. Chem* *255* : 9820-9823.

Enns, CA, and HH Sussman.( 1981b). Similarities between transferrin receptor proteins on human reticulocytes and human placentae. *J. Biol. Chem.* *256* : 12620-12623.

Eriksson, S, A Graslund, S Skog, L Thelander, and B Tribukait.( 1984). Cell cycle dependent regulation of mammalian ribonucleotide reductase. *J. Biol. Chem* *259* : 11695-11700.

Estrov, Z, A Tawa, and XH Wang.( 1987). In vitro and in vivo effects of deferoxamine in neonatal acute leukaemia. *Blood* *69* : 757-761.

Finch, CA, K Denelbeiss, and JC Cook et al.( 1970). Ferrokinetics in man. *J. Clin. Invest* 49: 17-53.

Fisbach, FA, DW Gregory, PM Harrison, TG Hoy, and JM Williams.( 1971). On the structure of haemosiderin and its relation to ferritin. *J. Ultrastruct. Res.* 37 : 495-503.

Florence, AT, and D Attwood.(1981). In *Physicochemical Principles of Pharmacy*. 329. London: Macmillan.

Foa, P, AT Maiolo, L Lombardi, L Villa, and EE Polli.( 1986). Inhibition of proliferation of human leukemic cell lines by deferoxamine. *Scand. J. Haematol* 36 : 107-110.

Foley, AA, and GW Bates.( 1988). The influence of inorganic anions on the formation and stability of Fe-transferrin-anion complexes. *Biochim. Biophys. Acta* 965 : 154-162.

Forsbeck, K, and K Nilsson.( 1983). Iron metabolism of established human haematopoietic cell lines in vitro. *Exp. Cell Res.* 144 : 323-332.

Forsbeck, K, and K Nilsson.( 1985). The dynamic morphology of the transferrin - transferrin receptor system in human leukaemia/lymphoma cell lines and its relation to iron metabolism and cell proliferation. *Scand. J. Haematol.* 35 : 145-154.

Forsbeck, K, K Bjelkenkratz, and K Nilsson.( 1986). Role of iron in the proliferation of the established human tumour cell lines U-937 and K-562: Effects of suramin and a lipophilic iron chelator (PIH). *Scand. J. Haematol* 37 : 429-437.

Fritch, G, J Treumer, DT Spira, and A Jung.( 1985). *Plasmodium vinckea* : Suppression of mouse infections with desferrioxamine B. *Exp. Pathol.* 60 : 171-174.

Funk, F, C Lecrenier, E Lesuisse, RR Crichton, and W Schneider.( 1986). A comparative study on iron sources for mitochondrial haem synthesis including ferritin and transit pool species. *Eur. J. Biochem.* 157 : 303-309.

Galbraith, RM, P Werner, P Arnaud, and GMP Galbraith.( 1980). Transferrin binding to peripheral blood lymphocytes activated by phytohemagglutinin involves a specific receptor interaction. *J. Clin. Invest* 66 : 1135-1143.

Ganeshaguru, K, AV Hoffbrand, RW Grady, and A Cerami.( 1980). Effect of various iron chelating agents on DNA synthesis in human cells. *Bioch. Pharmacol.* 29 : 1275-1279.

Goodman, LS, and A Gilman.(1975).*The Pharmacological Basis of Therapeutics*. 5th ed. New York: Macmillan Publishing Co.

Gordon-Smith, EC.(1981). Inherited haemolytic anaemias. In *Postgraduate Haematology*. Edited by A. Hoffbrand and S. Lewis. 176-178. London: Heinemann.

Grady, RW, and C Hershko.( 1990). An evaluation of the potential of HBED as an orally effective iron-chelating drug. *Semin. Haematol.* 27 : 105-111.

- Graham, JM, and TC Ford.(1983). Enzymic and Chemical Assays. In *Iodinated density gradient media*. Edited by D. Rickwood. 195-216. Oxford: IRL Press.
- Graham, JM, T Ford, and D Rickwood.( 1990). Isolation of the major subcellular organelles from mouse liver using Nycodenz gradients without the use of an ultracentrifuge. *Anal. Biochem.* 187 : 318-323.
- Green, CJ, G Healing, S Simpkin, J Lunec, and BJ Fuller.( 1986a). Increased susceptibility to lipid peroxidation in rabbit kidneys: a consequence of warm ischaemia and subsequent reperfusion. *Comp. Biochem. Physiol.* 83 : 603-606.
- Green, CJ, G Healing, S Simpkin, J Lunec, and BJ Fuller.( 1986b). Desferrioxamine reduces susceptibility to lipid peroxidation in rabbit kidneys subjected to warm ischaemia and reperfusion. *Comp. Biochem. Physiol* 85B : 113-117.
- Green, CJ, G Healing, S Simpkin, J Lunec, and BJ Fuller.( 1986c). Reduced susceptibility to lipid peroxidation in cold ischaemic rabbit kidneys after addition of desferrioxamine, mannitol or uric acid to the flush solution. *Cryobiology* 23 : 358-365.
- Guesdon, J, T Teernynk, and S Avrameus.( 1979). The use of avidin biotin interaction in immunoenzymatic techniques. *J. Histochem. Cytochem.* 27 : 1131-1139.
- Gutteridge, JMC, DA Rowley, E Griffiths, and B Halliwell.( 1985). Low molecular weight iron complexes and oxygen radical reactions in idiopathic haemochromatosis. *Clin. Sci.* 68 : 463-467.
- Gutteridge, JMC, and B Halliwell.( 1989). Iron toxicity and oxygen radicals. *Bailliere's Clin. Haematol.* 2 : 195-256.
- Gyparaki, M, JB Porter, S Hirani, M Streater, RC Hider, and Er Huehns.( 1987). In vitro evaluation of hydroxypyridone iron chelators in a mouse model. *Acta Haematologica* 78 : 217-221.
- Haile, DJ, MW Hentze, TA Rouault, JB Harford, and RD Klausner.( 1989). Regulation of interaction of the iron-responsive element binding protein with iron responsive RNA elements. *Mol. Cell Biol.* 9 : 5055-5061.
- Hallberg, L, and L Hedenberg.( 1965). The effect of desferrioxamine on iron metabolism in man. *Scand. J. Haematol* 2 : 67-79.
- Halliwell, B, and JMC Gutteridge.( 1984). Oxygen toxicity, oxygen radicals, transition metals and disease. *Biochem. J.* 219 : 1-14.
- Halliwell, B, and JMC Gutteridge.( 1986). Oxygen free radicals and iron in relation to biochemistry and medicine. *Arch. Biochem. Biophys.* 246 : 501-514.
- Hanstein, WG, PV Sacks, and U Muller-Eberhard.( 1975). Properties of liver mitochondria

from iron-loaded rats. *Biochem. Biophys. Res. Commun.* *67* : 1175-1184.

Harrison, PM, GA Clegg, and K May.(1980). Ferritin structure and function. In *Iron in Biochemistry and Medicine*. Edited by A. Jacobs and M. Worwood. 131-162. Academic Press.

Harrison, PM.( 1986). The structure and function of ferritin. *Biochemical Education* *14* : 154-162.

Hentze, MW, TA Rouault, SW Caughman, A Dancis, JB Harford, and RD Klausner.( 1987). A *cis*-acting element is necessary and sufficient for translational regulation of human ferritin expression in response to iron. *Proc. Natl. Acad. Sci. USA* *84* : 6730-6734.

Hentze, MW, and P Argos.( 1991). Homology between IRE-BP, a regulatory RNA binding protein, aconitase and isoprpylmalate isomerase. *Nucl. Acids Res.* *19* : 1739-1740.

Hershko, C, JD Cook, and CA Finch.( 1973). Storage iron kinetics III. Study of desferrioxamine action by selective radioiron labels of RE and parenchymal cells. *J. Lab. Clin. Med.* *81* : 876-886.

Hershko, C, G Graham, GW Bates, and EA Rachmilewitz.( 1978). Non-specific serum iron in thalassaemia; an abnormal serum fraction of potential toxicity. *Br. J. Haematol.* *40* : 255-263.

Hershko, C, and EA Rachmilewitz.( 1979). Mechanism of desferrioxamine induced iron excretion in thalassaemia. *Brit. J. Haematol* *42* : 125-132.

Hershko, C, and DW Weatherall.( 1988). Iron chelating therapy. *CRC Crit. Rev. Clin. Lab. Sci* *26* : 303-345.

Hershko, C, G Link, A Pinson, A Avramovici-Grisaru, S Sarel, HH Peter, RC Hider, and RW Grady.( 1990). New orally effective iron chelators; Animal studies. *Ann. N.Y. Acad. Sci* *612* : 351-360.

Hershko, C, G Link, A Pinson, HH Peter, P Dobbin, and RC Hider.( 1991a). Iron mobilization from myocardial cells by 3-hydroxypyridin-4-one chelators: Studies in rat heart cells in culture. *Blood* *77* : 2049-2053.

Hershko, C, EN Theanacho, DT Spira, HH Peter, P Dobbin, and RC Hider.( 1991b). The effect of N-alkyl modification on the antimalarial activity of 3-hydroxypyridin-4-one oral iron chelators. *Blood* *77* : 637-643.

Heys, AD, and TL Dormandy.( 1981). Lipid peroxidation in iron overloaded spleens. *Clin. Sci.* *60* : 295-301.

Hibbs, JB, RT Read, and Z Vavrin.( 1984). Iron depletion: possible cause of tumour cell cytotoxicity induced by activated macrophages. *Biochem. Biophys. Res. Commun.* *123* : 716-723.

Hider, RC, G Kontoghiorghes, and J Silver.( 1982). Pharmaceutical Compositions. UK Patent GB 2118176A

Hider, RC, GJ Kontoghiorghes, J Silver, and MA Stockham.( 1984a). 1-hydroxypyridin-2-ones. UK Patent GB 2146990A

Hider, RC, G Kontoghiorghes, J Silver, and MA Stockham.( 1984b). Pharmaceutically active hydroxypyridinones. GB Patent 2146989

Hider, RC, S Singh, JB Porter, and ER Huehns.( 1990). Development of the Hydroxypyridin-4-ones as orally active chelators. *Ann. N.Y. Acad. Sci* 612 : 327-338.

Hider, RC, AD Hall, B Gudka, and S Singh.(1991). The exchange of iron between low molecular weight ligands and transferrin (Abstr.). Oxford:

Hoe, S, DA Rowley, and B Halliwell.( 1982). Reactions of ferrioxamine and desferrioxamine with the hydroxyl radical. *Chem. Biol. Interact.* 41 : 75-81.

Hoffbrand, AV, K Ganeshaguru, JWL Hooton, and MHN Tattersall.( 1976). Effect of iron deficiency and desferrioxamine on DNA synthesis in human cells. *Brit. J. Haematol* 33 : 517-526.

Hoffbrand, AV, AN Bartlett, PA Veys, NTJ O'Connor, and GJ Kontoghiorghes.( 1989). Agranulocytosis and thrombocytopenia in patient with Blackfan-Diamond anaemia during oral chelator trial. *Lancet* 2 : 457.

Huebers, H, B Josephson, B Huebers, E Csiba, and C Finch.( 1981). Uptake and release of iron from human transferrin. *Proc. Nat. Acad. Sci. USA* 78 : 2572-2576.

Huebers, HH, and CA Finch.( 1987). The physiology of transferrin and transferrin receptors. *Physiol. Rev.* 67 : 520-582.

Iancu, TC, and HB Neustein.( 1977). Ferritin in human liver cells of homozygous beta-thalassaemia. *Br. J. Haematol* 37 : 527-535.

Iancu, TC.( 1989). Ultrastructural pathology of iron overload. *Baillieres Clin. Haematol.* 2 : 475-495.

Jacobs, A.( 1977). Low molecular weight intracellular iron transport compounds. *Blood* 50 : 433-439.

Jin, Y, A Baquet, A Florence, RR Crichton, and YJ Schneider.( 1989). Desferrithiocin and Desferrioxamine B cellular pharmacology and storage iron mobilization. *Biochem. Pharmacol.* 38 : 3233-3240.

Keberle, H.( 1964). The biochemistry of Desferrioxamine and its relation to iron metabolism. *Ann. N.Y. Acad. Sci.* 119 : 758-768.



Klausner, RD, J Van Renswoude, G Ashwell, C Kempf, AN Schechter, A Dean, and KR Bridges.( 1983). Receptor mediated endocytosis of transferrin in K562 cells. *J. Biol. Chem.* 258 : 4715-4724.

Klausner, RD, and JB Harford.( 1989). Cis-trans model for post-transcriptional gene regulation. *Science* 246 : 870-872.

Klebanoff, S.( 1975). Antimicrobial mechanism in neutrophil polymorphonuclear leukocytes. *Semin. Haematol.* 12 : 117-142.

Kontoghiorghes, GJ, and AV Hoffbrand.( 1986). Orally active alpha ketohydroxypyridone iron chelators intended for clinical use: in vivo studies in rabbits. *Brit. J. Haematol* 62 : 607-613.

Kontoghiorghes, GJ, L Sheppard, AV Hoffbrand, J Charalambous, J Tiperkae, and MJ Pippard.( 1987a). Iron chelation studies using desferrioxamine and the potential oral chelator 1,2-dimethyl-3-hydroxypyridin-4-one in normal and iron-overloaded rats. *J. Clin. Pathol.* 40 : 404-408.

Kontoghiorghes, GJ, MA Aldouri, AV Hoffbrand, J Barr, B Wonke, T Kourouclaris, and L Sheppard.( 1987b). Effective chelation of iron in  $\beta$  thalassaemia with the oral chelator 1,2-dimethyl-3-hydroxypyridin-4-one. *Br. Med. J.* 295 : 1509-1512.

Kontoghiorghes, GJ, MA Aldouri, AV Hoffbrand, J Barr, B Wonke, T Kouroucalaris, and L Sheppard.( 1987c). Effective chelation of iron in  $\beta$  thalassaemia with the oral chelator 1,2-dimethyl-3-hydroxypyrid-4-one. *Br. Med. J.* 295 : 1509-1512.

Kontoghiorghes, GJ, P Nasser-Sina, JG Goddard, JM Barr, P Nortey, and LN Sheppard.(1989). Safety of oral iron chelator L1. *Lancet* 2 : 457-458.

Kontoghiorghes, GJ, AN Bartlett, AV Hoffbrand, JG Goddard, L Sheppard, J Barr, and P Nortey.( 1990). Long-term trial with the oral iron chelator 1,2-dimethyl-3-hydroxypyrid-4-one (L1). *Brit. J. Haematol* 76 : 295-300.

Krishan, A.( 1975). Rapid cytofluorometric analysis of mammalian cell cycle by propidium iodide staining. *J.Cell Biol.* 66 : 188-193.

Kumar-Jain, M.(1988)*Introduction to Biological Membranes*. 2nd Edition ed. John Wiley and Sons.

Laub, R, YJ Schneider, JN Octave, A Trouet, and RR Crichton.( 1985). Cellular pharmacology of Deferoxamine B and derivatives in cultured rat hepatocytes in relation to iron mobilization. *Biochem. Pharmacol.* 34 : 1175-1183.

Lederman, HM, A Cohen, JWW Lee, MH Freedman, and EW Gelf.( 1984). Deferoxamine: a reversible S-phase inhibitor of human lymphocyte proliferation. *Blood* 64 : 748-753.

Leo, AJ, C Hansch, and D Elkins.( 1971). Partition coefficients and their uses. *Chem. Rev.* 71 : 525-560.

- Levin, VA.( 1980). Relationship of octanol/water partition coefficient and molecular weight to rat brain capillary permeability. *J. Med. Chem.* 23 : 682-687.
- Libschitz, DA, J Dugard, MO Simon, TH Bothwell, and RW Charlton.( 1971). The site of action of desferrioxamine. *Br. J. Haematol.* 20 : 395-404.
- Lloyd, JB, H Cable, and C Rice-Evans.( 1991). Evidence that desferrioxamine cannot enter cells by passive diffusion. *Biochemical Pharmacology* 41 : 1361-1363.
- Lucarelli, G, M Galimberti, P Polchi, E Angelucci, D Baronciana, C Giardini, F Manneti, P Politi, SMT Durazzi, F Albertini, and P Muretto.(1989).Bone marrow transplantation in thalassaemia. The experience of Pesaro. In *Advances and Controversies in Thalassaemia. Bone Marrow Transplantation and Other Approaches*. Edited by G. Buckner, R. Gale and G. Lucarelli. New York: Liss.
- Mann, S, VJ Wade, DPE Dickson, NMK Reid, RJ Ward, M O'Connell, and TJ Peters.(1988). Structural specificity of haemosiderin iron cores in iron-overloaded diseases. *FEBS Lett.* 234 : 69-72.
- Martell, A.(1989).*Development of Iron Chelators for Clinical Use*. Amsterdam: Elsevier.
- Mattia, E, K Rao, DS Shapiro, HH Sussman, and RD Klausner.( 1984). Biosynthetic regulation of the human transferrin receptor by desferrioxamine in K562 cells. *J. Biol. Chem.* 259 : 2689-2692.
- May, WS, and G Tyler.( 1987). Phosphorylation of the surface transferrin receptor stimulates receptor internalization in HL60 leukemic cells. *J. Biol. Chem* 262 : 16710-16718.
- May, BK, CR Bhasker, MJ Bawden, and TC Cox.( 1990). Molecular regulation of 5-aminolevulinate synthase. Diseases related to heme biosynthesis. *Mol. Biol. Med.* 7 : 405-421.
- McArdle, MJ, and EH Morgan.( 1982). Transferrin and iron movements in rat conceptus during gestation. *J. Reprod. Fertil.* 66 : 529-536.
- McClelland, A, LC Kuhn, and FH Ruddle.( 1984). The human transferrin receptor gene: Genomic organization, and the complete primary sequence of the receptor deduced from a cDNA sequence. *Cell* 39 : 267-274.
- McCord, JM.( 1985). Oxygen-derived free radicals in post ischemic tissue injury. *N. Engl. J. Med.* 312 : 159-167.
- Mehta, J, S Singhal, R Revanker, A Walvalker, A Chablani, and BC Mehta.( 1991). Fatal systemic lupus erythematosus in patient taking oral iron chelator L1. *Lancet* 337 : 298.
- Mendelsohn, J, I Trowbridge, and J Castagnola.( 1983). Inhibition of human lymphocyte proliferation by monoclonal antibody to transferrin receptor. *Blood* 62 : 821-826.

- Modell, CB, and J Beck.( 1974). Long term desferrioxamine therapy in thalassaemia. *Ann. N.Y. Acad. Sci* 232 : 201-210.
- Modell, B.( 1977). Total management of thalassaemia major. *Arch. Dis. Childhood* 52 : 485-500.
- Modell, B.( 1979). Advances in the use of iron-chelating agents for the treatment of iron overload. *Prog. Haematol.* 11 : 267-312.
- Moran, PL, and PA Seligman.( 1989). Effects of transferrin-indium on cellular proliferation of a human leukemia cell line. *Cancer Res.* 49 : 4237-4241.
- Morley, CGD, and A Bezkorovainy.( 1985). Cellular iron uptake from transferrin id endocytosis the only mechanism. *Int. J. Biochem.* 17 : 553-564.
- Muirden, KD.( 1966). Ferritin in synovial cells in patients with rheumatoid disease. *Ann. Rheum. Dis.* 25 : 387-401.
- Mulligan, MM, B Althus, and MC Linder.( 1986). Non-ferritin, non-heme iron pools in rat tissues. *Int. J. Biochem.* 18 : 791-798.
- Neckers, LM, and J Cosman.( 1983). Transferrin receptor induction in mitogen stimulated human T lymphocytes is required for DNA synthesis and cell division and is regulated by interleukin-2. *Proc. Natl. Acad. Sci. USA* 80 : 3494-3498.
- Nicolini, C.( 1976). The principles and methods of cell synchronization in cancer chemotherapy. *Biochim. Biophys. Acta.* 458 : 243-282.
- Nocka, KH, and LM Pelus.( 1988). Cell cycle specific effects of Deferoxamine on human and murine haematopoietic progenitor cells. *Cancer Res.* 48 : 3571-3575.
- Nunez, NT, V Gaete, JA Watkins, and J Glass.( 1990). Mobilization of iron from endocytotic vesicles. *J. Biol. Chem.* 265 : 6688-6692.
- O'Connell, MJ, RJ Ward, H Baum, and TJ Peters.( 1985). The role of iron in ferritin and haemosiderin mediated lipid peroxidation in liposomes. *Biochem. J.* 229 : 135-139.
- O'Connell, MJ, B Halliwell, CP Moorhouse, OI Aruoma, H Baum, and TJ Peters.( 1986). Formation of hydroxyl radicals in the presence of ferritin and haemosiderin. *Biochem. J.* 240 : 297-300.
- Octave, JN, YJ Schneider, RR Crichton, and A Trouet.( 1983). Iron mobilization from cultured hepatocytes: Effects of Desferrioxamine B. *Biochem. Pharmacol.* 32 : 3413-3418.
- Oldendorf, WH.( 1974). Lipid solubility and drug penetration of the blood barrier. *Proc. Soc. Exp. Biol. Med.* 147 : 813-824.

- Osheroff, MR, Km Schaich, RT Drew, and DC Borg.( 1985). Failure of desferrioxamine to modify the toxicity of paraquat in the rat. *J. Free Radical Biol. Med.* 1 : 71-82.
- Owen, D, and LC Kuhn.( 1987). Noncoding 3' sequences of the transferrin receptor gene are required for mRNA regulation by iron. *EMBO J.* 6 : 1287-1295.
- Page, MA, E Baker, and EH Morgan.( 1984). Transferrin and iron uptake by rat hepatocytes in culture. *Am. J. Physiol.* 746 : G26-G33.
- Pelosi-Testa, E, U Testa, P Samoggia, G Salvo, A Camagna, and C Peschle.( 1986). Expression of transferrin receptor in human erythroleukemic lines: regulation in the plateau and exponential phase of growth. *Cancer Res.* 46 : 5330-5334.
- Pelus, LM, S Saletan, RT Silver, and MAS Moore.( 1982). Expression of Ia antigens on normal and chronic myeloid leukemic human granulocyte-macrophage colony forming cells (CFU-GM) is associated with regulation of cell proliferation by prostaglandin E. *Blood* 59 : 284-292.
- Peterson, CM, JH Graziano, RW Grady, RL Jones, HV Vlassara, VC Canale, DR Miller, and A Cerami.( 1979). Chelation therapy in  $\beta$  thalassaemia major: a one year double blind study of 2,3-dihydroxybenzoic acid. *Exp. Haematol.* 7 : 74-80.
- Pippard, MJ, GT Warner, ST Callender, and DJ Weatherall.( 1977). Iron absorption in iron loading anaemias: effect of subcutaneous desferrioxamine infusions. *Lancet* 2 : 737-739.
- Pippard, MJ, DK Johnson, and CA Finch.( 1982). Hepatocyte iron kinetics in the rat explored with an iron chelator. *Brit. J. Haematol* 52 : 211-224.
- Pippard, MJ, and DW Weatherall.( 1984). Iron absorption in iron-loading anaemias. *Haematologica* 17 : 407-414.
- Pippard, MJ, MJ Jackson, K Hoffman, M Petrou, and CB Modell.( 1986). Iron chelation using subcutaneous infusions of diethyl triaminepenta-acetic acid. *Scand. J. Haematol.* 36 : 466-472.
- Pippard, MJ.(1989). Clinical use of iron chelation. In *Iron in Immunity, Cancer and Inflammation*. Edited by M. d. Sousa and J. Brock. John Wiley and Sons Ltd.
- Pollack, S, RN Rossan, DE Davidson, and A Escajadillo.( 1987). Desferrioxamine supresses *Plasmodium falciparum* in aotus monkeys. *Proc. Soc. Exp. Biol. Med.* 184 : 162-164.
- Polson, RJ, AM Jawad, A Bomford, H Berry, and R Williams.( 1986). Treatment of rheumatoid arthritis with desferrioxamine. *Q. J. Med.* 61 : 1153-1158.
- Ponka, P, J Borova, J Neuwirt, O Fuchs, and E Necas.( 1979). A study of intracellular iron metabolism using pyridoxal isonicotyl hydrazone and other synthetic chelating agents. *Biochim. Biophys. Acta.* 586 : 278-297.

- Ponka, P, D Richardson, E Baker, HM Schulman, and JT Edward.( 1988). Effect of pyridoxal isonicotinoyl hydrazone and other hydrazones on iron release from macrophages, reticulocytes and hepatocytes. *Biochim. Biophys. Acta* 967 : 122-129.
- Porter, JB, M Gyparaki, LC Burke, ER Huehns, P Sarpong, V Saez, and RC Hider.( 1988). Iron mobilization from hepatocyte monolayer cultures by chelators: the importance of membrane permeability and the iron binding constant. *Blood* 72 : 1497-1503.
- Porter, JB, RC Hider, and ER Huehns.( 1989). The development of iron chelating drugs. *Baillieres Clin. Haematol.* 2 : 257-292.
- Porter, JB.( 1989). Oral iron chelators: Prospects for future development. *Eur. J. Haematol.* 43 : 271-285.
- Porter, JB, and ER Huehns.( 1989). The toxic effects of desferrioxamine. *Baillieres Clin. Haematol.* 2 : 459-474.
- Porter, JB, KP Hoyes, R Abeysinghe, ER Huehns, and RC Hider.( 1989). Animal Toxicology of iron chelator L1. *Lancet* 2 : 156 (Letter).
- Porter, JB, J Morgan, KP Hoyes, LC Burke, ER Huehns, and RC Hider.( 1990). Relative oral efficacy and acute toxicity of hydroxypyridin-4-one iron chelators in mice. *Blood* 76 : 2389-2396.
- Porter, JB, KP Hoyes, RD Abeysinghe, PN Brooks, ER Huehns, and RC Hider.( 1991). Comparison of the subacute toxicity and efficacy of 3-hydroxypyridin-4-one iron chelators in overloaded and non-overloaded mice. *Blood* 78 : 2727-2734.
- Pratten, MK, R Duncan, and JB Lloyd. (1980). Adsorptive and passive pinocytotic uptake. In *Coated Vesicles*. Edited by C. Ockleford and A. Whyte. 179-218. Cambridge University Press.
- Propper, RD, SB Shurin, and DG Nathan.( 1976). Reassessment of the use of deferrrioxamine B in iron overload. *New Engl. J. Med.* 294 : 1421-1423.
- Rao, K, JB Harford, T Roualt, A McClelland, FH Ruddle, and RD Klausner.( 1986). Transcriptional regulation by iron of the gene for the transferrin receptor. *Mol. Cell. Biol.* 6 : 236-240.
- Reddel, RR, DW Hedley, and RL Sutherland.( 1985). Cell cycle effects of iron depletion on T-47D human breast cancer cells. *Exp. Cell Res.* 161 : 277-284.
- Rice-Evans, C, E Baysal, S Singh, SA Jones, and JG Jones.( 1989). The interactions of desferrioxamine and hydroxypyridone compounds with haemoglobin and erythrocytes. *FEBS Lett.* 256 : 17-20.
- Richter, GW.( 1978). The iron-loaded cell - the cytopathology of iron storage. *Am. J. Pathol*

91 : 363-396.

Richter, GW.( 1984). Studies on iron overload. Rat liver siderosome ferritin. *Lab. Invest.* 50 : 26-35.

Robbins-Browne, RM, and JK Prpic.( 1983). Desferrioxamine and systemic yersiniosis. *Lancet* 2 : 1372.

Roberts, S, and A Bomford.( 1988). Chelation of transferrin iron by desferrioxamine in K562 cells. *Biochem. J.* 254 : 869-875.

Roberts, PJ.( 1990). Development, characterization and subcellular location of DNase activity in HL-60 cells and monocytes. *Blood* 75 : 976-983.

Rocchi, E, P Gilbertini, M Cassanelli, A Pietrangelo, A Borghi, M Pantaleoni, J Jensen, and E Ventura.( 1986). Iron removal therapy in porphyria cutanea tarda: phlebotomy versus slow subcutaneous desferrioxamine infusion. *Br. J. Dermatol* 114 : 621-629.

Rouault, TA, CK Tang, S Kaptain, WH Burgess, DJ Haile, F Samaniego, OW McBride, JB Harford, and RD Klausner.( 1990). Cloning of the cDNA encoding an RNA regulatory protein - the human iron-responsive element-binding protein. *Proc. Natl. Acad. Sci. USA* 87 : 7958-7962.

Rouault, TA, CD Stout, S Kaptain, JB Harford, and RD Klausner.( 1991). Structural relationship between an iron-regulated RNA binding protein (IRE-BP) and aconitase: Functional implications. *Cell* 64 : 881-883.

Rubinstein, M, P Dupont, JP Doppee, C Dehon, J Ducobu, and J Hainaut.( 1985). Ocular toxicity of desferrioxamine. *Lancet* 1 : 817.

Ruutu, R.( 1975). Determination of iron and unsaturated iron binding capacity in serum with ferrozine. *Clin. Chim. Acta* 61 : 229-235.

Sahasrabudhe, DM, J Dusel, and S Jedlika.( 1991). Suppression of delayed type hypersensitivity by desferoxamine. *J. Immunother.* 10 : 112-119.

Samson, D, D Halliday, and I Chanarin.( 1977). Reversal of ineffective erythropoiesis in pernicious anaemia following B12 therapy. *Br. J. Haematol* 35 : 217.

Schlabach, MR, and GW Bates.( 1975). The synergistic binding of an anion and Fe<sup>3+</sup> by transferrin. *J. Biol. Chem.* 257 : 2182-2188.

Schneider, C, MJ Owen, D Banville, and JG Williams.( 1984). Primary structure of the human transferrin receptor deduced from the mRNA sequence. *Nature* 311 : 675-680.

Selden, C, M Owen, JPM Hopkins, and TJ Peters.( 1980). Studies on the concentration and intracellular localization of iron proteins in liver biopsy specimens in patients with iron

overload with special reference to their role in lysosomal disruption. *Br. J. Haematol* 44 : 593-603.

Seligman, PA.( 1983). Structure and function of the transferrin receptor. *Prog. Haematol.* 13 : 131-147.

Sephton-Smith, R.( 1962). Iron excretion in thalassaemia major after administration of chelating agents. *Br. Med. J.* ii : 1577.

Serna, FJ De La, M Praga, F Gilsanz, JL Rodicio, LM Ruilope, and JM Alcazar.( 1988). Improvement in the erythropoiesis of chronic haemodialysis patients with desferrioxamine. *Lancet* 2 : 181-184.

Seymour, CA, and TJ Peters.( 1978). Organelle pathology in primary and secondary haemochromatosis with special references to lysosomal changes. *Br. J. Haematol.* 40 : 239-253.

Sibille, JC, JN Octave, YJ Schneider, A Trouet, and RR Crichton.( 1982). Transferrin protein and iron uptake by cultured hepatocytes. *FEBS Lett.* 150 : 365-369.

Singh, S, RC Hider, and JB Porter.( 1990). Separation and identification of desferrioxamine and its iron chelating metabolites by high-performance liquid chromatography and fast atom bombardment mass spectrometry. *Anal. Biochem.* 187 : 1-8.

Skinner, MK, and MD Griswold.( 1983). Sertoli cells synthesize and secrete transferrin like protein. *J. Biol. Chem* 255 : 9523-9525.

Soltys, HS, and JI Brody.( 1970). Synthesis of transferrin by human peripheral blood lymphocytes. *J. Lab. Clin. Med* 75 : 250-257.

Stein, BS, and HH Sussman.( 1983). Peptide mapping of human transferrin receptor in normal and transformed cells. *J. Biol. Chem* 258 : 2668-2673.

Stoorvogel, W, HJ Geuze, and GJ Strous.( 1987). Sorting of endocytosed transferrin and asialoglycoprotein occurs immediately after internalization in HepG2 cells. *J. Cell. Biol.* 102 : 1261-1268.

Summers, MR, A Jacobs, D Tudway, P Perera, and C Ricketts.( 1979). Studies in desferrioxamine and ferrioxamine metabolism in normal and iron loaded subjects. *Br. J. Haematol.* 42 : 547-555.

Sun, IL, W Toole-Sims, FL Crane, ES Golub, T Diaz de Pagan, DJ Morre, and H Low.( 1987). Retinoic acid inhibition of transplasmalemma diferric transferrin reductase. *Biochem. Biophys. Res. Commun.* 146 : 976-981.

Sussman, HH.(1989).Iron and tumour cell growth. In *Iron in Immunity Cancer and Inflammation*. Edited by M. D. Sousa and J. Brock. 261-282. Chichester, UK.: Wiley.

Sutherland, R, D Delia, C Schneider, R Newman, J Kemshead, and M Greaves.( 1981).

Ubiquitous cell surface glycoprotein is proliferation associated receptor for transferrin. *Proc. Natl. Acad. Sci. USA* 78 : 4515-4519.

Taetle, R, K Rhyner, D Castagnolo, and J Mendelsohn.( 1985). Role of transferrin, Fe and transferrin receptors in myeloid leukaemia cell growth. *J. Clin. Invest* 75 : 1061-1067.

Taetle, R, JM Honeysett, and R Bergeron.( 1989). Combination iron depletion therapy. *J. Natl. Cancer Inst.* 81 : 1229-1235.

Tangeras, A, T Flatmark, D Backstrom, and A Ehrenberg.( 1980). Mitochondrial iron not bound in heme and iron-sulfur centers. *Biochim. Biophys. Acta* 589 : 162-175.

Tangerus, A.( 1985). Mitochondrial iron not bound in heme and iron-sulfur centers and its availability for heme synthesis in vitro. *Biochim. Biophys. Acta* 843 : 199-207.

Taylor, PD, IEG Morrison, and RC Hider.( 1988). Microcomputer analysis of non-linear analysis to metal-ligand equilibria. *Talanta* 35 : 507-512.

Thelander, L, and P Reichard.( 1979). Reduction of ribonucleotides. *Ann. Rev. Biochem.* 48 : 133-158.

Thelander, L, A Graslund, and M Thelander.( 1983). Continual presence of oxygen and iron required for mammalian ribonucleotide reductase: possible regulation mechanism. *Biochem. Biophys. Res. Commun.* 110 : 859-865.

Thorstensen, K, and I Romslo.( 1988). Uptake of iron from transferrin by isolated rat hepatocytes. *J. Biol. Chem.* 263 : 8844-8850.

Thorstensen, K, and I Romslo.( 1990). The role of transferrin in the mechanism of cellular iron uptake. *Biochem. J.* 271 : 1-10.

Titeaux, M, U Testa, F Louache, P Thomopoulos, H Rochant, and P Breton-Gorius.( 1984). The role of iron in the growth of human leukemic cell lines. *J. Cell Physiol* 121 : 251-256.

Wagstaff, M, M Worwood, and A Jacobs.( 1978). Properties of human tissue isoferritins. *Biochem. J.* 173 : 969-977.

Ward, PA, GO Gill, R Kunkel, and C Beauchamp.( 1983). Evidence for role of hydroxyl radical in complement and neutrophil dependent tissue injury. *J. Clin. Invest* 72 : 789-801.

Ward, PA, JS Warren, GO Till, J Varani, and KJ Johnson.( 1989). Modification of disease by preventing free radical formation: a new concept in pharmacological intervention. *Baillieres Clin. Haematol.* 2 : 391-402.

Weaver, J, and S Pollack.( 1989). Low Mr iron isolated from guinea pig reticulocytes as AMP-Fe and ATP-Fe complexes. *Biochem. J.* 261 : 787-792.

Weaver, J, and S Pollack.( 1990). Two types of receptor for iron on mitochondria. *Biochem.*



J. 271 : 436-466.

Weinberg, ED.( 1984). Iron withholding: a defense against infection and neoplasia. *Physiol. Rev.* 64 : 65-102.

Weinberg, K, J Champagne, C Lenarsky, J Peterson, T Nguyen, B Felder, and R Parkman. (1988). Desferrioxamine (DFO) inhibition of interleukin 2 receptor (IL2R): potential therapy of graft versus host disease (GVHD). *Blood* 68 : 286 (Abstr.).

Weir, MP, JF Gibson, and TJ Peters.( 1984a). Biochemical studies on the isolation and characterisation of human spleen haemosiderin. *Biochem. J.* 223 : 31-38.

Weir, MP, JF Gibson, and TJ Peters.( 1984b). Haemosiderin and tissue damage. *Cell Biochem. Function* 2 : 186-194.

White, GP, R Bailey-Wood, and A Jacobs.( 1976a). The effect of chelating agents on cellular iron metabolism. *Clin. Sci. Mol. Med.* 50 : 145-152.

White, GP, A Jacobs, RW Grady, and A Cerami.( 1976b). The effect of chelating agents on iron mobilization in chang cell cultures. *Blood* 48 : 923-929.

Williams, CH, and H Kamin.( 1962). Microsomal triphosphopyridine nucleotide-cytochrome c reductase of liver. *J. Biol. Chem.* 237 : 587-595.

Worwood, M.( 1986). Serum ferritin. *Clin. Sci.* 70 : 215-220.

Wright, JA, RG Hards, and JE Dick.( 1981). Studies of ribonucleotide reductase activity in intact permeabilized cells: a genetic approach. *Advances in Enzyme Regulation* 19 : 105-127.

Yinnon, AM, EN Theanacho, RW Grady, DT Spira, and C Hershko.( 1989). Antimalarial effect of HBED and other phenolic and catecholic iron chelators. *Blood* 74 : 2166-2171.

Young, SP, A Bomford, and R Williams.( 1984). The effect of the iron saturation of transferrin on its binding and uptake by rabbit reticulocytes. *Biochem. J.* 219 : 505-510.

Zerial, M, P Melancon, C Schneider, and H Garoff.( 1986). The transmembrane segment of the human transferrin receptor functions as a signal peptide. *EMBO J.* 5 : 1543-50.

Zerial, M, M Soumelainen, M Zanetti-Schneider, C Schneider, and H Garoff.( 1987). Phosphorylation of the human transferrin receptor by protein kinase C is not required for endocytosis and recycling in mouse 3T3 cells. *EMBO Journal* 6 : 2661-2667.

## **APPENDICES**

## APPENDIX 1

Plasticware, glassware and reagents were purchased from the following manufacturers:

### PLASTICWARE

All plasticware was of tissue culture grade unless otherwise indicated.

30ml Universal containers	Sterilin Ltd
35mm Petri dishes	Hounslow, UK.
50ml polythene tubes, 5 and 10ml graduated pipettes	
7ml Bijou bottles	Falcon (Becton Dickinson Labware)
Microtest flexible assay plates	California, USA.
Tissue culture flasks	
25ml graduated pipettes	
15ml screw cap conical tubes	
Flowpore D 0.2 and 0.45 $\mu$ M filters	Flow Labs Ltd
96 well E.I.A Microtitration plate	Rickmansworth, Herts, UK.
Syringes (1-50ml capacity)	Sabre International Products Ltd Reading, Berks, UK.
LP3 and LP4 polystyrene tubes	L.I.P (Equipment and Services) Ltd. Shipley, W.Yorks, UK.

1.8ml cryotubes	Nunc (Gibco Ltd)
96 well tissue culture plates	Paisley, UK.
1.5ml microcentrifuge tubes	Treff
	Degeirsheim, Switzerland.
0.5ml, 2.5ml Combitips	Eppendorf
	Hamburg, Germany
6ml scintillation vials and screw cap	Hewlett Packard
Fibreglass filterpaper	Whatman International Ltd
	Maidstone, UK.

### GLASSWARE

For general use glassware was Pyrexware which was washed routinely in detergent and rinsed in distilled water. Other glassware is listed below.

Microscope slides	British Drug House (BDH)
glass cover slips	Poole, UK.
1ml and 2ml graduated pipettes	Volac (John Poulter Ltd)
	Barking, Essex, UK.
Pasteur pipettes	Bilbate Ltd
	Daventry, UK.

## GENERAL REAGENTS

All reagents were Analar or tissue culture grade where possible.

Ammonium ferric citrate British Drug House

Ammonium ferrous sulphate

Hepes (N-2-hydroxyethylpiperazine-N-2-ethenesulphonic acid)

Magnesium chloride

Sodium acetate

Sodium chloride

Sodium hydroxide

Sodium iodide

Trizma Base

Boric acid Fisons

Diamino-ethane-tetra-acetic acid Loughborough, UK.  
(disodium and dipotassium salts)

Disodium tetraborate

Glycine

Acridine orange Sigma

Adenosine triphosphate Poole, Dorset, UK.

Aprotinin

Barium hydroxide solution

*Crotalus atrox* venom

Cytochrome *c*

Dithiothreitol

Ethidium bromide

Imidazole

*p*-Nitrophenyl β-D-galactopyranoside

Phenylmethanesulphonyl-fluoride

Propidium iodide

RNAase (Type 1-A)

Sigmacote

Sodium azide

Transferrin (holo- and apo, human, approximately 98% pure)

Tween 20 and 80

Zinc sulphate solution

Phytohaemagglutinin

Wellcome Pharmaceuticals

Beckenham, Kent, UK.

DEAE Sepharose CL-6B

Pharmacia LKB Ltd

Ficoll-Hypaque.

Milton Keynes, UK.

Affigel

Biorad

Richmond, California, USA.

### TISSUE CULTURE MEDIA

Iscoves minimum Dulbeccos medium

Gibco Ltd

Penicillin and Streptomycin

Paisley, UK.

RPMI 1640 medium

Foetal calf serum

Northumbria Biologicals Ltd

Northumberland, UK.

Agar

Difco

Detroit, USA.

PBS Tablets

Oxoid Ltd

Basingstoke, UK.

### SOLVENTS

Acetone

May and Baker Lab Products

Ethanol

Manchester, UK.

Formaldehyde

Methanol

Hisafe scintillation fluid

Pharmacia LKB Ltd

Milton Keynes, UK.

### RADIOISOTOPES

[<sup>14</sup>C] cytidine diphosphate (20 $\mu$ Ci/ml, disodium salt)

Amersham International

[<sup>3</sup>H] leucine (1mCi/ml)

Amersham, Berks, UK.

[<sup>14</sup>C] sucrose (200 $\mu$ Ci/ml)

[<sup>3</sup>H]thymidine (1mCi/ml)

[<sup>3</sup>H]uridine (1mCi/ml)

[<sup>59</sup>Fe] Ferrous sulphate

New England Nuclear

(Dupont Ltd) Stevenage, UK.

## APPENDIX 2: BUFFERS AND MADE UP REAGENTS

### PHOSPHATE BUFFERED SALINE (PBS)

This was prepared from Oxoid tablets. One tablet was dissolved in 100ml distilled water and the pH was checked and adjusted as necessary.

### TRIS-HCl BUFFER pH 8.0

This buffer was prepared as a stock solution of 1M as described below, and diluted with distilled water to the required molarity. The pH was checked and adjusted as necessary.

25ml of 121.15g/l Tris[hydroxymethyl]aminomethane was mixed with 41.6ml 1N HCl and made up to 100ml with distilled water.

### 0.05M CITRATE PHOSPHATE BUFFER pH4.3, pH5.0

This buffer was used at pH4.3 for the  $\beta$  Galactosidase assay, and at pH5.0 for the ferritin ELISA.

SOLUTION (A) Citric acid ( $C_6H_8O_7 \cdot H_2O$ ) 10.51g/l

SOLUTION (B) Disodium Phosphate ( $Na_2HPO_4 \cdot 2H_2O$ ) 17.8g/l

The above solutions were mixed in the proportions given below and the pH was checked.

pH 4.3 56.4ml (A) + 43.6ml (B).

pH 5.0 49ml (A) + 51ml (B).

### 0.1M BORATE SALINE BUFFER pH8.4

This buffer was used for the ferritin ELISA

SOLUTION (A) Sodium tetraborate (Borax) 9.6g/l + 29.2g/l NaCl

SOLUTION (B) Boric acid 12.37g/l + 29.2g/l NaCl

Mix 46.3ml (A) with 53.7ml (B) and titrate to pH8.4



### **APPENDIX 3.**

#### **MEASUREMENT OF SERUM IRON LEVELS**

The iron content and unsaturated iron binding capacity (UIBC) of three batches of FCS were determined by the method of Ruutu (1975), using the iron chelating dye ferrozine.

#### **METHODS**

##### **A) DETERMINATION OF IRON**

250mg of ferrozine (disodium salt of 3-(2-pyridyl)-5,6-bis (4-phenylsulphonic acid)-1,2,4,-triazine), 10g of ascorbic acid and 30g of Triton X-100 were dissolved in 1L of 0.4M glycine/HCl buffer pH 3.1. The reagent for blank samples was as above but without the ferrozine.

A stock standard solution containing 2.0mmol/L of iron in 0.02M HCl. Working standards containing 0-60  $\mu\text{mol/L}$  of iron were prepared by dilution of the stock standard solution with iron free water.

For the assay 300 $\mu\text{l}$  of sample or standard was mixed with 800 $\mu\text{l}$  of the ferrozine colour reagent. Samples were incubated for 45 minutes and the absorbance was read at 560nm with a Pye Unicam SP-800 spectrophotometer. A blank was prepared for each serum sample.

The iron content of the samples was determined by subtracting the absorbance of each serum blank from the absorbance of the respective serum and the result was read from the standard curve.

##### **B) DETERMINATION OF UIBC**

The colour reagent was prepared by dissolving 1.35g of ferrozine per litre of iron-free water. The buffer for UIBC measurement was 0.25M Tris/HCl pH8.4 containing 15g/L Triton X-100 and 10.0g/L ascorbic acid to give a final pH of 7.95.

Standards and a UIBC saturation solution containing 200µmol Fe were prepared by dilution of the stock standard with iron-free water as above.

UIBC was determined by adding 300µl of serum to 800µl of Tris buffer and 150µl of the saturation solution. After 10 minutes 150µl of the colour reagent was added. Standards were prepared by mixing 300µl of the working standard solutions, 800µl of Tris buffer and 150µl of water. After 10 minutes 150µl of the colour reagent was added. A blank was prepared for each serum sample by substituting water for the colour reagent.

After 45 minutes the absorbance of the solutions was measured at 560nm. The amount of unbound iron was calculated from the standard curve as described above. The UIBC was obtained by subtracting the amount of unbound iron from the amount of iron added per litre of serum.

## RESULTS

Serum Batch	Serum Iron (µM)	UIBC (µM)	TIBC (µM)	% Saturation
1	34.3	102.2	136.5	25.1
2	32.6	102.4	134.0	24.3
3	30.7	102.9	133.6	22.9
Mean	32.5	102.5	134.7	24.1
S.E.M	1.9	0.3	2.6	0.9